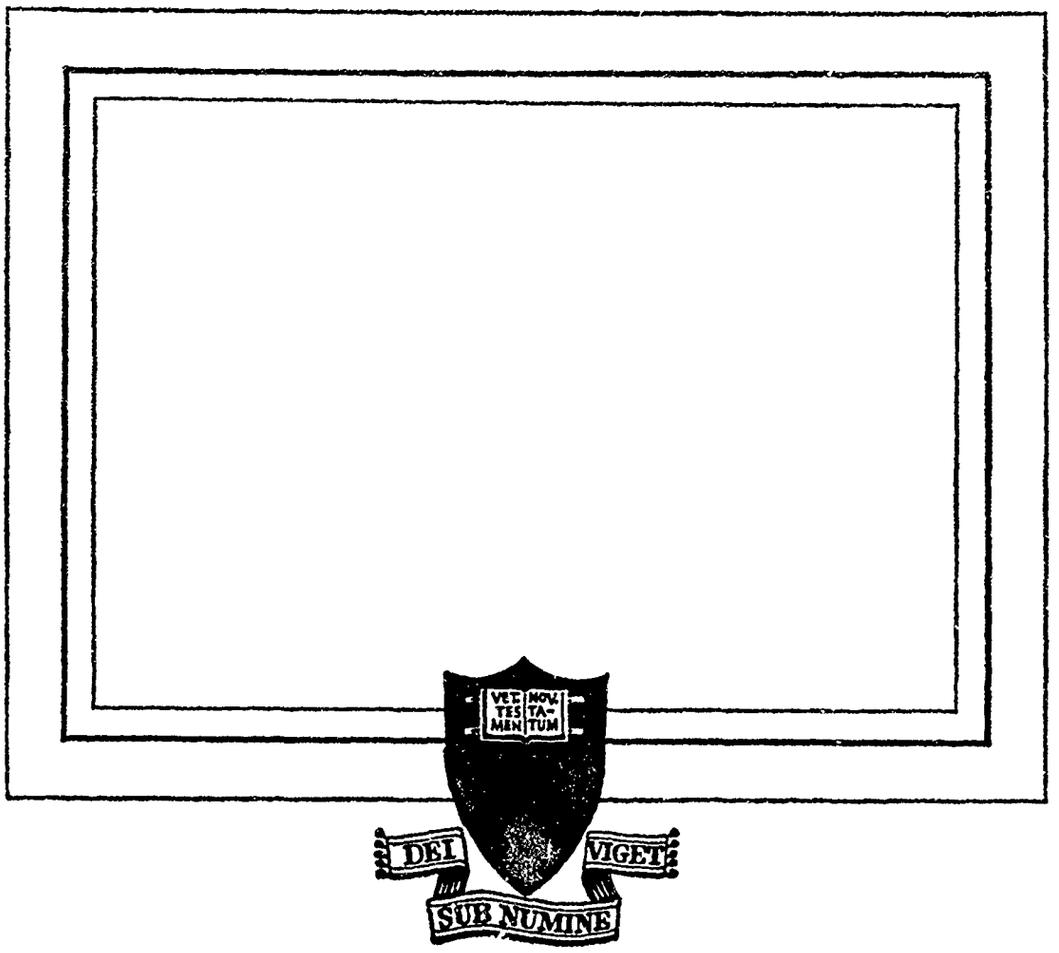

Research Sponsored by:

Power Branch
Office of Naval Research
Department of the Navy

PRINCETON UNIVERSITY

DEPARTMENT OF

AEROSPACE AND MECHANICAL SCIENCES

1. Distribution of this document is unlimited.

250

THE BURNING MECHANISM OF AMMONIUM PERCHLORATE-BASED COMPOSITE SOLID PROPELLANTS

Aerospace and Mechanical Sciences Report
No. 830

by

J. A. Steinz, P. L. Stang, and M. Summerfield

ONR CONTRACT Nonr 1858(32)

February 1969

Transmitted by:

Martin Summerfield
Principal Investigator

1. Distribution of this document is unlimited.

Qualified requestors may obtain additional copies from the Defence Documentation Center. All others should apply to the clearinghouse for Federal Scientific and Technical information.

Guggenheim Laboratories for the Aerospace Propulsion Sciences
Department of Aerospace and Mechanical Sciences
PRINCETON UNIVERSITY
Princeton, New Jersey

ABSTRACT

Theories of propellant burning are briefly reviewed in the light of previous studies of the burning behavior and flame structure of composite ammonium perchlorate (AP) propellant. Those studies showed that the granular diffusion flame (GDF) theory conforms to the known structure of the propellant flame, and is quantitatively valid for a wide class of practical AP propellants, much more so than any other theory proposed for composite propellants.

A comprehensive survey of all available burning rate data extending over the range 1-100 atm, serves to delineate, (1), the domains of burning behavior of AP propellant, and (2), the domain of validity of the GDF theory. This survey shows that whenever the AP loading is high, the AP particles are medium-sized, and the fuel is of the type that does not melt readily, an AP-based propellant burns normally, i.e., it has a monotonic log-log burning rate-pressure curve that is of steadily decreasing slope as pressure is increased. Of all the burning rate equations proposed, the GDF equation, $1/r=a/p+b/p^{1/3}$, fits the data of this class of propellants best. When the propellant is severely underoxidized, has small AP particles, and/or has a fuel that melts easily, abnormal burning in the form of plateaus, mesas, or extinctions, at intermediate pressure (20-200 atm) is the result. No burning rate equation has been proposed that applies to this category of propellants. The transition between abnormal and normal burning, and hence also, the boundary of validity of the GDF theory, is defined for propellants with difficult-to-melt fuels, by: $\phi_o \gtrsim (0.30 - 0.10 \log_{10} d_m)$ and $d_m \lesssim 250\mu$, where ϕ_o = equivalence ratio and d_m = mean AP paricle size in microns.

The trend towards the above anomalous burning behavior is quite regular with respect to the effects of AP loading, AP particle size, and relative meltability of the fuel: reduction of AP particle size, and/or reduction of AP content, and/or substitution of a more readily meltable fuel, causes a progressively stronger deviation from the normal monotonic log-log r-p curve in the usual rocket pressure range; first, a region of zero slope (plateau) appears; then, a region of negative slope (mesa) develcpes; finally, in the extremes of either of these parameters, steady self-sustained burning is no longer possible in this anomalous burning range.

Various observations of the flame and of the propellant surface after extinguishment, show that whenever a propellant burns in this anomalous way, the flame suffers temporary localized extinctions which serve to reduce the mean burning rate for the particular physical conditions. The burning surface appears then always to be covered by a molten fuel layer. These observations suggest that it is the molten fuel layer that causes the intermittent burning behavior; it would do so by covering the AP particles exposed at the regressing propellant surface, thereby de-

pleting the gas phase flame of the necessary oxidizer gases. This phenomenon can be put to practical use in the sense that hot plateau-burning propellants can be made by using a fuel that forms a molten layer on the propellant surface.

Extension of the work to subatmospheric pressures shows that in this low pressure range, too, the relative meltability of the fuel plays an important role in determining the burning behavior. As a general phenomenon, AP propellants show no indication of melting (they usually char), have burning rates in the 0.05-1.0 atm range that fall on a straight line with slope 0.6-0.9 when plotted as (log r) vs. (log p). These results are in qualitative accord with the predictions of the GDF theory but only when it is extended to include explicitly the pressure dependence of the kinetic rate of the first stage flame. This first stage flame consists of the exothermic redox reaction between the gases produced by the dissociative sublimation of AP. It can be shown theoretically that, above 10 atm, it is valid to treat the first stage as having zero thickness and to disregard its pressure dependence, as was done in the original formulation of the GDF theory (1960). It can be shown also that such simplification is not permissible at subatmospheric pressures.

Extinctions below 1 atm were noted for propellants not prone to melting, i.e., those that had a dry charred appearing burned surface. Such extinctions appear to be due to escape of unreacted AP from the flame zone, together with peripheral convective cooling of the flame at the strand edges. The extinction pressure might well be lower than 0.05 atm in rocket chambers, under adiabatic conditions, but this possibility was not tested.

The polyurethanes of this study showed markedly different behavior in that the extinction pressure is much higher (up to several atm); also, the burning rate curve bends downwards as soon as the extinction pressure is approached. Various indications are that this behavior is due to the meltability properties of these fuels: a very easily meltable urethane causes extinction above 1 atm and a less meltable urethane causes extinction at pressures closer to 0.1 atm. These extinctions seem to be due to either partial coverage of the AP particles at the propellant surface or expulsion of solid AP + liquid fuel globules from the propellant surface into the afterburning zone; whichever occurs, depends on whether the thickness of the molten fuel layer (related to the thickness of the thermal layer in the solid phase) is respectively, comparable to, or much larger than, the mean size of the AP particles. Exceptional behavior was also found with polysulfide-AP propellant, in the range where a solid porous residue is formed as a combustion product (below 0.05 atm). This can be plausibly explained by assuming that the porous ash retains the heat generated by the gaseous flame.

This study puts on rational grounds the burning mechanism of AP composite solid propellants of both standard and non-standard formulation. The findings on flame structure are important for understanding steady state burning rates, non-steady burning (instability), extinguishment, and ignition.

ACKNOWLEDGEMENTS

This research under Contract Nonr 1858(32) was sponsored by the Power Branch, Office of Naval Research, Department of the Navy.

Dr. R. Roberts, Head, Power Branch, was the Technical Supervisor for this project. Mr. R. D. Jackel, also of the Power Branch, was the Project Monitor.

The authors are especially indebted to Mr. C. R. Felsheim who is in charge of the technician group concerned with solid propellants and who so willingly spent much of his time processing the many specialized propellants needed for this study.

We also extend a special word of thanks to Lead Technician Mr. E. R. Crosby and Undergraduate Mr. V. S. Natiello; the former provided help in many practical experimental matters, no matter what the circumstances; the latter spent many long hours obtaining much of the burning rate data used in this document.

Other people who have given of themselves at various times over the past few years are: Messrs. L. Kurylko, H. Ayres, S. O. Morris, J. H. Semler, J. A. Batson and G. H. Hart. Their assistance and advice is gratefully acknowledged.

This document was typed by Miss D. Morris, Mrs. D. Guest and Mrs. E. Bartlebaugh. Their patient and skillful handling of this task is very much appreciated.

TABLE OF CONTENTS

		Page
TITLE PAGE		(i)
ABSTRACT		(ii)
ACKNOWLEDGEMENTS		(iv)
TABLE OF CONTENTS		(v)
LIST OF TABLES		(ix)
LIST OF FIGURES		(x)
SECTION I	INTRODUCTION	1
SECTION II	PREVIOUS STUDIES OF THE MECHANISM OF BURNING	2
A.	Flame Structure and Surface Decomposition Process	2
(i)	Gaseous Fuel-Oxidant Flame	2
(ii)	Ammonium Perchlorate Decomposition Process	3
(a)	Bulk Degradation of Pure AP	4
(b)	Burning Behavior of Pure AP	5
(iii)	Fuel Decomposition Process	9
(iv)	Sub-Surface and/or Heterogeneous Reactions; Plausibility and the Search for Evidence	11
(v)	Structure of Regressing Propellant Surface	14
(vi)	Physical Picture of Burning Process	15
B.	AP Composite Propellant Burning Rate Behavior and Solid Propellant Burning Rate Theories That Have Been Proposed	16
(i)	Summary of AP Composite Propellant Burning Rate Behavior	17
(ii)	Theories of Solid Propellant Burning	19
SECTION III	THE GRANULAR DIFFUSION FLAME THEORY	24
A.	Physico-Chemical Model	24
B.	General Equations for a Three-Stage Flame Model	27
C.	GDF Theory With Collapsed A/PA Flame	29
(i)	Theoretical Treatment of Collapsed A/PA-GDF Model	29
(ii)	Comparison of Diffusion Theory Burning Rate Equations With Burning Rate - Pressure Data	33
D.	GDF Theory With Distended A/PA Flame	36
(i)	Reaction Times for A/PA and O/F Stages	36
(ii)	Derivation of Distended A/PA-GDF Theory	37

		Page
	E. Discussion of Theoretical Predictions; Collapsed A/PA-GDF Model Compared to Distended A/PA-GDF Model	38
	F. Major Conclusions Summarized	42
SECTION IV	COMPOSITE PROPELLANT BURNING BEHAVIOR IN 1-100 ATM RANGE: NORMAL BURNING, PLATEAU BURNING, AND INTERMEDIATE PRESSURE EXTINCTION	43
	A. Findings by Previous Investigators	43
	B. Experimental Results of This Investigation	44
	(i) The Effect of AP Particle Size	45
	(ii) The Effect of AP Loading	45
	(iii) The Effect of Increasing Strand Size	45
	(iv) The Effect of Fuel Type	46
	(v) Various Qualitative Observations	48
	C. Interpretation of Results; Phenomenon of Intermittent Burning	48
	D. Concluding Remarks	51
SECTION V	COMPOSITE PROPELLANT BURNING BEHAVIOR AT SUBATMOSPHERIC PRESSURES	52
	A. Review of Findings by Previous Investigators	52
	B. Experimental Results of This Investigation	53
	(i) Burning Rates	53
	(ii) Subsidiary Semi-Quantitative Observations	56
	C. Discussion of Results; Relation to Earlier Experimental and Theoretical Findings	57
	D. Concluding Remarks	61
SECTION VI	MAJOR CONCLUSIONS OF THIS STUDY	62
SECTION VII	EXTENDED CONSIDERATIONS FOR OTHER PROPELLANT SYSTEMS AND PHYSICAL SITUATIONS	64
	A. Oxidizer Substitution	65
	B. Catalyst Additives	67
	C. Aluminum Additions	69
	D. Effects of Different Fuels	72
	E. Pure Double-Base Propellants	72
	F. Propellant Behavior Under Other Physical Situations	74
LIST OF SYMBOLS		77
LIST OF ABBREVIATIONS		79
LIST OF REFERENCES		82
TABLE I		100
FIGURES 1 to 27		101

		Page
APPENDIX A	LISTING OF PHYSICAL CONSTANTS AND CALCULATED PREDICTIONS FOR GRANULAR DIFFUSION FLAME THEORY (Collapsed and Distended A/PA Flames)	128
	Tables II(A) to II(D)	130
APPENDIX B	REVIEW OF BURNING RATE BEHAVIOR OF AP PROPELLANTS AND FIT OBTAINED BY VARIOUS PROPOSED BURNING RATE EQUATIONS	133
	Tables III(A), III(B), and IV	134
	Figures B-1 to B-59	137
APPENDIX C	EXPERIMENTAL PROCEDURES AND ACCURACY OF MEASUREMENTS	196
	(i) Propellant Manufacturing Process	196
	(ii) Propellant Quality Control Tests	198
	(a) Propellant Hardness and Uncured Viscosity	198
	(b) Finished Propellant Density	198
	(iii) Oxidizer Particle Size Measurements	200
	(a) Sedimentation Technique	201
	(b) Miscroscopic Technique	202
	(c) Accuracy of Sedimentation Technique	203
	(iv) Burning Rate Measurements	203
	(a) Burning Rates at Subatmospheric Pressures	203
	(1) Apparatus	203
	(2) Experimental Procedure and Data Reduction	204
	(b) Burning Rates in the Range 1-100 atm	205
	(1) Apparatus	205
	(2) Experimental Procedure	206
	(c) Accuracy of Burning Rate Measurements	206
	(1) Effect of Strand Surface Treatment	206
	(2) Effect of Nitrogen Purge Rate	207
	(3) Effect of Strand Size	207
	(4) Effect of Fuse Wires	208
	(5) Condition of Regressing Surface: Flatness and Inclination to Direction of Travel	208
	(6) Accuracy and Reproducibility of Burning Rate Measurements	208
	Table V	210
	Figures C-1 to C-15	211
APPENDIX D	SPECIFICATIONS OF ALL PROPELLANT FORMULATIONS USED IN THIS INVESTIGATION: Conditions of Manufacture, Propellant Composition, Propellant Density, and AP Particle Size	226
	Tables VI(A) and VI(B)	227
	Figures D-1 and D-3	228

		Page
APPENDIX E	ERRORS ASSOCIATED WITH DENSITY MEASUREMENTS	231
(i)	Loss of Fuel During Manufacturing	231
(ii)	Displacement Fluid	231
(iii)	Error Incurred by Neglecting Volume Displaced by the Wire Suspending the Sample in the Displacement Fluid	232
(iv)	Error in Weight Measurements	232
(v)	Error in Fuel Density	232
(vi)	Error in AP Density	232
(vii)	Error Analysis of Propellant Density Measurements	232
(viii)	Reproducibility of Density Measurements	234
APPENDIX F	DISTRIBUTION LIST	236
APPENDIX G	D.D. FORM 1473	Last page

LIST OF TABLES

Table No.	Title	Page
I	Comparison of Calculated and Measured Combustion Products and Heat of Reaction for Pure AP	100
II	Theoretical Predictions of Granular Diffusion Flame Theory	130
II(A)	Collapsed A/PA-GDF Predictions for Case When E_s=15 kcal/mole	130
II(B)	Collapsed A/PA-GDF Predictions for Case When E_s=30 kcal/mole	131
II(C)	Distended A/PA-GDF Predictions for ϵ=0 and E_s=15 kcal/mole	132
II(D)	Distended A/PA-GDF Predictions for ϵ=0.75 and E_s=15 kcal/mole	132
III	Summary of Behavior of AP-Based Propellants in 1-100 atm Range	134
III(A)	Propellants With Fuels That do not Melt Readily	134
III(B)	Propellants With Fuels That Form Molten Layer on Burning Surface	135
IV	Properties of Selected Fuel-Binder Systems	136
V	Comparison of Mean Particle Diameters Obtained by Microscopic and Sedimentation Techniques (for As Received "Spherical" Ammonium Perchlorate)	210
VI(A)	Specifications of All Propellant Formulations Used for 1-100 atm Burning Rate Studies	227
VI(B)	Specifications of All Propellant Formulations Used for Subatmospheric Burning Rate Studies	227

LIST OF FIGURES

Figure	Caption	Page
1	Two-Stage Granular Diffusion Flame Model for Ammonium Perchlorate-Type Composite Solid Propellants	101
2	Correlation of Burning Rates with: $(1/r) = (a/p) + (b/p^{1/3})$	102
3	Burning Behavior and Regimes of Validity of GDF Theory for AP Based Propellants with Fuels That do not Melt Readily	103
4	Correlation of Burning Rates with: $(1/r)^2 = (a/p)^2 + (b/p^{1/3})^2$	104
5	Correlation of Burning Rates with: $(1/r) = (a/p) + (c)$	105
6	Pressure Dependence of Reaction Times of Ammonia/Perchloric Acid and Oxidant/Fuel Reactions	106
7	Heat Supply to Propellant Surface by A/PA and O/F Stages in the Granular Diffusion Flame Model	107
8	Granular Diffusion Flame Theory Predictions Plotted as (p/r) vs. $(p^{2/3})$ for Collapsed and Distended A/PA Flames	108
9	Pressure Dependence of Burning Rate Predicted by the Granular Diffusion Flame Theory for the Cases: (1) Premixed Ammonia/Perchloric Acid Flame is Distended (2) Premixed Ammonia/Perchloric Acid Flame is Collapsed	109
10	Effect of Activation Energy of Surface Reaction on Burning Rate Behavior of Granular Diffusion Flame Theory with Collapsed A/PA Flame Zone	110
11	Pressure Dependence of Flame Zone Thicknesses Predicted by Granular Diffusion Flame Theory with Distended A/PA Flame	111
12	Effect of AP Loading on Burning Rate Behavior of Polysulfide (LP3/GMF)-AP Propellant (From Bastress Ref. 14)	112
13	Effect of AP Particle Size on Burning Rate Behavior of Polysulfide-AP Propellant (From Bastress)	113
14	35% LP3/GMF + 65% AP Data of Fig. 13 Plotted as (p/r) vs. $(p^{2/3})$	114
15	Effect of AP Particle Size on Burning Rate Behavior of 25.0% PBAA/EPON + 75.0% AP Propellant ($\psi_o = 0.334$)	115
16	Effect of AP Loading on Burning Rate Behavior of PBAA/EPON-AP Propellant (Bimodal AP: 30% 5μ + 70% 45μ)	116
17	GDF Correlation of Highly Loaded AP Propellants With Fuels That do not Melt Readily	117
18	Burning Rate Behavior of AP-Based Propellants With Fuels That do not Melt Readily	118

Figure	Caption	Page
19	Burning Rate Behavior of Unimodal AP Propellants With Polyurethane Fuels That Melt Readily	119
20	Burning Rate Behavior of Bimodal AP Propellants With Polyurethane Fuels That Melt Readily	120
21	Burning Rate Behavior of PIB/MAPO-AP Propellants (PIB/MAPO Fuel is Readily Meltable)	121
22	Burning Rates of DB and CMDB Propellants (Pure NC/TEGDN and NC/TEGDN-AP Mixtures)	122
23	GDF Correlation of DB and CMDB Propellants (Pure NC/TEGDN-AP Mixtures)	123
24	Comparison of GDF Theory Predicted Surface Temperature With Measurements for AP-Based Propellants	124
25	Burning Rate - Pressure Dependence at Subatmospheric Pressures for Ammonium Perchlorate with Different Binders	125
26	Effect of Binder-Type on Burning Rate of Ammonium Perchlorate Propellants (mean particle size of AP is 5 micron)	126
27	Burning Rate of 35% Polysulfide + 65% NH_4ClO_4 With Varying Mean Oxidizer Particle Size	127
B-1 to B-59	Burning Rates of All Propellants Listed in Table III (88 different formulations) Plotted Four Ways: (a) (log r) vs. (log p) (b) $(p/r)_2$ vs. $(p^{2/3})$ (c) $(p/r)^2$ vs. $(p^{2/3})^2$ (d) (p/r) vs. (p)	137 to 195
C-1	Ammonium Perchlorate Particle Size Distributions Determined by Microscopic Technique	211
C-2	Ammonium Perchlorate Particle Size Distributions Determined by Sedimentation Technique	212
C-3	Apparatus for Measuring Burning Rates at Subatmospheric Pressures	213
C-4	Close-Up of Optical System Used to Measure Burning Rates at Subatmospheric Pressures	214
C-5	Photographic Records of Strands Burning at Subatmospheric Pressures	215
C-6	Propellant Burning Rates Determined by Two Independent Means of Data Reduction	216
C-7	Exploded View of Strand Burner for Measuring Burning Rates in 1-100 atm Range	217
C-8	Close-Up of Strand Holder Prior to Test (1-100 atm Strand Burner)	218
C-9	Instrumentation for Measuring Burning Rates in 1-100 atm Range	219
C-10	Typical Test Record from 1-100 atm Strand Burner	220
C-11	Effect of Condition of Surface of Strand on Burning Rate of 25% PBAA/EPON + 75% AP (80μ Mean Particle Diameter)	221

Figure	Caption	Page
C-12	Effect of Nitrogen Purge Rate on Mean Burning Rate of 25% PBAA + 75% Ammonium Perchlorate (Mean Size = 80μ)	222
C-13	Effect of Strand Size on the Burning Rate Behavior of 25% PBAA/EPON + 75% Ammonium Perchlorate (Mean AP Size = 80μ)	223
C-14	Batch to Batch Reproducibility of PBAA/EPON-AP Propellant; Mean Particle Size of AP is 80 Micron	224
C-15	Duplication of Bastress' Data for Polysulfide Propellants	225
D-1	AP Particle Size Distributions A to D (of Table VI) Determined by Sedimentation Technique	228
D-2	AP Particle Size Distributions E to G (of Table VI) Determined by Sedimentation Technique	229
D-3	AP Particle Size Distributions H to K (of Table VI) Determined by Microscope Method	230
E-1	Effect of Immersion into Displacement Fluid on the Measured Density of 25% PBAA/EPON + 75% AP (80μ Unimodal)	235

SECTION I

INTRODUCTION

The ultimate aim of the study of the steady-state burning characteristics of a composite solid propellant is to deduce enough information about the flame mechanism to be able to predict or modify at will the combustion performance of any propellant before deciding upon its use. In this way, the expensive and time-consuming process of having to take recourse to repetitive experimental testing, as has been done to date, can be avoided. On a broader scale, a detailed fundamental understanding of the burning mechanism should serve as a foundation for the prediction of solid propellant burning behavior in the more complicated non-steady situations, viz., ignition, extinguishment, and instability. All of these combustion characteristics should be deducible from a knowledge of the structure and internal processes of the flame.

A composite solid propellant is one in which the oxidizer exists as a finely divided crystalline solid bonded in a matrix of some suitable plastic fuel. The burning mechanism for such a propellant is a very complex process. The flame wave is driven by several physical processes and many chemical reactions, acting simultaneously or in succession. It is the purpose of burning mechanism research to identify the most important physical processes and reaction steps in the flame and then, knowing their character, incorporate them into a theory of flame propagation that can predict burning rate behavior over the entire range of propellant parameters of interest. Experimental observations of the structural features of the flame and diagnostic measurements of various flame properties are essential for developing a theory based on a valid physical model. However, direct observations are not always possible; in such cases, inferences drawn from comparison between burning rate theory and experiment can be very helpful in distinguishing the roles played by the various processes internal to the flame. This combination of flame structure observations and interpretation of rate data is the approach that has been adopted in this investigation.

This study is concerned with the burning mechanism of composite solid propellants using ammonium perchlorate as the oxidizer. It covers the burning behavior of a wide range of AP-based propellants from 0.01 atm to 100 atm, and also determines the range of applicability of the granular diffusion flame theory, in its original form (Ref. 1), as well as in a form extended to include the AP decomposition process in a more sophisticated way. Much of the work to be reported herein has already been previously published (Refs. 2,3 and 4), when major conclusions were reached, in order to expedite scientific communication at logical times. This document strives to present all the results of this investigation, as well as the previous results of other workers, on a unified basis; it also includes many of the details that are of interest but could not have been put into the earlier papers.

SECTION II

PREVIOUS STUDIES OF THE MECHANISM OF BURNING

It is important to review previous work on flame structure and burning rate behavior in order to obtain a physical picture of the burning process in a solid propellant. In the following subsections, the significance of the gaseous fuel-oxidant flame, of the fuel and oxidizer decomposition process, and of the physical state of the regressing propellant surface is discussed. The lack of evidence for significant solid phase and/or heterogeneous reactions is indicated. The burning rate behavior of AP based composite solid propellants with respect to such variables as pressure, oxidizer particle size, and propellant composition is also described. The various theories that have been proposed in the literature are briefly discussed in terms of these findings and some of these theories are then rejected on the basis of these findings. Finally, the ranges of validity of those theories that still qualify are determined in Section III, by systematic comparison with experimental burning rate data.

A. Flame Structure and Surface Decomposition Process

(i) Gaseous Fuel-Oxidant Flame

In general, conductive heat feedback to the propellant surface from the high temperature gas phase reaction zones adjacent to the surface is the main energy flux that drives the flame wave in a solid propellant*. The energy arriving at the propellant surface by conductive heat feedback is used to heat the solid to the surface temperature and also to gasify the condensed-phase propellant constituents. The decomposed fuel and oxidizer gases emerge from the surface in an initially unmixed state. Thus, the final oxidizer-fuel (O/F) flame process must be dependent on both the diffusional mixing rate and the chemical reaction rate between the fuel and oxidizer decomposition products.

Sutherland's(7) thermocouple and spectral emission survey traverses, Zenin et al's(6) thermocouple traverses, and also, the spectral intensity profile measurements of Povinelli(8), and of Derr and Osborne(9), all show that the O/F flame occurs within a distance of about 100 microns (or less) from the regressing

---

*Blair et al's calculations(5) and Zenin et al's recent measurements(6) show that the contribution of the radiative heat feedback to the propellant surface amounts to only about 1% of the total heat fed back, in the burning of propellant strands at normal rocket pressures; in rocket motors with cylindrical grains, the radiative heat feedback contribution is expected to be about 6%(5).

propellant surface in the 1-5 atm pressure range*. This distance is sufficiently small for the O/F flame to be significant in its energy contribution towards establishing the burning rate. Neither Sutherland's(7), Cole's(12), nor Silla's(13) direct or schlieren photographs show any evidence of turbulent motion in the immediate vicinity of the regressing propellant surface. Also, the Reynolds number based on flame thickness is of the order of 20(Ref. 14); by analogy to fluid flow in packed beds, such a low value for the Reynolds number is not sufficient to establish fully turbulent flow (see Refs. 1 and 15).

A corroborative inference that the O/F flame is significant, can also be drawn from the fact that many burning rate studies (1-4,16,17) have shown composite solid propellant burning rates to be dependent on AP particle size. In fact, with the use of a "loose-granule" burner in which the particle size of the fuel and AP can be varied independently, McAlevy et al(18,19) have shown that particle size effects come about through the size of the fuel interstices between the AP particles; in a composite solid propellant, the oxidizer particle size and the scale of the fuel interstices can not be varied independently.

(ii) Ammonium Perchlorate Decomposition Process

Much attention has been given to the degradation mechanisms of propellant constituents. Owing to the difficulty of making

---

*Flame thicknesses of as much as 1 millimeter have been reported in the literature(10,11). However, as noted by Povinelli(8), the apparent (recorded) thickness of the flame must be corrected for by the distance traversed by the burning surface during the time that the emission spectrum is being recorded; the image of the emission is smeared by the linear displacement of the flame (during the time that the shutter of the recording instrument is open). Thus, Povinelli(8) found that an apparent flame thickness of about 2mm is the result of a flame that is in reality only about 200 microns thick. In view of this finding of Povinelli, it seems likely that the values for flame thickness quoted by Refs. 10 and 11, are too large only because the correction required, to account for the smearing of the flame image, was not applied to their raw data.

Derr and Osborne(9) noted temperature irregularities at distances as much as 1 mm from the burning surface. These irregularities were offered as evidence of chemical reaction and therefore, as evidence also of a very thick O/F flame. However, as pointed out by Summerfield et al(1), this unsteadiness in both space and time is more likely to be the result the unmixedness that must be present in the gas phase flame of a composite (heterogeneous) solid propellant. Thus, the distance from the burning surface at which the adiabatic flame temperature is first reached, is more representative of the effective thickness of the O/F flame. This effective thickness has been found to be about 100μ at 1 atm(6-9) and this thickness is the thickness to use in an equivalent one-dimensional model of the combustion process.

direct measurements at the high surface heating rates ($> 10^5$ °C/sec), and at the high surface temperature (600-900°C) typically encountered during propellant burning, most of this work has been confined to the study of AP and fuel decomposition at low temperatures (200-400°C), during slow heating (less than 1°C/sec) of the sample as a whole. Although these low temperature bulk degradation experiments provide an insight into the detailed mechanism of AP decomposition, it is doubtful whether kinetic rates obtained from such experiments can be extrapolated over the many orders of magnitude to propellant burning conditions, especially when it is realized that degradation in bulk is not the same as degradation at the surface of the sample; for instance, escape of the reaction products is more seriously impeded when the sample is heated uniformly in depth.

(a) Bulk Degradation of Pure AP

The decomposition mechanism of ammonium perchlorate was first seriously studied by Bircumshaw and Newman(20,21). They showed the mode of degradation to depend on the prevailing pressure and temperature conditions. In vacuo and below 300°C, only 30% decomposition occurs. The remaining 70% is a porous solid residue chemically identical to the starting material but which does not react further unless "rejuvenated" by exposure to a solvent vapor such as, water vapor, or methyl alcohol vapor. Jacobs(22) found that moderate pressures of ammonia retards this low temperature reaction. If, in vacuo, only the temperature is raised up to 250°C, decomposition remains constant at 30% but pure sublimation increases with increase in temperature. Beyond 280°C, sublimation still increases with increase in temperature but the amount of decomposition decreases with increase in temperature. Above 400°C, no solid residue remains behind. The effect of increased pressure is to retard pure sublimation and to increase the extent of chemical reaction. Sublimation was hardly noticeable at atmospheric pressure. The solid-to-gas phase transition (whether sublimation or decomposition) does not take place uniformly throughout the AP sample; it spreads hemispherically outwards from certain nucleation sites at the surface of the AP.

It is believed(23,24) that decomposition of ammonium perchlorate proceeds by continued surface diffusion of free perchloric acid to these reaction sites(see above). Neither infrared(25) nor mass spectroscopic(26) investigations could reveal the presence of the NH_4ClO_4 molecule in the gas phase. Thus, as is generally agreed (22-35,38-45), AP degradation involves as a first step dissociative sublimation of a loosely held NH_3:$HClO_4$ complex, physically adsorbed at the decomposing AP surface. Further chemical reaction between the resulting gaseous NH_3 and $HClO_4$ is then possible depending on the prevailing physical conditions.

Recently, Jacobs(22) proposed a unified mechanism incorporating this dissociative sublimation step. He imagines the step towards the adsorbed state to be accomplished by a proton transfer mechanism. At low temperatures, both NH_3 and $HClO_4$ desorb but recombine in the

gas phase to form gaseous NH_4ClO_4, i.e., pure sublimation occurs. At low temperatures and increased pressures, the NH_3 does not desorb but remains physically adsorbed, acting as an inhibitor to further desorption of the perchloric acid. The perchloric acid decomposes in the gas phase. As the temperature is increased, the NH_3 is driven off the surface and reacts with the decomposed perchloric acid. His pressure measurements show that here, namely, at significant pressure and above about 350°C, the overall decomposition, consisting of dissociative sublimation of the AP followed by reaction between the NH_3 and $HClO_4$, has an activation energy of 39 kcal/mole. His weight loss measurements gave a value of 30 kcal/mole for the activation energy of the dissociative sublimation step.

As shown by Jacobs and Whitehead, in an extensive review of the literature(24), the latter value of 30 kcal/mole agrees fairly well with that obtained by others for the dissociative sublimation step; the quoted values usually fall in the range 20 - 30 kcal/mole, the most common occurrence being at the upper limit of this range. It is to be noted that the value of 30 kcal/mole is about half of the value of the heat of dissociative sublimation of AP, 58 kcal/mole(28-30). The implication of this might be that this AP gasification step follows the Clausius-Clapeyron equilibrium vaporization law. (See, however, Section IIA(vi).)

Another point to be made is Sammons' observation(31) that highly purified AP (as opposed to commercial-grade AP) has a much higher activation energy for the dissociative sublimation step, around 100 kcal/mole. As noted in Refs. 22 and 24, this high value of the activation energy, together with the fact that the addition of impurities accelerates the rate of decomposition of AP, suggests that it is the impurities that form the nucleation sites rather than dislocations in the crystal lattice, as has been suggested earlier(32).

(b) Burning Behavior of Pure AP

Ammonium perchlorate is sufficiently exothermic in its decomposition that it can burn of its own accord(33-35). The previous studies of the decomposition mechanism of AP suggests that during the burning of an AP monopropellant stick, the flame wave is driven by conductive heat feedback to the regressing AP surface from the exothermic gas phase reaction between the NH_3 and the $HClO_4$. This heat is used to heat up the solid phase from its initial temperature to the surface temperature and also to overcome the heat needed for the solid-to-gas phase dissociative sublimation step near the surface of the AP.

When heated, the condensed-phase AP goes through an orthorhombic to cubic lattice phase transition. This lattice transition occurs at 240°C(21,36) and is endothermic to the amount of 20 cal/gm(36). The transition appears to have no effect on the decomposition mechanism of AP other than to retard the rate of

decomposition at the transition temperature(21). The rate of decomposition at this temperature is too small to be important in the burning of pure AP because the relaxation time for conduction in the solid phase is very small (about 1 msec). However, the heat of transition should be taken into account in theories of propellant burning.

The dissociative sublimation step is of zeroth order (with respect to pressure) and is endothermic to the amount of 500 cal/gm(28-30). Because this gasification process occurs in depth below the surface and because the activation energy for this process is 30 kcal/mole, the apparent activation energy during linear surface pyrolysis (as opposed to bulk degradation) is expected to be about 15 kcal/mole*. Thus, the approximate value of 20 kcal/mole obtained by several linear pyrolysis studies (38-41), is in good agreement with bulk degradation data. (See also the review of these data by Refs. 41 to 44.)

Friedman et al(45) have made some measurements of the gaseous ammonia/perchloric acid reaction at 367°C and found that the extent of decomposition of the $HClO_4$ is increased by the presence of the NH_3, i.e., the NH_3 reacts with the $HClO_4$. No further kinetic measurements of this reaction appear to have been made because premixed $NH_3/HClO_4$ flames are plagued by the formation of solid perchlorate(46) and opposed-jet $NH_3/HClO_4$ flames can not be made to burn stably(47,48).

Because of the above difficulties, and in the hope that the character of the $NH_3/HClO_4$ reaction may be nevertheless revealed, the emphasis has recently fallen on the study of pure $HClO_4$ flames and $HClO_4$-hydrocarbon flames. The main result of interest in these studies is that $HClO_4$-hydrocarbon flames are typically three times faster than hydrocarbon-oxygen-nitrogen flames of the same equivalence ratio and flame temperature(49-53)#. Another point worthy of note is that premixed fuel-$HClO_4$ flames have an activation energy that is much lower than that of the pure $HClO_4$ decomposition

---

*Consider decomposition to occur in a layer of thickness L_s below the surface regressing at rate r. Then the mass rate of decomposition below the surface is:

$$\dot{m} = (\rho_c \mathcal{E} L_s) = \rho_c r$$

where r = (regression rate) $\sim \exp(-E_s/RT_s)$

$\mathcal{E}$ = (reaction rate) $\sim \exp(-E_B/RT_{eff})$

and L_s = (thermal wave thickness) = (α_c/r)

From the above one obtains:

$$r \sim \exp(-E_s/RT_s) \sim \exp(-E_B/2RT_{eff})$$

Calculations of the rate of decomposition in the solid phase show that it is significant only when T_{eff} approaches T_s. Thus, $T_{eff} \approx T_s$ and so, the apparent activation energy during linear pyrolsis is half of that measured in bulk degradation experiments. (This conclusion can also be inferred from the relations given in Ref. 37.)

flame. For instance, the H_2-$HClO_4$ flame has an activation energy of 15 kcal/mole(49) as compared to 45 kcal/mole for the pure $HClO_4$ flame(56).) These results suggest that the $NH_3/HClO_4$ reaction is fast and has a low activation energy, as may be expected.

The character of the $NH_3/HClO_4$ flame is further elucidated by studying the burning behavior of an AP monopropellant stick. Friedman(34) found that in order to account for the measured linear regression rate, surface temperature, and adiabatic flame temperature of pure AP, by conductive heat feedback from the premixed $NH_3/HClO_4$ gas phase flame (as suggested by the previously mentioned kinetic studies), this gaseous $NH_3/HClO_4$ flame zone must be less than 1 micron thick at 100 atm. Also, the measured burning rate-pressure dependence implies that the premixed gas $NH_3/HClO_4$ reaction is of second order(27), as is expected. Friedman further made the interesting observation(27,45) that the mass consumption rate of $HClO_4$-hydrocarbon flames corresponds closely to the mass consumption rate of an AP composite solid propellant at the same flame temperature and pressure, whereas the mass consumption rate of a similarly corresponding hydrocarbon-oxygen flame falls short by a factor of 5. Based on the assumption that the burning velocity of an $NH_3/HClO_4$ mixture is not much different from the burning velocity of an equivalent hydrocarbon/$HClO_4$ mixture*, this observation would imply that most of the heat (about 80%) needed to establish the burning rate of an AP propellant must come from the AP monopropellant flame, the rest coming from the slower fuel-oxidant flame following it. This implication, that most of the heat comes from the $NH_3/HClO_4$ flame, is in agreement with our understanding of the burning process of an AP composite propellant (see section III).

#That reaction with $HClO_4$ is much faster than reaction with O_2 is also demonstrated by the fact that premixed CH_4-$HClO_4$-O_2 flames have a two-stage character in which some CH_4 is oxidized by the $HClO_4$ in the first stage, and the remaining CH_4 reacts with the O_2 in the second stage(54). Fuel-rich premixed CH_4-$HClO_4$-N_2 flames show the same two-stage character(55); Ref.(55) concludes that "the two flame fronts result from the dual oxidizing action of the perchloric acid to produce both a chlorine-oxygen species, which reacts rapidly with the initial fuel molecule, and oxygen, which completes the combustion."

*The gases that serve as the fuel constituent in the gas phase flame of a solid propellant are hydrocarbon fragments of relatively large size (see next section). Thus, mixtures of these hydrocarbons with some oxidizers are expected to have higher burning velocities than mixtures of ammonia with the same oxidizer at the same equivalence ratio; these large hydrocarbon molecules are bound to have many weak bonds and are therefore unstable compared to NH_3 which has only a few strong bonds. However, this discrepancy in burning velocities is expected to be much less than a factor of 5, because, as shown by Ref. 57, the burning velocities of a wide range of hydrocarbons, covering both strongly bonded and weakly bonded hydrocarbons, fall within a factor of 2.

It has been found, quite generally(23,24,27,33-35), that pure AP can not burn of its own accord below 27 atm. Friedman(34) suggested that the growing importance of radiative heat loss from the burning surface, with reduction in pressure, may be the cause of such extinctions below 27 atm. However, as Johnson and Nachbar(58) point out, a heat loss is required that is at least five times larger than can be accounted for by radiation alone. In fact, Horton and Price(59) found that minimizing radiative heat loss by using cylindrical grains instead of end-burning grains did not lower the extinction pressure of pure AP. On the other hand, they found that the use of an epoxy resin surface inhibitor lowered the extinction limit from 23 atm to 3 atm. Thus, one must also call upon the fact that the burning process becomes more inefficient(17,33-35) as the lower combustion limit is approached.

Calculations based on measured products of decomposition of AP (see Table I), show that the exothermic heat of decomposition of AP is about 20% less than for the case where the products are assumed to be in equilibrium (270 cal/gm compared to 330 cal/gm). These calculations also suggest that the inefficiency (loss of available heat) grows with decreasing pressure. This loss of available heat can be overcome by preheating the AP(33), by supplying radiative heat to the regressing AP surface(34) or, as noted above, by adding a small amount of fuel to the AP. In fact, Powling et al(33) found that a minimum adiabatic flame temperature of about 950°C is necessary for continued burning of AP. For instance, they found that the addition of only 3.85% paraformaldehyde depresses the lower extinction limit to 1 atm. In this case they measured the flame temperature to be 1000°C. It compares rather well with Friedman's measured value of 950°C for pure AP(34,35). Therefore, the presence of the fuel assists the AP flame by providing a hotter environment that helps overcome the reaction incompleteness.

A final point of interest is that the burning rate of sticks of pressed ammonium perchlorate powder is dependent on the particle size of the AP powder(60,61). Shannon and Peterson (60,61) suggested that this particle size dependence comes about through the fact that the time to ignition of each AP particle is dependent on the size of the particle. The resulting burning rate equation, derived by adding the ignition time and consumption time of each AP particle, $1/r = k_1 d^{0.8} + k_2$ (where k_1, and k_2 are constants), was found to fit the measured burning rate data quite well. In fact, extrapolation of this equation to zero particle size, led to a burning rate that agrees well with Hightower and Price's(62) value for a pure AP crystal. However, comparison of the magnitude of the terms in this proposed equation, when fitted to the measured burning rate data,

shows that the ignition time can be as long as 60% of the particle consumption time (in the case of AP powder with 265μ particle size at about 1000 psia pressure). Such long ignition times seem unlikely for such large AP particles.

A more likely explanation for the burning rate-particle size dependence of pressed AP powders revolves about the fact that the very thin $NH_3/HClO_4$ gas phase flame surrounds each AP particle that is exposed at the burning surface; as long as the AP particle is much larger than the thickness of this $NH_3/HClO_4$ gas phase zone (about 1 micron at normal rocket pressures), the burning rate of a stick of pressed AP powder will be inversely proportional to the AP particle size*. The data of Shannon and Peterson(60,61), for pressed AP powder larger than about 30μ, have been plotted to test whether this inverse dependence on particle size fits better than the equation proposed by Shannon and Peterson. It was found that both relations fit the data equally well. Thus, while the latter model (particle size effects due to $NH_3/HClO_4$ surrounding each AP particle) seems more reasonable for the combustion of sticks of pressed AP, the applicability of either model is really still a matter of conjecture.

(iii) Fuel Decomposition Process

Very little is known about the decomposition process of the fuel constituent as it applies to the burning process of a composite solid propellant. Hardly any work has been done with the polymers that are commonly used in modern-day rocket technology. Those polymers that have been studied in detail, have generally been studied in bulk under conditions of very low pressure (to avoid a diffusion-limited process), low temperature (200-400°C, for slow reaction times to enable detailed measurements), and slow heating rates (to ensure a uniform temperature within the sample).

The mechanism of thermal degradation of polymeric substances has been extensively reviewed on several occasions(63-66). The mechanism of decomposition (pyrolysis) involves random scission and/or systematic unzipping of the polymer chain to produce generally a gaseous mixture of monomer units and/or chain fragments of varying sizes(63,66). For instance, polymethylacrylate yields only 0.7% monomer(66) (as witnessed by a rapid drop in the molecular weight at the beginning of the process), whereas polymethylmethacrylate yields 100% monomer (molecular weight reduces only slowly, particularly during first 20% of weight loss). Polystyrene(66), on the other hand, yields 40.6% monomer; it degrades first by random scission up to 30% weight loss and then, by unzipping of the remaining chain lengths. It has been found(66)

---

*Total AP surface area exposed to A/PA reaction zone = A = na
where n = (number of AP particles exposed)
$\sim$ (volume of each AP particle)$^{-1} \sim d^{-3}$
a = (exposed surface area of each AP particle) $\sim d^2$
Therefore $A \sim d^{-1}$

that the thermal stability of a polymer is enhanced by, (1) increased linearity of a chain involving paraffinic structure, (2) introduction of a double bond*, (3) introduction of a benzene ring into the backbone of the chain, (4) increased molecular weight, (5) increased degree of crosslinking, and (6) elimination of oxygen from the back bone of the chain. It is also generally true that the degradation process follows a first order (zero order with respect to pressure) Arrhenius kinetic law in which the activation energy varies between 30 and 60 kcal/mole depending on the polymer type and molecular weight(66). This process is endothermic to the amount of 10 to 20 kcal per mole of the monomer unit; polymers with a high monomer yield fall at the low end of this range and polymers with a low monomer yield fall at the upper end(63). Above 500°C, cracking of the large chains starts to become important and so, the effect of increased temperature is then generally to reduce the monomer yield(66). Indications are that the effect of elevated pressure is to reduce the monomer yield and to increase the proportion of dimer, trimer, etc. (63). These latter observations render questionable any attempt at extrapolating low temperature bulk degradation kinetic data to the temperature conditions typically encountered in composite propellant burning; the knowledge gained from such studies can only be of qualitative value and even then, considerable caution must be exercised in its use.

A few measurements(67-70) of the linear pyrolysis rates of polymers have been made using the hot-plate technique(71). These indicate also, that the surface pyrolysis mechanism is dependent on polymer type and molecular weight. The same studies show that the activation energy for the surface pyrolysis process is strongly dependent on the surface temperature, increasing from 10 kcal/mole above 800°K to a much higher value (that is strongly dependent on the polymer type) below 700°K#. This implies that the activation energy for fuel pyrolysis appropriate to composite propellant burning is much lower than is generally observed during bulk degradation. As an explanation for the observed variation in

---

*The presence of a tertiary carbon weakens it.

#This assumes that the hot-plate technique does not distort the Arrhenius plot of (r) vs $(1/T_s)$, by defective surface temperature measurement at high surface temperatures; at high surface temperature, the mass efflux rate is high causing the gas film thickness between the sample surface and the hot-plate to be large and so, the error in surface temperature measurement can be large also. There has been a controversy concerning this point(67,72,73). Cantrell's calculations(74) show that the effect of defective surface temperature measurement is merely to reduce the scatter and to displace the Arrhenius curve in the direction of higher T_s; no distortion in the pyrolysis curves is apparent.

activation energy with surface temperature, Chaiken et al(68) suggested that monomer formation and diffusion in the surface substrate is rate-controlling at low temperature, but that at high surface temperature, desorption of the monomer is the rate-controlling step. At this stage, interpretation of propellant burning behavior in terms of the detailed structure of the binder is extremely difficult. It must therefore await more definitive results of further research on polymer degradation mechanisms.

(iv) Sub-surface and/or Heterogeneous Reactions; Plausibility and the Search for Evidence

Exothermic reaction sites other than in the gas phase, i.e., in the solid phase and at the regressing propellant surface, are possible in principle. However, at this stage there appears to be no evidence that points to their being significant.

Hightower and Price(75) conducted very careful observational searches for sub-surface and interfacial reactions by taking high resolution photographs (1-2 microns) of sectioned propellant samples that had been extinguished. No evidence of their existence could be found. Similar observations were reported by McGurk(76). Powling's(43), West, et al's(77), and Nadaud's(78) searches for significant interfacial reactions, by measurement of the rate of flame penetration into the interface between the fuel and oxidizer, also yielded negative results; the rates had almost the same magnitudes as the burning rates for similar composite solid propellants at the same conditions. A wide variety of AP-binder combinations have been tested by these investigators and they all conform to these observations*. Similarly, McAlevy et al(19) noted that "loose-granule" burners have about the same burning rate as composite propellants of equivalent composition, again suggesting the lack of significant interfacial reactions; the voids between the loose particles in such an analog burner provide ample opportunity for possible interfacial reactions to become important.

McAlevy and Hansel(79) found that passing gaseous Cl_2 or NO_2 through a porous bed of polystyrene accelerated the regression caused by rocket exhaust gas impinging on the surface of the porous sample. This, they claimed to be evidence of heterogeneous reaction at the fuel surface. No evidence was offered to rule out the more likely possibility

---

*The exception is Nadaud's(75) finding for the rate of penetration of the flame at the interface between a slab of AP and a slab of polyisobutylene(PIB): above 20 atm, this penetration rate is faster than the burning rate of an equivalent PIB-AP composite propellant. The above remarks with respect to the possible significance of interfacial reactions do not hold for this particular propellant composition.

of accelerated gas phase reaction in the pores of the fuel sample. To the author's knowledge, the only evidence that exists to suggest that heterogeneous reactions may be important, is Pearson and Sutton's(80) finding that perchloric acid vapor ignites more readily with a solid fuel surface than with fuel vapors in the range 200-300°C. (The more meaningful comparison, however, would be between the gas phase reaction at 2000°C and the surface reaction at 500-600°C). Such heterogeneous reactions can only be important in crevices around the AP particles. Hightower found no such crevices. The only possibility that remains is that the crevices exist during burning but are filled up during the extinguishment process, but this seems unlikely. We conclude that there is no positive evidence of the existence of energetic heterogeneous reactions. Moreover, at this stage, there appears to be no need to call upon such reactions to explain composite propellant burning rate behavior, as will be shown below.

As noted below, several investigators have proposed that solid phase reactions are an important factor in the burning process of a solid propellant. The proponents of these reactions seldom define the exact meaning of their solid phase reactions. A true solid phase reaction, i.e., a solid-to-solid transition, can not be of major importance in determining the burning rate of a solid propellant because the exothermicity of these reactions seldom amounts to more than a few tens of calories per gram, far less than the total heat of reaction of a solid propellant (around 1000 cal/gm). The existence of significant interfacial solid phase reactions (between the solid fuel and the solid oxidizer) can be discounted also, because the reaction would cease as soon as contact between the solid fuel and the solid oxidizer is broken; the reaction could not last very long.

It is conceivable that gas-phase interfacial reactions in the crevices between the solid fuel and the solid oxidizer (most likely, heterogeneous attack of the solid fuel by gaseous perchloric acid) could take over soon after the solid phase interfacial reactions came to an end. However, as noted before, Hightower(75) found no evidence of the crevices that must exist if these interfacial reactions are to be important.

The only reaction that could conceivably be highly exothermic and could occur below the "surface" of the propellant, is a solid-to-gas phase transition. Such a reaction could take place in a thin porous region below the propellant "surface"--porous, because gases are evolved, and thin, because solid material would otherwise be spewed off the propellant surface if the reaction took place too far below the surface; no evidence of such surface disruptions has yet been reported. It is clear that such a solid-to-gas phase reaction can not be responsible for all the heat generated by the propellant

because the rate of this reaction is independent of pressure (concentration of solid reactants is independent of pressure) whereas the rate of the overall burning process is clearly dependent on the pressure; the burning rate of solid propellant is dependent on pressure. Obviously then, other gas phase reactions must also play an important role in the burning process.

Wenograd and Waesche(81,82) claimed on the basis of differential scanning calorimetry measurements, a refined form of differential thermal analysis, that the heat generated during the decomposition of PBAA-AP propellant, considered as purely due to solid phase reactions, is sufficient to account for observed propellant burning rates at 1 atm. The effect of pressure on the burning rate of a propellant is rationalized on the grounds that pressure affects the surface temperature and that this, in turn, affects the burning rate(83); it is assumed that the gasification process at the regressing propellant surface follows an equilibrium vaporization law. It is to be noted that differential thermal analysis, or any of its refinements, measures only the total heat release and can not identify where this heat is being generated. Further, the results of Wenograd and Waesche, above, can be equally well interpreted by assuming that the gas phase $NH_3/HClO_4$ is a major source of heat; to insist that solid phase reactions are of overriding importance would be to deny the significance of this $NH_3/HClO_4$ reaction, an already well established fact.

The most convincing evidence to the effect that solid phase reactions may contribute a significant part of the total heat of reaction is Inami, et al's(84) finding that the heat release rate during AP decomposition in bulk does not change when the pressure is varied from 1 atm to 13.5 atm. This invariance with pressure indicates that the process was probably in the solid phase, or otherwise, that the rate of this process is determined by a zeroth order solid-to-gas phase step.

It is interesting that, when the slow low-temperature heat release rates reported in Refs. 81-85 are extrapolated to the high temperature of 800°K at the surface of a burning propellant (admittedly a long extrapolation), it turns out that almost the entire energy identified as solid phase heat release must occur within a relatively thin zone of about 2-3 microns below the regressing surface at normal regression rates. (The significance of the thinness of this layer is further discussed in the summary of Section IIA(vi).) Flanagan(86) calculated that the heat released within this first two microns below the AP surface, is not sufficient to affect the burning rate; the stay-time is too short (compared to the reaction time) for the solid phase reaction to be significant in its effect on the burning rate. Caveny and Pittman(87) came to the same conclusion. These latter investigators also found experimentally that whereas (prior)

irradiation or thermal shocking of the AP accelerates the low-temperature decomposition (DTA results) of AP, the same treatment has no effect on the burning rate of an AP propellant. Based on the assumption that solid phase reactions are important at low temperatures, as is more likely, these experimental observations imply that these same solid phase reactions are too slow (compared to the stay time) to be important in the burning process of a composite propellant.

(v) Structure of Regressing Propellant Surface

The physical state of the regressing propellant surface, i.e., whether it is dry or molten, and its scale of roughness, can have important implications with respect to the burning mechanism.

Bastress'(14) photographic surveys of extinguished polysulfide-AP propellants show that the AP particles protrude above the fuel surfaces during combustion at low pressures but that the opposite is true at high pressure. That the pyrolysing oxidizer and fuel surfaces must in general lie in different planes is in accord with the "two-temperature" postulate proposed by Schultz and Dekker(88). The implication of such surface roughness with respect to the burning mechanism is that there is a particle size and a pressure above which the flame as a whole cannot be considered one-dimensional (see Section IIA(vi) below). This consideration implies the existence of boundaries (in particle size and in pressure) to the domain of validity of a one-dimensional theory.

Searches for a liquid layer and its consequences have also been conducted. While Sutherland's(7) photographs show $KClO_4$ propellants to have a mobile liquid layer of molten $KClO_4$ and KCl on the regressing propellant surface, both his and Bastress' (14) studies indicate that the burning surfaces of polystyrene-AP and polysulfide-AP propellants are dry, or at least so little molten as to leave the surface geography rigid. With such a dry and rigid surface, the heterogeneity of the propellant surface is propagated unchanged into the issuing gas stream.

Hightower's(62,75,89) and Boggs'(90) recent photographic studies of pure AP and carboxyl terminated polybutadiene-AP propellant surfaces indicate that both the AP and fuel melt to some degree during burning. However, the AP melt is very thin, at the most a few microns, and it seems that in most circumstances the layer would be relatively immobile. The problem is to determine for what conditions the presence of the molten layer may be important. It appears (see Section IV) that most AP-based propellants with fuels such as polystyrene, polysulfide and polybutadiene acrylic acid can be considered to have at least an immobile surface if not a dry surface provided the AP content is high (equivalence ratio*, ψ_o above about 0.4) and provided the AP particles are of medium sizes (in the approximate range 40-200μ). However, when the fuel is of the type that melts readily (i.e., particular polyurethanes) or when the fuel content is high and the AP particle size is small, the melt becomes

mobile, the burning rate is affected, and in the extreme, abnormal burning in the form of temporary localized extinctions is the result; the phenomenon of extinction appears to be directly related to the propellant surface condition#.

(vi) Physical Picture of Burning Process

From the previous paragraphs, it is apparent that the most important source of energy in driving the flame in an AP-based composite solid propellant is conductive heat feedback from the A/PA and O/F gas phase reaction stages. The second stage, the O/F stage, occurs considerably further away from the regressing propellant surface at normal rocket pressures than the A/PA stage. The scale of unmixedness, as it affects the O/F flame, appears to be an important aspect of the burning process. There is considerable evidence against the existence of significant solid phase and/or heterogeneous reactions.

As shown from calculations in Section III, the A/PA reaction stage in the burning of a composite propellant at rocket pressures is so thin compared to the oxidizer particle size and the O/F flame thickness that it may be considered in the burning rate theory to occur right at the regressing propellant surface, merely depositing its heat there as gasification takes place; in the limit, it can be shown that it may be considered infinitely thin and thus without any contribution toward the pressure dependence of burning rate. (See also Section III concerning breakdown of this assumption at subatmospheric pressures.) The amount of energy deposited at the propellant surface by the exothermic A/PA stage is off-set in part by the amount of heat required to decompose and vaporize the fuel binder. Sabadell(91) inferred from his thermocouple traces that the net amount of heat liberated at the propellant surface is about 130 cal/gm of propellant. (His resolution was insufficient to resolve the details of the surface decomposition process). This figure is in good agreement with the earlier estimate(1) of 100 cal/gm, where the net heat of decomposition of AP and the heat needed for gasification of

---

*Equivalence ratio is defined here as the mass fraction of oxidizing species (O, Cl, F...) present in the propellant (oxidizer and fuel) divided by the mass of oxidizing species present in the same propellant mixed to stoichiometric proportions. The stoichiometric ratio is taken as that which leads to the products H_2O, CO_2, SO_2, HCl, and N_2.

#Boggs(90) observed that the burning rate behavior of pure AP changes when the structure of the surface (on microscopic scale) changes. He suggested that this surface decomposition process may be the cause of the observed reduction in burning rate with increased pressure (between 2000 and 4000 psia), in the case of pure AP. While this factor may be the cause of abnormal burning in AP-based composite propellants, the meltability of the binder must also be important, as will be shown in Section IV.

the fuel were both taken into account.

Powling(42,43) has made composite plots of all his burning rate-surface temperature-pressure data for several AP composite propellant systems and several porous AP-gaseous fuel systems. He found that the surface gasification process is better described by an unopposed surface decomposition law of the Arrhenius type (in which the activation energy is about 30kcal/mole) than by a simple Clausius-Clapeyron equilibrium law.*

The thickness of the A/PA gas phase reaction, the thickness of the AP melt, and the depth below the surface to which solid phase reactions could be important, are all of the order of one micron at normal rocket pressures. In this context, therefore, the exact definition of a decomposing surface is obscure; however, from the standpoint of the solid-to-gas boundary condition in the theory, it makes little difference whether the heat of decomposition is considered to be liberated in the gas phase immediately above the surface, exactly at the surface, or in a thin solid or liquid phase layer below the surface. So far, no evidence has been found that conflicts with the view that the heat of decomposition is deposited at the AP surface, in the normal rocket pressure range; the assumption appears to break down only at subatmospheric pressures where the A/PA stage becomes distended (Section III(B)).

To portray the overall propellant surface as planar is admittedly difficult. In accord with the "two-temperature" postulate, the fuel and AP surfaces must be staggered. Moreover, conditions can arise in which a molten fuel layer covers the AP particles and this can cause abnormal burning behavior in the form of localized extinctions. Nevertheless, it seems plausible that the irregular surface geometry would not upset the one-dimensionality if the dimensions of the irregularities are sufficiently small.

B. AP Composite Propellant Burning Rate Behavior and Solid Propellant Burning Rate Theories That Have Been Proposed

Based on the previous discussion it is now possible to build plausible models of propellant burning so that theories of propellant burning may be formulated. In the final evaluation of these theories, it is necessary that their burning rate predictions with respect to pressure, propellant composition,

*It is difficult to believe that a composite propellant could vaporize strictly according to an equilibrium law because then both the forward and reverse kinetic processes must be equally probable; the binder in a typical composite propellant is a large complicated molecule and so, it is highly unlikely that the exact reverse of the decomposition-gasification process could occur.

and oxidizer particle size, be compared with experimental burning rate determinations*. Many theories can be rejected on the basis of their qualitative burning rate predictions (or, because some physical fact known about the flame structure, is violated). Thus, before discussing the various theories that have been proposed, the burning rate behavior of typical AP composite solid propellants is briefly described. More discussion of earlier findings on the burning rate behavior and of the mechanisms responsible for this behavior is deferred to Sections III, IV, and V.

(i) Summary of AP Composite Propellant Burning Rate Behavior

A survey of all available burning rate data in the range 1-100 atm (see Section IIIC(ii) shows that whenever the AP loading is high (equivalence ratio $\psi_o \gtrsim 0.4$), the AP particles are larger than about 40μ, and the fuel is of the type that does not melt readily, the burning rate-pressure curves (plotted as (log r) vs. (log p)) are monotonic with steadily decreasing slope as pressure is increased; around 100 atm the pressure exponent (n in the empirical equation $r=ap^n$) is about 0.3 and near 1 atm it lies between 0.6 and 0.9 depending on the fuel type. The effect of increasing AP content and/or decreasing AP particle size for this class of propellants is merely to increase the burning rate at all pressure levels between 1 and 100 atm.

As will be shown in Section IV, abnormal burning behavior results when the AP particle size is reduced to below 40μ or when the AP content is reduced to below the value for which $\psi_o = 0.4$. Reduction of either of these two parameters produces first, pronounced plateau burning behavior (n = o), and then, upon further reduction, a region of negative slope in the burning rate-pressure dependence curve (called mesa burning); for the smallest values of these parameters, a pressure range ($\sim$ 20-100 atm) can be found in which steady self-sustained burning is not possible. As also shown in Section IV, substitution of a fuel that is readily meltable, causes the same pronounced tendency toward plateau burning etc., even for mixtures with high AP loading ($\psi_o > 0.4$) and large AP particles (> 40μ).

Section V shows that AP composite solid propellants generally follow the equation $r = ap^n$ in the subatmospheric pressure range. The pressure exponent falls between 0.6 and 0.9 depending on the propellant type. The lowest pressure at which a propellant can be made to burn is about 0.01 atm. This low pressure extinction limit is dependent on AP particle size and fuel type. The effect of reduced AP particle size is to increase burning rate at all pressures, even as low as 0.1 atm.

---

*Comparison between theory and experiment in terms of other propellant behavior variables such as surface temperature and flame thickness, is also highly desirable. However, these measurements are not so readily obtained with the accuracy needed to establish the validity of any theory.

A few studies of AP propellant burning rate behavior in the very high pressure range have been done. It is found(92-94) that above about 200 atm, the pressure exponent increases with increasing pressure; in the 300-1000 atm range, the pressure exponent is of the order 1.5-2.0. One study(92) showed the tendency for the burning rate to become independent of binder properties and AP particle size. Another study(93) showed that the burning rate curves of AP-polyurethane propellant and pure AP monopropellant fall very close to each other above about 200 atm. It is interesting that $KClO_4$ propellants which do not posses an exothermic gas-phase oxidizer decomposition flame(95), do not show the upward bend in the burning rate curve at these very high pressures; rather they bend downwards(92). These findings together with Bastress'(14) observation that the AP surface recedes below the fuel surface at high pressures, suggest that the AP decomposition flame has a controlling influence on the burning rate in the very high pressure range(93,96).

It is appropriate to mention that several attempts have been made to study the combustion mechanism of a composite propellant by so-called analog techniques. One method, the "loose-granule" burner which was first used by Burger and van Tiggelen(97,98) and which has since been actively employed by McAlevy et al (18,19,79), has been very successful in elucidating some aspects of the burning mechanism. This method involves the study of the burning behavior of a packed bed of solid oxidizer granules (or solid fuel granules) through which a predetermined amount of fuel gas (or oxidizer gas) is passed. The scale of granularity in this type of burner is of the same order as the size of the AP crystals typically used in a composite propellant. The results of studies with this analog burner are reported at various places throughout this document whenever these results are relevant to the discussion at hand.

Other analog burners that have been used involve large scale heterogeneity. These can only be used to provide an insight into the combustion mechanism of a composite propellant if their behavior is studied at a low enough pressure that the thickness of the gas phase flame is of the same order as the scale of heterogeneity (unmixedness), as is the case in a composite solid propellant. Unfortunately, various studies of the burning behavior of large ammonium perchlorate speres ($\sim$ 1 cm diameter)(41,99) and of thick ($\sim$ 1 cm) binder-ammonium perchlorate sandwiches(43,77, 78,100) have been carried out at very high pressure with very little attention being given to the scaling problem. Such results are of little use in interpreting the combustion mechanism of a composite propellant. The point should however be made that the flame at the interface between the solid fuel and solid AP of a binder-AP sandwich, on a microscopic scale, does represent the conditions at the interface between the solid binder surface and the solid AP surface of a composite propellant.

(ii) Theories of Solid Propellant Burning

In consideration of the above described findings concerning AP propellant flame structure and burning rate behavior, those theories that portray a diffusion flame structure with finite chemical reaction rates(1,27) would appear to be consistent, at least qualitatively, with the known facts. Those theories(101-103) that have been derived for homogeneous (double base) propellants are obviously not applicable to composite propellants. Other theories which consider solid phase reactions, heterogeneous reactions or the AP monopropellant flame to be rate-controlling, suffer from various objections detailed below.

The first of the diffusionally controlled models of propellant burning, the columnar diffusion flame model, was proposed by Rice(104) in 1945. Here the flame was assumed to occur at the interface between fuel and oxidizer streams pyrolysing off the regressing surface. Although the model gives the correct qualitative dependence of burning rate on oxidizer particle size, neglect of finite reaction times and the assumption of a columnar flame geometry combine to cause the burning rate to be insensitive to pressure. The latter prediction is contrary to experimental observations. A more refined form of the theory was developed by Nachbar(105-107) in 1957. The burning rate was calculated for a geometrically simplified model consisting of alternate slabs of fuel and oxidizer. Due also to neglect of finite gas phase kinetics, this theory suffers from the severe shortcoming of having burning rate independent of pressure.

It is clear that the assumption of infinitely fast reaction kinetics in a diffusion flame must break down at some low pressure and that this breakdown could be the cause of a steady increase in the value of the pressure exponent as pressure is reduced. Also, most practical AP propellants exhibit a pressure exponent of about 0.3 in the range 70-100 atm. (Plateau burning is caused by a phenomenon that is of unsteady nature and hence, cannot be predicted by any model of steady state burning.) With these considerations in mind, Summerfield proposed the granular diffusion flame model. In this model it was assumed that local unmixedness causes the fuel gases to leave the surface in pockets which burn up in an atmosphere of oxidizer decomposition products; it was assumed also that the average fuel vapor mass per pocket is independent of pressure. Based on the hypothesis that at low pressure the burning rate is chemical reaction rate controlled while it is diffusionally controlled at high pressure, the asymptotic forms for burning rate were obtained. The burning rate at intermediate pressure was then expressed in the simplest manner by joining these two asymptotic forms as follows: $1/r=a/p+b/p^{1/3}$. As will be shown in Section IIIC(ii), this equation is remarkably successful in correlating composite propellant burning rate data over wide ranges of pressure, AP particle size, and AP loading; it is the most successful of all burning rate equations that have been proposed to date. It will be shown below that modification of the theory is necessary in the very low pressure range (< 1 atm).

Based on similar reasoning to the above, von Elbe, et al(27) have recently incorporated finite chemical reaction times into the columnar diffusion flame theory. As will be shown in Section IIIC(ii), the proposed burning rate equation, $1/r=a/p+c$, does not fit AP propellant burning rate data under any circumstances.

Arguing that the surface temperature of ammonium nitrate must be considerably less than that of typical binders during steady burning ($\sim 600^{\circ}K$ compared to $\sim 1000^{\circ}K$ respectively), Andersen(108) surmised that the fuel-oxidizer gas-phase reaction might be too far from the oxidizer surface to affect its regression rate. This idea of a burning rate controlled solely by an exothermic oxidizer decomposition reaction is the essence of the thermal layer theory developed by Chaiken(109). Although the physical picture might be roughly valid for ammonium nitrate propellants (the evidence is meager), the prediction that burning rate is linearly dependent upon pressure and insensitive to fuel type and fuel-oxidant mixture ratio renders it invalid for AP propellants from 1 to 100 atm. Chaiken's later attempt(110) to fix these defects by allowing for a certain degree of reaction of the ammonia/perchloric acid gas with the fuel vapors necessitated the introduction of two variable mixing factors, the values of which were not derived from fundamental principles; they were artificially used merely to suggest the importance of reaction with fuel vapor in the burning process of AP propellants. No burning rate predictions are possible with this theory until quantitative expressions are found for these two factors, even if they exist.

The fact that the pressure exponent of AP propellants at high pressures (200 to 1000 atm) is of the order 1.5 to 2.0 was taken by Irwin, Salzman and Andersen(93) as the cue to suggest that small cracks may be formed in the surface of the oxidizer, causing the exposed oxidizer surface area to increase progressively with increasing pressure. Based on the observation that the burning rate is mainly determined by the oxidizer decomposition flame at these very high pressures (see previous section), the net effect of the increased exposed oxidizer surface would be to increase the burning rate and the pressure exponent. In a later publication(96), it was shown that thermal stresses induced by the steep temperature gradient in the solid phase at these high pressures, is the most likely cause of surface cracks propagating into the solid phase. The model has been put into analytical form and the resulting two-parameter burning rate equation fits the data. However, the test is not sensitive and so, the idea cannot be considered proved. In this regard, it is interesting that Hermance(111,112) suggested that it is the onset of turbulence in the previously laminar fuel-oxidant flame which is responsible for the transition to a high pressure exponent at high pressures (see below).

Other models of propellant burning, some of which have not been formulated mathematically, have also received attention in the literature. Hicks(113) suggested that, at least during

ignition, the burning process is driven by exothermic solid phase reactions. Wenograd and Waesche(81-93) reported on the basis of their differential scanning calorimetry measurements (a refinement of the differential thermal analysis (DTA) technique), that the heat generated during pure AP decomposition at 1 atm, presumed to be purely due to solid phase reactions, is roughly sufficient to account for observed burning rates at 1 atm. The pressure dependence of burning rate for a composite propellant is explained on the assumption that the surface vaporization process is an equilibrium process and that therefore, increasing pressure increases the surface temperature, thereby increasing the burning rate also. Because DTA measurements are a measure only of the total heat released and not necessarily that due to solid phase reactions alone, the results can be said to be only qualitatively consistent with the trends expected from the solid phase reaction model proposed by Wenograd(81).

Andersen and Brown(114,115) proposed that heterogeneous reaction between the gaseous oxidizer decomposition products and solid fuel at the oxidizer interfaces is rate-controlling. No diagnostic test data to support the idea were advanced and no burning rate equation has been derived for the model; so, it must be regarded as an untested hypothesis.

A more elaborate theory along the same lines has recently been proposed by Hermance(111,112). In this theory account is taken of fuel pyrolysis, AP decomposition, heterogeneous reaction at the fuel surface, and a chemical-diffusion fuel-oxidant flame. It is assumed that the exothermic gaseous $NH_3/HClO_4$ reaction is collapsed to the regressing propellant surface, regardless of the pressure level. Heterogeneous reaction between the gaseous $HClO_4$ and the solid fuel is presumed to occur in crevices around the exposed AP particles. The ensuing gas-phase fuel-oxidant flame is treated as a columnar diffusion flame in which both second order chemical kinetics and diffusional mixing rates play important roles. The possibility of transition to a turbulent fuel-oxidant flame is allowed for. (This latter feature permits the theory to predict the high pressure exponents ($n \approx 1.75$) that have been observed in the 200-1000 atm range). The theory is involved, has many component elements, and its predictions are sensitive to the values of parameters chosen. The predictions can be made to fit the selected composite propellant burning rate data. Such fitting was done even for the burning rate curves of underoxidized propellants whose behavior is known by direct observation to be dependent on a phenomenon of unsteady nature described below (Section IV), the essential features of which are not incorporated into the model. The point is emphasized by the observation that whereas this unsteady phenomenon can explain both mesa and plateau burning behavior, the theory of Hermance can fit only plateau burning propellants; no mechanism has been included that will allow the theory to predict negative

exponents. At this stage, the values of parameters needed for the theory are not known accurately enough to test the validity of the solutions.

Recently, Fenn(116) proposed what he calls a "phalanx" flame model. Here, the burning process for a composite propellant is imagined to be driven by a gas-phase fuel-oxidant flame that is situated directly above the interface between the solid fuel surface and the solid oxidizer surface. Heat arrives at the regressing surface by conductive heat feedback through the gas phase and it is assumed that the flame stand-off distance is governed by a combination of chemical reaction rate, diffusional mixing rate, and quench distance; it is assumed that the relatively cold propellant surface quenches the flame. The burning rate equation derived, $1/r = A/p+Br/p^{n/2}$, was found to fit the burning rate data of Webb(120) as well as does the GDF equation (above) provided the loose parameter n is chosen to be 1.33. This particular value chosen for a best fit to the data, is not consistent with the theoretical development because the reaction order in the expression used for the quench distance, differs from the value assumed for the reaction order in the chemical reaction rate expression, namely 2.0. The latter is implied by the term A/p in the above equation. Another, less severe, criticism of the theory is that Hightower's observations of the fuel-oxidizer interfacial region(75) tend to deny the existence of crevices at these interfaces, a prerequisite for the model. It is not too surprising that Fenn's equation fits Webb's data as well as the GDF equation when n = 1.33, because in this circumstance, both equations display the same low pressure and high pressure asymptotic behavior (pressure exponents of 1.0 and 0.33 at low and high pressure, respectively).

Based on his survey of the literature, Powling(42) described AP-based propellants to burn with two gas phase reaction stages, the first, a premixed reaction between the sublimed NH_3 and $HClO_4$ and the second, an unmixed reaction between the pyrolysed fuel vapors and the combustion products of the first stage. Diffusional mixing plays an important role in the second flame stage. At very high pressures (above about 70 atm), he considers the $NH_3/HClO_4$ reaction zone to be confined very close to the surface of the regressing AP crystal. The effect of fuel type on the burning rate of AP-based propellants at these pressures is explained by the existence of a fuel/oxidizer diffusion flame at the binder/oxidizer boundaries, as in the phalanx flame model above. At low pressures (subatmospheric), he considers the two stages of the flame to merge forming a single premixed $NH_3/HClO_4$/fuel-vapor stage. This representation would explain why most propellants have a pressure exponent near unity at subatmospheric pressures but does not account for the observed persistence of particle

size effects at pressures as low as 0.1 atm.* These ideas have not been put into mathematical form for testing with propellant burning rate data. The possibility that the $NH_3/HClO_4$ reaction zone becomes distended at some low pressure is interesting and will be investigated in the next section.

Spalding(103) has developed a theory for the burning behavior of homogeneous propellants. Although the theory is obviously not applicable to AP composite propellants and probably not applicable to the common homogeneous propellants based on nitrocellulose (whose flame structures are obviously complex), it is of interest to note that he showed that low pressure extinction could be caused by radiative heat loss to the surroundings from the hot regressing propellant surface. Johnson and Nachbar(58) have also included this radiative heat loss term into their theory for pure AP monopropellant burning but found that the amount of heat lost is insufficient to account for the observed extinction behavior. The possibility that this mode of heat loss may be the cause of extinction at low pressures for composite solid propellants, has not yet been investigated. This possibility will be investigated in the next section.

From the above discussion it is concluded that, of all theories that have been proposed in the literature to date, only the columnar diffusion flame theory and the granular diffusion flame theory are consistent, qualitatively at least, with all that is known about the flame structure. (The heterogeneous reaction theory of Hermance can not be ruled out on the same grounds but it appears to be unnecessarily complex, incorporating processes that have not been proved to exist). The validity of either the granular diffusion flame model or the columnar diffusion flame model and the burning rate equations derived for them can be assessed by systematic comparison of the burning rate predictions with experimental burning rate data. Such comparisons will be made in the next section. The ideas propounded by Powling(42), that the $NH_3/HClO_4$ reaction stage could become distended at low pressures, and by Spalding (103), that radiative heat loss from the burning propellant surface could be significant at low pressures, will be analysed on theoretical grounds in the next section also.

*The persistence of oxidizer particle size effects on the burning rate down to pressures as low as 0.1 atm can be attributed to particle size dependent subsurface reactions and/or a gas phase flame that is not purely chemical reaction rate controlled, i.e., diffusion mixing processes still have effect at these low pressures. Further discussion of this matter is deferred to sections V and VI of this document.

SECTION III

THE GRANULAR DIFFUSION FLAME THEORY

In the original 1960 formulation(1) of the granular diffusion flame (GDF) theory, the pre-mixed ammonia-perchloric acid (A/PA) reaction zone was considered so thin compared to the overall temperature profile established by the oxidant-fuel (O/F) flame that it was identified as occurring entirely at the regressing propellant surface. The resulting burning rate equation was very successful in describing AP composite propellant burning rate behavior in the 1-100 atm range(3,4). However, as will be shown later, it breaks down at subatmospheric pressures.

Because the A/PA reaction rate is pressure sensitive, and because the thickness of the A/PA zone thus increases with reduction in pressure, the assumption that it is effectively collapsed must become invalid at some low pressure. Consequently, if the validity of the granular diffusion flame model is to be extended to very low pressures, the distributed nature of this reaction must be recognized. The model then possesses two gas phase reaction stages, the second stage, the fuel oxidation stage, still retaining its originally proposed character of a granular diffusion flame. A further modification of the theory lies in the observation that low pressure burning rate behavior is critically dependent on the sensitivity of pyrolysis rate (i.e., burning rate) to surface temperature. Therefore, variation of surface temperature with pressure must now be allowed for. Finally, since radiative heat loss from the burning propellant surface could be important, a term accounting for this form of heat loss, must be included.

In the sections below, the complete two-stage GDF model is described. The collapsed A/PA-GDF theory is then derived and its range of validity determined on the basis of all available AP composite propellant burning rate data in the range 1-100 atm. Finally, the complete (distended A/PA stage) GDF theory is derived and its implications with respect to AP propellant burning is discussed. The purpose of developing the complete two-stage granular diffusion flame theory is first, to extend the validity of the theory to very low pressures and second, to check a posteriori the validity of assuming an infinitely fast A/PA reaction in the 1-100 atm range.

A. Physico-Chemical Model

In constructing the granular diffusion flame model, it is assumed that the gasification process at the solid regressing surface is driven by conductive heat feedback from a two-stage flame occurring in the gas phase (see Fig. 1). This solid-to-gas step is generally endothermic for both the fuel and oxidizer

constituents. In the case of ammonium perchlorate, this step is the dissociative sublimation step yielding hot gaseous ammonia and perchloric acid. (See previous section.) The ammonia and perchloric acid become the reactants for a vigorous pre-mixed exothermic gas phase reaction occurring very close to the surface of the AP crystal (less than one micron at normal rocket pressures). The products of this reaction which are rich in oxygen and oxygen-containing compounds, now serve as a reactant in the ensuing fuel-oxidant gas-phase reaction which extends much further from the regressing propellant surface (about 20 micron at normal rocket pressures). Up to this point, the beginning of the O/F flame, the pyrolysed fuel gases are considered dispersed in the oxidant stream but still unmixed (pockets). In the one-dimensional energy equation written below, the fuel vapor plays the role of a diluent in this first stage. Since a composite propellant is of heterogeneous nature and the fuel and oxidizer gases therefore are unmixed when they emerge from the propellant surface, both the rates of diffusional mixing and chemical reaction determine the overall reaction rate of the fuel-oxidant redox reaction. In the granular diffusion flame model it is presumed that the fuel enters this flame zone in the form of tiny gas pockets and that the mass of these pockets is independent of pressure. These pockets burn up in an atmosphere of oxidizer decomposition products. Composite propellant burning is thus viewed as a three-step process in which the endothermic solid-to-gas phase step, the exothermic premixed $NH_3/HClO_4$ reaction, and exothermic fuel-oxidant reaction occur sequentially; the diffusional mixing and chemical reaction processes in the O/F flame zone occur simultaneously.

The granular diffusion flame is a one-dimensional model in which it is assumed that the A/PA and O/F reaction zones are planar and parallel to the regressing propellant surface. One-dimensionality can be assumed provided the depth of the thermal wave L_s in the solid phase and the O/F flame thickness L_{II} are large compared to the effective roughness dimension of the regressing propellant surface. The roughness scale of the surface is not known accurately but based on Bastress'(14) photographic study which shows the surface to be relatively smooth at normal rocket pressures, it could be of the order of 10 micron. (This figure will vary with particle size). On the assumption that this figure is correct, calculation of the pressure dependence of L_{II} and L_s (see Fig. 11) shows that the assumption of one-dimensionality will break down only when the pressure exceeds about 100 atm. It is recognized that at high pressures especially, the A/PA flame hugs the exposed AP crystal, leaving the fuel surface exposed only to the O/F flame. However, we can still represent this zone as a planar wave provided the temperature T_1, at the point of completion of the A/PA reaction, is obtained from mass flux average enthalpy, including both the gases in the A/PA reaction zone and the as yet unreacted fuel vapors. If we define T_1 this way, then by definition the enthalpy term in the 1-D energy equation is

satisfied. The same is true for the choice of the average surface temperature T_s. (The average T_1 and the average T_s selected to satisfy the one-dimensional energy equation may differ appreciably from the physically measured average values). Finally, in the energy equation there are one-dimensional heat conduction terms for the solid phase and for the O/F flame. We assume that the microscopic three-dimensional heat flow processes serve to smooth out the temperature profile so as to validate these one-dimensional heat conduction terms.

The assumption that the propellant flame is steady, is difficult to justify on fundamental grounds because, at any one point in the gas phase flame, the mixture ratio changes drastically every time an AP particle near that point burns out at the propellant surface. However, it is reasonable to expect that the flame of a composite propellant that has a large enough burning surface area (compared to the cross-sectional area of an AP particle), will behave steadily on a macroscopic scale and on a large time scale (compared to the transit time of the burning surface through an AP particle), because in the usual composite propellant, the scale of heterogeneity (particle size) is comparable to, or smaller than the characteristic dimension of the propellant flame (flame thickness); also, in the normally-used composite propellant, the transit time of the propellant surface through a solid oxidizer particle is much larger than the transit time through the layer of binder separating two successive oxidizer particles. This assumption, that the flame of a composite propellant behaves steadily, will become invalid when the oxidizer particles are large. However, it is likely that the assumption of one-dimensionality will break down for even smaller particle sizes.

In the treatment of the complete granular diffusion flame model it is assumed that the A/PA and O/F stages are independent of each other as far as their respective responses to pressure are concerned. In particular, their individual behaviors can be extrapolated to low pressure where the role of the A/PA flame becomes interesting. Their responses are inter-related, however, by virtue of the fact that energy is transferred across the boundary from the O/F flame to the A/PA flame. There is no evidence to suggest that perchloric acid vapor reacts faster with gaseous ammonia than with the gaseous pyrolysis products of the binder. (This evidence is necessary to justify such separate treatment of the O/F and A/PA flame stages.) In fact, Powling(42) suggested earlier that when the pressure is lowered, the A/PA stage becomes more distended, finally merging with the O/F flame. Thus, the exact nature of the gas phase flame zone(s) will remain open to question for the low(sub-atmospheric)pressure range until such time as the pertinent kinetic rate data have been obtained*. Certainly, however, it is valid to treat the

*The kinetic rate data of a premixed $HClO_4/NH_3$/hydrocarbon reaction would also have to be obtained before quantitative predictions are possible with Powling's model.

A/PA stage and the O/F stage as distinctly separate flame zones in the normal rocket pressure range because here, the thickness of the A/PA stage is much smaller than the size of the AP particle (1μ compared to 10-200μ); the physical situation does not give the perchloric acid vapor the chance to react with the binder pyrolysis products, except perhaps at the fringes of the exposed surfaces of the AP particles (where the AP particle surface and the binder surface meet), even if the $HClO_4$ were more reactive with the binder pyrolysis products than with the NH_3.

The granular diffusion flame theory postulates the existence of fuel pockets in the gas phase fuel-oxidant flame and also assumes that the mass of these fuel pockets is independent of pressure but increases with increasing oxidizer particle size. As indicated in Section II, various studies have shown the burning surface of a composite to be highly irregular, on a microscopic scale. Such surface irregularities, together with the fact that the fuel and oxidizer gases have different densities, could introduce sufficient disturbance at the propellant surface to periodically disrupt the vaporization of the fuel gases and in so doing, create fuel pockets which burn up in the surrounding atmosphere of oxygen-rich gases. These pockets would be irregular in shape but could be represented as effectively spherical in the theory.

It is logical to expect that the size of these fuel pockets would increase with increasing oxidizer particle size, because in a composite propellant, the oxidizer particle size and the size of the fuel interstice between the oxidizer particles are directly related; a larger exposed binder surface area is expected to generate larger fuel pockets. The assumption that the mass of each fuel pocket remains independent of pressure can be justified only on the basis that if this assumption is made, the burning rate equation resulting from the theory agrees well with the measured rate data of a wide range of practical rocket propellants (see later). A further point in defence of the existence of gaseous fuel pockets in the O/F flame of an AP composite propellant is that if the fuel and oxidizer gases are assumed to stream uniformly off the burning surface of the propellant (i.e., the columnar diffusion flame model), the resulting burning rate equation does not fit measured burning rate data under any circumstances (see also later). However, it is emphasized that, despite all these previous arguments, the question of the existence of fuel pockets still remains but a postulate upon which the GDF theory is based.

B. General Equations for a Three-Stage Flame Model

The complete three-stage model depicted in Fig. 1 can be solved by setting up integrated steady-state 1-D energy equations for various stations in the flame zone viz., in the solid just below the surface, in the gas just above the surface, at the point of completion of the $NH_3/HClO_4$ reaction, and at the point of completion of the fuel-oxidant reaction. In these

equations, the reference state will be considered as the energy of the unburned solid at the initial temperature T_o. A term accounting for radiation from the hot propellant surface to the surroundings is included. Simple calculation has shown that, provided no free carbon or other radiating solid particles are present in large amounts in the flame zone, radiation from the gas-phase flame is negligible by comparison.

With reference to Fig. 1 and the list of symbols at the end of the text, the intergrated energy equations are:

$$0 = \rho_c r \left[c_c(T_s - T_o) + \Delta h_{tr}\right] + \epsilon\sigma T_s^4 - \lambda_c \frac{dT}{dx}\Big|_{s,c} \tag{1}$$

$$= \rho_c r \left[c_g(T_s - T_o) + \Delta h_{tr} + \Delta h_s\right] + \epsilon\sigma T_s^4 - \lambda_g \frac{dT}{dx}\Big|_{s,g} \tag{2}$$

$$= \rho_c r \left[c_g(T_1 - T_o) + \Delta h_{tr} + \Delta h_s + \Delta h_I\right] + \epsilon\sigma T_s^4 - \lambda_g \frac{dT}{dx}\Big|_{1,g} \tag{3}$$

$$= \rho_c r \left[c_g(T_2 - T_o) + \Delta h_{tr} + \Delta h_s + \Delta h_I + \Delta h_{II}\right] + \epsilon\sigma T_s^4 - \lambda_g \frac{dT}{dx}\Big|_{2,g} \tag{4}$$

where r satisfies the Arrhenius expression for pyrolysis reaction, i.e.,

$$r = A \exp\left(-E_s/RT_s\right) \tag{5}$$

Upon introduction of the Mallard-le Chatelier approximation(Ref.117) that all temperature gradients in the gas phase are linear, and upon recognition of the fact that the temperature gradient is zero when the final flame temperature T_2 is reached, these energy equations reduce to:

$$0 = \rho_c r \left[c_c(T_s - T_o) + \Delta h_{tr}\right] + \epsilon\sigma T_s^4 - \lambda_c \frac{dT}{dx}\Big|_{s,c} \tag{1a}$$

$$= \rho_c r \left[c_g(T_s - T_o) + \Delta h_{tr} + \Delta h_s\right] + \epsilon\sigma T_s^4 - \lambda_g \left(\frac{T_1 - T_s}{L_I}\right) \tag{2a}$$

$$= \rho_c r \left[c_g(T_1 - T_o) + \Delta h_{tr} + \Delta h_s + \Delta h_I\right] + \epsilon\sigma T_s^4 - \lambda_g \left(\frac{T_2 - T_1}{L_{II}}\right) \tag{3a}$$

$$= \rho_c r \left[c_g(T_2 - T_o) + \Delta h_{tr} + \Delta h_s + \Delta h_I + \Delta h_{II}\right] + \epsilon\sigma T_s^4 \tag{4a}$$

$$\approx \rho_c r \left[c_g(T_{2(ad)} - T_o)\right] + \epsilon\sigma T_s^4 \tag{4b}$$

These equations can be solved simultaneously provided expressions for L_I and L_{II} can be inserted. In general, the flame zone thickness L and the reaction time τ are related by:

$$L = (\rho_c r / \rho_g)\tau \qquad (6)$$

Thus a quantitative estimate of the pressure dependence of τ_I and τ_{II} is needed. Such estimates require detailed assumptions concerning the structure of the two gaseous reaction stages.

In the sections below, τ_{II} is determined by specifying a granular diffusion (O/F) flame structure. Two cases of the granular diffusion flame theory are treated:

(a) The A/PA stage is effectively collapsed to the regressing propellant surface ($\tau_I = o$).

(b) The A/PA stage is distended and is governed by a premixed second order chemical reaction ($\tau_I \sim p^{-1}$).

C. GDF Theory With Collapsed A/PA Flame

(i) Theoretical Treatment of Collapsed A/PA-GDF Model

For this restricted case of the GDF theory, the heat of reaction of the AP-monopropellant flame is considered deposited at the regressing propellant surface. The pressure dependency of the burning rate then comes about only by virtue of the fact that the O/F chemical-diffusion flame reaction rate is pressure dependent. The relative roles played by diffusional mixing and chemical reaction in determining the rate of the O/F flame are difficult to analyze. Consequently, as was done in the original formulation(1), expressions will be derived for burning rate in the extremes of low pressure and high pressure where chemical reaction and diffusional mixing rates respectively, are known to be controlling; the burning rate at intermediate pressure is then taken as the simplest empirical formula which has these high and low pressure asymptotes and which has been found to fit experimental burning rate data best over the range 1-100 atm.

As in Ref. 1 for a second order gas phase reaction where the prevailing pressure is sufficiently low for the O/F flame (zone II of Fig. 1) to be chemical reaction rate-controlled (high diffusional mixing rate), the chemical mass conversion rate in a zone of length $L_{II,ch}$ at temperature T_g may be expressed as:

$$\rho_c r_{ch} = L_{II,ch}\, \mathcal{B}\, \rho_g^2 \exp(-E_2/RT_2) \qquad (7)$$

Assuming as an approximation that the effective gas temperature is close to the flame temperature i.e., $T_2 = T_g$, then

use of the perfect gas law simplifies the expression of $L_{II,ch}$ to:

$$L_{II,ch} = \alpha^2 \left(\rho_c r_{ch} T_2^2 / P^2 \right) \exp\left(E_2 / R T_2 \right) \qquad (8)$$

where α = constant

An implicit relationship for the burning rate at low pressure may now be found by substitution of $L_{II,ch}$ from Equation (8) for L_{II} in the heat balance equation (3a). Inherent to this step is the assumption that the pyrolysed fuel and oxidizer gases start to react immediately upon leaving the propellant surface. When it is noted that $T_1 = T_s$ in the case where the first gaseous reaction stage is very fast (implied by Equation (2a) when $\tau_I = 0$), burning rate at low pressure where it is chemical reaction rate controlled, can be written as:

$$\frac{1}{r_{ch}} = \alpha \sqrt{\frac{\left[c_g (T_s - T_o) + \Delta h_{t,r} + \Delta h_s + \Delta h_I + \frac{\epsilon \sigma T_s^4}{\rho_c r_{ch}} \right]}{\lambda_g (T_2 - T_s)}} \left(\frac{\rho_c T_2}{P} \right) \exp\left(\frac{E_2}{2 R T_2} \right) \qquad (9)$$

Again, as in Ref. 1, the burning rate at high pressure where it is diffusionally controlled, may be found. It is assumed that the mass μ of each of the fuel gas pockets, of effective diameter d_g, is independent of pressure but still directly related to the mean size of the solid oxidizer crystals d_m, through the size of the solid fuel elements between the crystals. Thus,

$$\mu = f(d) \sim \rho_g d_g^3 \qquad (10)$$

It is expected that the functional relationship $f(d)$ and hence μ, increases with the increasing oxidizer particle size d_m.

The overall flame thickness of the fuel-oxidant stage may be obtained from the average gas velocity V_{II} and the fuel pocket life time $\tau_{II,f}$, which is determined by the rate of supply of both fuel and oxidizer gases to the flame front enveloping each of the fuel pockets, i.e.,

$$L_{II,dif} = V_{II} \tau_{II,dif}$$

$$\sim \left(\frac{r_{dif} \rho_c}{\rho_g} \right) \left(\frac{d_g^2}{D_g} \right) \sim \left(\frac{r_{dif} \rho_c \mu^{2/3}}{\rho_2^{5/3} D_g} \right) \qquad (11)$$

While chemical reaction rates were identified with T_2 in the previous case, it would be more reasonable to identify diffusion

rate with T_s here. Thus use of the perfect gas law and the empirical relationship(Ref. 118):

$$\mathcal{D}_g \sim (T_g^{7/4}/p) \sim (T_s^{7/4}/p)$$

yields

$$L_{II,dif} = \beta(d) \frac{\rho_c r_{dif} T_2^{5/3}}{T_s^{7/4} p^{2/3}} \qquad (12)$$

where $\beta(d)$ is some constant, incorporating f(d).

Again, when it is noted that $T_1 = T_s$, substitution of $L_{II,dif}$ for L in the heat balance equation gives the asymptotic value for burning rate at high pressures:

$$\frac{1}{r_{dif}} = \beta(d)\left(\frac{\rho_c T_2^{5/6}}{p^{1/3} T_s^{7/8}}\right)\sqrt{\frac{\left[c_g(T_s-T_o)+\Delta h_{tr}+\Delta h_s+\Delta h_I+\frac{\epsilon\sigma T_s^4}{\rho_c r_{dif}}\right]}{\lambda_g(T_2-T_s)}} \qquad (13)$$

With these two asymptotic forms for burning rate, the burning rate at intermediate pressure can be expressed by some relation which reduces to these forms at the extremes of pressure. Many relations are possible, but the relation, $1/r=1/r_{ch}+1/r_{dif}$, originally proposed, has been very successful to date and has the appeal of simplicity. Thus:

$$\frac{1}{r} = \rho_c\sqrt{\frac{\left[c_g(T_s-T_o)+\Delta h_{tr}+\Delta h_s+\Delta h_I+\frac{\epsilon\sigma T_s^4}{\rho_c r}\right]}{\lambda_g(T_2-T_s)}}\left\{\frac{\alpha T_2}{p}\exp\left(\frac{E_2}{2RT_2}\right)+\frac{\beta(d)T_2^{5/6}}{p^{1/3}T_s^{7/8}}\right\} \qquad (14)$$

It is worth noting that considering T_s constant and radiative heat loss negligible reduces this equation to the earlier burning rate equation,

$$\frac{1}{r} = \frac{a}{p} + \frac{b(d)}{p^{1/3}} \qquad (15)$$

where a = chemical reaction time parameter

b = diffusion time parameter

The numerical values of a and b can be evaluated by fitting Equation (15) to experimental burning rate curves. Because Equation (14) and (15) display the same behavior in the range 1-100 atm (see below and Section IIID), α and β can be evaluated from a and b using a measured surface temperature at a particular pressure.

An implicit relationship between T_s and p can be found by substituting Equation (5) into Equations (14) and (4b):

$$\frac{\exp\left(\frac{E_s}{RT_s}\right)}{\rho_c A} = \sqrt{\frac{\left[c_g(T_s-T_o)+\Delta h_{fr}+\Delta h_s+\Delta h_I+\frac{\epsilon\sigma T_s^4}{\rho_c A}\exp\left(\frac{E_s}{RT_s}\right)\right]}{\lambda_g(T_2-T_s)}}\left\{\frac{\alpha T_2}{P}\exp\left(\frac{E_2}{2RT_2}\right)+\frac{\beta(d)T_2^{5/6}}{P^{1/3}T_s^{7/8}}\right\} \tag{16}$$

where

$$T_2 = T_{2(ad)} - \left[\epsilon\sigma T_s^4 \exp\left(E_s/RT_s\right)\right]\Big/\left(\rho_c c_g A\right) \tag{17}$$

The pressure dependence of burning rate for the collapsed A/PA-GDF model can now be obtained by solving Equation (16) for T_s (by trial and error) at every p and then inserting these values into Equation (14). These calculations have been performed*. The predictions are shown in Figs. 8, 9, 10, and 11, together with the predictions of the distended A/PA-GDF model. Discussion of these predictions is deferred to Section IIIE (after the complete two-stage GDF theory has been treated in Section IIID). What is of interest now, however, is that the burning rate-pressure predictions of the collapsed A/PA-GDF model behave in the same way as Equation (15) above about 1 atm; the predictions of the collapsed model and of Equation (15) fall on straight lines when plotted as (p/r) vs. $(p^{2/3})$ (see Fig. 8). Thus, the simplified burning rate Equation (15) proposed by Summerfield(Ref.1) is a good representation of the collapsed GDF model above 1 atm.

Equation (15) has been tested with a wide variety of AP composite solid propellants and has been found remarkably successful over the range 1-100 atm (to be shown below). Later, Penner(Ref. 119) contested this by proposing the same equation in slightly altered form; it was claimed by Ref. 119 that this alternate equation was equally good:

$$\left(\frac{1}{r}\right)^2 = \left(\frac{a}{p}\right)^2 + \left(\frac{b}{p^{1/3}}\right)^2 \tag{18}$$

*The numerical values assumed as typical for the physical constants are listed in Appendix A. The numerical values of the predictions for the collapsed A/PA-GDF model appear in Tables II(A) and II(B) of the same Appendix.

where a and b are the same parameters as in Equation (15), also representing the O/F flame chemical reaction and diffusional mixing times, respectively. In Ref. 119 the similarity of Equations (15) and (18) was obscured because (18) was presented in an algebraically altered form:

$$\frac{1}{r} = \frac{P^{1/2}}{\sqrt{a'/P + b' P^{1/3}}} \qquad (18a)$$

where $a' = a^2$ and $b' = b^2$.

Actually, Equation (18) was discussed four years before Ref.(120) in the Princeton thesis of M. J. Webb as a trial equation combining the high and low pressure burning rate asymptotes differently, according to: $(1/r)^2=(1/r_{ch})^2+(1/r_{diff})^2$. The resulting burning rate Equation (18) was found unsatisfactory.

The validity of either of Equations (17) or (18) can be established by systematically testing the fit obtained by each equation to all the available composite propellant r-p data. For the purpose of this comparison it is noted that these two equations are identical when the ratio (a/b) is zero or infinite; therefore, the predictions ought to be equally good for very coarse or very fine propellants. The greatest distinction between these equations in the 1-100 atm range will be for propellants with intermediate values of (a/b), i.e., moderate particle size. It can be shown that with (a/b) around 28 $(psia)^{2/3}$ the difference between the two equations is greatest; these propellants are the ones to use for the test.

At this point, it is noted that simply on the basis of flame structure observations, the columnar diffusion flame theory as modified in Ref. 27 is equally credible. The way to test its validity is to determine just as for Equations (15) and (18) whether the derived burning rate equation fits the available composite propellant r-p data. The relation proposed (using the same reasoning above for the GDF relation), is:

$$\left(\frac{1}{r}\right) = \left(\frac{a}{P}\right) + (c) \qquad (19)$$

where again, a and c are constants representing the chemical reaction rate and the diffusional mixing rate, respectively.

(ii) Comparison of Diffusion Theory Burning Rate Equations With Burning Rate-Pressure Data

Many systematic studies(1-4,7,14-17,120-126) of the effects of variables such as AP particle size, AP content, and fuel type on the burning rate behavior of composite solid propellants have been made. Aluminized propellants are not included in this survey; the specific role of added aluminum is deferred to the last section. A summary of all the available AP-propellant burning rate data (including new results to be discussed later) is

presented in Table III of the Appendix B. (Data obtained by various manufacturers are not included in Table III because they seldom span more than a five-fold factor in pressure; a factor of about one hundred-fold is needed to determine the validity of any burning rate equation.) The results of comparing Equations (15), (18) and (19) with all of these data are also included in the table.

The agreement (or lack of agreement) with the data was determined by plotting the data as (p/r) vs. $(p^{2/3})$, $(p/r)^2$ vs. $(p^{2/3})^2$, and (p/r) vs. (p). As seen from Equations (15), (18) and (19), rewritten in the form,

$$(p/r) = a + bp^{2/3} \tag{15c}$$

$$(p/r)^2 = a^2 + (bp^{2/3})^2 \tag{18c}$$

$$(p/r) = a + cp \tag{19c}$$

respectively, the data must fall on a straight line when plotted in this way, if the particular burning rate equation is to be valid. The burning rate data of all propellants included in Table III have been plotted in these three ways* and are shown in Figs. B-1 to B-59 of Appendix B. These figures include plots of (log r) vs. (log p) for the same propellants.

Careful scrutiny of the data in Table III(A) (see also notes at bottom of this page) shows that the granular diffusion flame equation, Equation (15), fits the burning rate data whenever the AP loading is high and the AP particles are of intermediate size. Typical of the fits obtained with the GDF theory are those shown in Fig. 2. Apparently AP content and AP particle size are interrelated in defining the boundary of validity of the GDF theory. Since different fuels are involved, the definition of a validity boundary would be more meaningful if done in terms of equivalence ratio φ_o, and the mean particle size d_m. Figure 3 shows the range of validity of the GDF theory,

---

*The exception is when the burning rate data obviously would not fit either of Equations (15), (18), and (19), i.e., when the (log r) vs. (log p) curve is not monotonic or when its slope is negative at any point.

NOTES:

(1) All fuels are here designated according to their major constituents; thus, PBHT/TDI denotes hydroxyl terminated polybutadiene prepolymer polymerized with 2, 4 toluene diisocyanate.

(2) The exact formulation of each fuel is given in Table IV of Appendix B. The data required for calculation of equivalence ratio (defined in footnote on Page 15) are also included in Table IV.

(3) A list of abbreviations for chemical names appears at the end of the text.

defined in this way, for the 81 different propellants of Table III(A), i.e., unimodal and bimodal* AP-based propellants with P13, LP3/GMF, EPON/TETA, PBAA/EPON, PBAN/MAPO, PBHT/TDI, PVC/DBS or NC/TEGDN fuel. As shown later, these fuels are of the type that do not melt readily. According to Fig. 3, the range of validity of the GDF theory for propellants with these fuels is: $\psi_o \gtrsim (0.58-0.10 \log_{10} d_m)$ and $d_m \lesssim 250\mu$ where d_m is in microns.

Table III(A) shows that the region of small ψ_o and small d_m in Fig. 3 is one of abnormal burning that shows up as plateau burning, mesa burning and extinguishment in the normal rocket pressure range. Discussion of studies of this behavior and also how similar behavior may be produced with some highly oxidized AP-propellants, is deferred to Section IV. The upper limit of validity of the GDF theory with respect to d_m ($\sim 250\mu$) has been estimated on the basis of two propellants that did not fit the theory. This boundary is ill-defined but it is reasonable, since it is logical to expect that there is some particle size above which the assumption of a one-dimensional flame in the GDF theory must break down.

Comparison of the fits obtained by Equations (15) and (18) (see Table III(A) and Figs. 3 and 4) shows that both equations fit the data of propellants within the above-defined range of validity (i.e., large ψ_o and medium d_m) equally well, as long as the ratio (a/b) is less than about 10 $(psia)^{2/3}$. However, only Equation (15) applies when (a/b) approaches 30 $(psia)^{2/3}$, the value for which the distinction between Equations (15) and (18) is greatest. These points are illustrated by Fig. 4 which shows the data of Fig. 3 replotted as $(p/r)^2$ vs. $(p^{2/3})^2$.

Finally, Table III(A) shows that of the 81 propellants tested, only two or perhaps three, are fitted by Equation (19). This is purely coincidental. The inability of Equation (19) to correlate the burning rate data of the propellants in Figs. 3 and 4 is demonstrated in Fig. 5.

Thus, the burning rate correlation proposed for the columnar diffusion flame model is not valid. Of the equations proposed for the GDF model, that originally proposed by Summerfield(1) (Eq. 15) is preferable. Webb(120) also arrived at the latter conclusion, though he did not have access to as much data at that time as is presently available. The Summerfield relation fits all those propellants with high

---

*In bimodal AP distributions, d_m is here defined as:

$$d_m = y_l d_l + (1 - y_l) d_s$$

where y_l = mass fraction of AP particles with mean diameter d_l
d_l = mean diameter of large AP particle size distribution
d_s = mean diameter of small AP particle size distribution

AP-content, medium-sized AP particles and fuels that fall into the class that do not melt and flow easily. The only data in the literature known to us which does not conform to the predictions of the GDF model are those of Adams, Newman and Robins(17) for pressed fuel-AP strands. There is no apparent explanation at this time for their observed burning rate behavior; the curves are highly unusual, compared with practical propellants known to us. We know of no other exceptions.

D. GDF Theory With Distended A/PA Flame

(i) Reaction Times for A/PA and O/F Stages

The solution of the complete granular diffusion flame model in which account is taken of the distributed nature (non-zero reaction time) of the A/PA flame stage, requires first, quantitative estimation of the pressure dependences of the reaction times τ_I and τ_{II}.

It is assumed that the premixed $NH_3/HClO_4$ is bimolecular and hence of second order. In that instance, τ_I is inversely proportional to pressure. Friedman(34) shows that, since the final flame temperature of pure burning AP is low, and since its linear burning rate is fairly high, the thickness of the A/PA flame must be a fraction of a micron at 50 atm. Due to the heating effect of the fuel-oxidant flame, the thickness of the A/PA reaction zone in a burning propellant will be still less, say 0.1 micron at 50 atm. This is to say that the reaction is accomplished at this temperature level in about 100 molecular collisions. This implies that the first gas phase stage has a reaction time of 1.3×10^{-7} sec; for other pressures (in atm units) we may write:

$$\tau_I = (6.5 \times 10^{-6}\ p^{-1}) \quad \text{seconds} \qquad (21)$$

τ_I is plotted as a function of pressure in Fig. 6.

An expression giving the pressure dependence of τ_{II} can not be obtained directly. However, a reasonable estimate of τ_{II} be inferred from the collapsed A/PA-GDF theory which is valid in the 1-100 atm range; the theory fits composite propellant burning rate data remarkably well in the 1-100 atm atm range and moreover, as will be shown later, the assumption of a collapsed A/PA flame is theoretically valid in this pressure range. Essentially, the method of inferring $\tau_{II}(p)$ from the collapsed A/PA-GDF theory is by fitting the theory to AP composite propellant burning rate data in the range 1-100 atm and extrapolating the resulting expression for $\tau_{II}(p)$ to pressures below 1 atm. Implicit to this latter step is the assumption that the A/PA and O/F reaction stages behave independently of each other as far as their response to pressure is concerned. It is to be noted that similar extrapolation of $\tau_{II}(p)$ can not be carried out indefinitely to high pressures

because L_{II} would become very small and soon approach the effective roughness dimension of the propellant surface. The one-dimensional character of the O/F flame would then be lost.

The variation of τ_{II} with pressure predicted by the collapsed A/PA-GDF model can be found by substituting Equation (14) into Equation (3a), at the same time noting that $T_1 = T_s$ in this case. This leads to the following expression for L_{II}.

$$L_{II} = \sqrt{\frac{\lambda_g (T_2 - T_s)}{\left[c_g(T_s - T_o) + \Delta h_{tr} + \Delta h_s + \Delta h_I + \frac{\epsilon \sigma T_s^4}{\rho_c r}\right]}} \left\{ \frac{\alpha T_2}{p} \exp\left(\frac{E_2}{2RT_2}\right) + \frac{\beta(d) T_2^{5/6}}{p^{1/3} T_s^{7/8}} \right\} \quad (22)$$

Substitution of Equations (14) and (22) into (6), together with application of the perfect gas law, then yields:

$$\tau_{II} = \frac{\rho_2}{\rho_c} \frac{L_{II}}{r} = \frac{pM_2}{RT_2} \left\{ \frac{\alpha T_2}{p} \exp\left(\frac{E_2}{2RT_2}\right) + \frac{\beta(d) T_2^{5/6}}{p^{1/3} T_s^{7/8}} \right\}^2 \quad (23)$$

where, again

$$T_2 = T_{2(ad)} - \left[\epsilon \sigma T_s^4 \exp(E_s/RT_s)\right] \Big/ (\rho_c c_g A) \quad (17)$$

It is interesting to note that the low and high pressure asymptotes for τ_{II} are proportional to p^{-1} and $p^{1/3}$ respectively, as expected for this model.

$\tau_{II}(p)$ may now be calculated from (23) by substituting $T_s(p)$ which in turn, can be obtained from Equation (16) by trial solution at every p. The variation $\tau_{II}(p)$ thus calculated, is shown in Fig. 6 for the values of physical constants listed in Appendix A.

Fig. 6 shows that in the range 10-100 atm, the first stage A/PA flame is more than 20 times faster than the second stage O/F flame. Our a priori assumption that the A/PA flame is collapsed in this pressure range, is consistent with this finding although not yet proved to be valid; for proof of this point, the complete two-stage GDF theory must be developed. Fig. 6 does show, however, that the assumption of a collapsed A/PA flame breaks down below 1 atm; τ_I and τ_{II} become comparable in magnitude in this range. Thus, also for the purpose of extending the validity of the GDF theory to very low pressure, the distended A/PA-GDF theory is treated below.

(ii) Derivation of Distended A/PA-GDF Theory

The complete two-stage gas phase reaction granular diffusion flame theory can be solved using $\tau_I(p)$, and $\tau_{II}(p)$ given in Fig. 6. However, due to the complexity of the equations, burning rate can not be written directly as a function of p, $\tau_I(p)$, and $\tau_{II}(p)$. Therefore, the equations had to be

solved by a numerical procedure. The equations rewritten in a form, convenient for iteration are:

From Equation (6) and the perfect gas law we obtain:

$$L_I = \left(\frac{R\rho_c}{M_1}\right)\frac{rT_1}{P}\tau_I \tag{6a}$$

$$L_{II} = \left(\frac{R\rho_c}{M_2}\right)\frac{rT_2}{P}\tau_{II} \tag{6b}$$

Equation (5) is:

$$r = A\exp\left(-E_s/RT_s\right) \tag{5}$$

Equation (4a) rewritten, becomes:

$$T_2 = T_{2(ad)} - \left(\epsilon\sigma T_s^4\right)/\left(\rho_c c_g r\right) \tag{4a}$$

Rearrangement of (2a) and substitution of (6a) yields:

$$T_1 = T_s\Big/\left\{1 - \frac{r^2\tau_I}{P}\left(\frac{R\rho_c^2}{\lambda_g M_1}\right)\left[c_g(T_s-T_0) + \Delta h_{tr} + \Delta h_s + \frac{\epsilon\sigma T_s^4}{\rho_c r}\right]\right\} \tag{2b}$$

Rearrangement of (3a) and substitution of (6b) gives:

$$r^2 = \frac{P}{\tau_{II}}\left\{\frac{M_2\lambda_g(T_2-T_1)}{\rho_c^2 RT_2\left[c_g(T_1-T_0) + \Delta h_{tr} + \Delta h_s + \Delta h_I + \frac{\epsilon\sigma T_s^4}{\rho_c r}\right]}\right\} \tag{3b}$$

This set of equations is solved at any particular pressure by assuming a trial value of T_s and then in sequence, determining τ_I and τ_{II} from Fig. 6, r from Equation (5), T_2 from Equation (4a), T_I from (2b), r from (3b) and T_s from (5). If the finally calculated value of T_s does not correspond to the initially assumed value, the procedure is repeated with a new trial value of T_s until they do agree. The results of calculations so performed, are shown in Tables II(C) and II(D) of Appendix A and in Figures 7, 8, 9, and 11. The values assumed for the physical constants are the same as before and appear in Appendix A.

E. Discussion of Theoretical Predictions; Collapsed A/PA-GDF Model Compared to Distended A/PA-GDF Model

One of the main objectives for carrying out the complete two-stage GDF theory, aside from its application to low pressure burning rates, is to determine purely theoretically the

range of validity of the earlier approximate version, the collapsed A/PA stage-GDF model. Figure 6 shows that the assumption $\tau_I = 0$ in the collapsed model is reasonable above about 10 atm ($\tau_I \ll \tau_{II}$). Figure 7 shows that the distended model does in fact behave like the collapsed model at all pressures above 10 atm, that is, that the energy per unit mass of unburned propellant arriving at the regressing surface by conduction from the A/PA stage* becomes independent of pressure above 10 atm; this is the essence of the collapsed A/PA-GDF model. The collapsed A/PA flame assumption is therefore justified for pressure levels above 10 atm.

An interesting point of the two-stage GDF theory (Fig. 7) is that the pressure dependence of the heat flow into the interior and hence of the propellant burning rate is almost entirely governed by the kinetics of the O/F granular diffusion flame at pressures above 10 atm, even though the heat feedback from this source is considerably less than the heat contributed by the AP-monopropellant reaction. This is because, compared to the O/F flame, the A/PA layer has a very small impedance to conductive heat feedback above 1 atm. In effect, the A/PA layer is so thin at these pressures (particularly above 10 atm) that the requirement of finite heat conduction through the layer (only finite amount of heat available) forces the temperature difference $(T_1 - T_s)$ across the layer to be small also. As shown in Table II(C) and II(D)(Appendix A), this temperature difference is several hundred degrees at subatmospheric pressure, but above 10 atm it goes below 100°C and is even less than 10°C at 100 atm. This is so, in spite of the fact that the heat generated by the A/PA reaction is sufficient to produce a temperature rise in pure AP monopropellant combustion of about 300°C(34). Thus, it is the pressure sensitivity of the "trigger" and not of the main source of heat feedback that is important in determining the pressure dependence of composite propellant burning rate at normal rocket pressures.

Fig. 6 shows that the assumption $\tau_I = 0$ in the collapsed model starts to break down below 10 atm (τ_I becomes comparable to τ_{II}). Fig. 8 shows that this partial breakdown of the assumption does not jeopardize our graphical test for the validity of the GDF theory, i.e., determining whether data taken in the usual 1-100 atm experimental range fall on a straight line when plotted as (p/r) vs. $(p^{2/3})$. In fact, this graphical test will never distinguish between the collapsed and the distended A/PA stage models since the predictions of both models fall on straight lines on the (p/r) vs. $(p^{2/3})$ plot. (The line for the two-stage flame falls higher on this plot because all physical constants were left the same but τ_I was increased when going to the

*The conductive heat feedback per unit mass of unburned propellant from the A/PA flame is given by:

$$Q_I = (\dot{Q}_I/\dot{m}) = \left[(T_1 - T_s)/L_I - (T_2 - T_1)/L_{II}\right] / (\rho_c r)$$

two-stage model.) Note that data taken in the 0.001 - 0.1 atm range where $\tau_I \approx \tau_{II}$ (and hence the models most dissimilar), can not distinguish between the collapsed A/PA flame or the distended A/PA flame either when plotted this way ($p/r - p^{2/3}$), because all such data points will cluster at the very low pressure end of this graph.

It is appropriate now to make the parenthetic remark that these findings validate the approach taken by Krier, T'ien, Sirignano and Summerfield(127) when they assumed the collapsed A/PA-GDF model to predict low frequency instability behavior of composite solid propellants at normal rocket pressure. Also, since $\tau_{II} \approx 1.5 \times 10^{-5}$ sec at these pressures, their quasi-steady treatment of the O/F flame reaction time is valid for low frequencies; above about 5000 cps, the dynamic lag of the O/F must be taken into account - the dynamic lag of the A/PA flame need only be considered when the frequencies approach 100 Kcps.

The above findings also show that the assumption of a collapsed A/PA flame breaks down at subatmospheric pressure. To discern the role played by the A/PA flame, burning rate data must be taken into this low pressure range where the A/PA stage of the gas phase flame represents a large part of the total reaction time. Fig. 9 compares the burning rate vs. pressure predictions of the two models on a log-log plot. As expected, their behavior is drastically different in the subatmospheric pressure range. In the case where τ_I is non-zero and where there is no radiative heat loss the (log r) vs. (log p) plot tends to follow a straight line with slope slightly less than unity. It is interesting to see that, for small values of the activation energy of the surface reaction E_s, the collapsed A/PA flame model predicts that the burning rate curve will bend concave upwards as the pressure is reduced and will level out asymptotically to some non-zero burning rate at zero pressure, regardless of radiative heat loss. Only the fact that the surface reaction is exothermic overall makes the burning rate non-zero at zero pressure. The transition from a finite pressure exponent to a pressure exponent of zero denotes the region where the second stage O/F flame, the only pressure sensitive process, becomes so distended that its heat flux to the pyrolyzing surface, that is, its contribution towards establishing the burning rate, becomes negligible; below about 0.01 atm, only the exothermic A/PA surface reaction (effectively of zeroth order when $\tau_I = 0$) controls the burning rate. This behavior would not exist in practice without some "artificial" means of ensuring that $\tau_I = 0$, or at least independent of pressure. This possibility will be referred to later.

It should be emphasized that the low pressure behavior predicted by the collapsed model is very sensitive to the choice of E_s (see Fig. 10) for when E_s is large and when there is radiative heat loss, then extinction will occur at some low pressure. The reason for this is that the surface reaction for large E_s is a more sensitive function of surface temperature than is the

radiative heat loss. Thus, at some low pressure, where the O/F flame is weak, the surface reaction, which is almost entirely the source of heat, can not overcome the heat loss. This is the pressure at which extinction occurs. In the case of the distended A/PA flame model, radiative heat loss will always cause extinction, because the surface pyrolysis is taken to be an endothermic process in this case, and the A/PA stage behaves in the same way as the O/F stage, the heat feedback declining as the pressure is reduced. This model predicts extinction at 0.022 atm (see Fig. 9).

Radiative heat loss has on various occasions been proposed as a factor responsible for low pressure extinction of solid propellants. It is characteristic of the theoretical predictions that radiative heat loss becomes steadily more important as the pressure is reduced. Consequently, just before the extinction point is reached, the burning rate pressure curve starts to bend downwards with reduction of pressure. Two other factors more likely to be responsible for extinction, are cooling of the gas phase flame by dilution with the entrained ambient gases (in a strand burner not an internal burning grain), and reduction of the amount of heat produced in the flame due to increased combustion inefficiency (seen in the products, both gaseous and solid) with reduction in pressure. A propellant strand, typically 5 millimeters square, will be particularly susceptible to cooling by dilution with the surrounding ambient gases at about 0.05 atm because as Fig. 11 shows, the calculated flame thicknesses of the A/PA and the O/F stages are then of the order of millimeters. This is a full order of magnitude higher in pressure than can be accounted for by radiative heat loss alone; so, convective heat loss is more likely to cause extinction at low pressures. The significance of combustion inefficiency in determining low pressure extinction behavior can not be calculated theoretically. One must rely on actual measurements of the heat generated as a function of pressure. Product analyses will be very useful for this purpose.

At the high pressure end of the burning rate curve, it is noted that propellant burning can be considered one-dimensional only if the O/F gas phase flame thickness and the thermal wave thickness* in the solid phase are large compared to the effective roughness dimensions of the propellant surface. (This is more nearly the size of the crevice between the particles of oxidizer, not the mean particle diameter.) If the significant dimension is of the order of 10 microns, then from Fig. 11, it is seen

---

*The solid phase thermal wave thickness is defined as the depth below the propellant surface at which $(T - T_o) = \frac{1}{e} (T_s - T_o)$ and is calculated from the usual equation for the temperature profile in a moving medium with conductive and convective heat flow:

$$(T - T_o)/(T_s - T_o) = \exp(-rx/\alpha_c)$$

that one-dimensional considerations break down above about 100 atm. Therefore, agreement with the granular diffusion flame one-dimensional theory must break down above 100 atm, and generally this is so. (See Section IIB(i)).

A final prediction of use in the later evaluation of the complete two-stage GDF theory is that surface temperature increases significantly with increase in pressure; it is about 600°K at 0.01 atm and about 1100°K at about 100 atm.

F. Major Conclusions Summarized

The collapsed A/PA-GDF model is theoretically a valid representation of AP composite solid propellants in the range 1-100 atm. The resulting burning rate equation $1/r=a/p+b/p^{1/3}$, agrees well with the burning rate data of a wide class of practical AP propellants over the range 1-100 atm. These are propellants with high AP loading, medium-sized AP particles, and/or fuels of the type that do not melt readily. The boundary of validity of the collapsed A/PA-GDF theory, specified in terms of equivalence ratio ψ_o and AP particle size d_m, is: $\psi_o \gtrsim (0.30 - 0.10 \log_{10} dm)$ and $d_m \lesssim 250\mu$.

The collapsed A/PA-GDF theory becomes invalid for the following cases:

(1) Above 100 atm - the flame loses its one-dimensional character.

(2) Between 1 and 100 atm when the propellant has low AP content, small AP particle size, and/or a fuel that melts and flows easily - a new phenomenon to be elucidated in Section IV comes into play.

(3) Below 1 atm - the A/PA flame becomes distended as will be showr by supporting data given in Section V.

SECTION IV

COMPOSITE PROPELLANT BURNING BEHAVIOR IN 1-100 ATM RANGE; NORMAL BURNING, PLATEAU BURNING AND INTERMEDIATE PRESSURE EXTINCTION

In Section IIIC(ii) it was found that AP-based composite solid propellants conform to the GDF theory whenever the AP loading is high and the AP particles are neither very small nor very large (see Fig. 3). These propellants are said to burn normally. Our review of all available burning rate data also showed that abnormal burning in the form of plateaus etc., ensues soon after either ψ_o or d_m are reduced below the value for which the GDF theory applies (the normal burning - abnormal burning boundary in Fig. 3). Bastress(14) was the first to have reported these effects of low AP loading and small AP particle size for underoxidized mixtures. The phenomenon responsible for this behavior in the particular underoxidized AP propellants that he studied has a very important implication, in the sense that we may find it possible to produce these desirable plateau burning and mesa burning regions in the normal rocket pressure range with highly oxidized practical propellants, once the phenomenon is understood. Further study of this anomalous kind of behavior is therefore well justified.

A. Findings By Previous Investigators

Figures 12 and 13 show burning rate curves reported by Bastress(14) for several AP-based composite propellant systems. These demonstrate that burning rate plateaus can be produced by lowering AP content and reducing AP particle size. With further reduction of oxidizer loading, a region of negative slope (mesa burning) in the burning rate versus pressure curve develops; for still lower loading, extinction occurs for pressures above about 800 psia. This behavior was observed for polysulfide (LP3/GMF)-AP, polyesterstyrene (P13)-AP, and epoxy (EPON/TETA)-AP propellants.* Rumbel(16) reported an identical effect of reduced AP content in polyvinyl chloride (PVC/DBS) based propellants.

Fig. 13 shows that similar regions of plateau burning, mesa burning and intermediate pressure extinction can be produced by reducing oxidizer particle size while oxidizer loading is held at a constant low value. The data reported by Rumbel(16) for PVC/DBS propellants also seem to indicate that small AP particles accentuate plateaus. The data of Fig. 13, replotted as (p/r) vs. $(p^{2/3})$ in Fig. 14, show that these propellants conform to the GDF correlation only in a relatively narrow intermediate range of particle size (50-200μ).

*The behavior characteristics of all propellants discussed in this section are summarized in Table III of Appendix B

This is because the equivalence ratio (ϕ_o=0.415) is small (see Fig. 3). A higher oxidizer loading would widen the range of applicability of the GDF equation. Fig. 14 also shows, as expected, that the b-parameter in the GDF correlation depends on mean AP particle size; empirically, this dependence turns out to be $b \propto d_m^{0.2}$. The small dependence of burning rate on the particle size implied by this small exponent is consistent with the data reported by Rumbel(16).

In the case of one of Bastress' propellants, a polystyrene propellant with 72.5% 20μ AP, extinction was found only in the range 300 to 1200 psia. (Reid(128) had previously found that this extinction pressure range for this particular propellant, narrows with increasing strand size.) Since other severely underoxidized propellants were not tested above 1600 psia, the upper limit of the apparatus, the latter observation might imply that a pressure exists for all such propellants above which steady self-sustained burning is again possible.

Bastress ascribed(14) the above behavior (plateaus and extinguishment) to spotty flame-outs* caused by intermittent local depletion of exposed oxidizer crystals at the decomposing propellant surface, a phenomenon that was thought to result from the large difference between the individual pyrolysis rates of the fuel and oxidizer under weak flame conditions. The contradiction in burning rate behavior between propellants of high oxidizer loading and those of low oxidizer loading suggested interesting implications from both the theoretical and practical points of view. It was important, therefore, to re-examine thoroughly the data and the underlying mechanism.

B. Experimental Results of This Investigation

As a first step, it was decided to try to reproduce the results of Ref. 14 in order to make sure that the observed burning rate curves, which seemed quite unusual, could not be attributed to defects in experimental technique or in propellant quality. Steps were taken in the new experiments to modify the existing burning rate apparatus and to modify the test procedures in order to obtain more accurate measurements; also more careful propellant and quality control methods were instituted. A detailed account of these efforts is given in Appendix C; it covers the experimental procedures followed (propellant manufacture, propellant quality control, and burning rate measurements), and also the accuracies involved in following these procedures. Appendix D gives a listing of the physical properties of all the propellants used in this study.

*These temporary localized extinctions have since been observed photographically by Barrère and Nadaud(123).

In summary, the result of the above described efforts was that the curves for polysulfide (LP3/GMF) propellants containing 65% ammonium perchlorate with different particle sizes reported in Ref. 14 were found to be reproducible. (See Figure C-15 of Appendix C.) Similar plateau and extinguishment behavior was found also with polybutadiene acrylic acid (PBAA/EPON) propellants containing 75% AP of different mean sizes. Very careful measurement of propellant density in all test propellant strands excluded void content as a possible cause of the burning rate anomalies. It was concluded, therefore, that the anomalies are an inherent characteristic of small AP particle size propellants, particularly when severely underoxidized.

The effects of AP content, AP particle size, fuel-type and strand size, some of which were covered in Ref. 14, have been studied more extensively in the present investigation. These latest findings are:

(i) The effect of AP particle size in PBAA/EPON propellants, loaded with 75% AP shown in Fig. 15, was found to be consistent with the earlier findings described above. In line with the boundary of validity of the GDF theory defined in Fig. 3, none of these propellants fit the theory; the equivalence ratio is too low (0.334). Fig. 15 also shows that the addition of a small percentage of medium-sized AP particles (10% 80μ) to a predominately small unimodal particle size distribution (90% 5μ) is instrumental in suppressing the phenomenon responsible for mesa burning, though the amount added is obviously not sufficient to avoid extinction.

(ii) The effect of AP loading in PBAA/EPON propellants with a bimodal AP distribution (30% 5μ + 70% 45μ) shown in Fig. 16, is also consistent with earlier findings. As expected from the correlation of Fig. 3, only that propellant with the highest AP content (80%) in this series, conforms to the GDF correlation. Fig. 17 shows the data of this propellant plotted as (p/r) vs. $(p^{2/3})$, together with the data of other bimodal propellants with similar binders to be discussed in paragraph (iv) below.

(iii) The effect of increasing strand size from 1/8 inch square to 3/8 inch square was not completely negligible. In the search for the above-described extinction phenomena, for example, it was found that the extinction pressure is raised from 375 to 600 psia in the case of PBAA/EPON-AP propellant with 5μ mean particle size. (See Fig. C-13 of Appendix C.) Reduction of the drift velocity of nitrogen past the strand* from about 2 ft/sec

*Throughout this study, nitrogen at room temperature was allowed to flow slowly past the strand in order to prevent possible preheating of the strand by reverse flow of the hot combustion products and also to prevent the flame from flashing down the side of the strand, in cases where the applied surface inhibitor was not fully effective.

to zero was found to raise the extinction pressure from 500 to 600 psia in the case of the 1/4 inch square strands; this effect is not likely to be as great in the case of large strands. On the other hand, variation of strand size did nothing to alter the burning rates, except in the case of the smallest strands (1/8 inch) where the burning rates were reduced by about 15%; even so, all the burning rate curves were found to have the same shape (see Fig. C-13 of Appendix C.). The narrowing of the extinction pressure range with increasing strand size was also observed by Reid(126) with polystyrene-polyester propellant; for strands larger than 5/16 inch square, no extinction region could be found at all.

(iv) The effect of fuel type has been found significant in determining the burning rate behavior of composite solid propellants. Preliminary studies of the behavior of various polymer types during degradation in bulk* (Table IV of Appendix B) show that they fell into two classes according to their melting properties: (1) those for which the melting temperature is significantly lower (100-150°C) than the temperature at which 50% weight loss occurs in 30 minutes (i.e., ESTANE/POLYOL, PIB/MAPO, and POLYOL/TDI); and (2) those for which these two temperatures are about equal (i.e., PBAA/EPON, PBAN/MAPO, PBCT/EPOXY, and PBHT/TDI.) Because of the coincidence of these two temperatures, polymers of the latter category are less likely to form a thick molten fuel layer at the surface of a burning solid propellant. Thus, based on the assumption that knowledge gained from bulk degradation and melting studies is indicative of the behavior of the polymer during propellant burning (high heating rate at the decomposing surface), we will henceforth refer to polymers of class (1) as being of the type that melts readily; similarly then, class (2) is of the type that does not melt easily. It so happens that the polymers tested do not differ greatly in their volatility characteristics**; the temperatures for 50% decomposition all fall between 270°C and 340°C. (See Table IV).

The burning rate behavior of propellants with the above fuels were systematically studied. Fig. 17 shows data of highly loaded ($\psi_o \approx 0.52$) bimodal (30% 40μ + 70% 180μ) AP propellants with fuels that do not melt readily (class 2), namely PBAA/EPON, PBAN/MAPO, and PBHT/TDI, plotted as (p/r) vs. ($p^{2/3}$). They fit the GDF correlation quite well, although beyond about 1000 psi there is a tendency to break away from a straight line fit. Fig. 18 shows the same data plotted as (log r) vs. (log p), together with the data of propellants with the same fuels but with

---

*The polymer samples were placed in an oven at a preset temperature for 30 minutes. The percent weight loss during this time and the physical state of the polymer, i.e., molten or not, were recorded.

**The exception is paraformaldehyde, for which the temperature for 50% decomposition in 30 min. is about 100°C. It agrees well with the value 120°C reported by Ref. 42.

severely underoxidized propellants show strange inflections in the burning rate curve and do not fit the GDF correlation. If the results of these propellants (concerning the fit obtained by GDF correlation) are plotted on Fig. 3, it is seen that these propellants are consistent in their behavior with that of all other propellants previously reviewed. Thus, the correlation of Fig. 3 applies to AP propellants with fuels that do not form a thick molten layer.

The burning rate curves for propellants with fuels that do melt readily (ESTANE/POLYOL, POLYOL/TDI and PIB/MAPO) show exceptional behavior with respect to the correlation found in Fig. 3. Figs. 19 and 20 show the r-p behavior exhibited by the two AP-polyurethane (ESTANE/POLYOL and POLYOL/TDI) propellants. It is apparent from this figure that these propellants show marked tendencies toward the same kind of plateau burning and intermediate pressure extinction that is typical of points below the line in Fig. 3, but they show this anomalous behavior at much higher AP loadings than one would expect for propellants with fuels that do not melt readily.* Thus, when the representative points of these abnormal propellants are placed on Fig.3, they fall in the domain for normal burning. The same considerations apply to the PIB/MAPO-AP propellants of Fig. 21, although it is obvious that this system does not behave exactly like the polyurethane-based propellants.

A final observation concerning the previous burning rate curves is that the low pressure extinction limit for propellants with readily meltable binders is higher than the low pressure extinction limit for comparable propellants with fuels that do not melt readily (compare Figs. 15, 16, and 18-21). Fig. 18 shows that the low pressure extinction limit of the POLYOL/TDI-AP propellant is raised when the AP mean particle size is reduced, at least for the polyurethane propellants. The same trend has been reported by Peterson et al(129,130) for aluminized polyurethane-AP propellants.

Some work has been done also with double base (DB) and composite modified double base (CMDB) propellants using nitrocellulose powder plasticized in triethylene glycol dinitrate (TEGDN) as the binder. As seen from Figs. 22 and 23, the burning rate behavior of the CMDB propellants with 40% AP of varying particle size is well described by the GDF equation, while the pure DB propellant fits the power formula $r \propto p^{0.78}$, as expected for a premixed second-order flame rather than a GDF flame. Correspondingly, the visible gaseous flame of the CMDB propellant appeared relatively opaque, like that of an AP-composite propellant, while the gaseous flame of the pure DB propellant

*This type of burning rate behavior for unaluminized polyurethane propellants has been confirmed by Dr. H. J. Wiegand at Aerojet-General Corporation where a great deal of experience with polyurethane propellants exists. Similar results for polyurethane propellants have been reported also by Mr. T. W. Boggs of the Naval Weapons Center. (Private communication.)

appeared transparent and homogeneous. (No dark zone usually observed(128,131,132) below about 800 psi for NC/NG double base propellants could be seen with our particular DB propellant composition; this puzzling point deserves further investigation.) It appears that the addition of 40% AP to double-base propellant converts the gaseous flame from a premixed reaction zone to a zone dominated by a chemical reaction-granular diffusion mechanism. It is interesting that the representative points for these CMDB propellants lie within the GDF theory validity region defined in Fig. 3 for propellants wit fuels that do not melt readily.

(v) Various qualitative observations have shown that the burning process is unsteady whenever the slope of the (log r)-(log p) is negative. High speed movies show that, under these circumstances, the flame is highly nonuniform, intermittently extinguishing in various localized portions of the strand surface; on the other hand, the flame is always uniform and steady when the burning rate curve has a positive slope. (Barrere(123) reported the same observations). Consistent with this is the finding that irregular pressure oscillations of up to 5 psi amplitude (depending on the propellant tested) persisted in the chamber whenever a strand burning test was made at a pressure in the mesa region; the pressure was always steady when the pressure exponent was positive.

A further observation of importance is that the burned surfaces of polyurethane-AP or polyisobutylene-AP propellant strands that had been ignited in the intermediate pressure range (several hundred psi) but suffered extinction, were covered by a molten fuel layer. (No exposed AP crystals could be seen). On the other hand, the AP crystals were clearly exposed on the burned surfaces of the same propellant that extinguished at the low pressure end of the burning rate curve (near 1 atmosphere). The 25% PIB/MAPO + 75% AP propellant that extinguished at all pressures between 1 and 100 atm (Fig. 21) had a molten fuel layer, the thickness of which increased with increasing test pressure. All propellant samples that extinguished at intermediate pressures had highly irregular burned surfaces, regardless of the fuel type used.

C. Interpretation of Results; Phenomenon of Intermittent Burning.

The consistency with which reduction of AP loading and reduction of AP particle size cause a propellant to burn abnormally indicates that the same underlying phenomenon of intermittent burning is responsible for plateau burning, mesa burning and intermediate pressure extinction. It is only a matter of the degree of this intermittency that determines whether a propellant will have a plateau region or a mesa region, or will extinguish at intermediate pressures. The

[illegible] fuel layer on the surface of propellants with readily meltable fuels (when burning at intermediate pressures) together with the fact that these propellants are far more prone to showing intermittent burning behavior, imply that it is the molten fuel layer that is causing the temporary localized extinctions. These temporary localized extinctions are imagined to occur through covering, on a local scale, of the AP particles by the molten fuel layer; this results in an O/F flame that is weakened by local depletion of oxidizer gases. The net effect of the temporary localized extinctions is to cause a reduction in the mean burning rate or perhaps even complete extinction of the propellant strand. Thus, a region of plateau or mesa burning can result, depending on the way in which the molten fuel layer responds to pressure, i.e., local conditions of temperature and temperature gradient.

In retrospect, it appears that all fuels melt to some degree (Sections IIB(v) and IVB). It is plausible therefore to say that even the abnormal burning behavior noted above for AP-composite solid propellants that are not readily meltable can also be explained in terms of the above suggested mechanism. Obviously, since the thickness of the molten layer is the important parameter, a propellant with less fuel (high ϕ_o) and with larger AP particles will be less prone to plateau behavior, etc. That the pressure range in which extinction occurs is narrowed by increased strand size is explained on the basis of the fact that the O/F flame is locally weakened during intermittent burning; a small strand will be more liable to complete extinction by cooling with the surrounding ambient gases. The effect of pressure on the tendency of a propellant to burn in intermittently (i.e., in what pressure ranges plateaus and mesas may be found) is not so clearly explained from a fundamental point of view; the physical properties of the polymers and AP are not well enough known. Visual examination of extinguished propellant strands shows that the molten fuel layer gets thicker as pressure is increased up 100 atm. (The implication is that the polymer is desorption limited at higher pressures, that is, at higher temperatures). On the other hand, it is apparent also that the molten fuel layer must be very thin at some very high pressure because under these circumstances the burning rate is high, and so the thickness of the thermal wave in the solid phase must be very thin. Thus, the melt is thickest at some intermediate pressure, and so intermittent burning which shows up as plateaus, etc., can be expected logically in this intermediate pressure range.

All propellants tested to date show behavior that is consistent with the above explanation. It is to be noted that the peculiarities of any particular burning rate curve such as the rather unusual inflections of the PIB/MAPO-AP propellant burning rate curve in Fig. 21 can not be explained at present; more detailed information about the response of the molten fuel layer to temperature and temperature gradient conditions is needed. A further note to be made is that while there are indications

that double base fuels can melt(133), these are usually so volatile compared to the AP that there is little opportunity for the AP particles to be covered. (The surface temperature of AP is typically 1000°K(40,68,109) near 1 atm, and that for the DB fuel is typically 500°K(91,134); thus, under the "two-temperature" postulate, the fuel surface recedes below the AP surface.) AP-based CMDB propellants are therefore not expected to burn intermittently. This does not mean that plateaus or mesas will not be observed with CMDB propellants, but rather that any plateau or mesa burning behavior shown by CMDB propellants will be the result of special catalysis as in pure DB propellants(135,136); the distinction is that plateau behavior in CMDB-AP propellants will be due to a steady phenomenon in which chemical kinetics play the determining role, whereas plateau behavior in "inert" binder-AP propellants is due to a phenomenon of unsteady nature in which the physical condition of the burning surface is the important factor.

Bastress(14) previously proposed an alternative mechanism for intermittent burning whereby the large difference between the pyrolysis rate of the fuel and AP causes a localized depletion of exposed AP crystals on the surface of a propellant in cases where the AP particles are small. That hypothesis explains the effects of AP particle size, AP loading and strand size, but does not account for the fact that propellants made with readily meltable fuels are far more prone to intermittent burning. The presently suggested mechanism, whereby intermittent burning is attributed to the role played by the molten fuel layer on the burning surface, accounts for all the effects that have been observed. In our opinion this is now the preferred explanation.*

In the context of the above suggested intermittent burning mechanism, i.e., the role played by the molten fuel layer, it is to be expected that the transition boundary between normal and intermittent burning behavior defined in Fig. 3, will be rather diffuse because the melting properties of the individual binders have not been taken into account.

---

*Boggs(90) recently reported some findings concerning the burning behavior of pure AP that may have some bearing on the phenomenon of intermittent burning in AP-based composite solid propellants: he showed that pure AP has a log(burning rate)-(log pressure) curve that has a steep negative slope in the 2000-4000 psia range and suggested that the observed occurrence of a froth in the thin molten layer at these pressures may cause this mesa burning behavior by, in some way, impeding heat transfer to the condensed phase. The idea is still too vaguely defined to incorporate into a consistent model of propellant burning for testing against known AP-based propellant burning behavior. Certainly, however, it is clear that the role played by the molten AP layer can not be the only important factor in explaining plateau burning behavior, etc. in AP propellants; the role played by the molten fuel must be important also.

As a final point it is noted that the particular low pressure extinction behavior of certain propellants with readily meltable fuels (i.e., one, the relatively high value of this limit, and two, the tendency for this value to increase with reduction in AP particle size and/or AP content), may also be explainable on the basis of the role played by the molten fuel layer. The thermal wave in the solid phase increases with reduction in pressure and consequently, the thickness of the molten layer (if it exists at these pressures) will also increase; ultimately, at some low pressure, it may be thick enough to partially cover the AP particles and thereby cause extinction of the already weak gaseous O/F flame. For non-meltable propellants, extinction at low pressure is explained on the basis of heat loss, combustion inefficiency, and dilution of cold ambient gas in the strand burner. (See next section.) The distinction is that for meltable fuels, the drowning of the AP particles may represent an even stronger mechanism for extinction.

D. Concluding Remarks

The results of this section and the mechanism proposed for the phenomenon of intermittent burning are all consistent with the general picture of AP propellant burning. Localized extinctions causing plateaus, etc., only become important when AP content is low, AP particle size is small, or when the fuel is of the type that forms a thick molten layer on the regressing propellant surface. In the sense that the assumption of a dry planar burning surface in the GDF theory breaks down for these cases, the intermittent burning phenomenon is consistent with the GDF theory, also. The GDF theory is only valid for those propellants which are not susceptible to intermittent burning, i.e., those with medium-size AP particles, high AP loading and fuels that do not melt readily. For these cases, the assumption of a dry planar burning surface appears to be valid.

SECTION V

COMPOSITE PROPELLANT BURNING BEHAVIOR AT SUBATMOSPHERIC PRESSURES

The purpose of studying low pressure burning behavior is to obtain information concerning the detailed structure of the flame zone. It is known that the fuel-oxidant reaction zone becomes very weak at very low pressures. Thus, at low pressures, the nature of any remaining exothermic reactions occurring at or near the propellant surface is more clearly manifested in the overall propellant burning behavior. Burning rates and extinction behavior have been measured for a number of propellant systems and will be reported below. These results are then interpreted in terms of the theoretical predictions made in Section III.

A. Review of Findings by Previous Investigators

Several experimental studies of low pressure solid propellant combustion phenomena have been made in the past. These were in the main restricted to measurements of surface temperature(29,42,43,91,137-141) and burning rate(12,13,42, 120,123,140,143)as a function of various parameters such as pressure, propellant composition and oxidizer particle size.

All available surface temperature-pressure dependence measurements(91,137-141) have been reviewed. These are shown in Fig. 24, compared to the theoretical predictions of the complete two-stage granular diffusion flame theory. It is seen that the theoretically predicted rise of surface temperature with pressure agrees quite well with the data, especially when it is realized that, as pointed out by Powling(142), both the infra-red radiometer and thermocouples are expected to record a lower pressure dependence than is actually the case. This low apparent pressure dependence is due to the fact that the temperature profile becomes steeper with increased pressure and hence burning rate. Bobolev et al's thermocouple measurements(141) have been omitted from the figure because they report rather low values (600-700°K in the 50-200 atm range) and moreover, they report a decrease in T_s with increased p. Selzer's measurements(138) for particle sizes larger than 100μ have also been omitted, but because of unduly large scatter. Beckstead and Hightower(139) indicate that the actual value of surface temperature could be 200°C higher than reported by them because of the presence of a thin molten layer on the AP crystal.

The burning rate-pressure dependence of AP composite propellants in the subatmospheric range(12,13,42,120,123, 140,143) has also been reviewed in detail. Fig. 25 is a composite plot of all the available data and includes some of the data of this study (to be discussed in greater detail below). This figure shows that subatmospheric burning

rates generally tend to follow a straight line on the (log r) vs. (log p) plot; the slope of this line is usually around 0.7 but in the case of some binder types such as polyesterstyrene, paraformaldehyde and polyisobutylene, it is close to unity.*

Of critical importance to this investigation is the behavior of the propellant at the very lowest pressures. This requires, amongst others, very careful determination of the low pressure extinction limit and also of the shape of the burning rate curve near this extinction limit; it is only in this range where the detailed interpretations as to the role played by the A/PA flame, radiative heat loss, combustion inefficiency, etc., can be made. Since in most cases, previous workers did not report the extinction pressure, or take sufficiently many data points to establish the exact detailed shape of the r-p curve at very low pressure, further work seemed necessary. The experimental results obtained for this study are reported below.

B. Experimental Results of This Investigation

(i) Burning Rates

A description of the propellant manufacturing process, the propellant quality control methods used, and the burning rate measurement technique followed, together with the accuracies involved in each of these procedures, is to be found in Appendix C. The specifications of all propellants used in this investigation i.e., AP particle size, propellant composition and propellant density compared to its theoretical density, are listed in Table VI of Appendix D. The properties and formulations of each binder-type used are given in Table IV of Appendix B.

Fig. 26 shows our results obtained for the effect of several binders on the burning rate at subatmospheric pressures. This set of curves represents propellants loaded as highly as is practically feasible with 5 micron mean particle size unimodal AP.** (The AP content and corresponding equivalence ratio for each propellant are both listed in the figure). Fig. 26 shows that propellants with polybutadiene acrylic acid (PBAA/EPON) and carboxyl terminated polybutadiene (PBCT/EPOXY) binder behave in the usual way, i.e., follow straight lines on the (log r) vs. (log p) plot. This is also true of the hydroxyl terminated

---

*Theoretically the pressure exponent is less than unity because at these low pressures, the two gas phase reaction stages are essentially second order reaction rate controlled and the surface temperature decreases with reduction in pressure; this T_s-p dependence decreases the value of the pressure exponent. The slight differences in the pressure exponent observed for the different binder types will depend on the individual binder properties.

**The reason for the choice of this particular set of parameters is that preliminary tests have shown that propellants with the highest possible loading of very fine AP burn to lower pressures than propellants more highly loaded with coarse AP; it is very low pressure burning behavior that is of primary interest here.

polybutadiene (PBHT/TDI) when copper chromite is added. (Note that PBHT cured with TDI is a polyurethane(144).) The pressure exponents for all three of these propellants lie between 0.68 and 0.78 and they all extinguish at about 0.045 atm.

As seen from Fig. 25, our results agree fairly well with those obtained by other investigators for similar propellant systems. The most marked difference between our burning rate curves and those of other investigators is that our curves extend down to lower pressures. We found that the propellants we tested could only be made to burn at very low pressures by first igniting the strand above about 0.3 atm and then slowly reducing the pressure to the desired test pressure; if the pressure is reduced too rapidly, then extinction will inevitably occur. In this study, the extinction pressure for a particular propellant was taken as the lowest pressure (out of a number of tests) at which the propellant could be made to burn. These extinction tests were done taking extreme care to reduce the pressure as slowly as possible. The extinction pressure determined in each of these tests, generally fell within 10% of each other. Some tests done with the PBAA/EPON-AP propellant showed that the extinction pressure is strand-size dependent: the extinction pressure was lowered by almost a factor of 2 when the strand size was increased from 0.25 inch square cross-section to 0.6 inch square cross-section. The burned surface of extinguished samples of all three propellants (PBAA/EPON, PBCT/EPOXY, and PBHT/TDI with copper chromite) looked porous and dull black (charred) when observed through a microscope; it appeared as though it were dry during burning.

Contrary to the general trend described above, hydroxyl terminated polybutadiene (a polyurethane) has a burning rate curve which bends concave downwards below 0.3 atm (Fig. 26). Also, the extinction pressure of this propellant is rather high (0.18 atm). The burned surface of extinguished samples of this propellant had a glistening black appearance. It had a large number of depressions of about 1 mm diameter and the bottom of these depressions was the same color as the unburned propellant (white). Little conical flamelets of about 1 mm base diameter and about 1 mm height could be seen darting about the propellant surface when the propellant was burning at a very low pressure near the extinction pressure. These observations suggest that a mass of molten fuel* containing solid AP particles is present on the burning propellant surface and that globules of this mixture periodically erupt from the surface. (The exothermic $NH_3/HClO_4$ reaction is severely inhibited due to encapsulation of the AP particles by the molten fuel.) These globules are presumably carried into the afterburning

*Polyurethanes show generally a tendency to melt(144). However, as shown in Section IVB(d), this polyurethane (PBHT/TDI) melts less readily than, say, POLYOL/TDI and ESTANE/POLYOL.

zone where they burn up and thus contribute little towards the heat needed for gasification at the propellant surface. This inefficiency in the burning process can explain the drooping of the burning rate curve at low pressures as well as the observation that the extinction pressure is higher than that of the PBAA/EPON-AP and PBCT/EPOXY-AP propellants whose burning surface appears dry. These observations fall in line also with the findings of Section IV for propellants with the readily meltable polyurethanes, i.e., POLYOL/TDI and ESTANE/POLYOL: these extinguish at pressures of the order of several atm depending on AP particle size and AP loading.

As seen in Fig. 26, the addition of 0.75% copper chromite to PBHT/TDI-AP propellant has the effect of increasing the burning rate at all pressures, but more important, the burning rate curve now follows a straight line all the way down to the extinction pressure which is the same as that of the PBAA/EPON-AP and PBCT/EPOXY-AP propellants. Moreover, the burned surface of extinguished samples of the PBHT/TDI-copper chromite propellant had the same appearance as that of PBAA-AP and PBCT-AP propellants, that is, it appeared dry during burning. These observations concerning the effect of copper chromite on the burning behavior of PBHT-AP propellant are reasonable because copper chromite is known to be a very good catalyst for AP decomposition(23,24); a likely explanation of these observations is that the addition of copper chromite will allow the same or more AP decomposition at a surface temperature lower than the melting temperature of PBHT/TDI binder.

Figure 27 shows polysulfide (LP3/GMF) propellant to behave in a completely different way: the burning rate curve bends concave upwards below 0.05 atm and there is a strong tendency for the burning rate to become independent of pressure at very low pressure ($\sim$ 0.005 atm); the extinction pressure is an order of magnitude lower than that of the PBAA-AP and PBCT-AP propellants. It is significant that the burning rate curve starts bending up at about the pressure below which the propellant leaves a porous but very firm solid residue as a combustion product. The peculiar characteristic that polysulfide propellant forms an "ash", was discovered by Most(140). In this study it was found that the "ash" starts forming unstably below 0.053 atm but then a firm layer of solid residue builds up on the regressing interface to a thickness of 1 - 2 mm and then suddenly burns away. Below about 0.040 atm, the propellant burns in cigarette-fashion leaving the solid residue intact. There is no evidence of a visible flame. The rate of progress of the interface into the unburned propellant is here taken as the burning rate of the propellant. The scatter in our burning rate results is rather large ($\pm$ 5%) in the range 0.005-0.05 atm. This scatter in the results is due to the fact that the burning process is somewhat irregular at these pressures and also to the fact that an oil film which produces small random distortions had to be used to prevent coating of the window by

the excessive amounts of white fumes produced at these low pressures. (See Appendix C for further details of experimental procedure.) Our burning rates compare well with those obtained by Most(140) in the 0.2-1.0 atm pressure range.

The effect of oxidizer particle size on the burning rate of LP3/GMF-AP propellant (with ϕ_o= 0.42) was investigated and is shown in Fig. 27. Although the scatter is quite large, increase of particle size does appear to depress the burning rate. The effect of particle size appears to be larger in the 0.005-05 atm than the 0.1-1.0 atm pressure range. In view of the fact that both the 15μ and 25μ propellants had densities within 1% of theoretical, it seems unlikely that the large void content (5%) of the 5μ propellant was the cause for its higher rate. (See Table VI(B) of Appendix D.) The pressure at which extinction occurs increases with increase of particle size. Particle size has no effect on the pressure at which the transition to ash formation occurs.

(ii) Subsidiary Semi-Quantitative Observations

When the pressure is around 0.05-0.06 atm, the flame of a "normal-burning" propellant i.e., PBAA/EPON-AP has the appearance of a two-stage flame. The first stage is a dark zone with no visible radiation and is 0.5-1.0 mm thick. This dark zone is followed by a very thin blue layer which marks the beginning of a long (several centimeters) yellow-to-orange colored zone. (The latter zone is blue when copper chromite has been added to the propellant.) At about 0.06 atm, the blue envelope is still largely planar and parallel to the propellant surface, but upon further reduction in pressure, especially very near the extinction pressure, it takes on a bulbous form. The dark region can be as thick as 3-5 mm when the pressure is very near the extinction pressure. When the dark zone is thick, white smoke (probably AP sublimate) can be seen to leave its edges. When the process of extinction is slow enough, it is always seen to start from the edges of the propellant strand. These qualitative observations suggest that the dark zone is the $NH_3/HClO_4$ reaction zone (NH radiates in the ultra-violet at 3360A(1,7) and that the blue envelope marks the onset of the pre-mixed fuel-oxidant reaction (probably CH or perhaps C_2 emission). It seems that low pressure extinction is due to convective heat loss at the flame periphery together with inefficient combustion associated with the escape of sublimed AP at the edges of the dark zone. These two forms of heat loss from the flame zone would explain the effect of strand size on the extinction pressure.

When burning LP3/GMF-AP propellant, it was observed that whenever the ash broke (under the influence of gravity) within about 2 mm from the regressing interface, then regression would immediately cease. This observation together with the fact that the burning rate curve changes character as soon as the ash starts forming, suggests that the presence of the ash is an important

aspect of the burning process. Ash formation is not a peculiarity of the mixture ratio, because the same phenomenon was observed for polysulfide propellant containing 75% bimodal AP. The pressure at which the transition to ash formation occurs is independent of the nature of the ambient gas (nitrogen or air). The ash itself is combustible; it is totally consumed when ignited in nitrogen or air above about 0.1 atm. Chemical analysis of the ash obtained from 35% LP3/GMF + 65% 5μ AP propellant ($\psi_c = 0.42$) has shown it to contain about 60% NH_4ClO_4 and about 10% NH_4Cl. Microscopic observation of the ash obtained from 25% LP3/GMF + 75% bimodal AP (5μ and 80μ in the ratio 30/70) revealed the presence of large unburned AP particles in the ash. The weight of ash obtained from the 35% LP3/GMF + 65% 5μ AP propellant at 0.03 atm amounted to about 30% of the original weight of the propellant. No accurate determination of the effect of pressure and particle size on this quantity could be made.

Burning at subatmospheric pressure is accompanied by the evolution of white fumes which solidify upon contact with a cold surface. In the case of LP3 propellant, it is larger in quantity and increases considerably as soon as the ash starts forming. This smoke was found to contain 25% ammonium perchlorate and 55% ammonium chloride. A trap was installed to determine the amount of smoke evolved per unit mass of propellant as a function of pressure and oxidizer particle size, but the results were inconclusive. The weight of sublimate caught was approximately 20% of the original weight of the propellant.

The presence of large amounts of AP in the ash as well as in the smoke constitute large sources of combustion inefficiency at low pressures. Another possible source of combustion inefficiency could be the ejection of AP particles from the regressing propellant surface. These would be carried into the afterburning zone where they burn up but contribute little towards the heat needed for gasification of the solid-phase propellant constituents at the regressing propellant surface. Microscopic examination of extinguished propellant surfaces revealed many deep holes, giving the impression that the oxidizer particles had been ejected from these holes. Those particles still intact were covered by a thin transparent yellow layer, like molten fuel. With 600μ particle size propellants many small particles were found lying at the bottom of the bell-jar after burning had taken place. Ohlemiller(145) has photographed particle tracks in the flame zone of PBAA-AP propellants. He calculated from the number of streaks that, under conditions of radiative-augmented burning or with 1% copper chromite additive, the AP ejection rate could be as high as 50% of that originally in the propellant, at low sub-atmospheric pressures.*

C. Discussion of Results; Relation to Earlier Experimental and Theoretical Findings

Low pressure burning behavior of composite solid propellants is critically dependent on fuel-type. One major determining

factor appears to be the relative meltability of the fuel. The low pressure extinction limit increases with increasing ease of melting of the fuel: (1), propellants with readily meltable fuels such as POLYOL/TDI and ESTANE/POLYOL, extinguish at several atm pressure; (2) propellants with obviously dry burning surfaces such as PBAA/EPON-AP, burn to pressures as low as 0.05 atm, and (3) PBHT/TDI-AP propellant which seems to be of intermediate meltability, extinguishes around 0.2 atm. Another major effect of the meltability of the fuel is shown by the fact that propellants with an obviously dry burning surface follow a straight line on the (log r) vs. (log p) plot, all the way down to the extinction pressure, whereas the propellants with meltable fuels all show a severe drop in the burning rate as soon as the extinction pressure is approached. Corroborative of these observed tendencies are our findings for PBHT/TDI-AP propellant with and without copper chromite: the addition of copper chromite changes the burning surface from molten to dry**, reduces the low pressure extinction limit from 0.18 atm to 0.05 atm, and removes the characteristic droop in the (log r) vs. (log p)curve near the extinction pressure; the curve becomes a straight line.

The anomalous low pressure burning behavior of PBHT/TDI-AP propellant is caused by expulsion of globules of molten fuel + AP particles from the burning surface into the afterburning zone leading to inefficient burning. This mechanism is plausible from a theoretical standpoint because below about 0.3 atm (where the anomalous behavior starts), the thickness of thermal layer in the solid phase below the surface and hence of the molten fuel layer, is large ($\sim$ 1 mm = 1000μ) compared to the mean AP particle size ($\sim$ 10μ). (See Fig.11). This mechanism is less likely to explain the high value of the low pressure extinction limit (several atm) for the propellants with the readily meltable polyurethanes of Section IV (ESTANE/POLYOL and POLYOL/TDI): as shown in Fig. 11, the depth of the thermal layer is only about 100μ at several atm and so, the melt is not likely to be thick enough to allow expulsion of AP particle + molten fuel mixture into the afterburning zone; furthermore, there is no physical evidence to suggest that such globules of propellant mixture are actually expelled from the flame zone in the case of these two polyurethane propellants. Thus, partial coverage

---

* It is interesting that a group of Russian workers, led notably by Bakhman, believe that there are regimes in which the dominant mode of heat release in the flame arises from the oxidizer particles burning up in the vaporized fuel gas stream as they are carried away from the surface. They consider this to be the normal mode, not the anomalous mode (as we do), but they do concede that under some circumstances such particle transport can lead to severe combustion inefficiency. This viewpoint is summarized in Ref.146.

** Presumably by allowing the same or more AP decomposition at a surface temperature that is lower than the melting temperature of the fuel.

of the AP particles at the burning surface by the molten fuel layer, as suggested in Section IV, is more likely to dominate during the low pressure burning of propellants based on POLYOL/TDI and ESTANE/POLYOL. More work is necessary to establish conclusively, the mechanism of burning at low pressure when the fuel is of the type that melts readily.

It is clear that when the burning surface is dry and charred as is the case with PBAA/EPON-AP, PBCT/EPOXY-AP and PBHT/TDI-AP-copper chromite, the burning process is more nearly "ideal". Comparison with the theoretical predictions shows that these propellants behave in a way that is in qualitative agreement with the granular diffusion flame theory when the $NH_3/HClO_4$ reaction stage is considered distended - they certainly do not correspond to the collapsed A/PA model. Most of the propellants studied by others (in Fig. 25) seem to be in qualitative accord with the distended A/PA-GDF model, also. Quantitative comparison between theory and experiment is not possible because combustion inefficiency, not accounted for by the theory, is an important factor in low pressure combustion.

In propellants with a dry burning surface, the pressure at which extinction occurs is dependent on the size of the strand. Pure radiative heat loss can not explain this. Both the predictions of theory and our observations of the flame indicate that the A/PA and O/F flame zones are thick enough (order of millimeters) at the extinction pressure, for the flame to be susceptible to convective cooling by the entrained ambient gases as well as to a significant loss of available heat due to escape of unreacted AP at the edges of the A/PA flame zone. No evidence has been found to show that radiative heat loss from the propellant surface is a major factor; radiative heat loss alone is not sufficient to account for the observed high values of the extinction pressure. Feinauer's(143) results, however, indicate that it is a contributory factor when carbon black has been added to the propellant.

It is relevant to mention that Ohlemiller(145) measured the regression rate of PBAA/EPON-AP propellant under conditions of radiative augmented burning at about 0.005 atm, almost ten times less than the extinction pressure of the propellant. He found, by comparing burning rates with radiative flux, that the overall burning process is endothermic to the amount of several hundred calories per gram of propellant. That the burning process is so highly endothermic at these low pressures is consistent with our deductions from our burning rates based on a distended A/PA-GDF flame model.

It seems that the mere presence of the ash is responsible for the ability of the LP3-AP propellant to undergo self-sustained combustion to pressures as low as 0.005 atm, an order of magnitude less than PBAA-AP and PBCT-AP propellants, and to maintain a relatively high burning rate at such low pressures. Two questions are of interest, one, why does it form, two, how does it sustain the burning rate. It is not clear why the ash forms. It may be

related to Bircumshaw and Newman's(20) discovery that only 30% of the original AP undergoes decomposition when the temperature is below about 350°C and that the remaining 70% is unreacted solid AP, and to the fact that the surface temperature and the temperature in the ash were measured by Most(140) to be 250-300°C. (The granular diffusion flame theory with a collapsed A/PA flame indeed predicts a low surface temperature, about 400°C below 0.01 atm.)

The LP3/GMF-AP burning-rate curve is the only curve that is similar in shape to that predicted by the GDF theory with a collapsed A/PA flame, when the activation energy of the surface reaction is 15 kcal/mole. (As is indicated in the review section, this value for E_s is reasonable.) Working backward from the measured asymptotic zero-pressure burning rate, the surface pyrolysis heat (including the endothermic dissociative sublimation step as well as the exothermic gas phase A/PA reaction step) comes out to be exothermic to the amount of 90 cal/gm. This figure falls 35% short of the previously assumed value of 130 cal/gm (based on the heats of transition of the various reaction steps and in rough agreement with the value measured at elevated pressure by Sabadell(91)). Considering the inaccuracies involved, it is indeed surprising that this defect is approximately the percentage of original AP found as undecomposed AP in the combustion product at these pressures. We therefore speculate that the A/PA reaction zone is the major source of heat in the pressure range where the ash forms. If so, then the shape of the burning rate curve implies that the reaction time of this zone τ_I becomes independent of pressure below 0.05 atm, in the ash formation regime, just like the theoretical burning rate curve for the collapsed A/PA model. We may then infer that the ash serves as a hot porous bed which ignites the desorbed NH_3 and $HClO_4$ vapors a short but fixed distance from the regressing interface and that this is the role of the ash in determining the unusual rate-pressure curve.

In this connection, it is pertinent to mention Pearson's(80) finding that hot solid surfaces drastically accelerate the ignition of these vapors. In line with our identification of the A/PA reaction zone as the major heat source, it is expected that both burning rate and extinction pressure are dependent on the total surface area of AP particles exposed to the A/PA reaction occurring in the pores of the ash. Thus, as observed experimentally, both burning rate and extinction pressure are dependent upon oxidizer particle size. (see footnote on p. 9). However, this interpretation is obscured by the fact that combustion inefficiency, an important parameter, is also expected to be particle size dependent.

It is to be noted that the peculiar behavior shown by the polysulfide propellant (LP3/GMF-AP) below about 0.05 atm could also be ascribed to the possibility that some solid phase interfacial reaction capable of generating about 100 cal/gm of heat, becomes rate-controlling at these very low pressures. The overwhelming importance of such a zeroth order solid phase interfacial

reaction would explain the observed zero slope of the (log r)-(log p) curve in this low pressure range, and would explain also the observed inverse dependence of burning rate on AP particle size. However, such a solid phase interfacial reaction has not been identified in its details, and furthermore, it does not seem necessary to assume the importance of such a solid phase reaction to explain the present results. Thus, for the present, the preferred interpretation of the behavior shown by the polysulfide-AP propellants at very low pressures, is that the A/PA reaction stage plays the dominant role in the burning process under these conditions. This interpretation, of a dominant A/PA stage, is consistent with all else that is known about the burning behavior of an AP propellant, whereas the interpretation of a dominating solid phase reaction is not -- the significance of the solid interfacial reaction would be invoked merely to explain the exceptional low pressure behavior shown by polysulfide-AP propellants.

D. Concluding Remarks

The results of this section show that the collapsed A/PA-GDF theory can not in general be used to describe AP composite propellant burning rate behavior. (The exception is LP3/GMF-AP propellant; it forms an ash.) However, as expected from theoretical considerations, the granular diffusion flame theory is in qualitative accord with subatmospheric burning rate data provided the A/PA reaction stage is considered distended. Extinction at low pressure of propellant strands whose burning surface is dry, appears to be due to the combined effect of convective heat loss with the surrounding ambient gases and loss of available heat due to loss of unreacted AP at the gaseous flame edges; when the fuel melts, it is the very presence of this molten layer that causes extinction to occur at considerably higher pressures.

Before leaving this account of this two-stage gas phase flame propagation theory and its various predictions we must concede that solid phase interfacial reactions and heterogeneous reaction between the $HClO_4$ vapor or products and the solid fuel cannot be ruled out on the basis of the experimental evidence at hand. However, there is no evidence that brings them in as major contributory heat sources. The gas phase driving source seems to account for all the known facts.

SECTION VI

MAJOR CONCLUSIONS OF THIS STUDY

Itemized, the major conclusions of this investigation are:

(1) In terms of what is known about the gaseous flame structure of AP-based composite solid propellants, those theories that are based on a chemical reaction gas diffusion flame structure appear the most credible.

(2) Of these theories, the granular diffusion flame theory, resulting in the formula, $1/r = a/p + b/p^{1/3}$, is the most successful in fitting the data of conventional AP-based rocket propellants (high AP content and medium-sized AP particles) in the range 1-100 atm. More specifically, the theory is valid in the 1-100 atm range for propellants with fuels that do not melt readily, as long as $d_m \lesssim 250\mu$ and $\psi_o \gtrsim (0.58 - 0.10 \log_{10} d_m)$. The defined range of validity of the GDF theory includes an AP-based CMDB propellant but not the corresponding DB propellant.

(3) The assumption of an effectively dry, planar burning surface in the GDF theory breaks down whenever the AP particle size or AP content is lower than defined by $\psi_o = (0.58-0.10 \log_{10} d_m)$, or whenever the fuel is of the type that melts readily.

(4) Under the circumstances specified by (3) a new phenomenon, intermittent burning, that is responsible for plateaus, mesas and intermediate pressure extinction, takes over; reduction of the AP particle size, or lowering of the AP content, or substitution of a more readily meltable fuel (i.e., that which forms a thicker molten layer), all progressively produce plateaus, mesas and intermediate pressure extinction ranges, in that order.

(5) It appears that this phenomenon of intermittent burning is caused by the presence of a molten fuel layer that covers the AP particles at the burning surface. This observation can be used to practical advantage in the sense that a hot plateau burning propellant can be produced by using a fuel that is known to form a molten layer on the regressing propellant surface. The ESTANE/POLYOL and POLYOL/TDI (polyurethane) binders of this study are two such fuel systems.

(6) The GDF theory breaks down at pressures above about 100 atm when the AP particles are of intermediate size ($\sim 20 - 250\mu$), and at pressures below 100 atm when the particles are large ($\gtrsim 250\mu$), due to the fact that the flame can no longer be considered one-dimensional.

(7) The assumption of a collapsed A/PA flame in the GDF theory breaks down below 1 atm; the A/PA stage must be considered distended below 1 atm and this affects the theoretical burning rate curve greatly.

(8) Normal-burning propellants, i.e., those with a dry burning surface such as PBAA/EPON-AP, conform in burning rate to the granular diffusion flame theory in the subatmospheric pressure range all the way down to about 0.05 atm.,but only when the A/PA reaction zone is considered distended in the theory.

(9) Combustion inefficiency in the form of unreacted AP in the combustion product is significant at low subatmospheric pressures.

(10) The dominant cause of low pressure extinction (at about 0.05 atm.) in the normal burning propellants of (8) in strand form appears to be convective cooling by the entrained ambient gases in the combustion chamber together with loss of available heat due to escape of unreacted AP from the edges of the A/PA flame zone. In motors under more nearly adiabatic conditions, these losses might be avoidable and still lower pressures might be attainable.

(11) The existence of a molten fuel layer can play a more important role in determining the low pressure extinction limit than the various heat loss mechanisms indicated in (10): it seems that extinction is caused by expulsion of globules of molten fuel + AP particles into the afterburning zone when the thermal layer and hence, the depth below the regressing surface to which the fuel is in the molten state, is large compared to the mean AP particle size; a molten fuel layer comparable in thickness to the mean size of the AP particles can cause extinction only by drowning of the AP particles.

(12) Exceptional behavior has been found with polysulfide (LP3/GMF)-AP propellant; it is able to burn to extremely low pressures (0.005 atm) because of the fact that it forms a protective ash that retains the heat of the exothermic A/PA flame close to the solid surface.

SECTION VII

EXTENDED CONSIDERATIONS FOR OTHER PROPELLANT SYSTEMS AND PHYSICAL SITUATIONS

This study has put on rational grounds the burning mechanism of AP-based composite solid propellants. By relying, in large measure, on the results of previous workers and by also confining attention to the still unknown areas, it was possible to define the domains in which different phenomena play the determining role. In this way, the range of validity of the granular diffusion flame theory could be defined. The success of these efforts lead to the conviction that the physico-chemical model underlying the GDF theory is the correct one for normal AP composite propellants; no other theory has been published that (1), conforms to all the known facts about the flame structure, (2), agrees quantitatively with the burning rates of normal AP propellants, and (3), finds rational explanation of its validity boundaries in terms of breakdown of some assumption, often predictable from the theory itself*.

Many of the details of the burning process undoubtedly remain to be explored. However, from a phenomenological standpoint, there appears little to be gained from further research in this area, unless, of course, contradictory evidence of a reliable nature should turn up. Therefore, it is now worthwhile to move ahead with studies designed to capitalize on the knowledge thus far obtained.

Many areas remain open for further study. Of particular interest as an extension to this project, are the effects of different oxidizers, catalyst additives and metal additives. The behavior of propellants under conditions of high pressure (100-1000 atm, and higher), centrifugal acceleration, erosive burning, and high ambient temperature, is still unknown from a combustion mechanistic standpoint. These all should be viewed in the light of the granular diffusion flame model. Another area that has received only cursory attention of late, is the realm occupied by double-base and composite modified double-base propellants. The following considerations, revealed by the literature and this investigation, should be borne in mind when extending the work to these areas of research.

---

*These are necessary but not sufficient conditions for proof of the validity of a theory of propellant burning. It would have been desirable to test also the burning rate-pressure dependence predictions of the GDF theory with respect to all other conceivable parameters, including the dependent variables such as, the surface temperature, the final flame temperature, and the thickness of the various reaction stages. However, presently available experimental techniques do not allow measurement of these other parameters with the accuracy required to test quantitatively the predictions of a burning rate theory.

A. Oxidizer Substitution

Much can be learned by noting the effects of substituting different oxidizers, particularly ammonium nitrate (AN) and potassium perchlorate (KP). They are the predecessers to AP in the solid propellant rocket industry and have consequently been subjected to much study(36,68,95,150-153). Their properties are fairly well known compared to other oxidizers currently receiving developmental attention. They therefore are of interest insofar as they help clarify the combustion mechanism of other more practical oxidizers. At present they have little practical value because of the low specific impulse of propellants based on them: KP yields a large proportion of KCl (high molecular weight) in the rocket exhaust gases and AN is not very energetic.

Most valuable for further elucidation of the combustion mechanism is the substitution of KP. It differs from AP in that it has an obviously mobile liquid layer at the burning surface(1,7), it is more stable than AP to thermal decomposition(36), but most interesting of all, it does not have the equivalent of an A/PA flame, i.e., an exothermic gas phase oxidizer decomposition flame very close to the regressing propellant surface(95). The consequences of the latter can best be determined by setting $\Delta h_I = \mathcal{T}_I = o$ (and $T_1 = T_s$) in the GDF theory. One obvious prediction that can be made without performing the calculations is that the absence of an exothermic reaction site close to the surface will cause KP propellants to extinguish sooner (at higher pressures) than AP propellants. Indications from the literature are that this is generally so. Another obvious result of not having an exothermic KP decomposition flame is that KP can not sustain combustion on its own.

It is interesting that the very absence of a fast exothermic oxidizer decomposition flame, close to the regressing surface of a KP propellant, may be construed as evidence that the exothermic A/PA reaction stage in the flame of an AP composite propellant is directly responsible for the particular combustion instability behavior and the particular very high pressure (above about 500 atm) burning rate behavior shown by AP propellants. Summerfield and Krier(154) note that AP propellants are far more prone to unstable burning than KP propellants and furthermore, their experimental and theoretical studies(127,154,155) show that the A/PA reaction stage is all important in determining the combustion instability behavior of an AP propellant. That the A/PA reaction stage is important for determining the very high pressure burning rate behavior of an AP propellant is suggested by Hall, Wenograd, and Coles(92) observation that a KP propellant has a much lower pressure exponent above 500 atm than is characteristic of an AP propellant in the same pressure range ($\sim$0.3 compared to $\sim$2.0). Corroborative of this assertion that the A/PA reaction stage is all important in determining the very high pressure burning rate of AP propellants, are their observations that AP particle size

and binder type have no effect on the burning rates of these propellants at these high pressures.

Because pure KP can not burn of its own accord, KP propellants with volatile fuels (NC-based DB fuels are excellant in this regard) may extinguish due to coverage of the fuel surface by the molten oxidizer ($KCl + KClO_4$)*, the inverse situation of what has been found at normal rocket pressures with the AP + readily meltable fuel mixtures of this study: KP is more stable to pyrolysis than the volatile fuel and so, the surface of the KP will project further into the O/F flame thereby providing ample opportunity for the molten oxidizer layer to overrun the fuel surface; coverage of the binder surface by the molten KP layer is expected to starve the O/F flame of the necessary fuel pyrolysis products+. The tendency toward intermittent burning would thus become greater with increasing KP particle size and KP loading.

Intermittent burning behavior is not expected with ammonium nitrate (also readily meltable) + nonmeltable-fuel propellants because the AN is not so stable thermally as either AP or KP(36) and furthermore, as indicated in Refs. 68 and 108, AN decomposes exothermally in the gas phase, the reactants being NH_3 and HNO_3, the dissociative gasification products of NH_4NO_3. The only time that intermittent burning could still occur is when a fuel that is considerably more volatile than AN (such as perhaps paraformaldehyde) is used; AN is not very energetic and so, it alone, probably could not sustain combustion if it were to cover the fuel.

The remarks made above concerning the possibility of finding intermittent burning with propellants based on KP and AN, are necessarily vague because the phenomenon of intermittent burning is still not well enough understood to make firm predictions. Furthermore, our knowledge of the relevant properties of the oxidizer and binder constituents, i.e., the relative meltability and the relative volatility, is at present only of a qualitative nature.

In comparing the effects of different oxidizers it should be borne in mind that oxidative potential varies from compound to compound. The oxidative potential would have a significant effect on the final adiabatic flame temperature and hence burning rate. For instance, in the case of AP, KP, and AN propellants, the stoichiometric (O/F) ratio decreases in the order

---

*Indications are that KCl, an inert to the combustion process, builds up in the molten layer of decomposing KP(95).

+It is unlikely that a premixed O/F flame could result due to mixing of the liquid fuel and the liquid oxidizer at the propellant surface. They are not easily miscible in the short period of time required (order of milliseconds); for this to be possible, both the liquid fuel and the liquid oxidizer must have low viscosity and also low surface tension.

KP > AP > AN (see Table III of Appendix B); generally, the burning rates decrease in that order also (150-153). Another factor to be remembered, although probably not too important in the combustion process because of the low temperatures involved, are the solid phase transitions that occur in various crystalline substances; AP has only one transition at 240°C(20) whereas AN has four in the temperature range below 150°C(36).

Other oxidizers of current practical interest are the high energy, fast burning rate, nonmetallic perchlorates such as hydroxyl ammonium perchlorate (HAP), hydrazinium monoperchlorate (HP), hydrazinium diperchlorate (HDP), and nitronium perchlorate (NP)(36). Unfortunately, their application is still plagued by developmental problems relating to their thermal stability, storability, impact and friction sensitivity, and hygroscopicity(36). The research effort in this field of high energy oxidizers is still in its infantile stages; only now, are papers starting to appear in this field (156-165). The only general remarks that can be made is that they usually melt around 200°C(36) and that they usually decompose in a manner similar to ammonium perchlorate, i.e., they go through a dissociative gasification step followed by an exothermic gas-phase reaction stage(36,160-162). More definitive results must become available before meaningful speculations as to the effect of these oxidizers can be made. The same is true of those oxidizers used as high energy additives such as RDX (cyclo trimethylene trinitramine) and HMX (cyclo tetramethylene tetranitramine)(36).

B. Catalyst Additives

Considerable work has been done concerning the effect of catalysts on the decomposition of AP. Jacobs and Whitehead(24) have recently reviewed the literature and find that catalysts generally fall into three catagories:

(1) Those which accelerate the high temperature reaction of AP ($> 350°C$) such as copper chromite and copper II oxide. (They probably promote heterogeneous decomposition of the gaseous perchloric acid (and/or ammonia).)

(2) Those which accelerate the low temperature reaction of AP ($< 300°C$) such as the ions, Ag^+, Cd^+, and the anions, MnO_4^-, ClO_3^-. (They could accelerate the proton transfer process but no concrete proposals have been made.)

(3) Those which cause the AP to melt and thereby accelerate the proton transfer initiation step, i.e., the metal oxides such as MgO, CdO, and ZnO. (The metal oxide is believed to combine with some of the AP to form the metal perchlorate which in turn forms a eutectic with the remaining AP.)

The catalysts of class (2) should have no significance on the burning rate of an AP composite propellant because of the

low temperatures at which they operate; reactions at these low temperatures ($< 300^{o}C$) are too slow compared to the stay time to be significant in propellant combustion; the fast, high-temperature reactions that follow, do all the chemical conversion in the burning of a solid propellant.

The mechanism proposed for catalysts of the third category, suggests that the action of these catalysts is to accelerate the dissociative gasification step of AP and to cause the AP to melt more so than it does when the catalyst is not present. This, of course, is subject to the conditions that either the catalyst is dispersed uniformly in the AP crystal lattice or, when the catalyst is not included in the AP, that the pressure is low enough so that the long times associated with slow burning rates may allow for sufficient spreading of the AP melt across the AP particles from the edges of the AP particles where the catalyst particles are. (It does not seem likely that significant gas-phase reactions in crevices between the solid fuel and the solid AP would be caused by these catalysts because the molten AP, if sufficiently mobile, would tend to fill up these crevices.) The result of faster dissociative gasification of AP can not be accounted for by the GDF theory as it stands at present, because this step is taken to be infinitely fast. The effect of a thicker, more mobile, molten oxidizer layer might be to induce intermittent burning if the binder is very volatile compared to the oxidizer and if conditions are such that the oxidizer can not sustain combustion on its own (see previous section).

The proposed action of class (1) catalysts is plausible for AP propellant burning at low pressures. However, it is hard to reconcile with the flame structure known to prevail at normal rocket pressures, unless, the catalyst is dispersed uniformly through the AP crystal lattice; in terms of the GDF theory, the A/PA flame is exceedingly thin compared to the mean AP particle size and so, it is unlikely that the gaseous $HClO_4$ (or NH_3) will be able to diffuse laterally across the AP crystal to the adjacent catalyst particles, there to react heterogeneously, before they, the NH_3 and the $HClO_4$, have a chance to react together in the A/PA flame. Neither is it likely that catalyst particles are attacked heterogeneously while they are being carried through the O/F flame - the stay time is short and also, the catalyst particles are present usually only in small quantities ($\sim$1% by weight). Yet, it is known that copper chromite, for instance, has a significant effect on the burning rate at all pressures, at least below 100 atm(1). Two possible modes of catalytic activity remain for the normal rocket pressure range: (1), one or more of the O/F flame reactants react heterogeneously with the surface of the catalyst particles while they are still embedded in the propellant surface, and (2), the existence of gas-phase or heterogeneous reactions in crevices between the solid fuel and solid AP is promoted by the presence of catalyst particles at the interface between the solid AP and solid fuel. The latter possibility seems more credible. This latter mechanism would

cause burning rate acceleration by virtue of accelerated AP decomposition kinetics and also, by virtue of the increased area for gasification of the propellant constituents; the burning surface would be conical around each catalyst particle.

The high speculative nature of the previous paragraphs is a direct indication of how little is known about the details of catalyst effects. This is the case despite the great deal of work that has been done already. The only way in which the mechanism could be fully resolved is to do systemic tests concerning the effects of various catalysts on the burning rate-pressure dependence of propellants, together with direct microscopic observations of the details of the regressing propellant surface. The latter is by far the most difficult. One interesting set of tests that does not appear to have been done, and that would clarify many of the previously outlined thoughts, is to determine the burning rate-pressure dependence and the microscopic surface structure of (1), a propellant without catalyst, (2), the same propellant with fine catalyst particles mixed uniformly in with the fuel and oxidizer, and (3), the same propellant with the same amount of the same catalyst, present now as a uniformly dispersed inclusion in the AP crystal structure.

C. Aluminum Additions

The interest in aluminum for solid propellants stems from the fact that its addition produces a high specific impulse (151,166) and furthermore, it suppresses combustion instability(154,167,168). Studies concerning the effects of aluminum addition have been mainly of qualitative nature, attention being confined almost exclusively to the structure of the flame.

It has been found quite generally that the aluminum accumulates on the propellant surface in molten form. Refs. 165, 168 to 173 show that the Al particles melt as they emerge from the propellant surface and then agglomerate. The agglomerates remain on the propellant surface for a short period of time and are then carried off by the surrounding gas stream into the afterburning zone. Soon after the molten aluminum emerges from the propellant surface, it is covered by an oxide layer due to heterogeneous surface attack by the surrounding oxidizer gases. The oxide layer resists further chemical attack. A luminous zone is established around the agglomerate soon after it leaves the propellant surface (sometimes also while it is still on the propellant surface). The agglomerates do not decrease noticeably in size before they leave the gaseous (O/F) flame zone.

Crump has made systematic measurements of the average Al agglomerate size(171) as a function of various propellant parameters and has found that it depends only on the amount of Al present in the space between adjacent AP particles, i.e., it

depends only on AP particle size and aluminum content but not on aluminum particle size, at least, not as long as the Al particle size is smaller than about 150μ. Crump found that the average size of the Al agglomerates is of order 100-300μ, even when the original Al particles are as small as 5μ.

The effect of added aluminum on the burning rate of a composite propellant is hard to predict because there are several competing effects:

(1) The Al particles have high heat capacity and act as a heat sink while being heated to the propellant surfact temperature; heat that may otherwise be used to effect decomposition of the fuel and AP, is used up and as a result, the burning rate decreases.

(2) Heat feedback into the solid phase interior from the gaseous flame is increased locally by the high conductivity of each Al particle; the burning surface regresses conically around each Al particle and so, the burning rate increases by virtue of the increased surface area for gasification. (This effect is far more important for Al wires than for spherical Al particles (16,174)).

(3) The molten Al tends to accumulate, forming a blanket over the propellant surface(168,171); it might suppress the decomposition of the fuel and AP, thereby decreasing the burning rate. (This effect has been observed with propellants with abnormally high Al concentrations(171) and also for aluminized propellants burning in acceleration fields(175,176); these acceleration forces prevent the Al agglomerates from leaving the propellant surface and escaping into the afterburning zone (175-178).)

(4) The Al agglomerates burn partially in the gaseous flame zone and the effect of the heat released in this flame zone is to increase the burning rate; in terms of Crump's pocket model for aluminized propellant burning(171), the burning rate should then be dependent on aluminum content but not on the mean particle size of the Al.

(5) The Al agglomerates burning in the gaseous flame zone and in the afterburning zone, radiate heat back to the propellant surface and the effect of this is to cause a higher burning rate(6,179). (This effect is small for the usual composite propellant mixtures because as shown by direct measurement in Ref. 6, the radiative heat feedback contribution from the hot Al agglomerates amounts to no more than 10% of the total heat fed back to the propellant surface*.)

(6) The Al agglomerates pass through the O/F flame zone unreacted and burn up far away from the propellant surface; the heat released by the Al burning far away from the propellant surface, has no effect on the burning rate but the heat needed to melt the Al reduces the burning rate slightly.

The most important of the above six possible effects of Al addition can be identified by a process of elimination. As has been noted already, the effect of radiative heat feedback (Item (5) above) is expected to be minor for most AP-Al based propellant mixtures (O/F flame temperature usually less than about 2600°K). Also mentioned before is that the effect of suppressing AP and binder decomposition by forming a molten Al blanket (that covers the propellant surface (Item (3))), is important only for propellants with abnormally high Al content or aluminized propellants burning in strong acceleration fields.

The roles played by factors (1) and (2) above, are harder to assess. It is doubtful whether the effects of Al acting as a thermal ballast in the solid phase heat-up zone (Item (1)) and of Al causing local increased heat conduction into the solid phase heat-up zone (Item (2)), will result in a significant increase of burning rate when the Al particles are small and spherical, as they usually are: these effects counteract each other, but more important, the net result of these effects, still felt, will be restricted to the depth of one Al particle diameter below the propellant surface. The views expressed in this paragraph are confirmed by implication of the success of the findings described in the paragraph below.

Whether the Al agglomerates release a significant amount of heat in the flame zone (Item (4)) and thereby effect the burning rate, or whether they act purely as an inert condensed-phase material passing through the flame zone (Item (6)), can be inferred from the results of a systematic study done by Hart and Merkle(181) of the parameters affecting the burning rate-pressure dependence of aluminized AP propellants. They found that: (a), the burning rate of an aluminized propellant is independent of the Al particle size, at least, as long as this particle size is smaller than about 150u; (b), the effect of increasing Al content while keeping AP content constant, is to increase the burning rate significantly; and (c), changing Al content does not change the burning rate provided the AP/binder ratio is kept constant. These results are all in agreement with Crump's findings of the structure of an aluminized propellant flame (summarized earlier).

---

*However, when the O/F flame temperature exceeds about 2600°K, the melting temperature of the oxide layer that covers the Al agglomerates, i.e., when the propellant has a high AP content, the Al will burn in the gas phase(180) and the Al will then radiate heat back to the propellant surface at an effective black body temperature that is much higher than the local equilibrium temperature(179); according to Ref. 180, the radiative heat feedback contribution could then be as high as the conductive heat feedback from the O/F flame, i.e., as much as 30% of the total heat feedback. It should be noted also that the radiative heat feedback will be dependent on pressure, because the radiating temperature is itself pressure dependent.

The above findings of Hart and Merkle, as well as the subsequent calculations of Hart(181) based on these results, show that Al acts merely as an inert in the flame zone of an AP propellant, at the most, absorbing the small amount of heat needed to melt the Al at the propellant surface. Any burning rate changes that come about by the addition of Al, will be by virtue only of the fact that the AP/binder ratio of the propellant has been changed. In fact, the burning rate of an aluminized propellant can be predicted merely as the burning rate of an unaluminized propellant with the same ratio of AP to binder. The implication of this conclusion is that the other five possible effects of Al additions (listed before) are not important in the burning process of an AP propellant.

D. Effects of Different Fuels

The effect of fuel-type on the burning mechanism of a composite solid propellant has been covered to some extent by this investigation. It was found that the burning behavior of these propellants is linked directly to the gross meltability properties of the fuel. Further progress is hindered by the fact that the detailed degradation mechanism of polymeric systems under the high temperature and surface heating rate conditions encountered in propellant combustion, is unknown. Most desirable would be information regarding the heat of gasification, the kinetics of degradation, and the gaseous pyrolysis products. (The present understanding of fuel decomposition at low temperature and during bulk heating can not be extrapolated to the conditions of a burning propellant - at most, one can only make educated guesses of the gross behavior properties, as has been done in this investigation).

Methods of obtaining the desired information are difficult to contrive. At present, it seems that the study of the behavior of the fuel during steady radiative heating, together with radiometer surface temperature measurements conducted at a wavelength different from that of the radiative input, would be the most rewarding. (The disadvantages of the hot-plate and porous-plate technigues of surface heating of fuels are that the degradation products coat the plate or clog the pores, and also, the surface temperature can not be accurately measured.) The knowledge thus gained, will permit more exact description, in the GDF theory, of the role played by the fuel. In consequence, more accurate burning rate predictions should be possible.

E. Pure Double-Base Propellants

Considerable effort went into the study of double-base (DB) propellants, particularly during the 1940's and early 1950's(91,95,101,102,128,131-136,182-186). However, since the advent of ammonium perchlorate-based composite solid propellants in the last decade, the interest in the mechanism of burning of pure DB propellants has been only spasmodic. As a

result, the armament rocket and gun ballistics industry which still makes extensive use of DB formulations, must rely heavily on expensive and time-consuming development of an empirical nature, much more so than the industry using AP composite propellants. The benefit to be derived from further detailed study of DB propellants is obvious.

The general structural features of double-base propellant flames are fairly well known. It is generally agreed that DB propellant, usually a colloid of NC with NG, TEGDN, or DEGDN (see list of abbreviations), burns with a three-stage flame (132-134). The first stage is believed to be a zeroth order (with respect to pressure), net exothermic solid-to-gas reaction in which the rate-determining step is the breaking of the N-O bond of the nitro-organic material(131,183-185). This is believed to occur in the "foam-zone" below the propellant "surface"(102). The surface temperature is about 500°K(91,134). The first reaction stage produces NO_2, aldehydes, etc., which react vigorously in the gas phase, the second stage, very close to the propellant surface. The products of this second stage (NO + oxidizible material) then react in a third, gaseous, stage further out in the gas stream(131,133). About half the total heat of reaction of the propellant is already expended at the end of the second reaction stage and the temperature is then about 1500°K(131). The remaining heat of reaction is released in the third stage and this release of heat causes the final flame temperature to be about 3000°K(131). The distance of the third reaction zone from the propellant surface is strongly dependent on the pressure(128,131,132); at low pressure ($\sim$10 atm), this reaction zone is preceded by a thick ($\sim$ 1 cm) dark zone in which no reaction occurs; this dark zone quickly diminishes to zero thickness (the luminous fronts of the 2nd and 3rd stages merge) when the pressure is increased beyond 50 atm. Below 40 atm, the total measured heat of reaction diminishes rapidly with reduction in pressure until, at about 10 atm, the heat of reaction is about half its high pressure (and theoretical) value(131,133,186). This severe drop in the heat of reaction is probably due to the fact that in low pressure strand burnings, there is ample opportunity for the partially reacted gases to escape from the edges of the thick dark non-reacting zone into the surrounding atmosphere.

The above findings concerning the flame structure imply that the burning rate at high pressure depends on the heat generated in all three stages, whereas, at low pressure, it depends only on the heat generated in the first, zeroth order stage. In detail, this first stage probably consists of an endothermic gasification step followed by an exothermic gas phase reaction, just like the first stage of an AP composite propellant flame. It is not certain whether this first stage responds to pressure just like the A/PA flame, i.e., distends with reduction in pressure to finally cause extinction, or, whether the exothermic gaseous step of the 1st stage is entrapped in the foam zone, thus retaining the heat generated (like the polysulfide propellant of this study). The former

possibility leads to a pressure exponent near unity at low pressure while the latter possibility yields a pressure exponent that tends to zero at low pressure. Both types of burning rate behavior have been observed with various propellant formulations(131). It has been suggested that those additives that cause a zero pressure exponent at low pressure, do so because they promote the surface reaction(131). Other additives produce further complicating features such as plateaus and mesas at intermediate pressures(135,136). The action of these additives is not fully understood. The problem is really that no burning rate measurement series have been made in which the many propellant parameters have been systematically varied. Thus, no systematic trends or regularity in the burning rate behavior can be discerned from the data. So, it is not yet possible to make meaningful interpretations as to the combustion mechanism; the position is still too murky to venture any specific predictions concerning the burning rate behavior.

Two theories of DB propellant burning have been formulated on the basis of the previously described picture of propellant burning(101,102). They are expectedly involved. They contain so many unknown, and hence adjustable parameters that testing of their validity is impossible at this stage. Even so, the paucity of data precludes meaningful comparison with the theoretical predictions. A systematic survey of DB propellant burning rate behavior is long overdue.

The position with composite modified double-base propellants is similar, although not so severe. Here again, very few studies have been made. The findings of this investigation suggest that CMDB propellants burn in a fashion similar to the common composite propellants. The nature of the DB fuel does not seem to be so important when AP is added and the complexities of the two-stage flame with its concomitant problem of combustion inefficiency, seem to disappear. Thus, it appears that much of the information needed to understand the mechanism of CMDB propellant burning can be drawn from that which has been learned about the common AP composites.

F. Propellant Behavior Under Other Physical Conditions

The present understanding of the steady state burning behavior of propellants in the domain of high pressure (above 100 atm) is poor. There have not been sufficiently many studies of the burning rate behavior and flame structure to establish conclusively the dominant mechanism of burning at these very high pressures. Several mechanisms have been proposed (see Section II) but more experimental work is necessary before the applicability of any of the proposed theories(93,96,116) can be determined.

Of obvious practical interest is also the response of a solid propellant to high initial temperature conditions(187); at present, the rocket engineer must still rely on empirical

data concerning the effect of this parameter. The prediction of burning rate as a function of initial temperature is the natural outcome of any theory of propellant burning. It is necessary to compare the predictions of the theory with the data. Such comparisons are all too little done. In this context, it is to be noted that nothing can be learned of the fundamental combustion mechanism if tests are made in which this parameter is varied, because all possible reactions within the flame wave are strongly temperature dependent and the functional relationship is approximately the same in all cases; the result of a particular reaction can not be separated from overall propellant performance data if only the initial temperature is varied.

The behavior of propellants in nonsteady pressure fields, in fields of high centrifugal acceleration, and under conditions conducive to erosive burning, should also be predictable from the fundamentals of the burning process. In many cases, such prediction is still not possible. Sometimes, the physics of the burning process are not adequately accounted for. Often, the reason for this is that the problem is so complex that the details of the flame wave can not be inferred from the overall propellant burning characteristics alone; also, direct, detailed observations of the structure of the flame are usually not possible in these difficult physical situations. Thus, recourse must be had to the knowledge gained from the study of propellants burning under conditions of steady-state in which the outside influences of gasdynamic pressure, temperature, and velocity fields, etc., are absent. In essence, we should incorporate, or at least be consistent with, the detailed propellant combustion model that has been developed for steady state conditions.

To review the state of affairs concerning the burning behavior of propellants in the previously mentioned, more complex physical situations is beyond the scope of this work. However, a few brief remarks seem appropriate.

All theories for the burning behavior in an erosive environment(188-193) result in expressions that relate the augmentation in the burning rate to the heat transferred through the boundary layer, from the hot by-flowing combustion product gases to the regressing propellant surface. The consequences of the combustion zone close to the propellant surface are left as a side issue. It would be useful now to include this combustion zone into the theoretical formulation. Only then can absolute burning rate predictions be made for propellants burning in an erosive environment, as a function of the independent propellant parameters of importance.

It is surprising that some theories of nonsteady solid propellant burning(194-196) deny even the most obvious facts concerning the structure of a composite propellant flame, such as its heterogeneity. Much of the turmoil in this field is caused by an insistance to use simple one-stage premixed flame

theories for composite solid propellants. (These theories probably do not apply to homogeneous DB propellants either; DB propellant flames consist of several stages.) For a more detailed criticism of previous nonsteady theories, and for a presentation of a new approach that recognizes the flame zone, see Ref.127.

Examples of where attempts have been made to include the known flame structure of a composite solid propellant, are those theories that have been proposed for the burning behavior when the propellant is subjected to high acceleration fields: Glick's theory(178) for unaluminized propellant employs the GDF model, and Crowe's theory(177) for aluminized propellants (later modified by Glick(178)) takes account of already published flame structure observations. However, these theories have only met with partial success (in the sense that only qualitative behavior trends are explained). So, it is apparent that, here too, further work is required.

LIST OF SYMBOLS

a - chemical reaction time parameter in burning rate equations (15), (18) and (19)

b - diffusion time parameter in burning rate equations (15) and (18)

a' - chemical reaction time parameter in burning rate equation (14)

b' - diffusion time parameter in burning rate equation (14)

c - specific heat; also diffusion time parameters in burning rate equation (19)

d - mean oxidizer particle size

d_g - effective diameter of gaseous fuel pockets

p - pressure

r - burning rate

x - distance from propellant surface (Fig. 1)

y_1 - mass fraction of large particles in bimodal particle size distribution

A - pre-exponential factor for surface pyrolysis reaction (Eq. (5))

B - pre-exponential factor for gas phase reaction (Eq. (7))

D - diffusion coefficient

E - activation energy

L - thickness of zones in propellant flame (Fig. 1)

M - Molecular weight

Q - conductive heat feedback from gaseous reaction stage to propellant surface per unit mass of propellant consumed

$\dot{Q}$ - conductive heat flux from gaseous reaction stage to propellant surface

R - universal gas constant

T - absolute temperature

V - average gas velocity

Δh - enthalpy required to effect a change of state

α_c - $(\lambda/\rho c)_c$ - thermal diffusivity of solid phase

α - constant related to a through equations (14) and (15)

β - constant related to b through equations (14) and (15)

ϵ - emissivity of propellant surface

λ - thermal conductivity

μ - average mass of gaseous fuel pockets

ρ - density

σ - Boltzmann constant

τ - reaction time

ψ_o - equivalence ratio (defined in footnote on p. 15)

Subscripts

I - first stage gas phase reaction zone (A/PA flame)

II - second stage gas phase reaction zone (O/F flame)

1 - condition at end of stage I (A/PA flame)

2 - condition at end of stage II (O/F flame)

ad - adiabatic condition

c - solid phase

eff - effective value

f - flame front around each gaseous fuel pocket

g - gas phase

l - mean diameter of large particles in bimodal particle size distribution

m - mean diameter of oxidizer particles (unimodal or bimodal distribution)

o - initial condition

s - propellant surface (or mean diameter of small articles in bimodal particle size distribution)

tr - orthorhombic to cubic lattice phase change in solid AP

LIST OF ABBREVIATIONS

Oxidizers:

AN	- Ammonium nitrate
AP	- Ammonium perchlorate
KP	- Potassium perchlorate

Binders:

(See Table IV of Appendix B for exact chemical formulations.)

EPON/TETA	- Epoxy with amine cure and plasticizer.
ESTANE/POLYOL	- Diisocyanate terminated polyester with polyol cure (a polyurethane).
LP3/GMF	- Polysulfide with dioxime cure.
NC/TEGDN	- Nitrocellulose in triethylene glycol dinitrate (a plastisol).
P13	- Polyesterstyrene (free radical polymerized).
PBAA/EPON	- Polybutadiene acrylic acid with epoxy cure.
PBAN/MAPO	- Polybutadiene acrylic acid acrylonitrile with imine cure.
PBCT/EPOXY	- Carboxyl terminated polybutadiene with epoxy cure.
PBHT/TDI	- Hydroxyl terminated polybutadiene with diisocyanate cure (a polyurethane).
PF	- Paraformaldehyde (polyoxymethylene).
PIB/MAPO	- Polyisobutylene with imine cure and plasticizer.
POLYOL/TDI	- Polyol with diisocyanate cure (a pulyurethane).
PVC/DBS	- Polyvinylchloride in dibutyl sebacate (a plastisol).

Chemicals:

DBP	- Dibutyl phthalate (Fisher Scientific Co.).
DBS	- Dibutyl sebacate (Matheson, Coleman and Bell).
DOA	- Dioctyl adipate (Pfaltz and Bauer, Inc.).

EPON 812	- Epoxy (Triglycidyl ether of glycerol) (Shell Chemical Co.).
EPON 828	- Epoxy (Diglycidyl ether of bisphenol A) (Shell Chemical Co.).
ERL 0500	- Epoxy (N,N - Diglycidyl-p-aminophenyl ether) (Union Carbide Co.).
ESTANE	- Diisocyanate terminated polyol (B. F. Goodrich Chem. Co.).
FERRO 121	- Barium ricinoleate (modified, (Ferro Corporation).
GMF	- Paraquinone dioxime.
LECITHIN	- Phosphatidyl choline (W. A. Cleary Corporation).
LP3	- Polysulfide (Thiokol Chemical Corp.).
LUPERSOL DDM	- 60% Methyl ethyl ketone peroxide in dimethyl phthalate (Wallan & Tiernan Co.).
MAPO	- Tris [1-(2-methyl) aziridinyl] phosphine oxide (Interchemical Corp.).
NC	- Nitrocellulose (component of Ball powder "A" consisting of 98.5% NC (12.6%N) and 1.5% 2 Nitrodiphenylamine) (Olin Mathieson Chemical Corp.).
NG	- Nitroglycerine.
P13	- Polystyrene-polyester copolymer (Rohm & Haas Co.).
PBAA	- Polybutadiene acrylic acid copolymer (American Synthetic Rubber Corp.).
PBAN	- Polybutadiene acrylic acid acrylonitrile terpolymer (B. F. Goodrich Chem. Co.).
PBCT	- Carboxyl terminated polybutadiene (Hycar) (B. F. Goodrich Chem. Co.).
PBHT	- Hydroxyl terminated polybutadiene (PBD-R-45) (Sinclair Petrochemicals Inc.).
PF	- Paraformaldehyde (Matheson, Coleman and Bell).
PIB	- Carboxyl terminated polyisobutylene (Enjay Chem. Co.).
Polycin 51	- Propylene glycol monoricinoleate (Baker Caster Oil Co.).

Polyol	- Mixture of PPG and TMP (proportions given Table IV).
PPG	- Polypropylene glycol (Voranol P-2000) (Dow Chemical Co.).
PVC	- Polyvinyl chloride (Geon 121) (B. F. Goodrich Chem. Co.).
TDI	- Toluene diisocyanate (Hylene-T) (E. I. duPont de Nemours & Co., Inc.).
TEGDN	- Triethylene glycol dinitrate (Propellex, Div. of Chromalloy Corp.).
TETA	- Triethylene tetramine (Matheson, Coleman and Bell).
TMP	- Trimethylol propane (Celanese Chemical Co.).
S	- Sulphur (Matheson, Coleman and Bell).
St. Oct.	- Stannous Octoate (K & K Laboratories, Inc.).

LIST OF REFERENCES

1. Summerfield, M., Sutherland, G. S., Webb, M. J., Taback, H. J. and Hall, K. P., "Burning Mechanism of Ammonium Perchlorate Propellants," Solid Propellant Rocket Research, Progress in Astronautics and Rocketry Series, Vol. 1, Academic Press, New York, 1960, pp. 141-182.

2. Steinz, J. A. and Summerfield, M., "Mechanism of Burning of Composite Solid Propellants with Special Reference to Low Pressure Combustion Phenomena," To be published in Advances in Chemistry Series, American Chemical Society, 1969; presented at the Symposium on Manufacture, Hazards and Testing of Propellants, 153rd National Meeting, American Chemical Society, Miami, Florida, April 9-14, 1967.

3. Steinz, J. A., Stang, P. L. and Summerfield, M., "Effects of Oxidizer Particle Size on Composite Solid Propellant Burning: Normal Burning, Plateau Burning and Intermediate Pressure Extinction," Proceedings of the 4th ICRPG Combustion Conference, CPIA Publication No. 162, Vol. 1, Dec. 1967, pp. 499-512.

4. Steinz, J. A., Stang, P. L. and Summerfield, M., "The Burning Mechanism of Ammonium Perchlorate-Based Composite Solid Propellants," AIAA 4th Propulsion Joint Specialist Conference, Cleveland, AIAA Preprint 68-658, June 1968.

5. Blair, D. W., Bastress, E. K., Hermance, C. E., Hall, K. P. and Summerfield, M., "Some Research Problems in the Steady-State Burning of Composite Solid Propellants," Solid Propellant Rocket Research, Progress in Astronautics and Rocketry Series, Vol. 1, Academic Press, New York, 1960, pp. 183-206.

6. Zenin, A. A., Glaskova, A. P., Leipunski, O. J. and Bobolev, V. K., "Effects of Metallic Additives on the Deflagration of Condensed Systems," Twelfth Symposium (International) on Combustion, University of Poitiers, France, July, 1968, Paper No. 4.

7. Sutherland, G. S., "The Mechanism of Combustion of an Ammonium Perchlorate-Polyester Resin Composite Solid Propellant," Ph.D. Thesis, Department of Aeronautical Engineering, Princeton University, May, 1956.

8. Povinelli, L. A., "A Study of Composite Solid-Propellant Flame Structure Using a Spectral Radiation Shadowgraph Technique," AIAA J., Vol. 3, No. 9, 1965, pp. 1593-1598.

9. Derr, R. L. and Osborne, J. R., "Temperature Profile Measurements in a Composite Solid Propellant Flame," Proceedings of the 4th ICRPG Combustion Conference, CPIA Publication No. 162, Vol. 1, Dec. 1967, pp. 491-497.

10. Penzias, G. J., Liang, E. T. and Tourin, R. H., "Infrared Radiation and Temperature Measurements in Solid Propellant Flames. I. Preliminary Study of Arcite 368," The Warner and Swasey Company Rept. TR-800-5, Oct. 1962.

11. Waesche, R. H. W., "The Effects of Pressure on the Emission Spectra of Solid Propellants," Proceedings of the 3rd ICRPG Combustion Conference, CPIA Publication No. 138, Vol. 1, Feb. 1967, p. 123.

12. Cole, R. B. and Wenograd, J., "Solid Propellant Combustion Mechanism Studies," Aerospace and Mechanical Sciences Rept. No. 446-o, Princeton University, June, 1965.

13. Silla, H., "Burning Rates of Composite Solid Propellants at Subatmospheric Pressure," ARS J., Vol. 31, No. 9, 1961, pp. 1277-1278.

14. Bastress, E. K., "Modification of the Burning Rates of Ammonium Perchlorate Solid Propellants by Particle Size Control," Ph.D. Thesis, Department of Aeronautical Engineering, Princeton University, Jan. 1961.

15. Bernard, R. A. and Wilhelm, R. F., "Turbulent Diffusion in Fine Beds of Packed Solids," Chem. Eng. Progress, Vol. 46, May 1950, pp. 233-244, cited by Ref. 1.

16. Rumbel, K. E., "Polyvinyl Chloride Plastisol Propellants," to be published in Advances in Chemistry Series, American Chemical Society, 1969; presented at the Symposium on Manufacture, Hazards and Testing of Propellants, 153rd National Meeting, American Chemical Society, Miami Beach, Florida, April 9-14, 1967. Also with other authors: Quarterly Reports dating back to 1952, Atlantic Research Corporation, Alexandria, Virginia.

17. Adams, G. K., Newman, B. H. and Robins, A. B., "The Combustion of Propellants Based Upon Ammonium Perchlorate," Eighth Symposium (International) on Combustion, The Williams & Wilkins Co., Baltimore, 1962, pp. 693-705.

18. McAlevy, R. F., Lee, S. H., Lastrina, F. A. and Samurin, N. A., "Further Studies of Ammonium Perchlorate Composite Propellant Deflagration by Means of Burner Analog Techniques," AIAA Preprint 67-101, AIAA 5th Aerospace Sciences Meeting, New York, Jan. 23-26, 1967.

19. McAlevy, R. F., Lee, S. Y., Cole, R. B., Lastrina, F. A., Samurin, N. A., "Investigation of the AP Composite Solid-Propellant Deflagration Mechanism by Means of Experimental Analog Techniques," AIAA J., Vol. 6, No. 7, 1965, pp. 1243-1251.

20. Bircumshaw, L. L. and Newman, B. H., "The Thermal Decomposition of Ammonium Perchlorate I," Proc. Royal Soc. (London), Vol. A227, No. 1168, 1954, pp. 115-132.

21. Bircumshaw, L. L. and Newman, B. H., "The Thermal Decomposition of Ammonium Perchlorate II," Proc. Royal Soc. (London), Vol. A227, No. 1169, 1955, pp. 228-241.

22. Jacobs, P. W. M. and Russell-Jones, A., "On the Mechanism of the Decomposition of Ammonium Perchlorate," AIAA J., Vol. 5, No. 4, 1967, pp. 829-830. Also Proceedings of the 3rd ICRPG Combustion Conference, CPIA Publication No. 138, Vol. 1, 1967, pp. 19-25.

23. Hall, A. R. and Pearson, G. S., "Ammonium Perchlorate: A Review of Its Role in Composite Propellant Combustion," R. P. E. Techn. Rept. 67/1, Jan. 1967. (To be published in part in "Oxidation and Combustion Reviews," Vol. 3, Elsevier).

24. Jacobs, P. W. M. and Whitehead, H. M., "Decomposition and Combustion of Ammonium Perchlorate," Final Report to Department of the Navy, U. S. Naval Weapons Center, China Lake, Calif., under Contract N60530-12591, by Department of Chemistry, University of Western Ontario, London, Ontario, Canada, Feb. 1968.

25. Mack, J. and Wilmot, G., "Infra-Red Spectra of Species Sublimed from Ammonium Perchlorate," Symposium on Molecular Structure and Spectroscopy at Ohio State University, Paper I3, June 11-15, 1962, cited by Ref. 22.

26. Heath, G. A. and Majer, J. R., "Mass Spectrometric Study of the Thermal Decomposition of Ammonium Perchlorate," Trans. Faraday Soc., Vol. 60, No. 502, 1964, pp. 1783-1791.

27. Von Elbe, A., King, M. K., McHale, E. T., Macek, A., Friedman, R. and Levy, J. B., "Chemical-Kinetic and Physical Processes in Composite Solid Propellant Combustion," Atlantic Research Corp. Rept. No. 66307, Jan. 1967.

28. Inami, S. H., Rosser, W. A. and Wise, H., "Dissociation Pressure of Ammonium Perchlorate," J. Phys. Chem., Vol. 67, No. 5, 1963, pp. 1077-1079.

29. Powling, J. and Smith, W. A. W., "The Surface Temperature of Burning Ammonium Perchlorate," Combustion and Flame, Vol. 7, No. 3, 1963, pp. 269-275.

30. Schultz, R. D. and Dekker, A. O., "Transition-State Theory of the Linear Rate of Decomposition of Ammonium Perchlorate," Sixth Symposium (International) on Combustion, Reinhold Publishing Corp., New York, 1957, pp. 618-626.

31. Sammons, G. D., "Application of Differential Scanning Calorimetry to the Study of Solid Propellant Decomposition," Proceedings of the 3rd ICRPG Combustion Conference, CPIA Publication No. 138, Feb. 1967, pp. 75-83.

32. Raevski, A. V., Manelis, G. B., Boldyrev, V. V. and Votinova, L. A., "The Part Played by Dislocations in the Thermal Decomposition of Ammonium Perchlorate Crystals," Doklady Akad. Nauk S.S.S.R., Vol. 160, 1965, pp. 1136-1137. Also Translation in Proc. Acad. Sci. U.S.S.R., Physical Chemistry Section, Vol. 160, 1965, pp. 158-159.

33. Aarden, E. A., Powling, J. and Smith, W. A. W., "Observations on the Burning of Ammonium Perchlorate," Combustion and Flame, Vol. 6, No. 1, 1962, pp. 21-33.

34. Levy, J. B. and Friedman, R., "Further Studies of Ammonium Perchlorate Deflagration," Eighth Symposium (International) on Combustion, The Williams & Wilkins Co., Baltimore, 1962, pp. 663-672.

35. Friedman, R., Nugent, R. G., Rumbel, K. E. and Scurlock, A. C., "Deflagration of Ammonium Perchlorate," Sixth Symposium (International) on Combustion, Reinhold Publishing Corp., New York, 1957, pp. 612-618.

36. Sarner, S. F., "Propellant Chemistry," Reinhold Publishing Corp., New York, 1966, p. 296.

37. Hart, R. W. and McClure, F. T., "Combustion Instability: Acoustic Interaction with a Burning Propellant Surface," J. Chem. Phys. Vol. 30, No. 6, 1959, pp. 1501-1514.

38. Andersen, W. H. and Chaiken, R. F., "On the Detonability of Solid Composite Propellants," Tech. Memo. No. 809, Aerojet-General Corp., Jan. 1959. Cited by Ref. 39.

39. Andersen, W. H. and Pesante, R. E., "Reaction Rate and Characteristics of Ammonium Perchlorate in Detonation," Eighth Symposium (International) on Combustion, The Williams and Wilkins Co., Baltimore, 1962, pp. 705-710.

40. Coates, R. L., "Linear Pyrolysis Rate Measurements of Propellant Constituents," AIAA J., Vol. 3, No. 7, 1965, pp. 1257-1261.

41. Barrère, M. and Williams, F. A., "Analytical and Experimental Studies of the Steady-State Combustion Mechanism of Solid Propellants," 25th Meeting of the AGARD Combustion and Propulsion Panel, La Jolla, April 1965.

42. Powling, J., "The Combustion of Ammonium Perchlorate-Based Composite Solid Propellants: A Discussion of Some Recent Experimental Results," E.R.D.E. Rept. No. 15/R/65, July 1965.

43. Powling, J., "Experiments Relating to the Combustion of Ammonium Perchlorate-Based Propellants," Eleventh Symposium (International) on Combustion, The Combustion Institute, Pittsburgh, 1967, pp. 447-456.

44. Jacobs, P. W. M. and Powling, J., "The Role of Sublimation of Ammonium Perchlorate Propellants," Twelfth Symposium (International) on Combustion, University of Poitiers, France, July, 1968, Paper No. 53.

45. Friedman, R., Levy, J. B., Copeland, B. K. W., Nugent, R. G., Shuman, M., Wallin, T. N. and Williams, E., "Research on Solid-Propellant Combustion," Atlantic Research Corp. Final Tech. Rept. under Contract AF 49(638)-813, Dec. 1961.

46. Cummings, G. A. McD. and Hall, A. R., "Perchloric Acid Flames. I. Premixed Flames with Methane and Other Fuels," Tenth Symposium (International) on Combustion, The Combustion Institute, Pittsburgh, 1965, pp. 1365-1372.

47. Sibbett, D. J. and Lobato, J. M., "Investigation of the Mechanism of Combustion of Composite Solid Propellants," Aerojet-General Corp. Rept. No. 1782, April 1960, (Astia AD246274). Cited by Ref. 23.

48. Cheselske, F. J., "Investigations of the Mechanisms of Decomposition, Combustion, and Detonation of Solids," Aerojet-General Corp. Rept. 0372-01F, March 1965.

49. Cummings, G. A. McD., and Pearson, G. S. "Perchloric Acid Decomposition Flame," Combustion and Flame, Vol. 8, No. 3, 1964, pp. 199-202.

50. Cummings, G. A. McD. and Hall, A. R., "Perchloric Acid Flames. I. Premixed Flames with Methane and Other Fuels," Tenth Symposium (International) on Combustion, The Combustion Institute, Pittsburgh, 1965, pp. 1365-1372.

51. Pearson, G. S., "Perchloric Acid Flames IV - Methane Rich Flames," Combustion and Flame, Vol. 11, No. 2, 1967, pp. 89-96.

52. Pearson, G. S., "Perchloric Acid Flames V - Ethylene-Rich Flames," Combustion and Flame, Vol. 11, No. 2, 1967, pp. 97-102.

53. Pearson, G. S., "Perchloric Acid Flames VI - Ethane-Rich Flames," Combustion and Flame, Vol. 11, No. 2, 1967, pp. 103-108.

54. Pearson, G. S., "Perchloric Acid Flames VIII - Methane-Rich Flames with Oxygen," Combustion and Flame, Vol. 12, No. 1, 1968, pp. 54-62.

55. Hall, A. R. and Pearson, G. S., "Perchloric Acid Flames: IX. Two-Flame Structure with Hydrocarbons," Twelfth Symposium (International) on Combustion, Poitiers, France, July 1968.

56. Levy, J. B., "The Thermal Decomposition of Perchloric Acid," J. Phys. Chem., Vol. 66, 1962, pp. 1092-1097.

57. Gaydon, A. G. and Wolfhard, H. G., "Flames - Their Structure, Radiation and Temperature," Chapman and Hall, Ltd., London, 1960, p.85.

58. Johnson, W. E. and Nachbar, W., "Deflagration Limits in the Steady Linear Burning of a Monopropellant with Application to Ammonium Perchlorate," Eighth Symposium (International) on Combustion, The Williams & Wilkins Co., Baltimore, 1962, pp. 678-689.

59. Horton, M. D. and Price, E. W., "Deflagration of Pressed Ammonium Perchlorate," ARS J., Vol. 32, No. 11, 1962, p. 1745.

60. Shannon, L. J. and Peterson, E. E., "Deflagration Characteristics of Ammonium Perchlorate Strands," AIAA J., Vol. 2, No. 1, 1964, pp. 168-169.

61. Shannon, L. J. and Peterson, E. E., "Burning Velocity of Ammonium Perchlorate Strands and Crystals," AIAA J., Vol. 6, No. 8, 1968, pp. 1594-1595

62. Hightower, J. D. and Price, E. W., "Combustion of Ammonium Perchlorate," Eleventh Symposium (International) on Combustion, The Combustion Institute, Pittsburgh, 1967, pp. 463-472.

63. Grassie, N., "Chemistry of High Polymer Degradation Processes," Interscience Publishers Inc., New York, 1956.

64. Wall, L. A., "Pyrolysis," Analytical Chemistry of Polymers, High Polymers Series, Vol. XII, Pt. II, Interscience Publishers, New York, 1962, pp. 181-248.

65. Grassie, N. "Thermal Degradation," Chemical Reactions of Polymers, High Polymers Series, Vol. XIX, Interscience Publishers, New York, 1964, pp. 565-644.

66. Madorsky, S. I., "Thermal Degradation of Organic Polymers," Interscience Publishers, John Wiley & Sons, Inc., New York, 1964.

67. Schultz, R. D. and Dekker, A. O., "The Absolute Thermal Decomposition Rates of Solids. Part I. The Hot-Plate Pyrolysis of Ammonium Chloride and the Hot-Wire Pyrolysis of Polymethylmethacrylate (Plexiglas IA)," Fifth Symposium (International) on Combustion, Reinhold Publishing Corp., New York, 1955, pp. 260-267.

68. Schultz, R., Green, L. and Penner, S. S., "Studies of the Decomposition Mechanism, Erosive Burning, Sonance and Resonance for Solid Composite Propellants," Third AGARD Colloqium on Combustion and Propulsion, Pergamon Press, New York, 1958, pp. 367-427.

69. Chaiken, R. F., Andersen, W. H., Barsh, M. K., Mishuck, E., Moe, G. and Schultz, R. D., "Kinetics of the Surface Degradation of Polymethylmethacrylate," J. Chem. Phys., Vol. 32, No. 1, 1960, pp. 141-146.

70. M. Guinet, "La Vitesse de Pyrolyse de Materiaux Composites," La Recherche Aéronautique, No. 80, Jan.-Feb. 1961, pp. 33-35.

71. Barsh, M. K., Anderson, W. H., Bills, K. W., Moe, G. and Schultz, R. D., "Improved Instrument for the Measurement of Linear Pyrolysis Rates of Solids," Rev. of Sci. Instr., Vol. 29, No. 5, 1958, pp. 392-395.

72. Andersen, W. H., "Comments on 'The Gas-Film Effects in the Linear Pyrolysis of Solids'," AIAA J., Vol. 2, No. 2, 1964, pp. 404-406.

73. Cantrell, R. H., "Reply by Author to W. H. Andersen," AIAA J., Vol. 2, No. 2, 1964, pp. 406-407.

74. Cantrell, R. H., "Gas-Film Effects in the Linear Pyrolysis of Solids," AIAA J., Vol. 1, No. 7, 1963, pp. 1544-1550.

75. Hightower, J. D. and Price, E. W., "Two-dimensional Experimental Studies of the Combustion Zone of Composite Solid Propellants," Proceedings of the 2nd ICRPG Combustion Conference, CPIA Publication No. 105, May 1966, pp. 421-432.

76. McGurk, J. L., "Microscopic Determination of Propellant Combustion Surface Temperatures," Proceedings of the 1st Combustion Instability Conference, CPIA Publication No. 68, Jan. 1965, pp. 345-359.

77. West, C. L., Golding, D. R. V. and Lo, G. A., "Macro-Combustion Studies of Ammonium Perchlorate-Hydrocarbon Binder," Proceedings of the 3rd ICRPG Combustion Conference, CPIA Publication No. 138, Vol. 1, Feb. 1967, pp. 113-117.

78. Nadaud, L., "Models Used at ONERA to Interpret Combustion Phenomena in Heterogeneous Solid Propellants," Combustion and Flame, Vol. 12, No. 3, 1968, pp. 177-195.

79. McAlevy, R. F. and Hansel, J. G., "Linear Pyrolysis of Thermoplastics in Chemically Reactive Environments," AIAA J., Vol. 3, No. 2, 1965, pp. 244-249.

80. Pearson, A. S. and Sutton, D., "Composite Solid Propellant Ignition: Ignition of Ammonia and Other Fuels by Perchloric Acid Vapor," AIAA J., Vol. 5, No. 2, 1967, pp. 344-346.

81. Wenograd, J., "Study of the Kinetics and Energetics of Propellant Decomposition Reactions and Application to Steady State Combustion Mechanism," Proceedings of the 3rd ICRPG Combustion Conference, CPIA Publication No. 138, Vol. 1, Feb. 1967, pp. 89-94.

82. Waesche, R. H. W. and Wenograd, J., "Decomposition Kinetics of PBAA Propellant," Proceedings of the 4th ICRPG Combustion Conference, CPIA Publication No. 162, Vol. 1, Dec. 1967, pp. 481-485.

83. Waesche, R. H. W., "Research Investigation of the Decomposition of Composite Solid Propellants," United Aircraft Research Laboratories, Final Rept. F910476-12, Sept. 1967.

84. Inami, S. H., Rosser, W. A. and Wise, H., "Heat-Release Kinetics of Ammonium Perchlorate in the Presence of Catalysts and Fuel," Combustion and Flame, Vol. 12, No. 1, 1968, pp. 41-44.

85. Rosser, W. A., Fishman, N. and Wise, H., "Ignition of Simulated Propellants Based on Ammonium Perchlorate," AIAA J., Vol. 4, No. 9, 1966, pp. 1615-1622.

86. Flanagan, D. A., "Analysis to Relate Subsurface Heating to Changes in Ammonium Perchlorate Crystal Structure," Appendix A (Unclassified) of Thiokol Chemical Corporation (Confidential) Progress Report, Sept. 1967.

87. Caveny, L. H. and Pittman, C. U., "Contribution of Solid-Phase Heat Release to AP Composite-Propellant Burning Rate," AIAA J., Vol. 6, No. 8, 1968, pp. 1461-1467.

88. Schultz, R. D. and Dekker, A. O., "Fundamental Studies of Aeroplex Propellant Rockets, Investigation of Solid Composite Propellants," Aerojet-General Corp. Rept. No. 576, Vol. 1 (Quarterly), Feb. 1952, pp. 6-10 (Confidential). Cited by Ref. 68.

89. Hightower, J. D., Price, E. W. and Zurn, D. E., "Continuing Studies of the Combustion of Ammonium Perchlorate," Proceedings of the 4th ICRPG Combustion Conference, CPIA Publication No. 162, Vol. 1, Dec. 1967, pp. 527-534.

90. Boggs, T. L. and Kraeutle, K. J., "Decomposition and Deflagration of Ammonium Perchlorate," Naval Weapons Center, Rept. NWC JP 4630, Oct. 1968.

91. Sabadell, A. J., Wenograd, J. and Summerfield, M., "Measurement of Temperature Profiles Through Solid Propellant Flames Using Fine Thermocouples," AIAA J., Vol. 3, No. 9, 1965, pp. 1580-1584.

92. Hall, K. P., Wenograd, J. and Cole, R. B., "Burning Rate Control Factors in Solid Propellants," Aeronautical Engineering Rept. Nos. 446 k & l, Princeton University, March 1962.

93. Irwin, O. R., Salzman, P. K. and Andersen, W. H., "Deflagration Characteristics of Ammonium Perchlorate at High Pressures," Ninth Symposium (International) on Combustion, Academic Press, New York, 1963, pp. 358-365.

94. Cole, R. B., "High Pressure Solid Propellant Combustion Using a Closed Bomb," Rohm and Haas Co. Special Rept. S-68, 1965.

95. Geckler, R. D., "The Mechanism of Combustion of Solid Propellants," Selected Combustion Problems, Butterworths, London, 1954, pp. 289-339.

96. Irwin, O. R., Salzman, P. K. and Andersen, W. H., "Mechanism of Accelerated Burning of Ammonium Perchlorate at High Pressures," AIAA J., Vol. 1, No. 5, 1963, pp. 1178-1180.

97. Burger, J. and van Tiggelen, A., "Contribution a l' Etude de la Combustion des Pondres Composites," Memoires Academie Royale de Belgigue, Tome XXXIV, fac. 3, 1964.

98. Van Tiggelen, A. and Burger, J., "Oxydations et Combustions (Chapitre XII) La Déflagration des Propeigols Solides et Hybrides," Revue de l' Institut Francais du Petrole, Vol. 11, No. 5, May 1966, pp. 816-868.

99. Barrère, M. and Nadaud, L., "Combustion of Ammonium Perchlorate Spheres in a Flowing Gaseous Fuel," Tenth Symposium (International) on Combustion, The Combustion Institute, Pittsburgh, 1965, pp. 1381-1394.

100. Friedman, R., Hertzberg, M., McHale, E. T. and von Elbe, G, "Composite Solid Propellant Flame Microstructure Determination," Atlantic Research Corp. Rept. prepared for NASA, NASA CR 66677, 1968.

101. Rice, O. K. and Ginnell, R., "The Theory of the Burning of Double-Base Rocket Powders," J. Phys. & Colloid Chem., Vol. 54, No. 6, 1950, pp. 885-917.

102. Parr, R. G. and Crawford, B. L., "A Physical Theory of Burning of Double-Base Rocket Propellants," J. Phys. & Colloid Chem., Vol. 54, No. 6, 1950, pp. 929-954.

103. Spalding, D. B., "The Theory of Burning of Solid and Liquid Propellants," Combustion and Flame, Vol. 4, No. 1, 1960, pp. 59-76.

104. Rice, O. K., "The Theory of Burning of Rocket Powders," OSRD Rept. No. 5574, 1955. Cited by Ref. 68.

105. Nachbar, W. and Parks, J. M., "A Sandwich Burner Model for the Composite Propellant," Lockheed Missile Systems Division Report LMSD-2191, AFOSR-TN 57-418, Sept. 1957. Cited by Ref. 106.

106. Nachbar, W., "A Theoretical Study of the Burning of a Solid Propellant Sandwich," Solid Propellant Rocket Research, Progress in Astronautics and Rocketry Series, Vol. 1, Academic Press, New York, 1960, pp. 207-226.

107. Nachbar, W. and Cline, G. B., "The Effects of Particle Size and Non-Stoichiometric Composition on the Burning Rates of Composite Solid Propellants," Fifth AGARD Colloqium on Combustion and Propulsion, The Macmillan Co., New York, 1963, pp. 551-568.

108. Andersen, W. H., Bills, K. W., Mishuck, E., Moe, G. and Schultz, R. D., "A Model Describing Combustion of Solid Composite Propellants Containing Ammonium Nitrate," Combustion and Flame, Vol. 3, No. 3, 1959, pp. 301-317.

109. Chaiken, R. F., "A Thermal Layer Mechanism of Combustion of Solid Composite Propellants: Application to Ammonium Nitrate Propellants," Combustion and Flame, Vol. 3, No. 3, 1959, pp. 285-300.

110. Chaiken, R. F. and Andersen, W. H., "The Role of Binder in Composite Propellant Combustion," Solid Propellant Rocket Research, Progress in Astronautics and Rocketry Series, Vol. 1, Academic Press, New York, 1960, pp. 227-249.

111. Hermance, C. E., "A Model of Composite Propellant Combustion Including Surface Heterogeneity and Heat Generation," AIAA J., Vol. 4, No. 9, 1966, pp. 1629-1637.

112. Hermance, C. E., "A Detailed Model of the Combustion of Composite Solid Propellants," Proceedings of the 2nd ICRPG/AIAA Solid Propulsion Conference, CPIA Publication, June 1967, pp. 89-103.

113. Hicks, B. L., "Theory of Ignition Considered as a Thermal Reaction," J. Chem. Phys., Vol. 22, Pt. 1, No. 3, 1954, pp. 414-429.

114. Andersen, R., Brown, R. S. and Shannon, L. J., "Ignition Theory of Solid Propellants," AIAA Solid Propellant Rocket Conference, Palo Alto, Jan. 1964, AIAA Preprint 64-156.

115. Andersen, R., Brown, R. S. and Shannon, L. J., "Heterogeneous Reaction in Ignition and Combustion of Solid Propellants," AIAA J., Vol. 2, No. 1, 1964, pp. 179-180.

116. Fenn, J. B., "A Phalanx Flame Model for the Combustion of Composite Solid Propellants," Combustion and Flame, Vol. 12, No. 3, 1968, pp. 201-216.

117. Mallard, E. and le Chatelier, H., Ann. mines 8, Series 4, p. 274 (1883). Cited by Ref. 27.

118. Penner, S. S., "Chemistry Problems in Jet Propulsion," p. 246, The Macmillan Co., New York, 1957.

119. Penner, S. S., "Combustion Research Related to Solid-Propellant Rocket Development," Chapter IV, "Chemical Rocket Propulsion and Combustion Research," Gordon and Breach Science Publishers, New York, 1962, pp. 99-143.

120. Webb, M. J., "The Dependence of Linear Burning Rate Upon Pressure for Ammonium Perchlorate-Polyester Resin Composite Solid Propellant," M.S.E. Thesis, Department of Aeronautical Engineering, Princeton University, May 1958.

121. Taback, H. J., "The Effects of Several Composition Factors on the Burning Rate of an Ammonium Perchlorate Solid Propellant," M.S.E. Thesis, Aeronautical Engineering Rept. No. 429, Princeton University, Sept. 1958.

122. Yamazaki, K., Hayashi, M. and Iwama, A., "The Effect of Sound Waves on the Burning Velocity of a Solid Propellant," Int. Chem. Eng., Vol. 5, No. 1, 1965, pp. 156-190.

123. Barrère, M. and Nadaud, L., "The Combustion Domaines of Composite Powders," La Recherche Aérospatiale, No. 98, 1964, pp. 15-29.

124. Kling, R. and Brulard, J., "Étude de la Combustion des Poudres Composites par la Microphotographic Ultra-Rapide," La Recherche Aéronautique, No. 80, 1961, pp. 3-11.

125. Nadaud, L., "La Combustion des Propergols Solides Métallisés," La Recherche Aéronautique, No. 85, 1961, pp. 3-14.

126. Capener, E. L., Dickinson, L. A. and Marxman, G. A., "Propellant Combustion Phenomenon During Rapid Depressurization," Stanford Research Institute Quarterly Rept. No. 1, Oct. 1965 (Contract NAS7-389).

127. Krier, H., T'ien, J.S., Sirignano, W. A. and Summerfield, M., "Nonsteady Burning Phenomena of Solid Propellants: Theory and Experiments," AIAA J., Vol. 6, No. 2, 1968, pp. 278-285.

128. Reid, D. L., "The Dependence of Several Solid Propellant Burning Anomalies on Flame Structure," M.S.E. Thesis, Department of Aeronautical Engineering, Princeton University, July 1957.

129. Peterson, J. A., Reed, R. and McDonald, A. J., "Control of Pressure Deflagration Limits of Composite Solid Propellants," AIAA J., Vol. 5, No. 4, 1967, pp. 764-770.

130. Peterson, J. A., Reed, R. and Cornia, R. P., "Comparative Extinction Characteristics of Fluorocarbon and Conventional Propellants," Proceedings of the 4th ICRPG Combustion Conference, CPIA Publication No. 162, Vol. 1, Dec. 1967, pp. 389-397.

131. Crawford, B. L., Huggett, C. and McBrady, J. J., "The Mechanism of the Burning of Double-Base Propellants," J. Phys. & Colloid Chem., Vol. 54, No. 6, 1950, pp. 854-862.

132. Heath, G. A. and Hirst R., "Some Characteristics of the High Pressure Combustion of Double-Base Propellants," Eighth Symposium (International) on Combustion, The Williams & Wilkins Co., Baltimore, 1962, pp. 711-720.

133. Huggett, C., "Combustion of Solid Propellants," Combustion Processes,High Speed Aerodynamics and Jet Propulsion Series, Vol. 2, Princeton University Press, Princeton, 1956, pp. 514-574.

134. Klein, R., Mentser, M., von Elbe, G. and Lewis, B., "Determination of the Thermal Structure of a Combustion Wave by Fine Thermocouples," J. Phys. & Colloid Chem., Vol. 54, No. 6, 1950, pp. 877-884.

135. Preckel, R. F., "Plateau Ballistics in Nitrocellulose Propellants," ARS J., Vol. 31, No. 9, 1961, pp. 1286-1287.

136. Preckel, R. F., "Plateau Ballistics in Nitrocellulose Propellants," AIAA J., Vol. 3, No. 2, 1965, pp. 346-347.

137. Powling, J. and Smith, W. A. W., "The Surface Temperature of Ammonium Perchlorate at Elevated Pressures," Tenth Symposium (International) on Combustion, The Combustion Institute, Pittsburgh, 1965, pp. 1373-1380.

138. Selzer, H., "The Temperature Profile Beneath the Burning Surface of a Composite Ammonium Perchlorate Propellant," Eleventh Symposium (International) on Combustion, The Combustion Institute, Pittsburgh, 1967, pp. 439-446.

139. Beckstead, M. W. and Hightower, J. D., "Surface Temperature of Deflagrating Ammonium Perchlorate Crystals," AIAA J., Vol. 5, No. 10, 1967, pp. 1785-1790.

140. Most, W. J. and Wenograd, J., "Solid Propellant Combustion Mechanism Studies," Aerospace and Mechanical Sciences Rept. 446-p, Princeton University, June 1965.

141. Bobolev, V. K., Glazkova, A. P., Zenin, A. A. and Leipunskii, O. T., "Temperature Profiles during Combustion of a Ammonium Perchlorate," Doklady Akad. Nauk S.S.S.R, Vol. 151, No. 3, 1963, pp. 604-607, Translation in Proc. Acad. Sci. U.S.S.R., Physical Chemistry Section, Vol. 151, 1963, pp. 644-647.

142. Powling, J. and Smith, W. A. W., "Measurement of the Burning Surface Temperatures of Propellant Compositions by Infra-red Emission," Combustion and Flame, Vol. 6, No. 3, 1962, pp. 173-181.

143. Feinauer, L. R., "Burning of Composite Ammonium Perchlorate Based Propellants Near Their Extinction Pressure," AIAA Student Journal, Vol. 3, No. 4, 1965, pp. 125-128.

144. Billmeyer, F. W., "Textbook of Polymer Science " Interscience Publishers, New York, 1965.

145. Ohlemiller, T. J. and Summerfield, M., "Radiation Augmented Burning of a Solid Propellant," Aerospace and Mechanical Sciences Rept. 799, Princeton University, July 1967.

146. Bakhman, N. N. and Belyaev, A. F., "Combustion of Heterogeneous Condensed Systems," Institute of Chemical Physics, Moscow Academy of Sciences, U.S.S.R., Nauka Publication, 1967; also, R.P.E. Translation No. 19, edited by G. S. Pearson, Nov. 1967.

147. Beachell, H. C., Hackman, E. E., "Combustion Characteristics of Crystalline Oxidizers," AFOSR Interim Scientific Report No. AFOSR 67-2419, University of Delaware, Newark, Delaware, Sept. 1967.

148. "Janaf Thermochemical Data," The Dow Chemical Company, Thermal Laboratory, Midland, Michigan.

149. Hansel, J. G., "Studies of the Linear Pyrolysis of Thermoplastics in Inert and Chemically Reactive Environments," Sc. D. Thesis, Stevens Institute of Technology, 1964, p. 99.

150. Warren, F. A. "Rocket Propellants," Reinhold Publishing Co., New York, 1958.

151. Barrère, M., Jaumotte, A., de Veubeke, B. F. and Vandenkerckhove, J., "Rocket Propulsion," Elsevier Publishing Co., Amsterdam, 1960.

152. Siegel, B. and Schieler, L., "Energetics of Propellant Chemistry," John Wiley & Sons, Inc., New York, 1964.

153. Shorr, M. and Zaehringer, A. J., "Solid Rocket Technology," John Wiley & Sons, New York, 1967.

154. Summerfield, M. and Krier, H., "Role of Aluminum in Suppressing Instability in Solid Propellant Rocket Motors," Aerospace and Mechanical Sciences Rept. No. 840, Princeton University, July 1968.

155. Krier, H. Mathes, H. B., Price, E. W. and Summerfield, M., "Entropy Waves Produced in Oscillatory Combustion of Solid Propellants," to be published in AIAA J. 1969.

156. Shidlovskii, A. A., Semishin, V. I. and Shmagin, L. F., "Thermal Decomposition and Combustion of Hydrazine Diperchlorate," Journ. of Applied Chem., U.S.S.R., Vol. 35, No. 4, 1962, pp. 734-759.

157. Gilliland, A. A., "Heat of Formation of Nitronium Perchlorate," Journ. of Research (Physics and Chemistry Section), Vol. 66A, Nov.-Dec. 1962, pp. 447-449.

158. Russell-Jones, A., "The Thermal Decomposition of Some Inorganic Perchlorates," Ph.D. Thesis, Imperial College of Science and Technology, London, Sept. 1964.

159. Caruso, R., Loprest, F. J. and Lum, A., "Heat of Formation of Hydrazinium Diperchlorate," J. Phys. Chem., Vol. 69, May, 1965, pp. 1716-1718.

160. Levy, J. B., von Elbe, G. Friedman, R., Wallin, T. and Adams, S. J., "The Deflagration of Hydrazine Perchlorate," Advanced Propellant Chemistry, Advances in Chemistry Series, Vol. 54, American Chemical Society Publications, 1966, pp. 55-72.

161. Grelecki, C. J. and Cruice, W., "Thermal Decomposition of Hydrazinium Monoperchlorate and Hydrazinium Diperchlorate," Advanced Propellant Chemistry, Advances in Chemistry Series, Vol. 54, American Chemical Society Publications, 1966, pp. 73-81.

162. Marshall, M. D. and Lewis, L. L., "Decomposition of Nitronium Perchlorate," Advanced Propellant Chemistry, Advances in Chemistry Series, Vol. 54, American Chemical Society Publications, 1966, pp. 82-92.

163. von Elbe, G. and McHale, E. T., "Branched-Chain Reactions in the Decomposition of Hydrazine-Based Oxidizers," Proceedings of the 3rd ICRPG Combustion Conference, CPIA Publication No. 138, Vol. 1, Feb. 1967, pp. 85-86.

164. McHale, E. T., Adams, S. J., von Elbe, G. and Levy, J. B., "The Deflagration of Hydrazine Diperchlorate," Combustion and Flame, Vol. 11, No. 2, 1967, pp. 141-149.

165. Price, E. W., "Solid Propellant Combustion: State of Knowledge 1967," Paper No. 3b, presented at the 62nd National Meeting of the American Institute of Chemical Engineers, Salt Lake City, Utah, May 21-24, 1967.

166. Cohen, M. S., "Advanced Binders for Solid Propellants - A Review," Advanced Propellant Chemistry, Advances in Chemistry Series, Vol. 54, American Chemical Society Publications, 1966, pp. 93-107.

167. Price, E. W., "Review of Experimental Research on Combustion Instability of Solid Propellants," Solid Propellant Rocket Research, Progress in Astronautics and Rocketry Series, Vol. 1, Academic Press, New York, 1960, pp. 561-602.

168. Watermeier, L. A., Aungst, W. P. and Pfaff, S. P., "An Experimental Study of the Aluminum Additive Role in Unstable Combustion of Solid Propellants," Ninth Symposium (International) on Combustion, Academic Press, New York, 1963, pp. 316-326.

169. Crump, J. E., "Surface Characteristics of Quenched Samples of Composite-Aluminum Propellants," Proceedings of the 1st ICRPG Combustion Instability Conference, CPIA Publication No. 68, Jan. 1965, pp. 361-366.

170. Crump, J. E., "Photographic Survey of Aluminum Combustion in Solid Propellants," Proceedings of the 1st ICRPG Combustion Instability Conference, CPIA Publication No. 68, Jan. 1965, pp. 367-370.

171. Crump, J. E., "Aluminum Combustion in Composite Propellants," Proceedings of the 2nd ICRPG Combustion Conference, CPIA Publication No. 105, May 1966, pp. 321-329.

172. Miller, R. R., "Some Factors Affecting the Combustion of Aluminum in Solid Propellants," Proceedings of the 2nd ICRPG Combustion Conference, CPIA Publication No. 5, May 1966, pp. 331-353.

173. Beckstead, M. W., Boggs, T. L., Crump, J. E., Dehority, G.L., Hightower, J. D., Kraeutle, K. J., Krier, H., Mathes, H.B., and Price, E. W., "Combustion of Solid Propellants and Low Frequency Instability," Progress Report NWC TP 4478, Naval Weapons Center, China Lake, Calif., April 1968.

174. Summerfield, M. and Parker, K. H., "Interrelations between Combustion Phenomena and Mechanical Properties in Solid Propellant Rocket Motors," Mechanics and Chemistry of Solid Propellants, Proceedings of the 4th Symposium on Naval Structural Mechanics, Office of Naval Research Structural Mechanics Series, Pergamon Press, London, 1967, pp. 75-116.

175. Andersen, J. B. and Reichenbach, R. E., "An Investigation of the Effect of Acceleration on the Burning Rate of Composite Solid Propellants," AIAA J., Vol. 6, No. 2, 1968, pp. 271-277. Also, U.S. Naval Postgraduate School Rept. NPS-57RV7071A, Monterey, Calif., July 1967.

176. Sturm, E. J. and Reichenbach, R. E., "An Experimental Study of the Effect of Solid Ingredient Particle Size on Burning Rates of Composite Solid Propellants in Acceleration Fields," Proceedings of the 4th ICRPG Combustion Conference, CPIA Publication No. 162, Vol. 1, Dec. 1967, pp. 467-480.

177. Crowe, C. T. and Willoughby, P. G., "Effect of Spin on the Internal Ballistics of a Solid Propellant Rocket Motor," AIAA Preprint No. 66-523, presented at the AIAA 4th Aerospace Sciences Meeting (West Coast), June 27-29, 1966; cited by Ref.175 . Also, "Investigation of Particle Growth and Ballistics Effects on Solid Propellant Rockets," United Technology Center Rept. UTC 2128-FR, June, 1966; cited by Ref. 176.

178. Glick, R. L., "An analytical Study of the Effects of Radial Acceleration Upon the Combustion Mechanism of Solid Propellant," Thiokol Chemical Corporation Rept. No. 42-66, NASA Rept. No. 66218, Dec. 1966. Also, "The Effect of Acceleration on the Burning Rate of Nonmetallized Composite Propellants," Proceedings of the 3rd ICRPG Combustion Conference, CPIA Publication No. 138, Vol. 1, Feb. 1967, p. 99.

179. Glassman, I., "Metal Combustion Processes," Presented at the ARS 14th Annual Meeting, Washington, D. C., Nov. 16-20, 1959, ARS Preprint 938-59. (Also, private communication.)

180. Glassman, I., "Combustion of Metals: Physical Considerations," Solid Propellant Rocket Research, Progress in Astronautics and Rocketry, Vol. 1, Academic Press, New York, pp. 253-257.

181. Hart, G. H. and Merkle, C. L., Princeton University, to be published. (Private communication.)

182. Gibson, R. E., "Origin and General Significance of Study of Kinetics of Propellants," J. Phys. & Colloid Chem., Vol. 54, No. 6, 1950, pp. 847-853.

183. Wilfong R. E., Penner, S. S. and Daniels, F., "An Hypothesis for Propellant Burning," J. Phys. & Colloid Chem., Vol. 54, No. 6, 1950, pp. 863-872.

184. Adams, G. K. and Wiseman, L. A., "The Combustion of Double-Base Propellants," Selected Combustion Problems, Butterworth's Scientific Publications, London, 1954, pp. 277-288.

185. Musso, R. C., "Decomposition Studies of CMDB Propellant Ingredients," Proceedings of the 3rd ICRPG Combustion Conference, CPIA Publication No. 162, Vol. 1, Dec. 1967, pp. 551-559.

186. Lenchitz, C. and Haywood, B., "Determination of the Role of the Ballistic Modifier in Propellant Combustion Using the Heat of Explosion Test," Combustion and Flame, Vol. 10, No. 2, 1966, pp. 140-146.

187. Glick, R. L., "Temperature Sensitivity of Solid Propellant Burning Rate," AIAA J., Vol. 5, No. 3, 1967, pp. 586-587.

188. Green, L., "Erosive Burning of Some Composite Propellants," Jet Propulsion, Vol. 24, No. 1, 1954, pp. 9-15.

189. Lenoir, J. M. and Robillard, G., "A Mathematical Method to Predict the Effects of Erosive Burning in Solid Propellant Rockets," Sixth Symposium (International) on Combustion, Reinhold, New York, 1957, pp. 663-667.

190. Vandenckerckhove, J., "Erosive Burning of Colloidal Solid Propellant," Jet Propulsion, Vol. 28, No. 9, 1958, pp. 599-603.

191. Tsuji, H., "An aerothermochemical Analysis of Erosive Burning of Solid Propellant," Ninth Symposium (International) on Combustion, Academic Press, New York, 1963, pp. 384-393.

192. Marklund, T. and Lake, A., "Experimental Investigation of Propellant Erosion," ARS J., Vol. 30, No. 2, 1960, pp. 173-178.

193. Lawrence, W. J. and Deverall, L. J., "The Erosive Burning Behavior of Selected Composite Propellants," Proceedings of the 4th ICRPG Combustion Conference, CPIA Publication No. 162, Vol. 1, Dec. 1967, pp. 459-465.

194. Friedly, J. C. and Peterson, E. C., "Influence of Combustion Parameters on Instability of Solid Propellant Rocket Motors," Part I: 'Development of Model and Linear Analysis,' AIAA J., Vol. 4, No. 9, 1966, pp. 1604-1610, Part II: 'Nonlinear Analysis,' AIAA J., Vol. 4, No. 11, 1966, pp. 1932-1937.

195. Denison, M. R. and Baum, E., "A Simplified Model of Unstable Burning in Solid Propellants," ARS J., Vol. 31, No. 8, 1961, pp. 1112-1122.

196. Marxman, G. A. and Wooldridge, C. E., "Effect of Surface Reactions on the Solid Propellant Response Function," AIAA J., Vol. 6, No. 3, 1966, pp. 471-478.

197. Flory, P. J., "Principles of Polymer Chemistry," Cornell University Press, Ithaca, New York, 1953.

198. Polymer Handbook, Interscience Publishers, New York, 1966.

199. Handbook of Epoxy Resins, McGraw-Hill Book Co., New York, 1967.

200. Handbook of Chemistry and Physics, 46th Edition, The Chemical Rubber Co., Cleveland, Ohio, 1965-1966.

201. The Condensed Chemical Dictionary, 5th Edition, Reinhold Publishing Corp., New York, 1956.

202. The Merck Index of Chemicals and Drugs, 6th Edition, Merck & Co., Inc., Rahway, N. J., 1952.

203. Dangerous Properties of Industrial Materials, Reinhold Publishing Corp., New York, 1963.

204. Schumacher, J. C., "Perchlorates: Their Properties, Manufacture and Uses," American Chemical Society Monograph Series, Reinhold Publishing Corp., New York, 1960.

205. Bastress, E. K., Hall, K. P. and Summerfield, M., "Particle Analysis of Ammonium Perchlorate by Liquid Sedimentation," AIAA J., Vol. 1, No. 5, 1963, pp. 1182-1184.

206. Dallavalle, M., "Micromeritics: The Technology of Fine Particles," 2nd Ed., Pitman Publishing Corp., New York, 1948, p. 68.

207. American Potash & Chemical Corp., Los Angeles, Calif., Bull. DEC -14.

208. "International Critical Tables of Numerical Data: Physics, Chemistry and Technology," Vol. 3, 1st Edition, 6th Impression, McGraw-Hill Book Co., Inc., New York, 1928.

TABLE I COMPARISON OF CALCULATED AND MEASURED COMBUSTION PRODUCTS AND HEAT OF REACTION FOR PURE AP

Moles Product per mole AP	EQUILIBRIUM CALCULATIONS				MEASUREMENTS*				Composition claimed as representative by Bircumshaw and Newman(28) & Huggett(133)		Analysis of B&N(20) data by Geckler(95)
	Beachell and Hackman(147)			Levy and Friedman(34)			Aarden et al(33)				
p (atm)	1	34	64	100	1	68	1	72	T < 300°C	T > 350°C	-
N_2	0.50	0.50	0.50	0.50	0.13	0.27	0.09	0.14	-	-	-
O_2	1.24	1.22	1.20	1.16	0.68	1.02	0.73	0.98	0.75	0.50	0.60
Cl_2	0.02	0.07	0.09	0.08	0.50	0.12	0.35	0.18	0.50	0.50	0.20
HCl	0.96	0.86	0.82	0.82	-	0.75	0.30	0.65	-	-	0.30
H_2O	1.52	1.57	1.59	1.59	2.00	1.62	1.85	1.67	2.00	2.00	1.80
NO	-	-	-	-	0.55	0.23	0.54	0.16	-	1.00	0.40
N_2O	-	-	-	-	0.10	0.12	0.15	0.23	0.50	-	-
NOCl	-	-	-	-	-	-	-	-	-	-	0.20
$HClO_4$	-	-	-	-	-	-	-	-	-	-	0.10
Cl	0.01	-	-	-	-	-	-	-	-	-	-
T_o (°K)	298	298	298			**	550++	293			
T_F (°K)	1375	1397	1403	1440		1203	1243	1203			
H_R (kcal/mole)+	38.3	39.2	39.5	39.5	31.4	32.7	28.7	32.4	***	***	29.4
h_R (cal/gm)+	326	334	336	336	267	278	244	276			250

NOTES:
* Mole fractions slightly adjusted in order to achieve mass balance.
\+ Heat of reaction calculated from product gas composition using heats of formation given in Ref. 148.
** Radiative augmented burning at 1 atm.
++ Preheated at 1 atm.
*** Too inaccurate to calculate reliable heat of reaction.

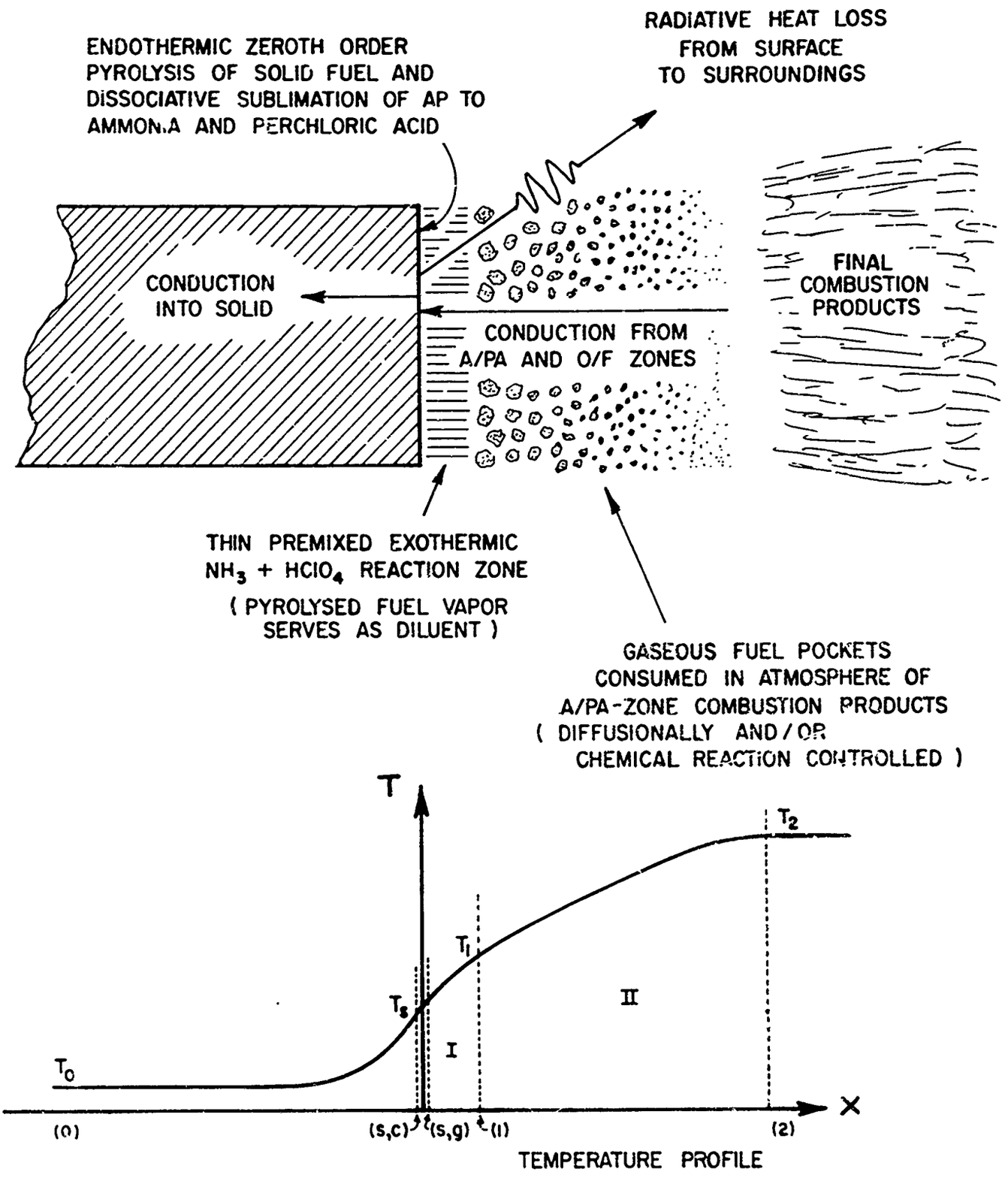

FIGURE 1 TWO-STAGE GRANULAR DIFFUSION FLAME MODEL FOR AMMONIUM PERCHLORATE-TYPE COMPOSITE SOLID PROPELLANTS

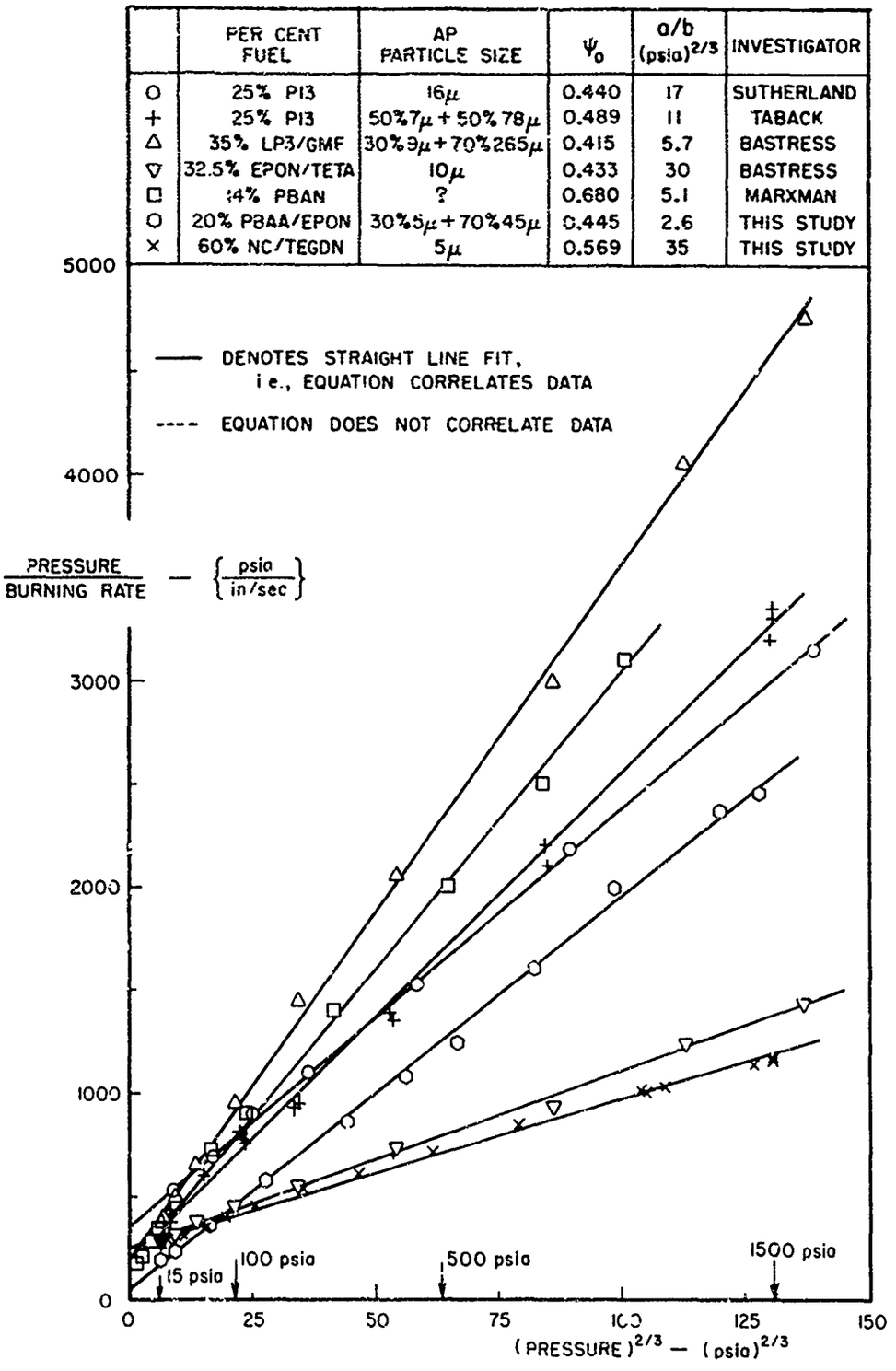

FIGURE 2 CORRELATION OF BURNING RATES WITH :

$$\left(\frac{1}{r}\right) = \left(\frac{a}{p}\right) + \left(\frac{b}{p^{1/3}}\right)$$

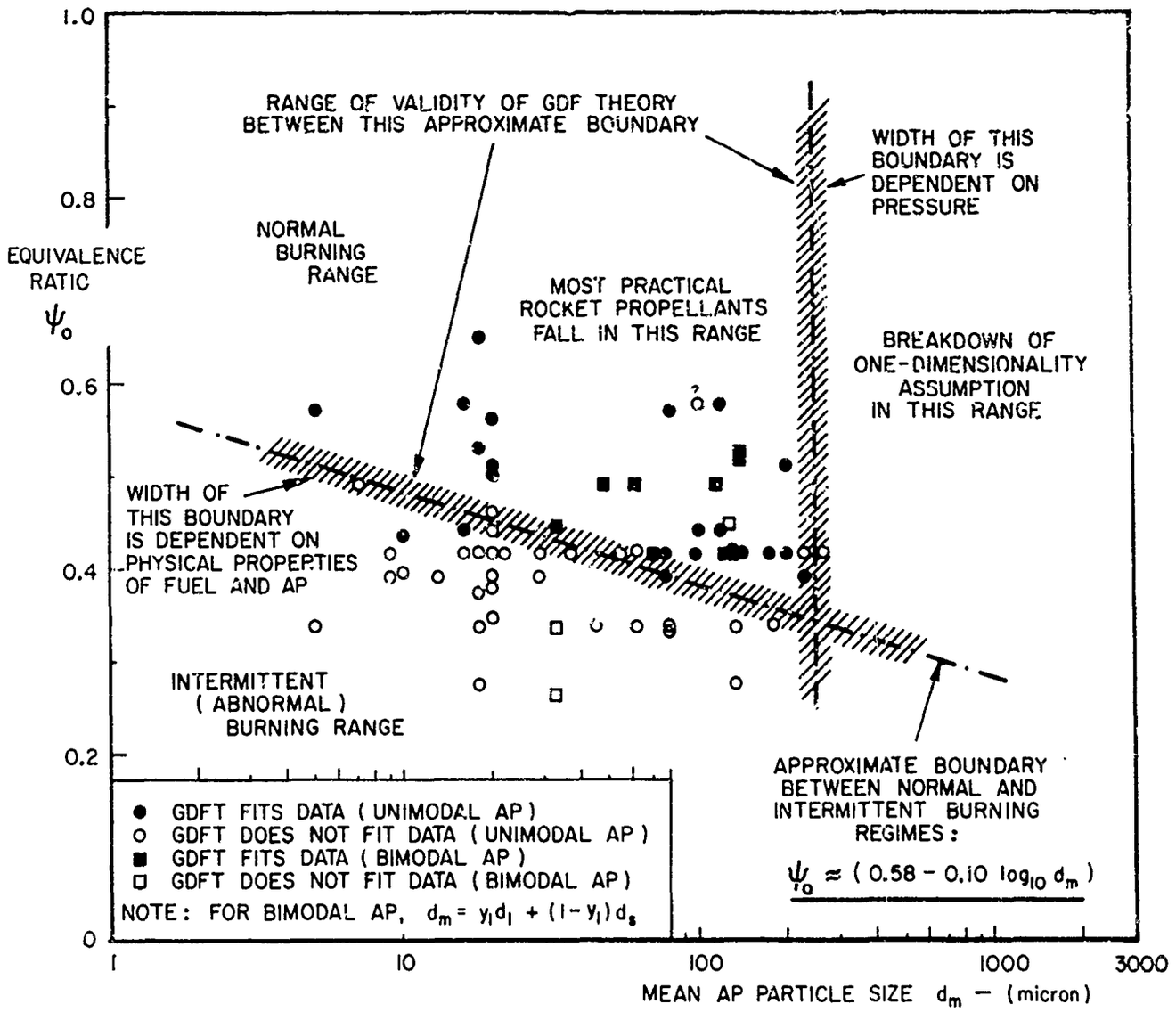

FIGURE 3 BURNING BEHAVIOR AND REGIMES OF VALIDITY OF GDF THEORY FOR AP BASED PROPELLANTS WITH FUELS THAT DO NOT MELT READILY

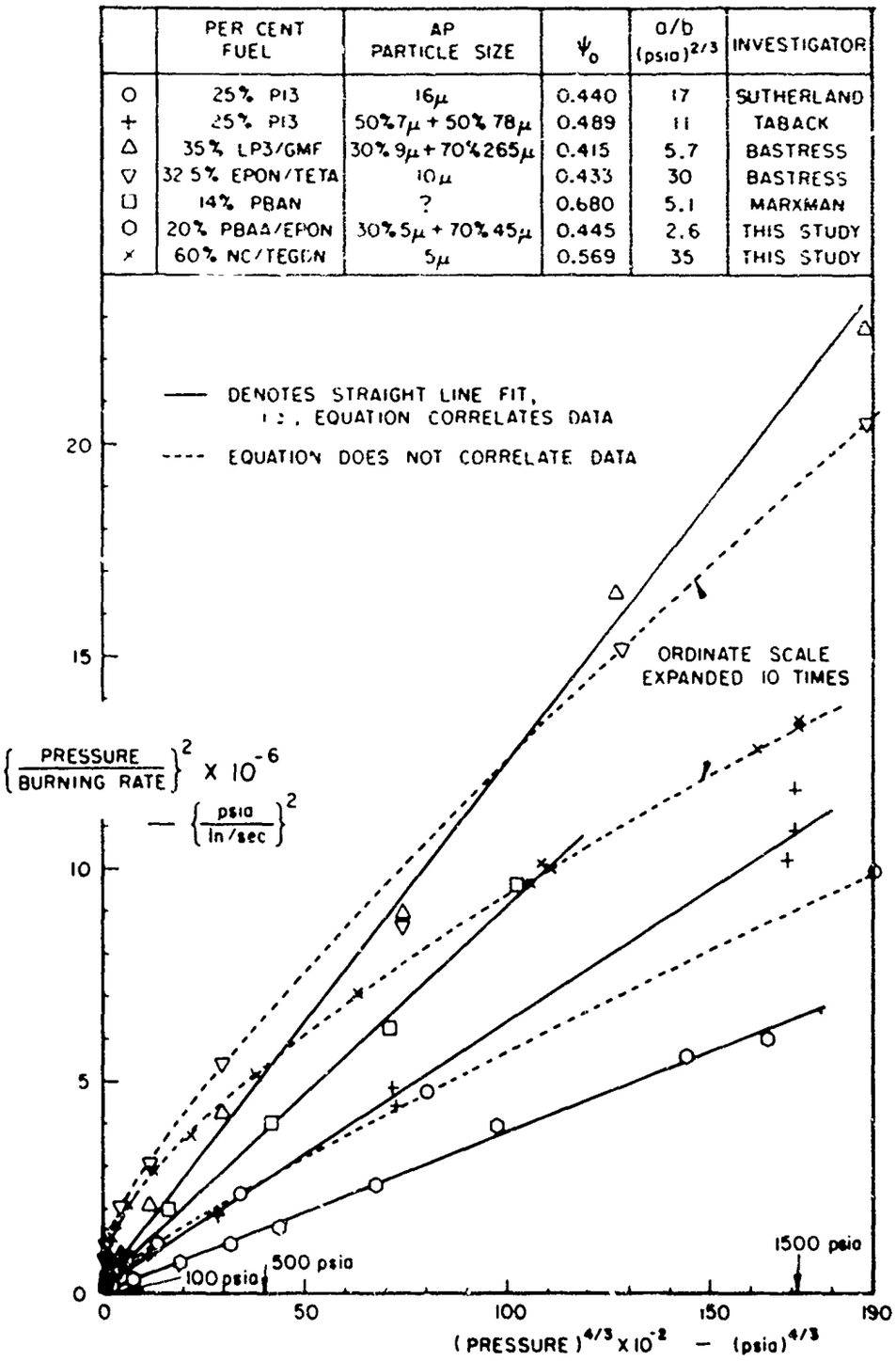

FIGURE 4 CORRELATION OF BURNING RATES WITH :

$$\left(\frac{1}{r}\right)^2 = \left(\frac{a}{p}\right)^2 + \left(\frac{b}{p^{1/3}}\right)^2$$

	PER CENT FUEL	AP PARTICLE SIZE	ψ_o	a/b $(psia)^{2/3}$	INVESTIGATOR
O	25% PI3	16μ	0.440	17	SUTHERLAND
+	25% PI3	50%7μ + 50%78μ	0.489	11	TABACK
△	35% LP3/GMF	30%9μ + 70%265μ	0.415	5.7	BASTRESS
▽	32.5% EPON/TETA	10μ	0.433	30	BASTRESS
□	14% PBAN	?	0.680	5.1	MARXMAN
O	20% PBAA/EPON	30%5μ + 70%45μ	0.445	2.6	THIS STUDY
×	60% NC/TEGDN	5μ	0.569	35	THIS STUDY

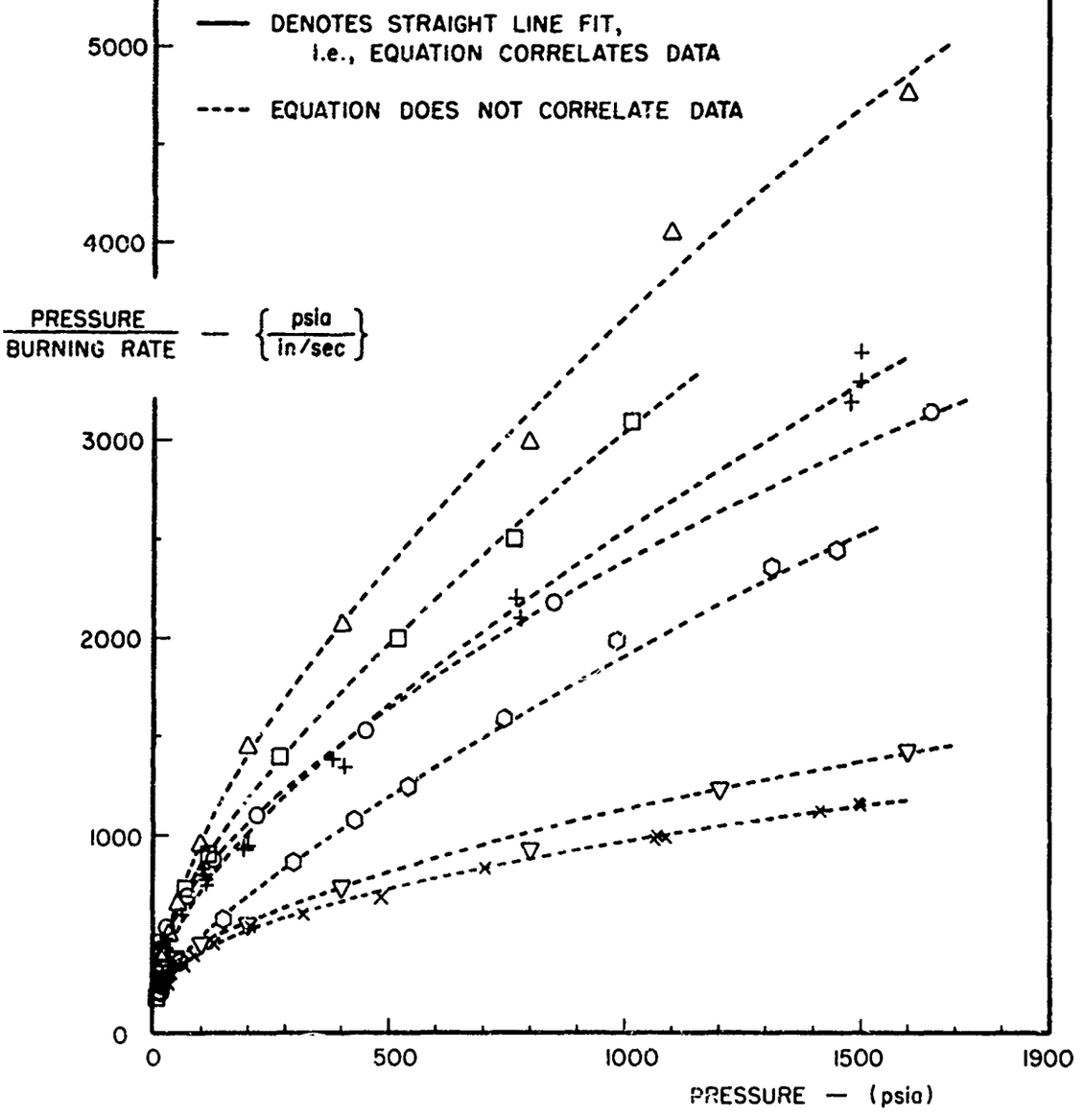

FIGURE 5 CORRELATION OF BURNING RATES WITH :

$$\left(\frac{1}{r}\right) \quad \left(\frac{a}{p}\right) + (c)$$

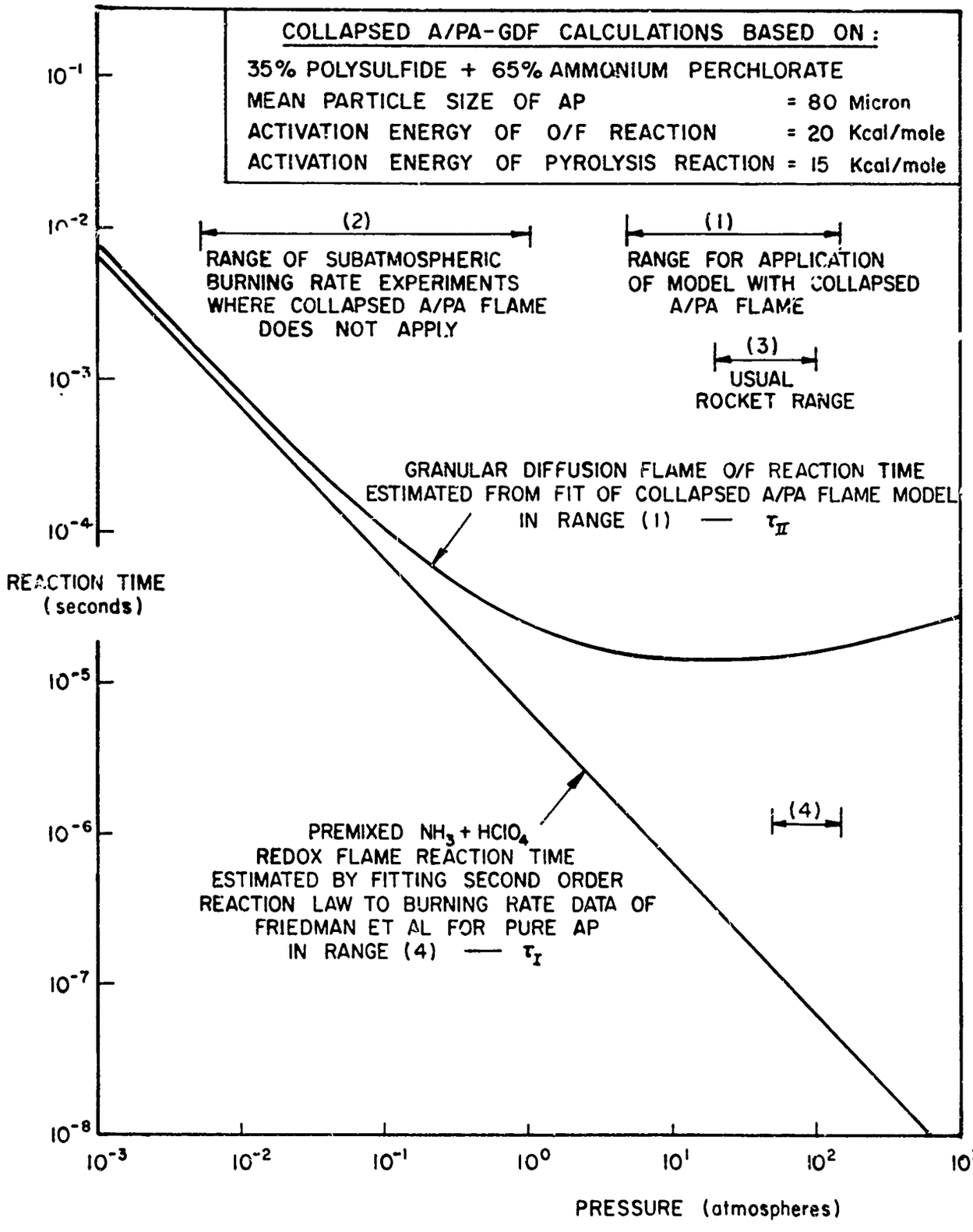

FIGURE 6 PRESSURE DEPENDENCE OF REACTION TIMES OF AMMONIA/PERCHLORIC ACID AND OXIDANT/FUEL REACTIONS

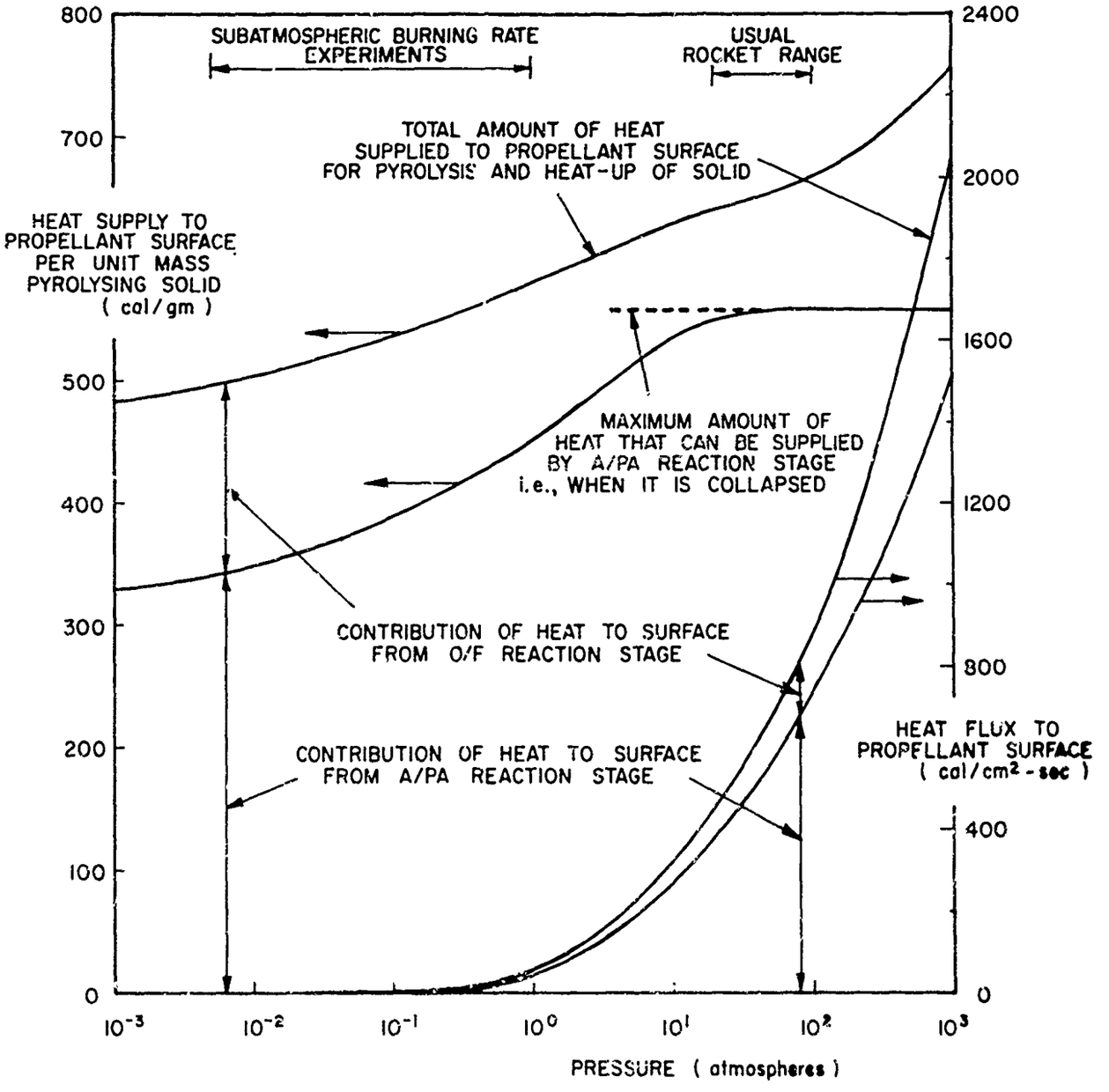

FIGURE 7 HEAT SUPPLY TO PROPELLANT SURFACE BY A/PA AND O/F STAGES IN THE GRANULAR DIFFUSION FLAME MODEL

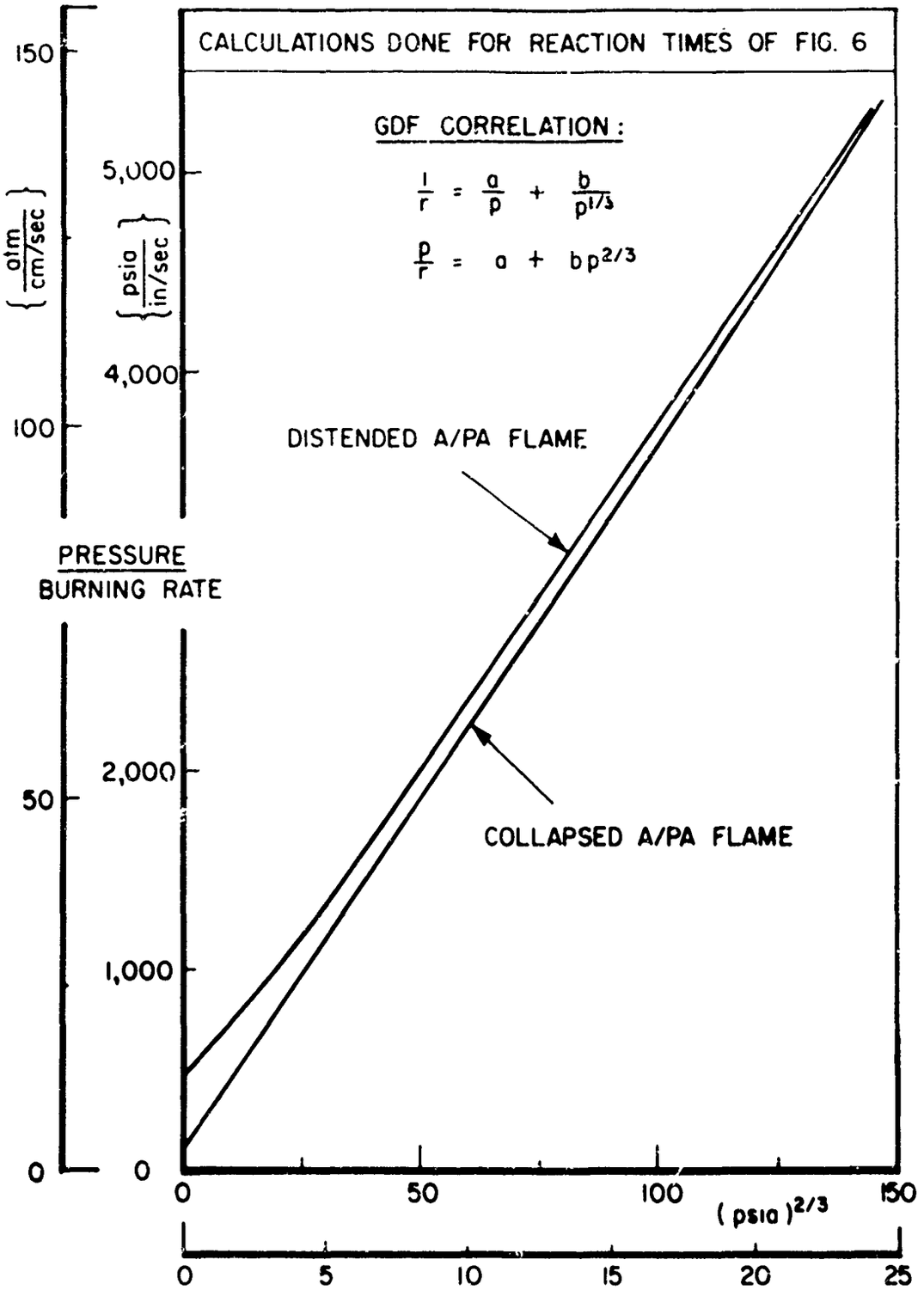

FIGURE 8 GRANULAR DIFFUSION FLAME THEORY PREDICTIONS PLOTTED AS (p/r) VS. $(p)^{2/3}$ FOR COLLAPSED AND DISTENDED A/PA FLAMES

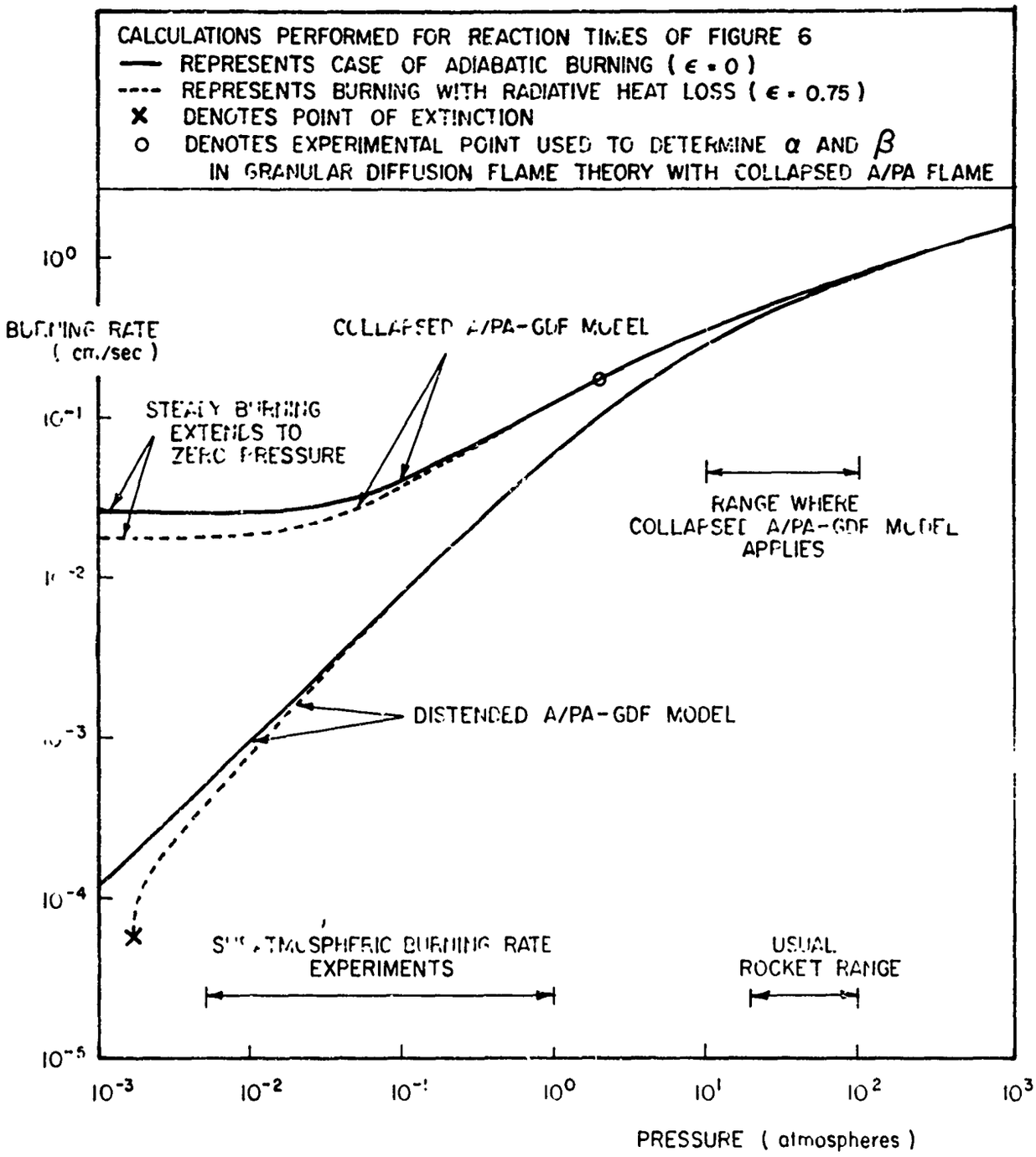

FIGURE 9 PRESSURE DEPENDENCE OF BURNING RATE PREDICTED BY THE GRANULAR DIFFUSION FLAME THEORY FOR THE CASES:

(1) PREMIXED AMMONIA/PERCHLORIC ACID FLAME IS DISTENDED.
(2) PREMIXED AMMONIA/PERCHLORIC ACID FLAME IS COLLAPSED.

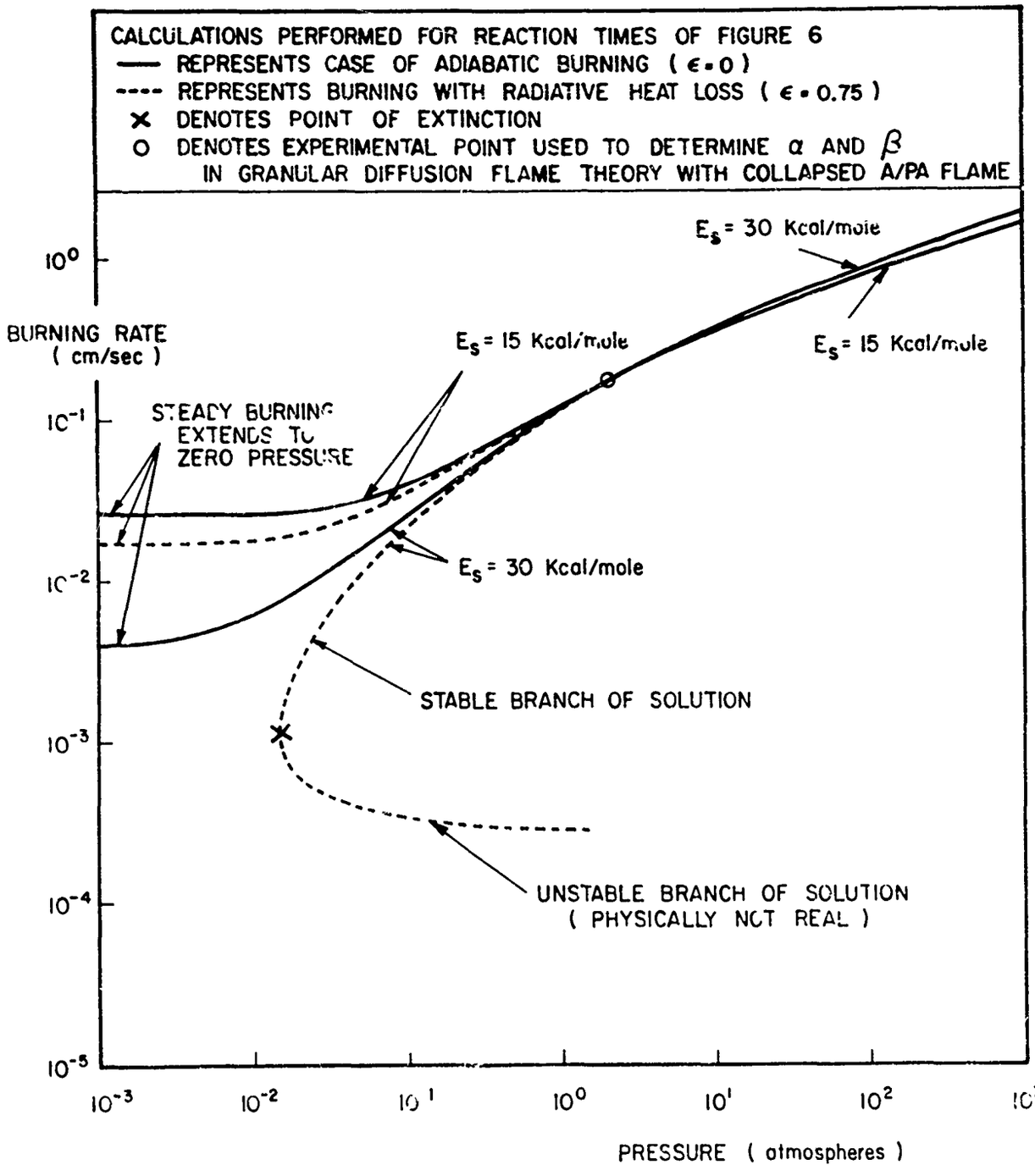

FIGURE 10 EFFECT OF ACTIVATION ENERGY OF SURFACE REACTION ON BURNING RATE BEHAVIOR OF GRANULAR DIFFUSION FLAME THEORY WITH COLLAPSED A/PA FLAME ZONE

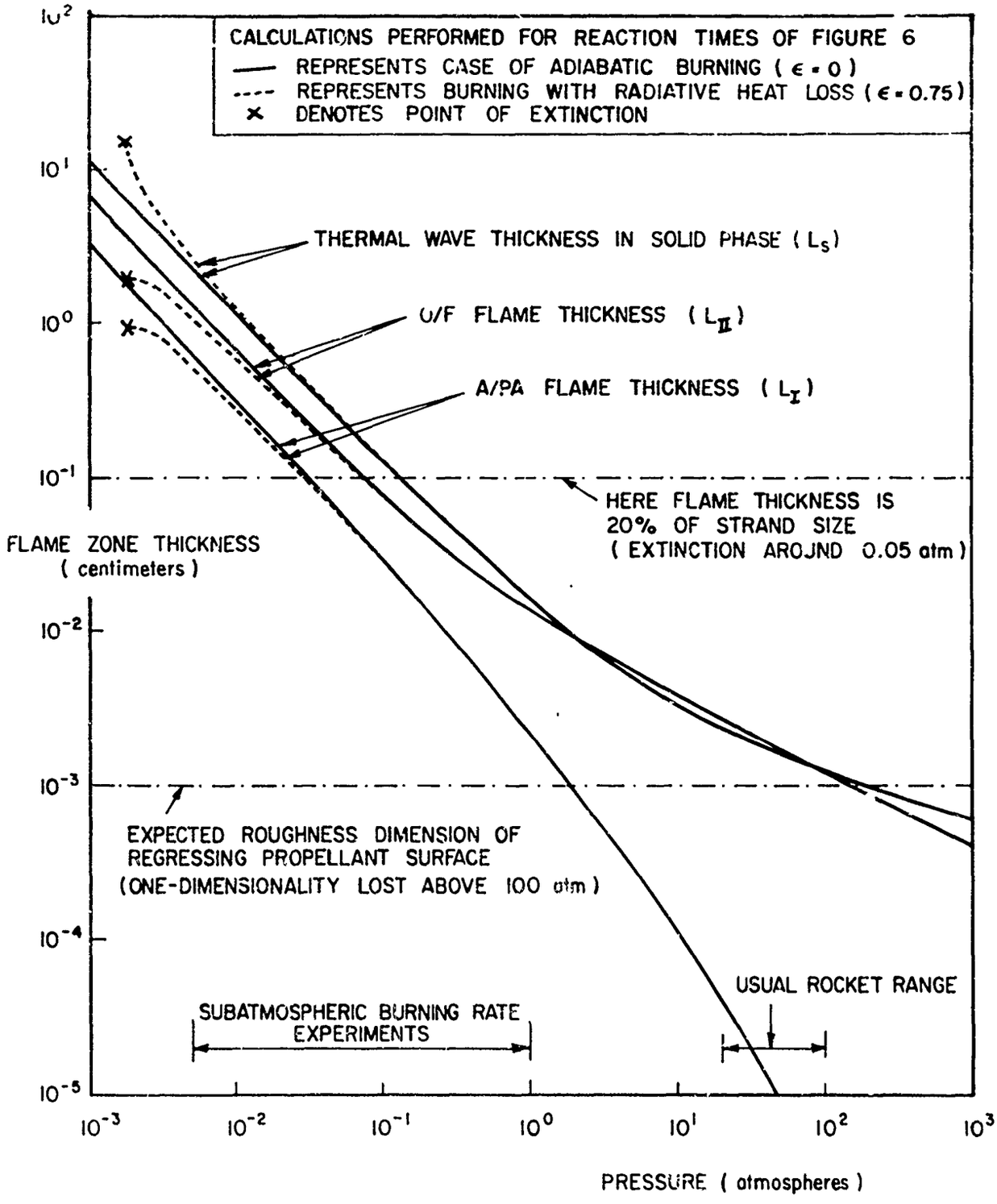

FIGURE 11 PRESSURE DEPENDENCE OF FLAME ZONE THICKNESSES PREDICTED BY GRANULAR DIFFUSION FLAME THEORY WITH DISTENDED A/PA FLAME

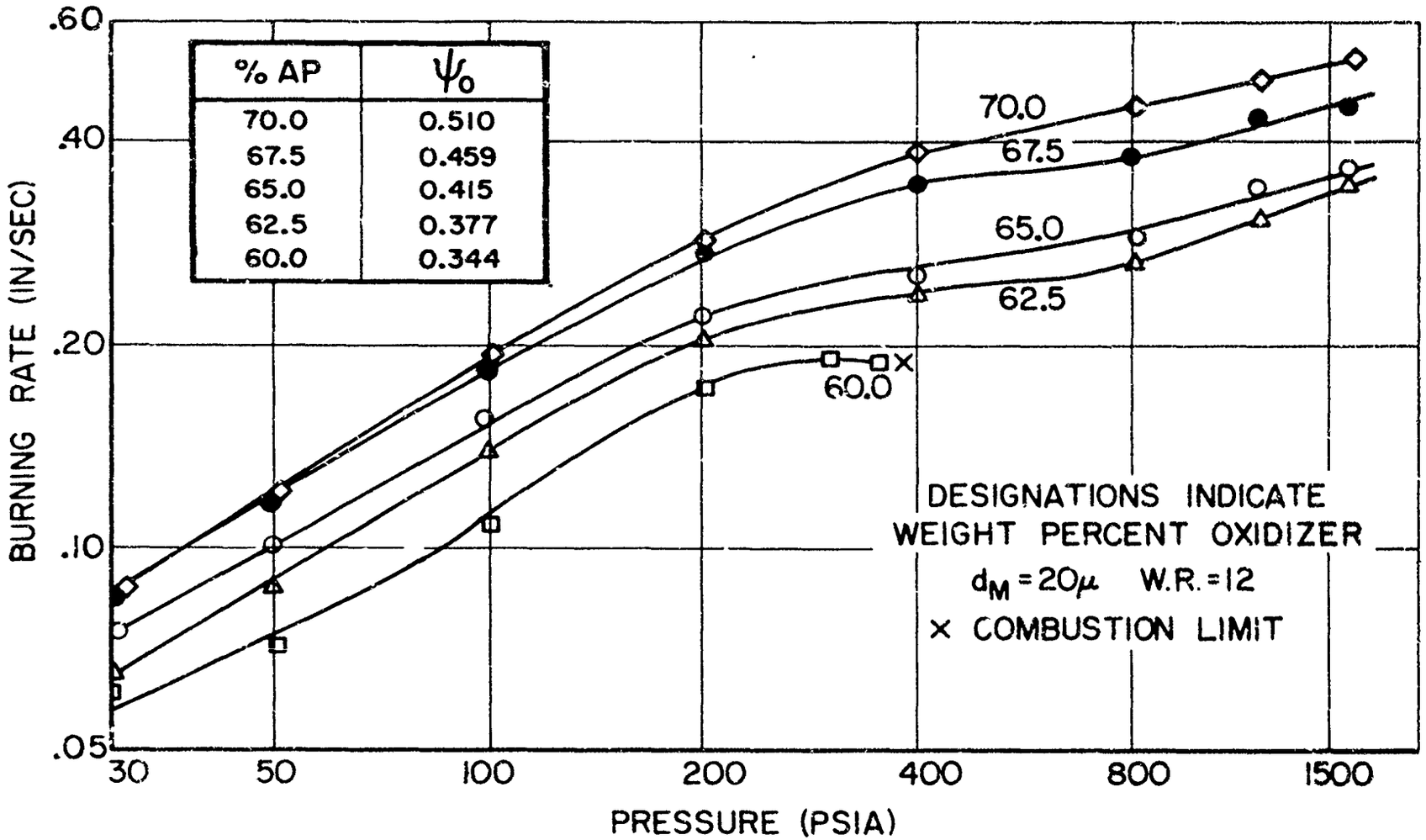

FIGURE 12 EFFECT OF AP LOADING ON BURNING RATE BEHAVIOR OF POLYSULFIDE(LP3/GMF)-AP PROPELLANT (FROM BASTRESS, REF. 14)

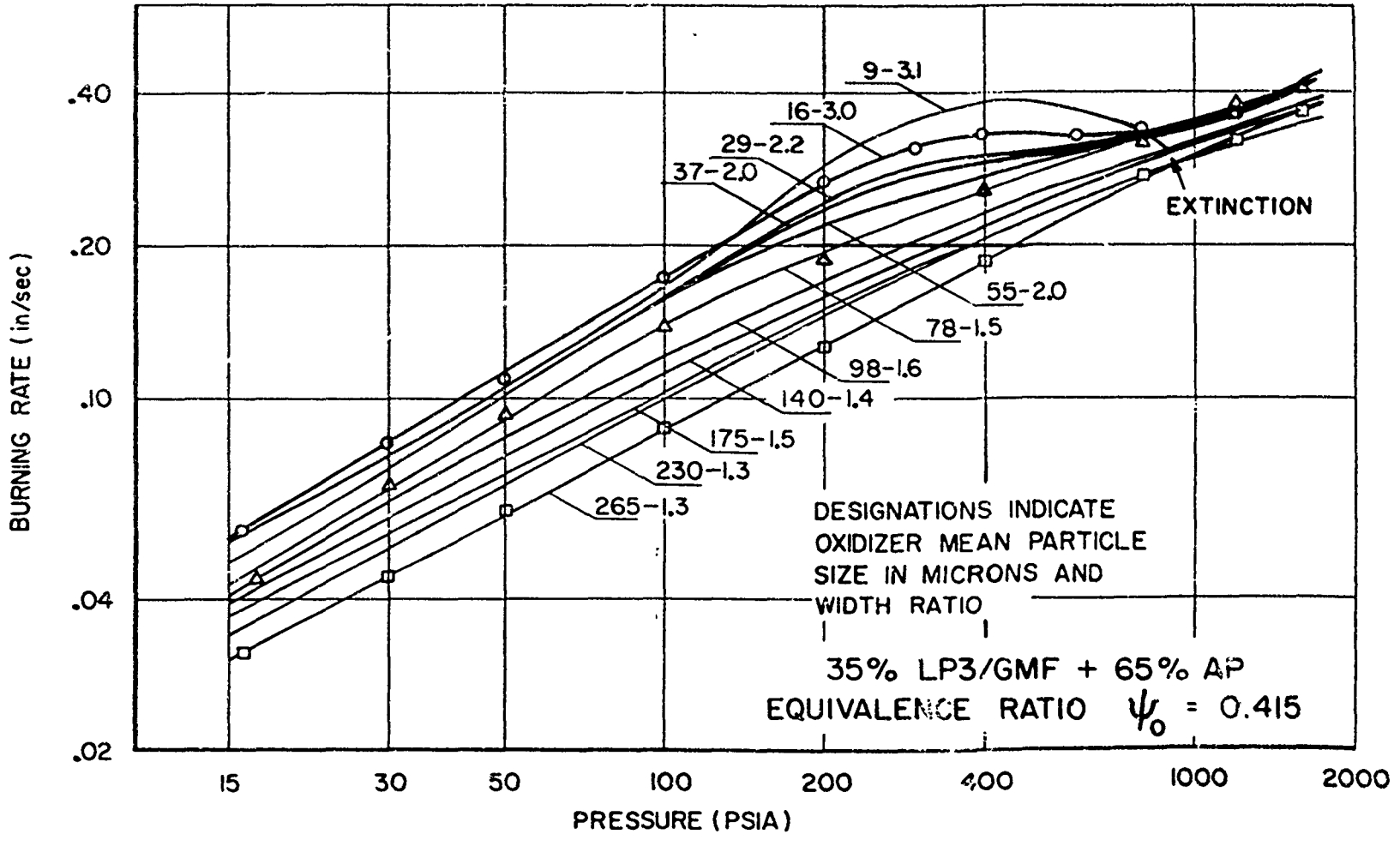

FIGURE 13 EFFECT OF AP PARTICLE SIZE ON BURNING RATE BEHAVIOR OF POLYSULFIDE-AP PROPELLANT (FROM BASTRESS)

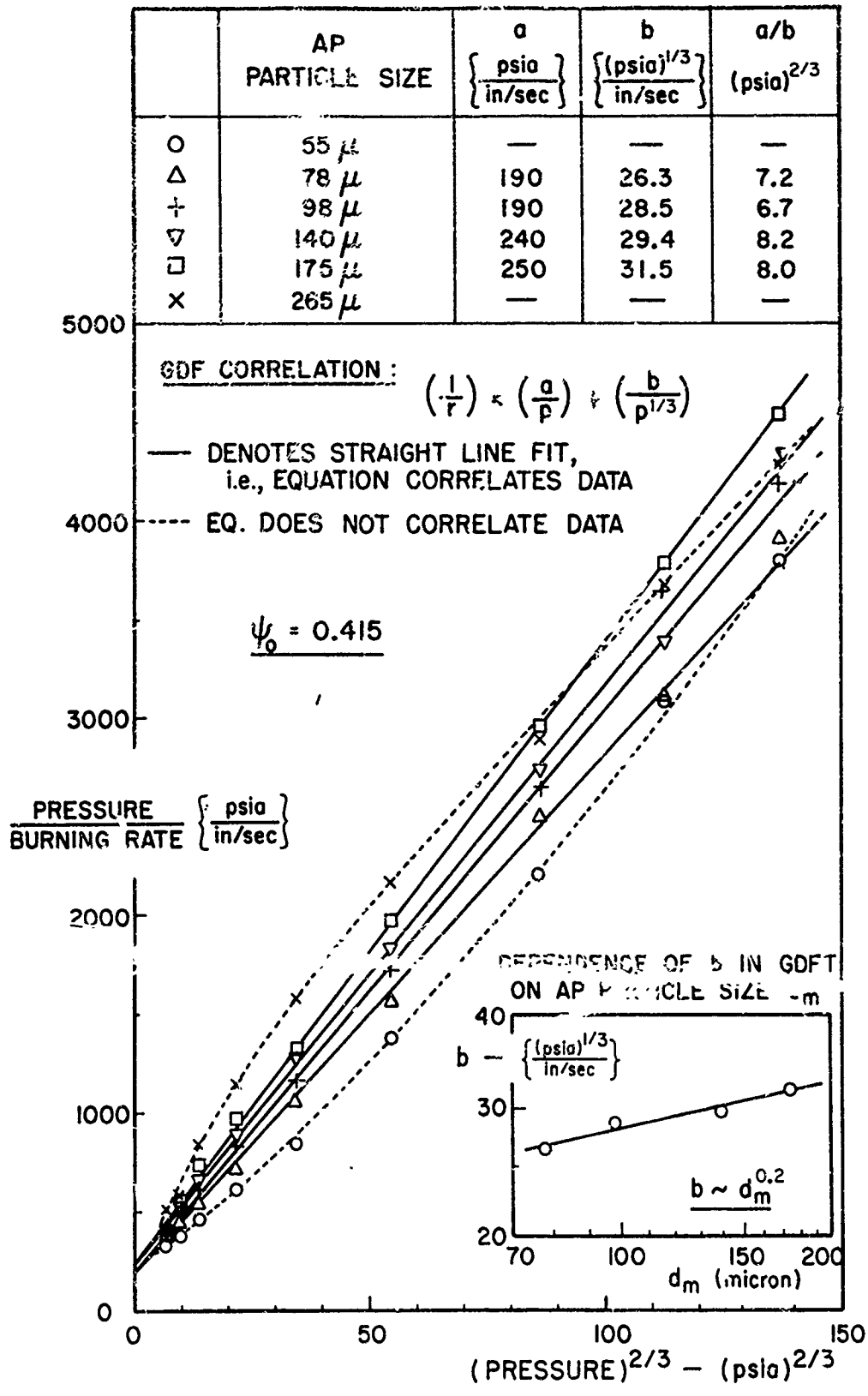

FIGURE 14 35% LP3/GMF + 65% AP DATA OF FIG. 12 PLOTTED AS (p/r) VS. ($p^{2/3}$)

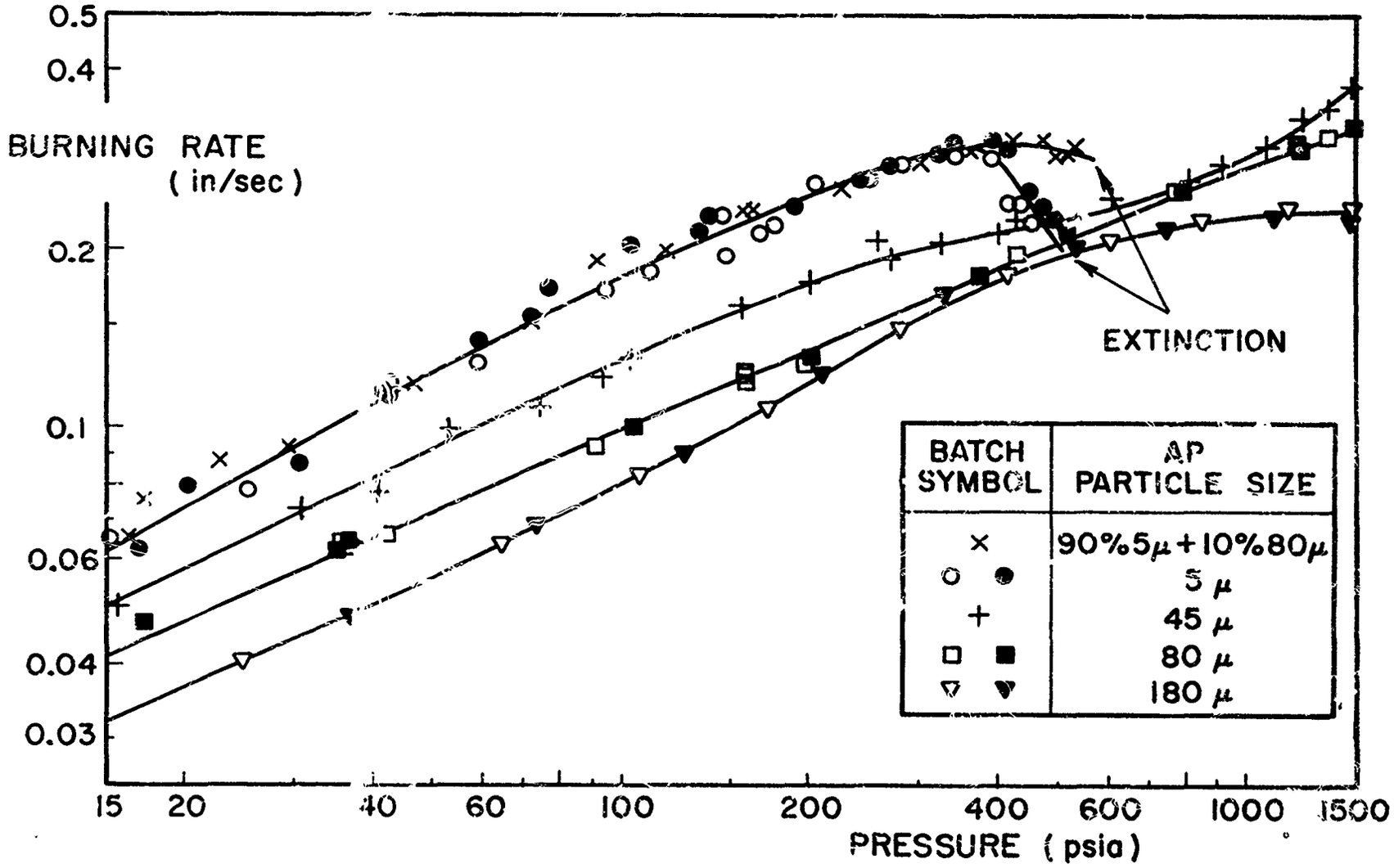

FIGURE 15 EFFECT OF AP PARTICLE SIZE ON BURNING RATE BEHAVIOR OF 25.0% PBAA/EPON + 75.0% AP PROPELLANT. (ψ_c = 0.337)

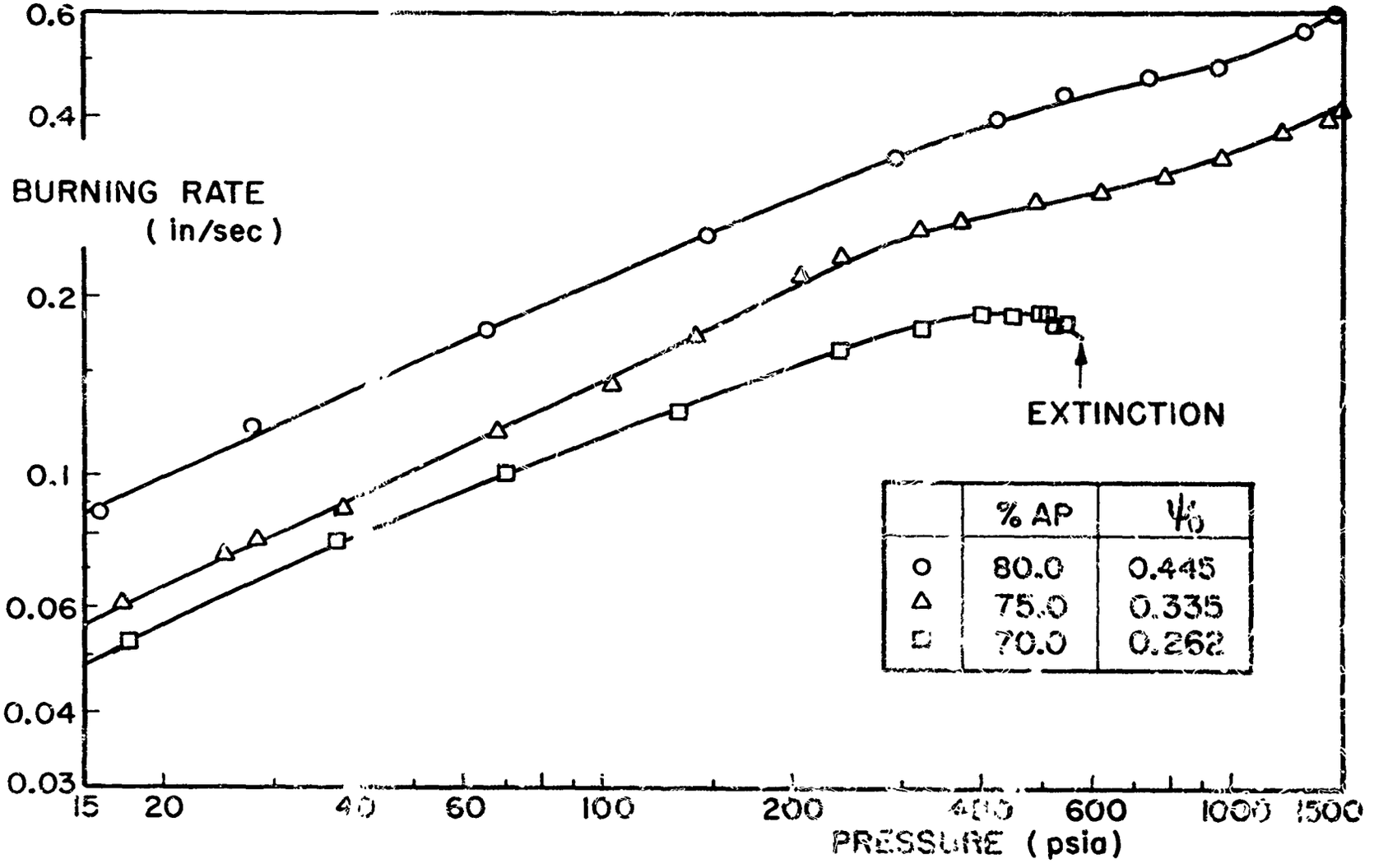

FIGURE 16 EFFECT OF AP LOADING ON BURNING RATE BEHAVIOR OF PBAA/EPON - AP PROPELLANT (BIMODAL AP: 30%5μ + 70%45μ)

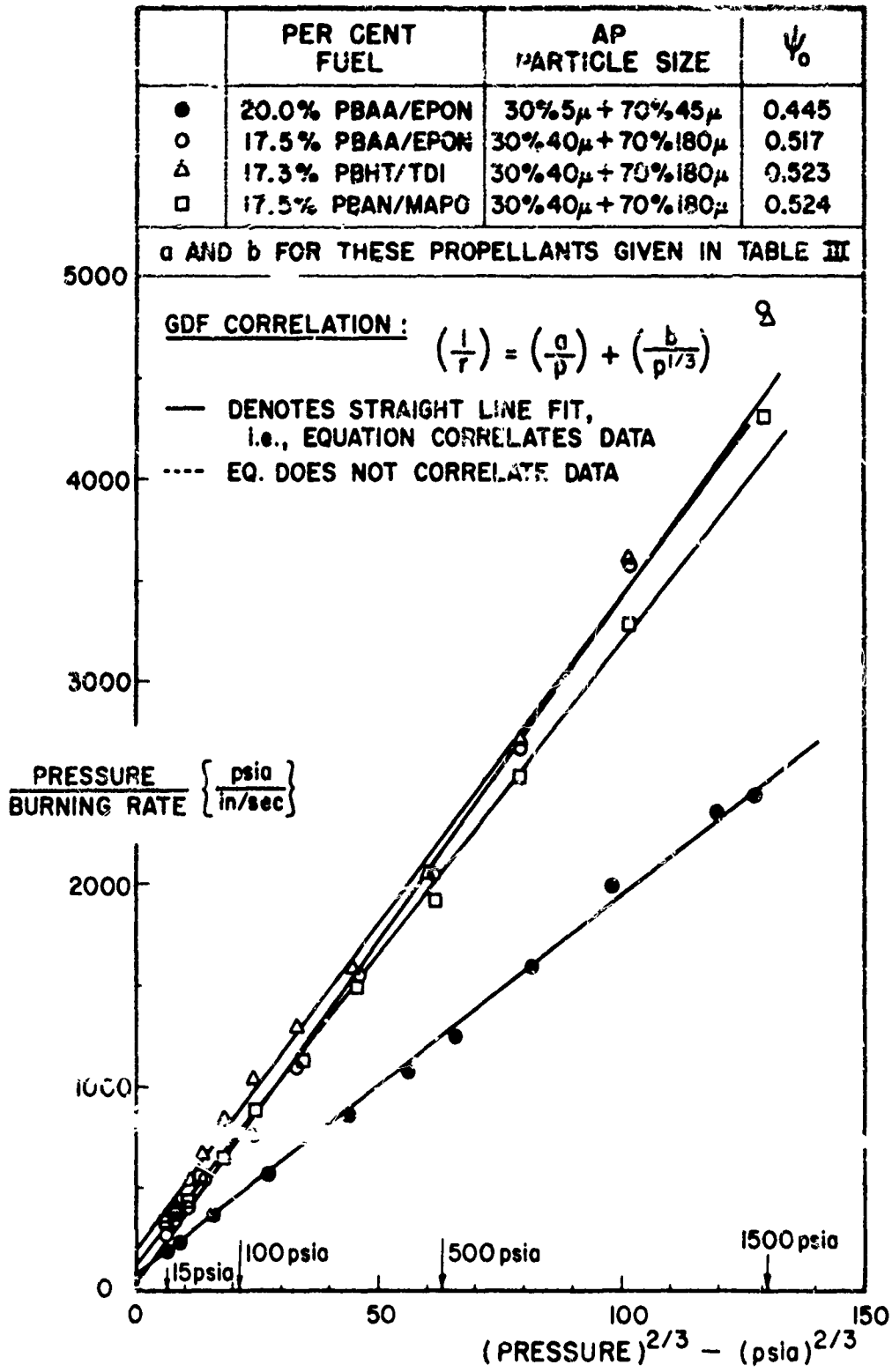

FIGURE 17 GDF CORRELATION OF HIGHLY LOADED AP PROPELLANTS WITH FUELS THAT DO NOT MELT READILY

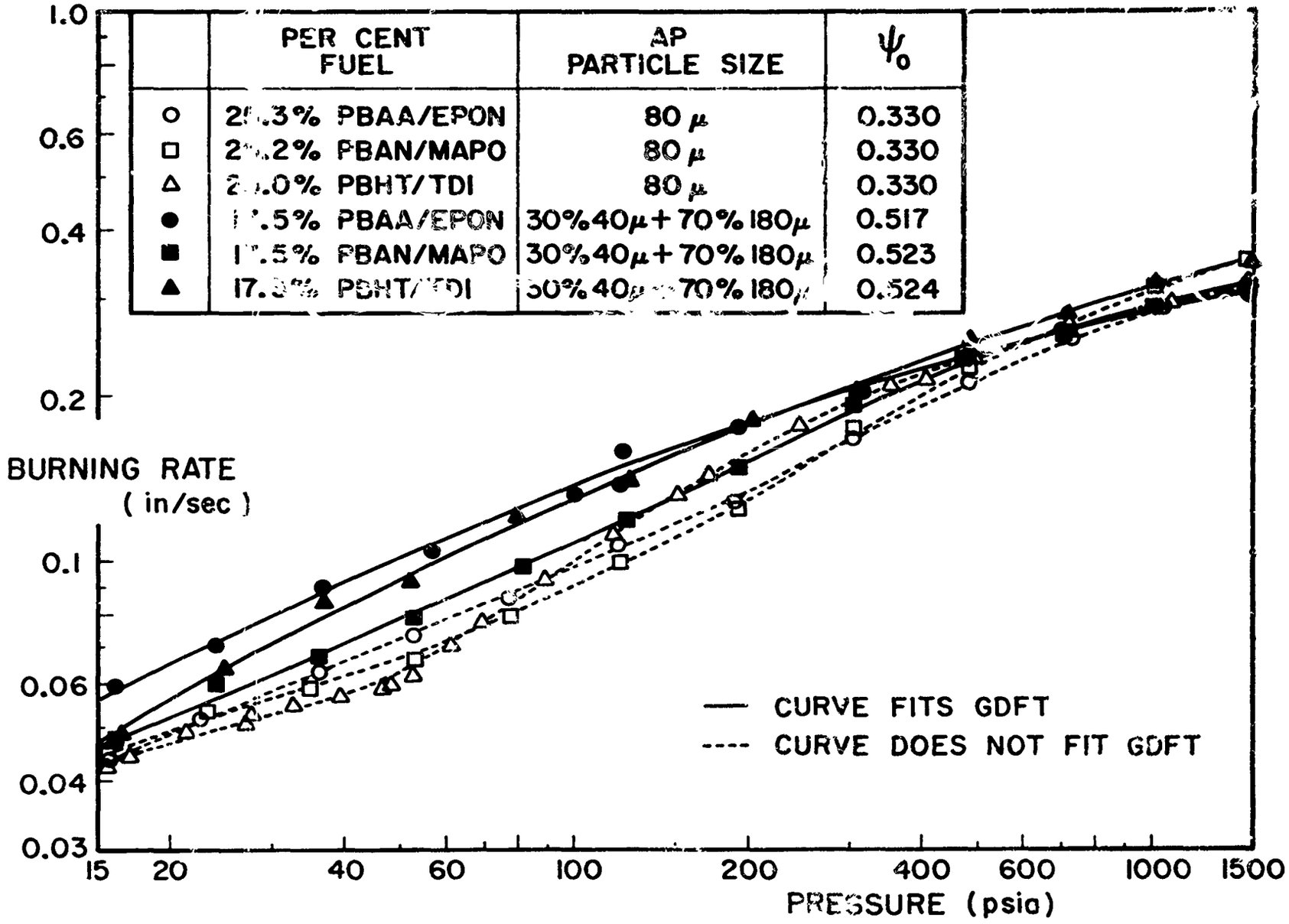

FIGURE 18 BURNING RATE BEHAVIOR OF AP-BASED PROPELLANTS WITH FUELS THAT DO NOT MELT READILY

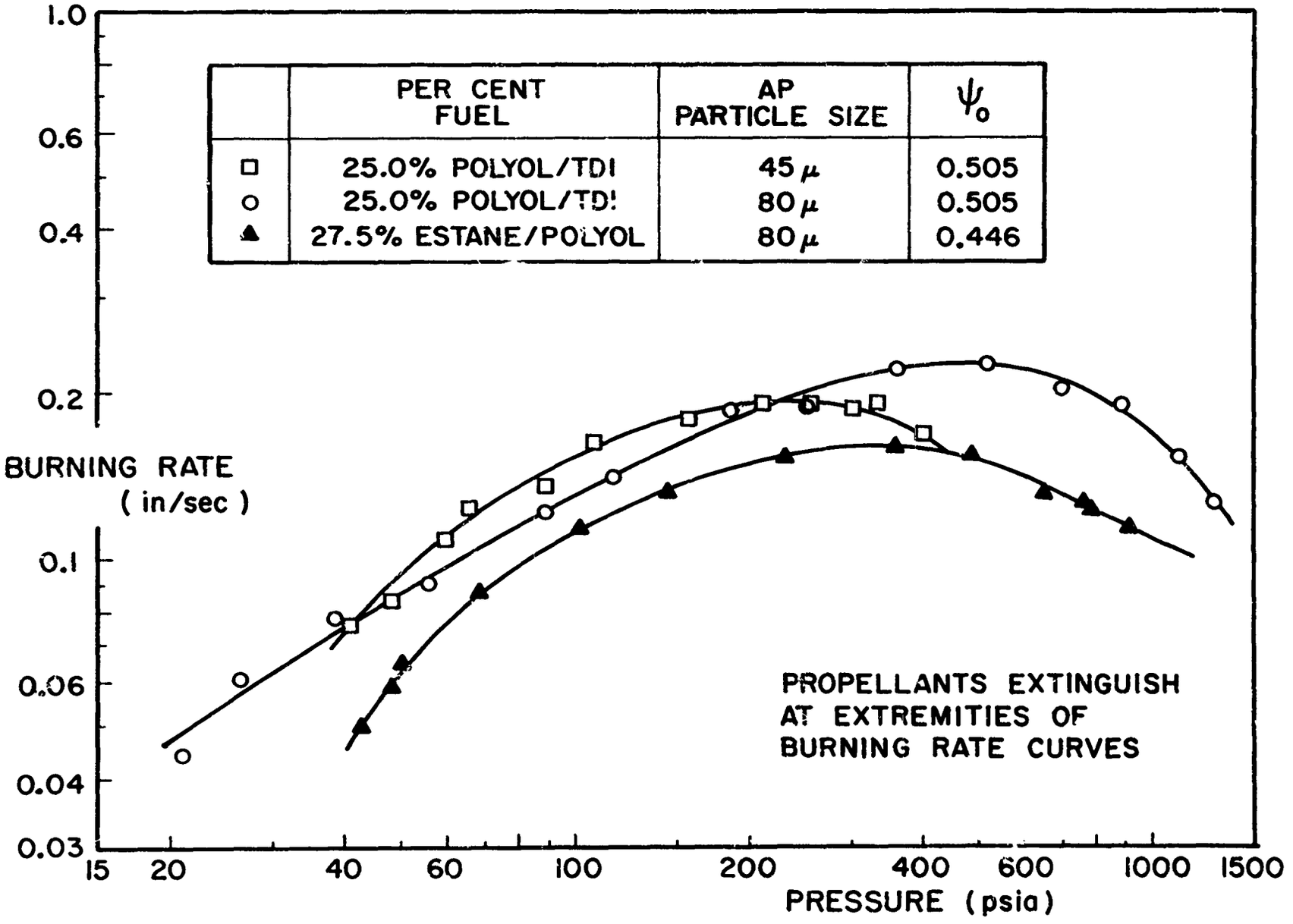

FIGURE 19 BURNING RATE BEHAVIOR OF UNIMODAL AP PROPELLANTS WITH POLYURETHANE FUELS THAT MELT READILY

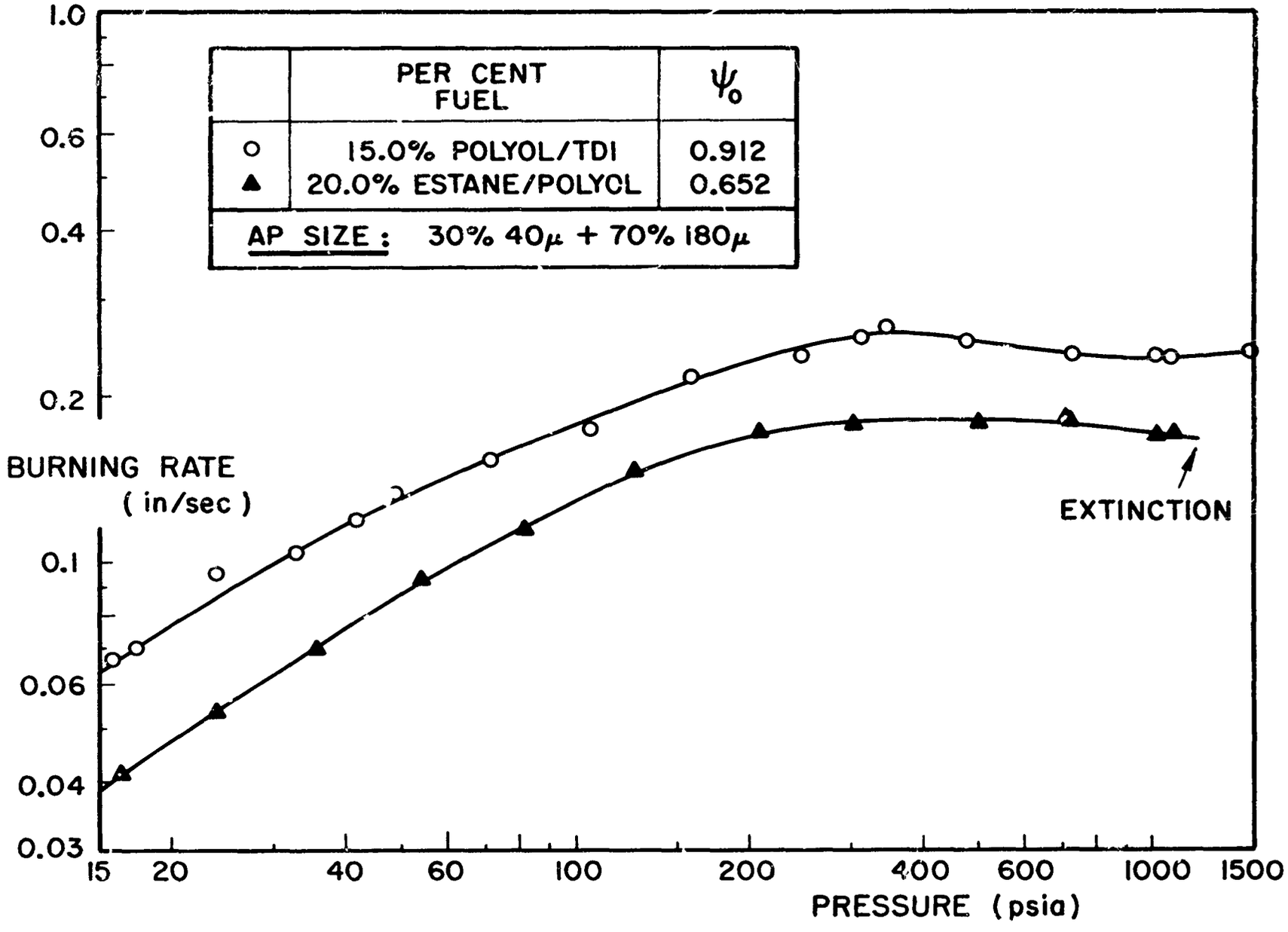

FIGURE 20 BURNING RATE BEHAVIOR OF BIMODAL AP PROPELLANTS WITH POLYURETHANE FUELS THAT MELT READILY

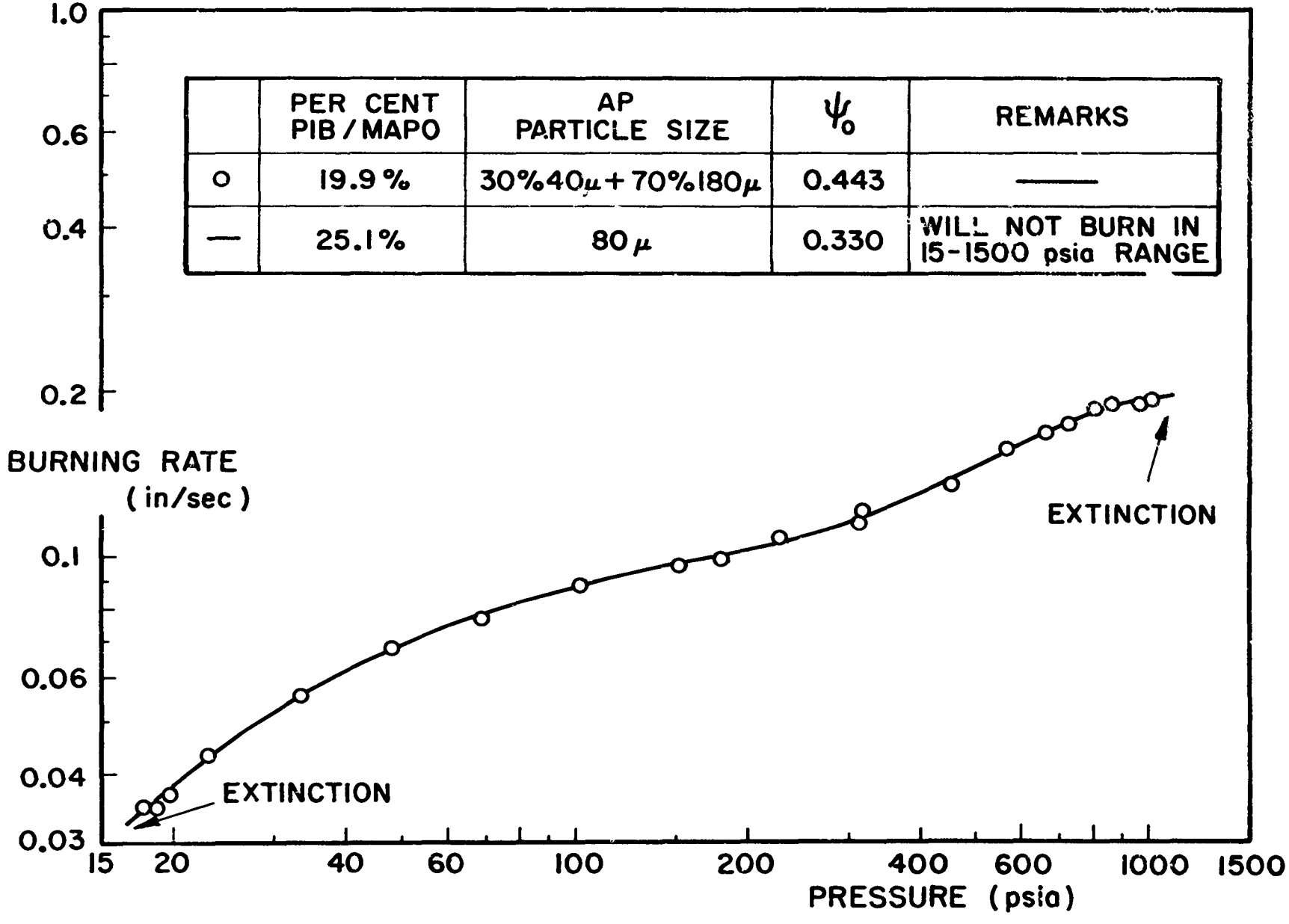

	PER CENT PIB / MAPO	AP PARTICLE SIZE	ψ_0	REMARKS
o	19.9 %	30%40μ + 70%180μ	0.443	——
—	25.1%	80 μ	0.330	WILL NOT BURN IN 15-1500 psia RANGE

FIGURE 21 BURNING RATE BEHAVIOR OF PIB/MAPO-AP PROPELLANT
(PIB/MAPO FUEL IS READILY MELTABLE)

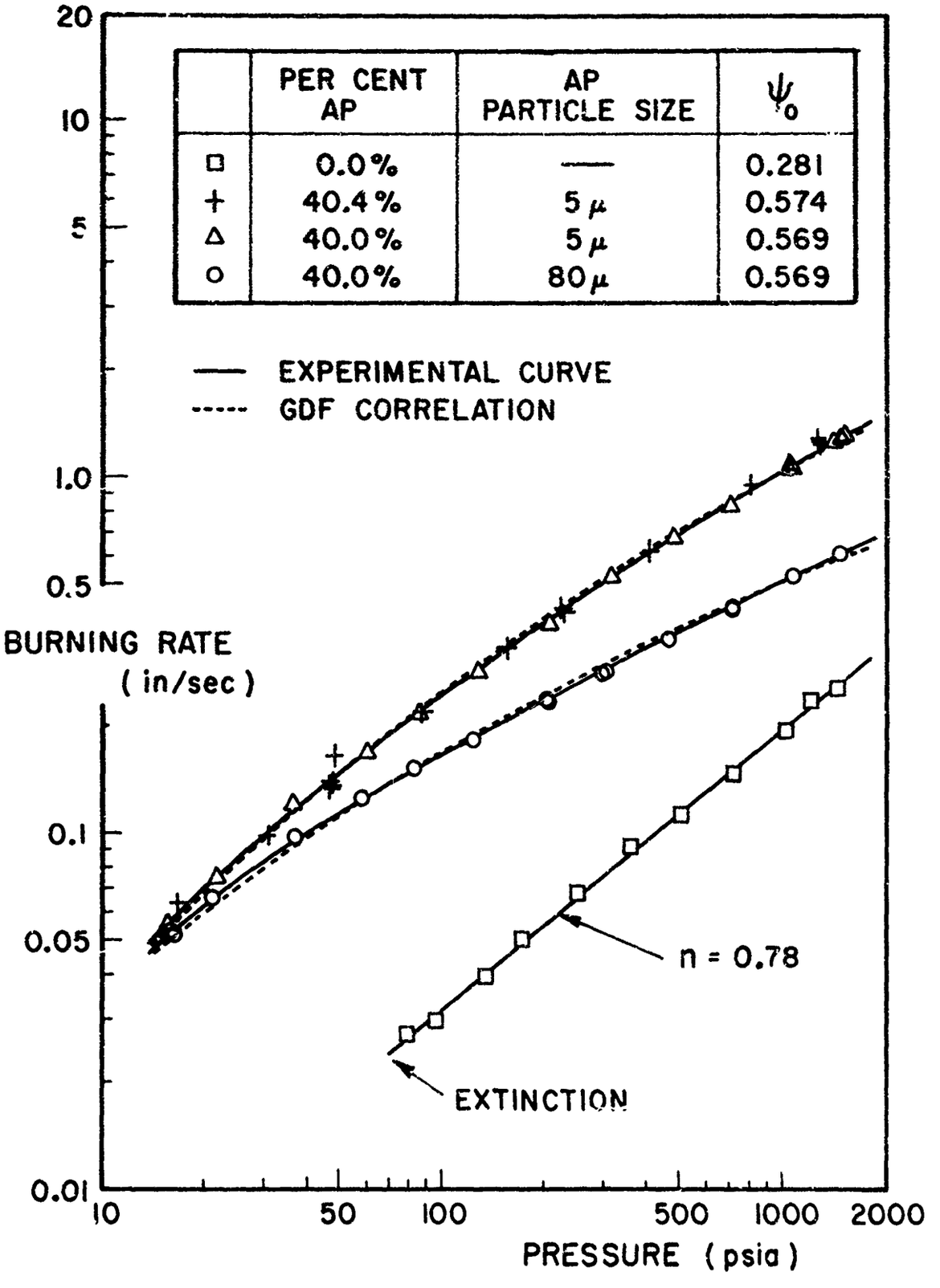

FIGURE 22 BURNING RATES OF DB AND CMDB PROPELLANTS (PURE NC/TEGDN AND NC/TEGDN-AP MIXTURES)

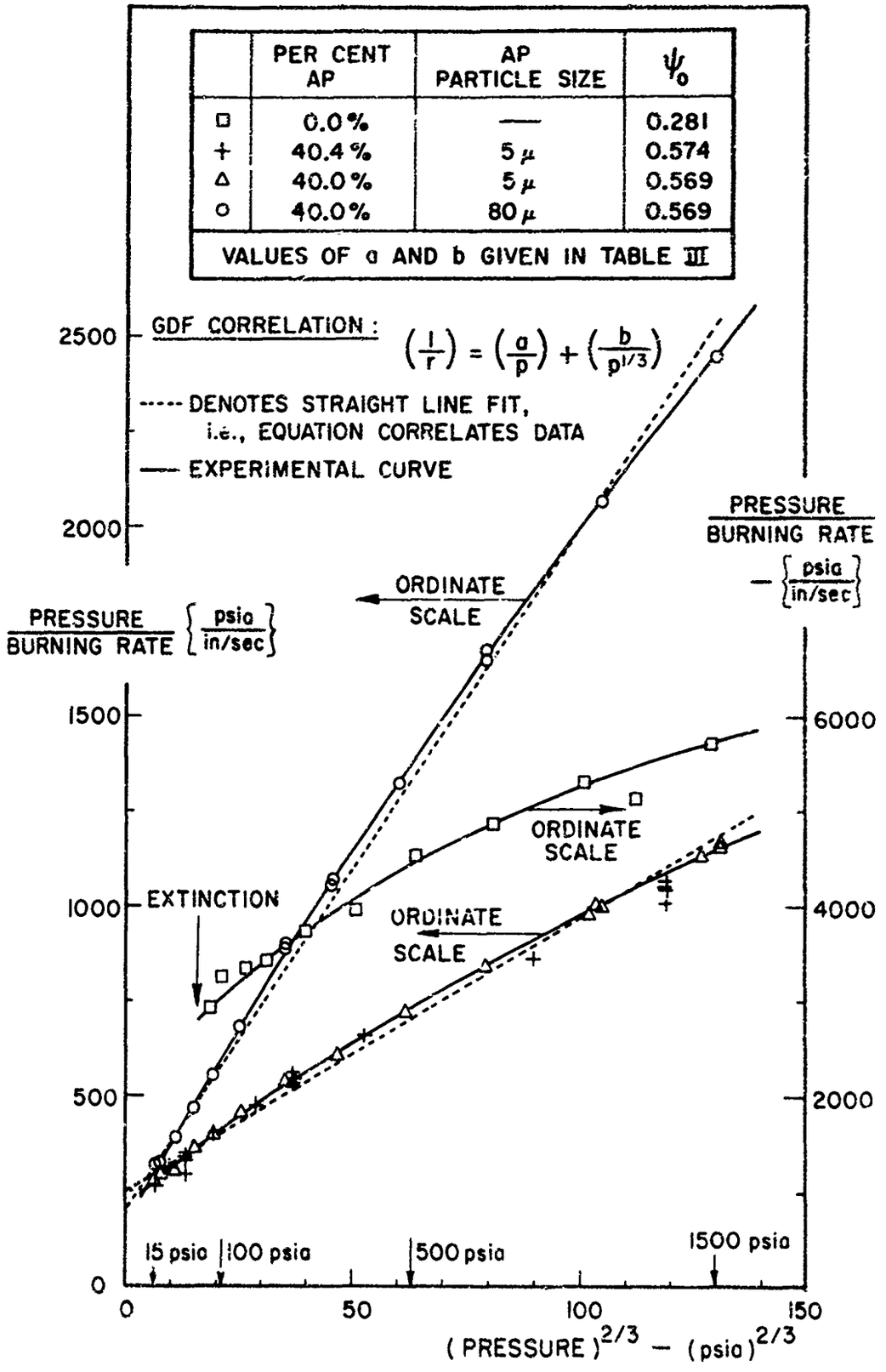

FIGURE 23 GDF CORRELATION OF DB AND CMDB PROPELLANTS (PURE NC/TEGDN AND NC/TEGDN-AP MIXTURES)

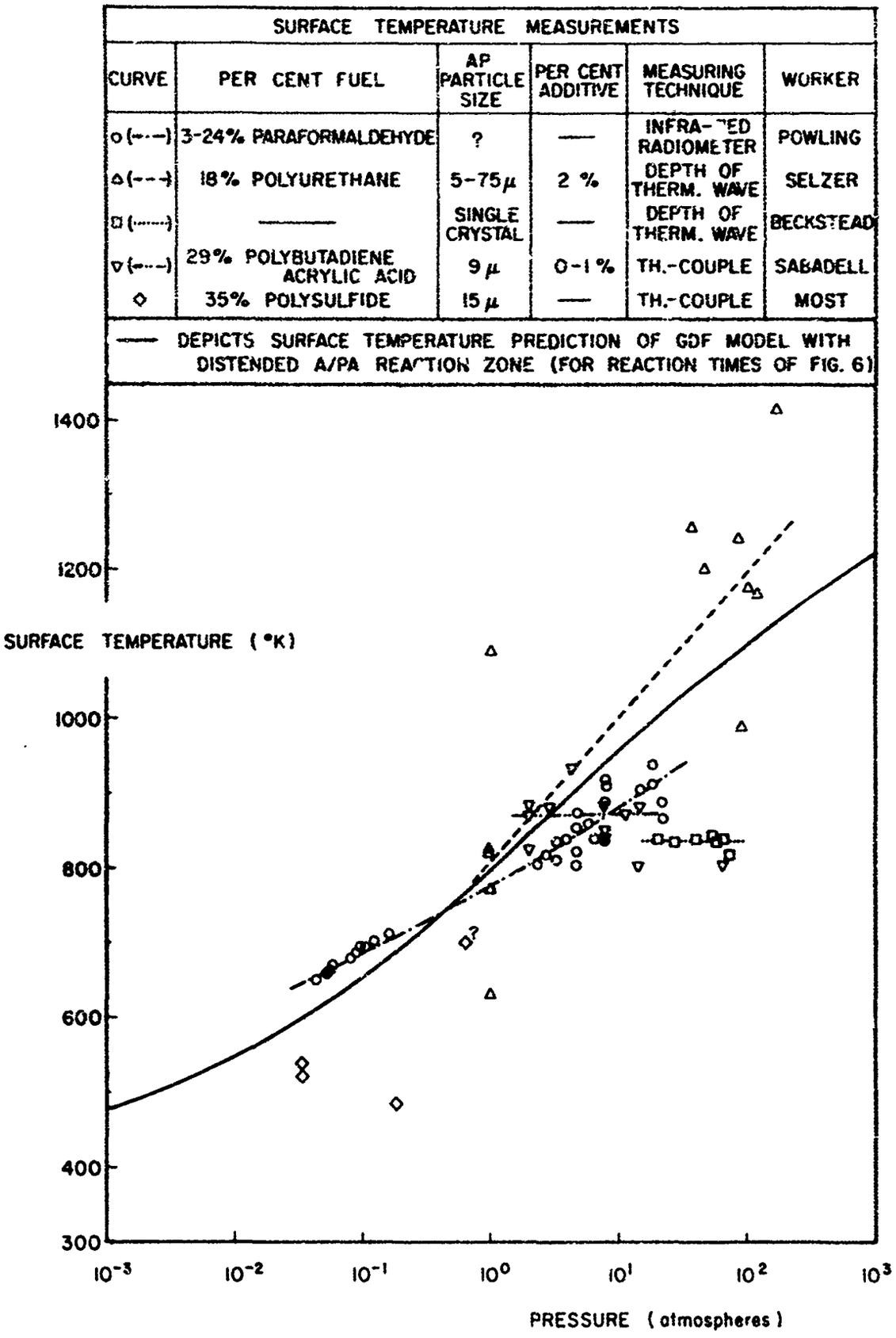

FIGURE 24 COMPARISON OF GDF THECRY PREDICTED SURFACE TEMPERATURE WITH MEASUREMENTS FOR AP-BASED PROPELLANTS

CURVE	PER CENT FUEL	AP PARTICLE SIZE	PER CENT ADDITIVE	INVESTIGATOR
A (——)	35% POLYSULFIDE	5 μ	——	THIS STUDY
B (——)	35% POLYSULFIDE	45 μ	——	THIS STUDY
C (------)	25% POLYBUTADIENE ACRYLIC ACID	5 μ	——	THIS STUDY
D (------)	25% POLYBUTADIENE ACRYLIC ACID	13 μ	——	COLE
E (------)	25% POLYBUTADIENE ACRYLIC ACID	188 μ	——	COLE
F (— — —)	25% PB (CARBOXYL-TERMINATED)	5 μ	——	THIS STUDY
G (— — —)	25% PB (HYDROXYL-TERMINATED)	5 μ	——	THIS STUDY
H (— — —)	25% PB (HYDROXYL-TERMINATED)	5 μ	0.75% CC	THIS STUDY
I (— — —)	20% POLYESTER RESIN	20 μ	——	WEBB
J (— — —)	20% POLYESTER RESIN	100 μ	——	WEBB
K (— — —)	20% POLYESTER RESIN	?	——	SILLA
L (— — —)	POLYVINYL CHLORIDE	50 μ	ALUMINUM	BARRÈRE
M (— — —)	POLYVINYL CHLORIDE	50 μ	——	BARRÈRE
N (------)	24.3% PARAFORMALDEHYDE	?	——	POWLING
O (------)	10% PARAFORMALDEHYDE	?	3% CC	POWLING
P (------)	11% POLYISOBUTYLENE	?	——	POWLING
Q (------)	18% PB ACRYLIC ACID (1/1 BIMODAL)	15μ + 230μ	——	FEINAUER
R (------)	20% PB ACRYLIC ACID (1/1 BIMODAL)	15μ + 230μ	2% CARBON	FEINAUER
S (------)	20% PB ACRYLIC ACID (1/1 BIMODAL)	15μ + 230μ	2% CC	FEINAUER

PB DENOTES POLYBUTADIENE ; CC DENOTES COPPER CHROMITE .

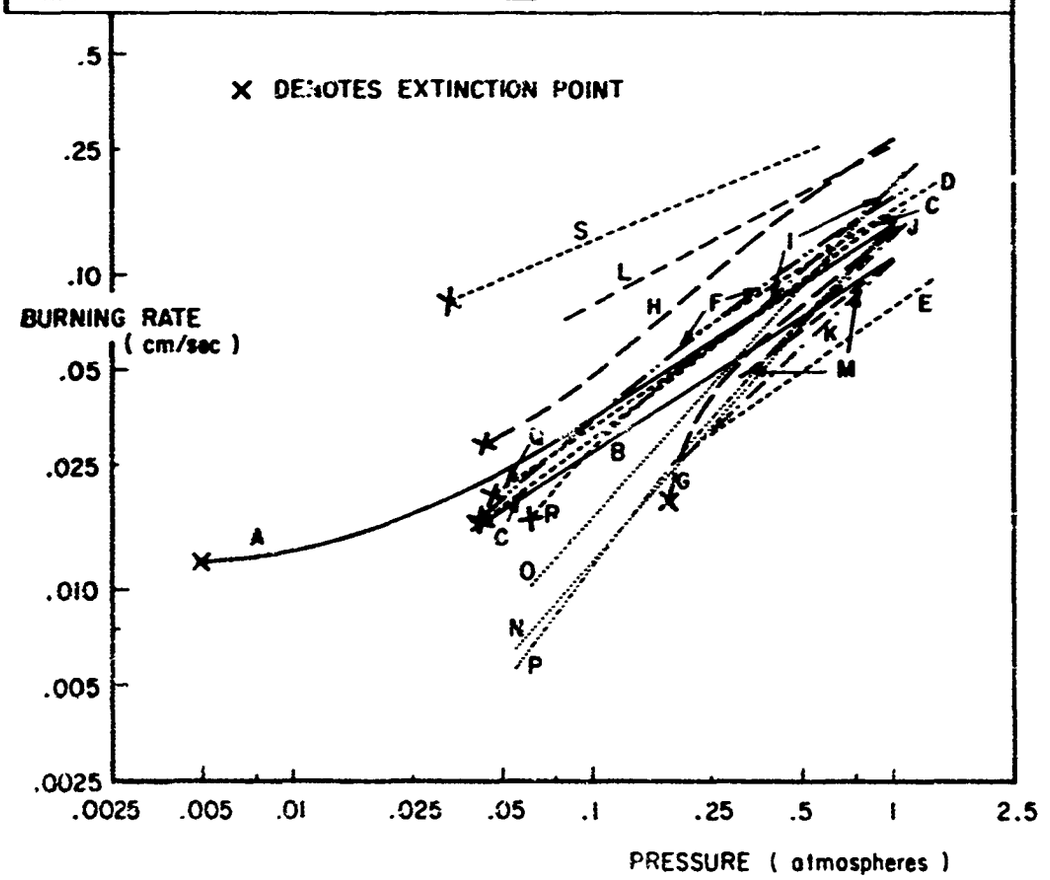

FIGURE 25 BURNING RATE – PRESSURE DEPENDENCE AT SUBATMOSPHERIC PRESSURES FOR AMMONIUM PERCHLORATE WITH DIFFERENT BINDERS

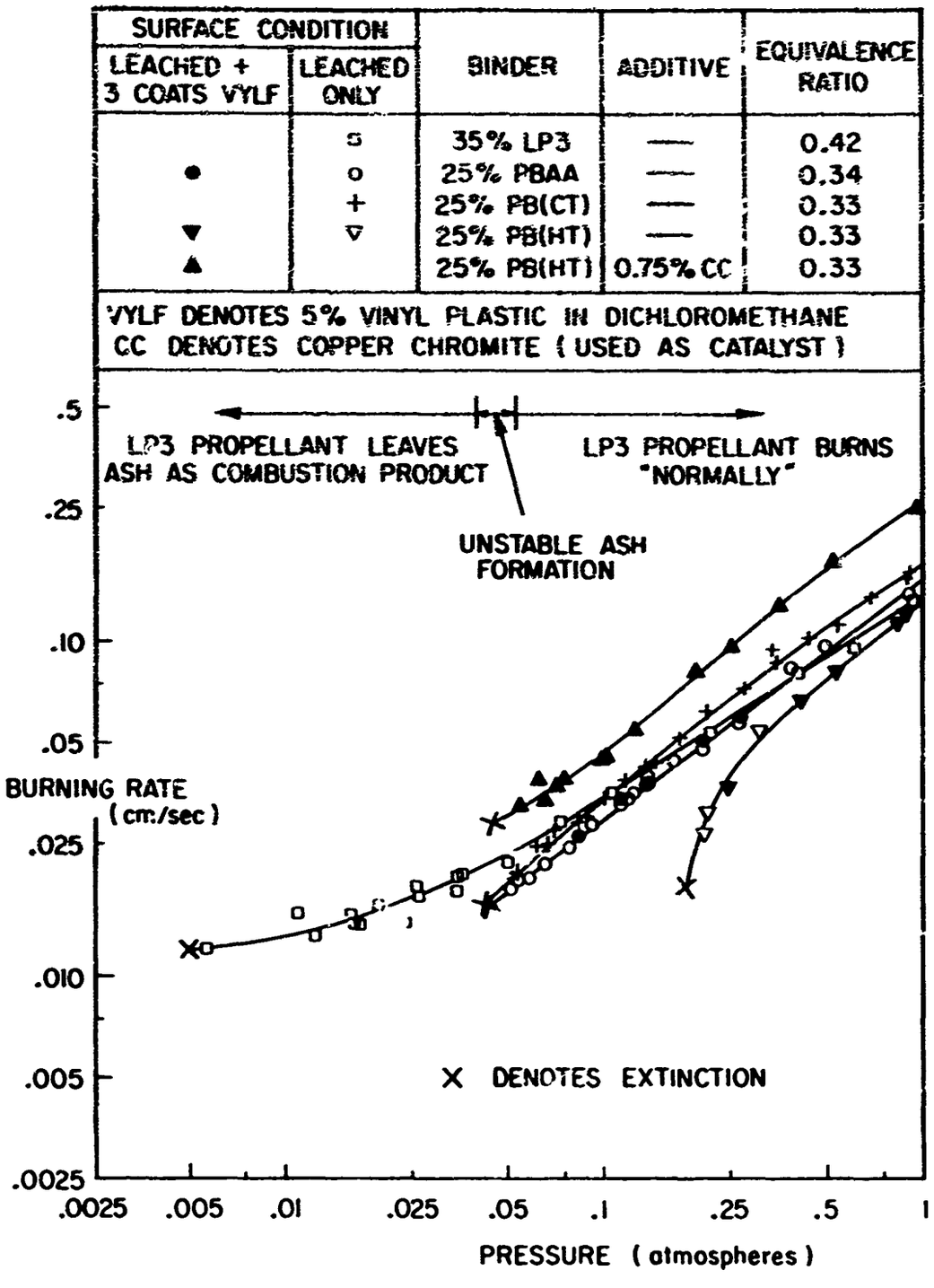

FIGURE 26 EFFECT OF BINDER-TYPE ON BURNING RATE OF AMMONIUM PERCHLORATE PROPELLANTS

(MEAN PARTICLE SIZE OF AP IS 5 MICRON)

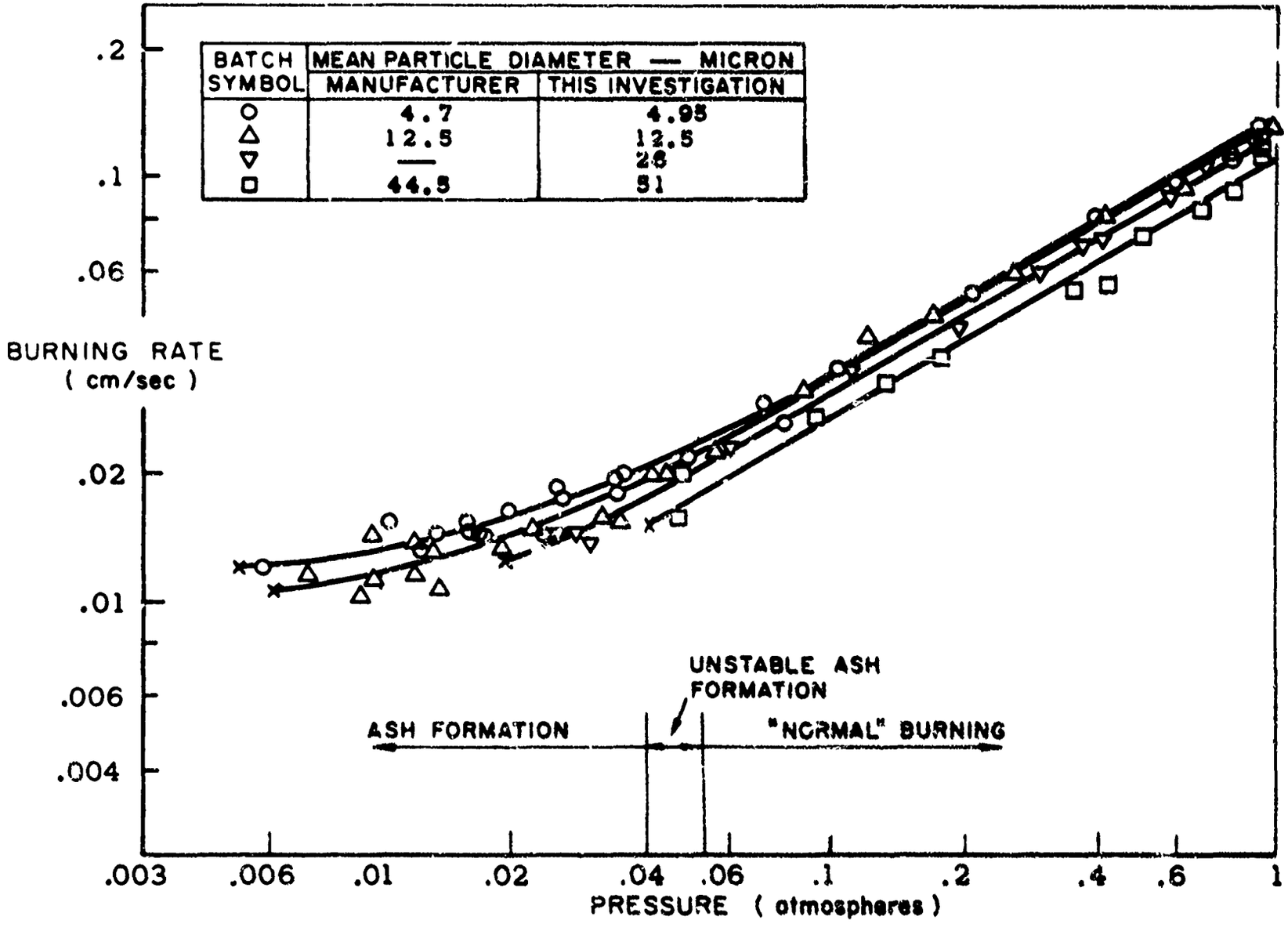

FIGURE 27 BURNING RATE OF 35% POLYSULFIDE + 65% NH_4ClO_4 WITH VARYING MEAN OXIDIZER PARTICLE SIZE

APPENDIX A

LISTING OF PHYSICAL CONSTANTS AND CALCULATED PREDICTIONS FOR GRANULAR DIFFUSION FLAME THEORY (Collapsed and Distended A/PA Flames)

The following numerical values were assumed as typical of AP composite propellants in the calculations:

$$C_c = 0.3 \text{ cal/gm } ^\circ\text{C}$$

$$C_g = 0.3 \text{ cal/gm } ^\circ\text{C}$$

$$\alpha_c = 10^{-3} \text{ cm}^2/\text{sec}$$

$$\epsilon = 0 \text{ or } 0.75 \text{ (estimated)}$$

$$\lambda_g = 2 \times 10^{-4} \text{ cal/cm sec } ^\circ\text{C}$$

$$\rho_c = 1.66 \text{ gm/cm}^3$$

$$E_2 = 20 \text{ kcal/mole}$$

$$E_s = 15 \text{ or } 30 \text{ kcal/mole}$$

$$M_1 = M_2 = 1.5$$

$$T_{2(ad)} = 2000^\circ\text{K}$$

$$(\Delta h_{tr} + \Delta h_s) = 430 \text{ cal/gm}$$

$$\Delta h_I = 560 \text{ cal/gm}$$

The values chosen for the various enthalpies of transition have been obtained by drawing the respective values for pure AP and typical fuels from the indicated references and converting them to their equivalent values for a typical propellant containing 70% AP, i.e., for pure AP, we assumed,

$$\Delta h_{tr} = 20 \text{ cal/gm (Ref. 36)}$$

$$\Delta h_s = 520 \text{ cal/gm (Refs. 28-30)}$$

$$(\Delta h_I + \Delta h_s) = -280 \text{ cal/gm (See Table I)}$$

$$\text{i.e., } \Delta h_I = (\Delta h_I + \Delta h_s) - \Delta h_s$$

$$= -520 - 280 = -800 \text{ cal/gm}$$

and for typical binders, we assumed:

$$\Delta h_{tr} = 0 \text{ cal/gm}$$

$$\Delta h_s = 175 \text{ cal/hm (Ref. 149)}$$

$$\Delta h_I = 0 \text{ cal/gm}$$

Note that in accord with Ref. 91, the net heat liberated at the regressing propellant surface when the A/PA flame is collapsed to the surface, is: $(\Delta h_s + \Delta h_I) \approx 140$ cal/gm.

The above values have been used in conjunction with the measurement (91)

$$T_s = 615^{\circ}C \approx 900^{\circ}K \text{ at } p = 30 \text{ psia}$$

and typical values of a and b for an 80μ mean oxidizer particle size propellant (3,4,14), namely,

$$a = 190 \text{ psia sec/in} = 32.8 \text{ atm sec/cm}$$

$$b = 25 \text{ (psia)}^{1/3} \text{ sec/in} = 25.9 \text{ (atm)}^{1/3} \text{ sec/cm}$$

to evaluate α and β from the identical Equations (14) and (15) and to evaluate A from Equation (5).

The numerical predictions of the granular diffusion flame theory (using the above values for the physical constants), are listed in the tables below for the cases where the A/PA stage is distended (τ_I finite) and where the A/PA flame is collapsed to the propellant surface ($\tau_I = 0$). The predictions are given for $\epsilon = 0$ (no radiative heat loss) and $\epsilon = 0.75$ (with radiative heat loss) in both cases.

TABLE II(A) COLLAPSED A/PA-GDF PREDICTIONS FOR CASE WHEN E_a = 15 kcal/mole

($\tau_I = 0 = L_I$)

Without Radiative Heat Loss ($\epsilon = 0$)				With Radiative Heat Loss ($\epsilon = 0.75$)			
T_s (^oK)	P (atm)	r (cm/sec)	L_{II} (cm)	T_s (^oK)	p (atm)	r (cm/sec)	L_{II} (cm)
1100.00	1.067×10^{2}	8.037×10^{-1}	1.226×10^{-3}	1100.00	1.020×10^{2}	8.037×10^{-1}	1.208×10^{-3}
1050.00	3.947×10^{1}	5.806×10^{-1}	2.074×10^{-3}	1050.00	3.803×10^{1}	5.806×10^{-1}	2.036×10^{-3}
1000.00	1.449×10^{1}	4.064×10^{-1}	3.705×10^{-3}	1000.00	1.411×10^{1}	4.064×10^{-1}	3.617×10^{-3}
950.00	5.398×10^{0}	2.738×10^{-1}	7.106×10^{-3}	950.00	5.328×10^{0}	2.738×10^{-1}	6.868×10^{-3}
900.00	2.042×10^{0}	1.766×10^{-1}	1.500×10^{-2}	900.00	2.052×10^{0}	1.766×10^{-1}	1.424×10^{-2}
850.00	7.631×10^{-1}	1.082×10^{-1}	3.659×10^{-2}	850.00	7.883×10^{0}	1.082×10^{-1}	3.339×10^{-2}
800.00	2.608×10^{-1}	6.231×10^{-2}	1.159×10^{-1}	800.00	2.876×10^{-1}	6.231×10^{-2}	9.515×10^{-2}
775.00	1.378×10^{-1}	4.605×10^{-2}	2.563×10^{-1}	750.00	8.754×10^{-2}	3.335×10^{-2}	4.069×10^{-1}
750.00	5.733×10^{-2}	3.335×10^{-2}	9.028×10^{-1}	725.00	3.836×10^{-2}	2.363×10^{-2}	1.329×10^{0}
740.00	3.025×10^{-2}	2.913×10^{-2}	2.604×10^{0}	710.00	1.563×10^{-2}	1.899×10^{-2}	5.938×10^{0}
735.00	1.361×10^{-2}	2.718×10^{-2}	1.120×10^{1}	705.00	6.045×10^{-3}	1.762×10^{-2}	3.503×10^{1}
734.00	8.366×10^{-3}	2.682×10^{-2}	2.842×10^{1}	704.50	4.465×10^{-3}	1.749×10^{-2}	6.304×10^{1}
733.50	4.095×10^{-3}	2.662×10^{-2}	1.145×10^{2}	704.00	2.040×10^{-3}	1.736×10^{-2}	2.935×10^{2}
733.40	2.569×10^{-3}	2.659×10^{-2}	2.868×10^{2}	703.90	1.067×10^{-3}	1.733×10^{-2}	1.060×10^{3}
733.35	1.275×10^{-3}	2.657×10^{-2}	1.148×10^{3}	703.88	7.366×10^{-4}	1.733×10^{-2}	2.215×10^{3}
733.34	8.039×10^{-4}	2.657×10^{-2}	2.870×10^{3}	703.87	4.597×10^{-4}	1.732×10^{-2}	4.873×10^{3}

TABLE II(B) COLLAPSED A/PA-CDF PREDICTIONS FOR CASE WHEN E_a = 30 kcal/mole

($\tau_I = 0 = L_I$)

Without Radiative Heat Loss ($\epsilon = 0$)				With Radiative Heat Loss ($\epsilon = 0.75$)			
T_s (^oK)	P (atm)	r (cm/sec)	L_{II} (cm)	T_s (^oK)	P (atm)	r (cm/sec)	L_{II} (cm)
1000.00	1.119×10^{2}	9.350×10^{-1}	1.610×10^{-3}	1000.00	1.065×10^{2}	9.350×10^{-1}	1.593×10^{-3}
975.00	3.722×10^{1}	6.365×10^{-1}	2.675×10^{-3}	975.00	3.575×10^{1}	6.365×10^{-1}	2.635×10^{-3}
950.00	1.306×10^{1}	4.244×10^{-1}	4.583×10^{-3}	950.00	1.269×10^{1}	4.244×10^{-1}	4.483×10^{-3}
925.00	4.963×10^{0}	2.771×10^{-1}	8.127×10^{-3}	925.00	4.898×10^{0}	2.771×10^{-1}	7.860×10^{-3}
900.00	2.042×10^{0}	1.776×10^{-1}	1.500×10^{-2}	900.00	2.052×10^{0}	1.766×10^{-1}	1.424×10^{-2}
875.00	8.904×10^{-1}	1.097×10^{-1}	2.906×10^{-2}	875.00	9.176×10^{0}	1.097×10^{-1}	2.668×10^{-2}
850.00	4.006×10^{-1}	6.624×10^{-2}	5.973×10^{-2}	850.00	4.293×10^{-1}	6.624×10^{-2}	5.163×10^{-2}
825.00	1.804×10^{-1}	3.881×10^{-2}	1.326×10^{-1}	825.00	2.071×10^{-1}	3.881×10^{-2}	1.021×10^{-1}
800.00	7.869×10^{-2}	2.199×10^{-2}	3.286×10^{-1}	800.00	1.031×10^{-1}	2.199×10^{-2}	2.011×10^{-1}
775.00	3.158×10^{-2}	1.201×10^{-2}	9.829×10^{-1}	775.00	5.389×10^{-2}	1.201×10^{-2}	3.732×10^{-1}
750.00	9.925×10^{-3}	6.299×10^{-3}	4.780×10^{0}	750.00	3.069×10^{-2}	6.299×10^{-3}	6.029×10^{-1}
740.00	4.696×10^{-3}	4.808×10^{-3}	1.578×10^{1}	725.00	1.978×10^{-2}	3.160×10^{-3}	8.008×10^{-1}
735.00	2.019×10^{-3}	4.188×10^{-3}	7.275×10^{1}	700.00	1.516×10^{-2}	1.510×10^{-3}	8.669×10^{-1}
734.00	1.236×10^{-3}	4.074×10^{-3}	1.871×10^{2}	680.00	1.597×10^{-2}	8.039×10^{-3}	7.665×10^{-1}
733.70	9.074×10^{-4}	4.039×10^{-3}	3.432×10^{2}	670.00	2.075×10^{-2}	5.784×10^{-4}	6.358×10^{-1}
733.50	6.071×10^{-4}	4.016×10^{-3}	7.594×10^{2}	660.00	4.200×10^{-2}	4.120×10^{-4}	4.213×10^{-1}
733.40	3.822×10^{-4}	4.006×10^{-3}	1.904×10^{3}	650.00	4.593×10^{-1}	2.903×10^{-4}	8.327×10^{-2}
733.35	1.905×10^{-4}	4.001×10^{-3}	7.627×10^{3}	648.30	2.415×10^{0}	2.733×10^{-4}	9.437×10^{-3}
733.34	1.203×10^{-4}	4.000×10^{-3}	1.907×10^{4}	648.10	1.327×10^{1}	2.713×10^{-4}	3.835×10^{-4}

TABLE II(C) DISTENDED A/PA-GDF PREDICTIONS FOR $\epsilon = 0$ and $E_a = 15$ kcal/mole

P (atm)	τ_I (sec)	τ_{II} (sec)	r (cm/sec)	T_s (^oK)	T_1 (^oK)	(T_1-T_s) (^oK)	L_I (cm)	L_{II} (cm)	L_s (cm)	Q_{TOT} (cal/gm)	Q_I (cal/gm)	Q_{II} (cal/gm)	$\dot{Q}_{TOT}$ (cal/cm^{2}sec)	$\dot{Q}_I$ (cal/cm^{2}sec)	$\dot{Q}_{II}$ (cal/cm^{2}sec)
10^3	6.50×10^{-9}	2.75×10^{-5}	1.64×10^{0}	1217	1217	0	5.81×10^{-8}	4.09×10^{-4}	6.12×10^{-4}	757	560	197	2055	1519	536
10^2	6.50×10^{-8}	1.74×10^{-5}	7.85×10^{-1}	1097	1104	7	2.72×10^{-6}	1.24×10^{-3}	1.28×10^{-3}	669	558	111	871	727	144
10^1	6.50×10^{-7}	1.43×10^{-5}	3.06×10^{-1}	962	1048	86	1.08×10^{-4}	3.98×10^{-3}	3.27×10^{-3}	629	534	95	319	271	48
10^0	6.50×10^{-6}	2.42×10^{-5}	6.06×10^{-2}	798	1168	370	2.15×10^{-3}	1.33×10^{-2}	1.65×10^{-2}	579	449	130	58.2	45.1	13.1
10^{-1}	6.50×10^{-5}	1.07×10^{-4}	8.05×10^{-3}	656	1223	567	2.85×10^{-2}	7.83×10^{-2}	1.24×10^{-1}	537	390	147	7.17	5.21	1.96
10^{-2}	6.50×10^{-4}	8.28×10^{-4}	8.73×10^{-4}	550	1253	703	3.40×10^{-1}	6.57×10^{-1}	1.15×10^{0}	505	349	156	0.731	0.505	0.226
10^{-3}	6.50×10^{-3}	7.86×10^{-3}	9.30×10^{-5}	472	1235	763	3.20×10^{0}	6.64×10^{0}	1.08×10^{1}	482	331	151	0.0743	0.0511	0.0232

Note: T_2 = constant = 2000^{o}K when $\epsilon = 0$.

TABLE II(D) DISTENDED A/PA-GDF PREDICTIONS FOR $\epsilon = 0.75$ and $E_a = 15$ kcal/mole

P(*) (atm)	τ_I (sec)	τ_{II} (sec)	r (cm/sec)	T_s (^oK)	T_1 (^oK)	T_2 (^oK)	(T_1-T_s) (^oK)	(T_2-T_1) (^oK)	L_I (cm)	L_{II} (cm)	L_s (cm)
10^0	6.50×10^{-6}	2.42×10^{-5}	5.99×10^{-2}	796	1150	1986	354	836	2.12×10^{-3}	1.32×10^{-2}	1.67×10^{-2}
10^{-1}	6.50×10^{-5}	1.07×10^{-4}	7.70×10^{-3}	655	1221	1951	566	730	2.73×10^{-2}	7.49×10^{-2}	1.30×10^{-1}
10^{-2}	6.50×10^{-4}	8.28×10^{-4}	7.82×10^{-4}	545	1119	1765	574	646	2.77×10^{-1}	5.89×10^{-1}	1.28×10^{0}
6.80×10^{-3}	9.70×10^{-4}	1.16×10^{-3}	5.15×10^{-4}	530	1095	1668	565	573	4.01×10^{-1}	7.98×10^{-1}	1.92×10^{0}
4.08×10^{-3}	1.57×10^{-3}	1.93×10^{-3}	2.95×10^{-4}	510	1012	1530	502	518	6.18×10^{-1}	1.27×10^{0}	3.39×10^{0}
2.82×10^{-3}	2.28×10^{-3}	2.80×10^{-3}	1.92×10^{-4}	495	880	1344	385	464	8.60×10^{-1}	1.76×10^{0}	5.21×10^{0}
2.04×10^{-3}	3.25×10^{-3}	3.95×10^{-3}	1.12×10^{-4}	478	722	1017	244	235	9.20×10^{-1}	1.97×10^{0}	8.93×10^{0}
1.87×10^{-3}	3.47×10^{-3}	4.20×10^{-3}	9.45×10^{-5}	473	677	892	204	215	9.56×10^{-1}	1.93×10^{0}	1.06×10^{1}
1.70×10^{-3}	No Solution Can Be Found (Extinction)										

Notes: *The calculations were not carried out above 1 atm because then the radiative heat loss is small compared to the other heat generation terms; above 1 atm, the predictions are the same as given in Table II(C) for case when $\epsilon = 0$.

APPENDIX B

REVIEW OF BURNING RATE BEHAVIOR OF AP PROPELLANTS AND FIT OBTAINED BY VARIOUS PROPOSED BURNING RATE EQUATIONS

The burning rate behavior of several AP-based composite solid propellants in the 1-100 atm range is summarized in Table III below. The fits obtained by 3 burning rate equations to the data, are also noted. The equations that have been tested are:

$$\left(\frac{1}{r}\right) = \left(\frac{a}{p}\right) + \left(\frac{b}{p^{1/2}}\right) \tag{15}$$

$$\left(\frac{1}{r}\right)^2 = \left(\frac{a}{p}\right)^2 + \left(\frac{b}{p^{1/2}}\right)^2 \tag{18}$$

$$\left(\frac{1}{r}\right) = \left(\frac{a}{p}\right) + (c) \tag{19}$$

The formulations and some physical properties of each of the fuels in Table III are listed in Table IV. (The information needed to calculate the empirical formula, molecular weight, etc., for each of the fuels indicated has been extracted from Refs. 36, 142, 197-203, and also from various manufacturers' data sheets. The manufacturer (or vendor) of each chemical pertinent to Tables III and IV, is noted in the list of abbreviations for chemical names, at the end of the text.)

In the figures following Tables III and IV are shown the actual burning rate data of all the propellants covered by Table III. Each propellant is referred to by the number assigned in the first column of Table III. The burning rate data of all the propellants are shown plotted in four ways: (log r) vs. (log p), (p/r) vs. $(p^{2/3})$, $(p/r)^2$ vs. $(p^{2/3})^2$, and (p/r) vs. (p). The latter three plots are to test respectively, the fits obtained by equations (15), (18), and (19); as indicated in Section IIIC(ii), when plotted this way, the burning rate data must fall on a straight line if the equation under consideration is to hold. The only time that the (p/r) vs. $(p^{2/3})$, etc., plots have been omitted is when Equations (15), (18), and (19) obviously do not fit the data, i.e., when the (log r) vs. (log p) curve is not monotonic and when this curve does not show a steadily decreasing positive slope with increasing pressure. Some of the plots appearing in this Appendix have already been presented in the main text of this document. For the sake of uniformity in this Appendix, they are repeated.

TABLE III SUMMARY OF BEHAVIOR OF AP-BASED PROPELLANTS IN 1-100 atm RANGE

TABLE III(A): PROPELLANTS WITH FUELS THAT DO NOT MELT READILY

INVESTIGATOR	FUEL	%AP	AP SIZE DISTRIBUTION	PER CENT ADDITIVE	ψ_o	FIT TO EQ.? (3)	FIT TO EQ.? (4)	FIT TO EQ.? (5)	a $\frac{psia}{lb/sec}$	b $\frac{(psia)^{1/3}}{lb/sec}$	a/b $(psia)^{2/3}$	ORIGINAL DATA IN FIGURES No.	REMARKS
1) SUTHERLAND	PIB	75	120$_\mu$	-	0.440	YES	YES	NO	275	41.8	6.6	1 - 4	LARGE SCATTER
2) "	PIB	80	120$_\mu$	-	0.577	YES	YES	NO	175	26.5	6	1 - 4	
3) "	PIB	75	16$_\mu$	-	0.440	YES	?	NO	350	20.9	17	1 - 4	
4) "	PIB	80	16$_\mu$	-	0.577	YES	YES	NO	210	17.1	12	1 - 4	
5) WEBB	PIB	75	COARSE	-	0.440	YES	YES	NO	90	39.4	2.3	5 - 8	LARGE SCATTER
6) "	PIB	75	FINE ($\sim 20_\mu$)	-	0.440	YES	YES	NO	110	22.9	4.8	5 - 8	LARGE SCATTER
7) "	PIB	80	FINE ($\sim 20_\mu$)	-	0.577	YES	YES	NO	110	15.3	7.2	5 - 8	LARGE SCATTER
8) "	PIB	80	COARSE	-	0.577	NO	NO	NO	-	-	-	5 - 8	PLATEAU, LARGE SCATTER
9) TABACK	PIB	77.5	$\sim 20_\mu$	0% COP. CHR.	0.501	YES	YES	NO	125	19.4	6.4	9 - 12	PLATEAU? LARGE SCATTER
10) "	PIB	77.5	$\sim 20_\mu$	0.5% COP. CHR.	0.511	YES	YES?	NO	130	12.7	10	9 - 12	LARGE SCATTER
11) "	PIB	77.5	$\sim 20_\mu$	2.5% COP. CHR.	0.560	YES	YES?	NO	125	9.5	13	9 - 12	LARGE SCATTER
12) "	PIB	77	7$_\mu$	-	0.489	NO	NO	?	-	-	-	13 - 16	PLATEAU? LARGE SCATTER
13) "	PIB	77	50% 7$_\mu$+50% ~78$_\mu$	-	0.489	YES	YES	NO	110	37.4	2.9	13 - 16	INFLECTION, LARGE SCATTER
14) "	PIB	77	25% 7$_\mu$+75% ~78$_\mu$	-	0.489	YES	YES?	NO	275	25.8	11	13 - 16	LARGE SCATTER
15) "	PIB	77	50% 7$_\mu$+50% ~230$_\mu$	-	0.489	YES	YES	NO	190	23.6	8.1	13 - 16	LARGE SCATTER
16) BASTRESS	PIB	72.5	9$_\mu$ (3.7 W.R.$_+^+$)	-	0.390	NO	NO	NO	-	-	-	17	EXT. $\gtrsim$ 300 psi
17) "	PIB	72.5	13$_\mu$ (4.7 W.R.$_+^+$)	-	0.390	NO	NO	NO	-	-	-	17	EXT. $\gtrsim$ 200 p
18) "	PIB	72.5	29$_\mu$ (3.6 W.R.$_+^+$)	-	0.390	NO	NO	NO	-	-	-	17	250 psi $\lesssim$ EXT. $\lesssim$ 1,000 psi
19) "	PIB	72.5	78$_\mu$ (1.5 W.R.$_+^+$)	-	0.390	YES	YES?	NO	420	28.8	15	17 - 20	
20) "	PIB	72.5	230$_\mu$ (1.3 W.R.$_+^+$)	-	0.390	YES	YES	NO	410	49.5	8.3	17 - 20	
21) "	PIB	72.5	$\sim 20_\mu$		0.796	NO	NO	NO	-	-	-	17	300 psi $\lesssim$ EXT. $\lesssim$ 1,000 psi
22) "	PIB	75	$\sim 20_\mu$	-	0.440	NO	NO	NO	-	-	-	17	INFLECTION; PLATEAU
23) YAMAZAKI	POLYSULFIDE	?	?	-	?	YES	YES	NO	120	31.2	3.8	42 - 45	LARGE SCATTER
24) BASTRESS	LP3/GMF	65	9$_\mu$(3.1 W.R.$_+^+$)	-	0.415	NO	NO	NO	-	-	-	21	EXT. $\gtrsim$ 800 psi
25) "	LP3/GMF	65	16$_\mu$(3.0 W.R.$_+^+$)	-	0.415	NO	NO	NO	-	-	-	21	PLATEAU (400-700 psi)
26) "	LP3/GMF	65	29$_\mu$(2.2 W.R.$_+^+$)	-	0.415	NO	NO	NO	-	-	-	21	INFLECTION
27) "	LP3/GMF	65	37$_\mu$(2.0 W.R.$_+^+$)	-	0.415	NO	NO	NO	-	-	-	21	INFLECTION
28) "	LP3/GMF	65	55$_\mu$(2.0 W.R.$_+^+$)	-	0.415	NO	NO	NO	-	-	-	21 - 24	$(p/r)-(p^{2/3})$ CONCAVE UP
29) "	LP3/GMF	65	78$_\mu$(1.5 W.R.$_+^+$)	-	0.415	YES	YES	NO	190	26.3	7.2	21 - 24	
30) "	LP3/GMF	65	98$_\mu$(1.6 W.R.$_+^+$)	-	0.415	YES	YES	NO	190	28.5	6.7	21 - 24	
31) "	LP3/GMF	65	140$_\mu$(1.4 W.R.$_+^+$)	-	0.415	YES	YES	NO	240	29.4	8.2	21 - 24	
32) "	LP3/GMF	65	175$_\mu$(1.5 W.R.$_+^+$)	-	0.415	YES	YES	NO	250	31.5	7.9	21 - 24	
33) "	LP3/GMF	65	230$_\mu$(1.3 W.R.$_+^+$)	-	0.415	NO	NO	NO	-	-	-	21 - 24	$(p/r)-(p^{2/3})$ CONCAVE DOWN
34) "	LP3/GMF	65	265$_\mu$(1.3 W.R.$_+^+$)	-	0.415	NO	NO	NO	-	-	-	21 - 24	$(p/r)-(p^{2/3})$ CONCAVE DOWN
35) "	LP3/GMF	65	22$_\mu$(1.2 W.R.$_+^+$)	-	0.415	NO	NO	NO	-	-	-	25	$(p/r)-(p^{2/3})$ CONCAVE UP
36) "	LP3/GMF	65	200$_\mu$/2.0 W.R.$_+^+$)	-	0.415	YES	YES	NO	315	30.6	10	25 - 28	
37) "	LP3/GMF	65	30% 9$_\mu$+70% 98$_\mu$	-	0.415	NO	NO	NO	-	-	-	25 - 28	$(p/r)-(p^{2/3})$ CONCAVE UP
38) "	LP3/GMF	65	30% 9$_\mu$+70% 175$_\mu$	-	0.415	YES	YES	NO	160	30.6	5.2	25 - 28	
39) "	LP3/GMF	65	30% 9$_\mu$+75% 265$_\mu$	-	0.415	YES	YES	NO	190	33.6	5.7	25 - 28	
40) "	LP3/GMF	65	30% 29$_\mu$+70% 175$_\mu$	-	0.415	YES	YES	NO	110	36.4	3.0	25 - 28	
41) "	LP3/GMF	65	30% 55$_\mu$+70% 175$_\mu$		0.415	YES	YES	NO	190	33.2	5.7	25 - 28	
42) "	LP3/GMF	70	20$_\mu$ (12 W.R.$_+^+$)	-	0.510	NO	NO	YES	-	-	-	29 - 32	$(p/r)-(p^{2/3})$ CONCAVE UP
43) "	LP3/GMF	67.5	20$_\mu$ (12 W.R.$_+^+$)	-	0.459	NO	NO	NO	-	-	-	29	INFLECTION
44) "	LP3/GMF	65	20$_\mu$ (12 W.R.$_+^+$)	-	0.415	NO	NO	NO	-	-	-	29	INFLECTION
45) "	LP3/GMF	62.5	20$_\mu$ (12 W.R.$_+^+$)	-	0.371	NO	NO	NO	-	-	-	29	PLATEAU?
46) "	LP3/GMF	60	20$_\mu$ (12 W.R.$_+^+$)	-	0.344	NO	NO	NO	-	-	-	29	EXT. $\gtrsim$ 400 psi
47) "	LP3/GMF	70	200$_\mu$ (2.6 W.R.$_+^+$)	-	0.510	YES	YES	NO	250	28.1	8.9	29 - 32	
48) TARRERE	PVC		'	-	?	YES?	YES?	NO	260	18.5	14	42 - 45	LARGE SCATTER
49) KUMBEI	PVC/DBS	80	18$_\mu$	-	0.698	YES	YES	NO	225	11.0	20	33 - 36	PRESSURE RANGE TOO SMALL FOR EFFECTIVE FIT OF EQ.? 3-5
50) "	PVC/DBS	75	18$_\mu$	-	0.529	YES	YES	NO	165	14.7	11	33 - 36	
51) "	PVC/DBS	70	18$_\mu$	-	0.417	NO	NO	NO	-	-	-	33 - 36	$(p/r)-(p^{2/3})$ CONCAVE DOWN
52) "	PVC/DBS	67.5	18	-	0.372	NO	NO	NO	-	-	-	33	INFLECTION
53) "	PVC/DBS	65	18$_\mu$	-	0.335	NO	NO	NO	-	-	-	33	INFLECTION
54) "	PVC/DBS	60	18$_\mu$	-	0.274	NO	NO	NO	-	-	-	33	BLISA (400- 900 psi)
55)	PVC/DBS	70	9$_\mu$	-	0.417	NO	NO	NO	-	-	-	37	INFLECTION
56) "	PVC/DBS	65	62$_\mu$	-	0.335	NO	NO	NO	-	-	-	37	PLATEAU
57) "	PVC/DBS	70	135$_\mu$	-	0.417	NO	NO	NO	-	-	-	37	INFLECTION
58) "	PVC/DBS	65	135$_\mu$	-	0.335	NO	NO	NO	-	-	-	37	PLATEAU
59) "	PVC/DBS	60	135$_\mu$	-	0.274	NO	NO	NO	-	-	-	37	PLATEAU (BLISA)

TABLE III(A): PROPELLANTS WITH FUELS THAT DO NOT MELT READILY - CONTINUED

INVESTIGATOR	FUEL	%AP	AP SIZE DISTRIBUTION	PER CENT ADDITIVE	ψ_o	FIT TO EQ.? (3)	(4)	(5)	a $\frac{psia}{in/sec}$	b $\frac{(psia)^{1/3}}{in/sec}$	a/b $(psia)^{2/3}$	ORIGINAL DATA IN FIGURES B-.....	REMARKS
60) EASTRESS	EPON/TETA	67.5	10μ (3.0 W.R.$^+$)	-	0.433	YES	NO	NO	260	8.7	30	38 - 41	
61) "	EPON/TETA	65	10μ (3.0 W.R.$^+$)	-	0.394	NO	NO	NO	-	-	-	38	MESA (400-800 psi)
62) MARXMAN	PBAN/?	86	?	-	0.680	YES	YES	NO	150	29.6	5.1	42 - 45	
63) "	PBAN/?	80	?	1.5% Fe_2O_3	0.440	YES?	YES	NO	140	18.7	7.5	42 - 45	
64) "	PBAN/?	70	?	10% Al	0.248	YES	YES	NO	170	34.4	4.1	42 - 45	
65) THIS STUDY	PBAN/MAPO	74.8	80μ	-	0.330	NO	NO	NO	-	-	-	46 - 49	INFLECTION
66) "	PBAN/MAPO	82.5	30%40μ+70%180μ	-	0.524	YES	YES	NO	190	31.4	6.1	50 - 53	
67) "	PBAA/EPON	75.1	5μ	-	0.337	NO	NO	NO	-	-	-	46	MESA(350-500psi);EXT ≥ 500psi
68) "	PBAA/EPON	75.1	45μ	-	0.337	NO	NO	NO	-	-	-	46	INFLECTION
69) "	PBAA/EPON	75.1	80μ	-	0.337	YES?	YES?	NO	230	34.5	6.7	46 - 49	INFLECTION?
70) "	PBAA/EPON	75.1	180μ	-	0.337	NO	NO	NO	-	-	-	46	n = 0 ABOVE 1000 psi
71) "	PBAA/EPON	75.1	90%5μ+10%80μ	-	0.337	NO	NO	NO	-	-	-	46	PLATEAU(350-550);EXT ≥ 550psi
72) "	PBAA/EPON	70.0	30%5μ+70%45μ	-	0.262	NO	NO	NO	-	-	-	50	EXT ≥ 600 psi
73) "	PBAA/EPON	75.0	30%5μ+70%45μ	-	0.335	NO	NO	NO	-	-	-	50 - 53	INFLECTION
74) "	PBAA/EPON	80.0	30%5μ+70%45μ	-	0.445	YES	YES	NO	50	19.1	2.6	50 - 53	
75) "	PBAA/EPON	80.1	30%7.5μ+70%180μ	-	0.448	NO	NO	YES	-	-	-	50 - 53	$(p/r)-(p^{2/3})$ CONCAVE UP
76) "	PBAA/EPON	82.5	30%40μ+70%180	-	0.517	YES	YES	NO	25	33.9	0.74	50 - 53	
77) "	PBHT/TDI	75.0	80μ	-	0.330	NO	NO	NO	-	-	-	46	INFLECTION
78) "	PBHT/TDI	82.7	30%40μ+70%180μ	-	0.523	YES	YES	NO	115	32.9	3.5	50 - 53	
79) "	NC/TEGDN#	0	-	-	0.281	NO	NO	NO	-	-	-	50 - 53	$r \propto p^{0.78}$ (70-1500 psia)
80) "	NC/TEGDN#	40.0	5μ	-	0.569	YES	NO	NO	230	7.15	35	56 - 57	
81) "	NC/TEGDN#	40.0	80μ	-	0.569	YES	NO	NO	207	17.9	12	56 - 57	

NOTES: *EQUIVALENCE RATIO ψ_o CALCULATED ASSUMING Al BURNS TO Al_2O_3 AT STOICHIOMETRY.

+W.R. DENOTES WIDTH RATIO I.E., RATIO OF DIAMETERS AT 90% AND 10% (BY WEIGHT) POINTS ON CUMULATIVE PARTICLE SIZE DISTRIBUTION CURVE.

#DENOTES ENERGETIC FUEL (DOUBLE-BASE).

TABLE III(B): PROPELLANTS WITH FUELS THAT FORM MOLTEN LAYER ON BURNING SURFACE

INVESTIGATOR	FUEL	%AP	AP SIZE DISTRIBUTION	PER CENT ADDITIVE	ψ_o	FIT TO EQ.? (3)	(4)	(5)	a $\frac{psia}{in/sec}$	b $\frac{(psia)^{1/3}}{in/sec}$	a/b $(psia)^{2/3}$	ORIGINAL DATA IN FIGURES B-.....	REMARKS
82) THIS STUDY	PIB/MAPO	74.9	80μ	-	0.330	NO	NO	NO	-	-	-	58	WILL NOT BURN (15-1500 psi)
83) "	PIB/MAPO	80.1	30%40μ+70%180μ	-	0.443	NO	NO	NO	-	-	-	59	INFLECTIONS; EXT. ≥ 1100 psi
84) "	ESTANE/POLYOL	72.5	80μ	-	0.446	NO	NO	NO	-	-	-	58	EXT. ≥ 1200 psia;EXT. ≤ 40 psia
85) "	ESTANE/POLYOL	80.0	30%40μ+70%180μ	-	0.652	NO	NO	NO	-	-	-	59	EXT. ≥ 1200 psi
86) "	POLYOL/TDI	75.0	45μ	-	0.505	NO	NO	NO	-	-	-	58	EXT. ≥ 450 psi; EXT. ≤ 40 psia
87) "	POLYOL/TDI	75.0	80μ	-	0.505	NO	NO	NO	-	-	-	58	EXT. ≥ 1350 psi; EXT. ≤ 40 psia
88) "	POLYOL/TDI	85.0	30%40μ+70%180μ	-	0.912	NO	NO	NO	-	-	-	59	SLIGHT MESA (400-1000 psi)

TABLE IV PROPERTIES OF SELECTED FUEL-BINDER SYSTEMS

BINDER DESIGNATION	BINDER FORMULATION	EMPIRICAL FORMULA*					BINDER DENS. (GM/CC)	APPROX. MELTING TEMP. (°C)	APPROX. TEMP. FOR 50% DECOMP. IN 30 MIN. (°C)	WT. PER CENT IN Al_2K_n AT STOICHIOMETRY+		
		C	H	O	N	OTHER				AP	AN	KP
EPON/TETA	89.35% EPON 818 + 9.75% DEP + 0.90% TETA	1.000	1.839	0.4335	0.005497	Cl 0.04019				83.86	87.85	84.68
ESTANE/POLYOL	92.05% ESTANE + 5.57% POLYCIN 51 + 1.59% TMP + 0.79% 1, 4 BUTANEDIOL	1.000	1.821	0.3183	0.02961	-	1.057	165-195	270	86.33	91.47	87.27
LP3/GMF	93.0% LP3 + 6.0% GMF + 1.0% S	1.000	1.967	0.3943	0.02846	S 0.3761	1.302			82.74	89.09	77.94
NC/TEGDN	66.67% TEGDN + 32.83% NC + 0.50% 2 NITRODIPHENYLAMINE	1.000	1.765	1.415	0.3538	-	1.410			62.50	73.95	55.12
P13	90.8% P13 + 9.2% DBP + (NUODEX COBALT + LECITHIN + LUPERSOL)#	1.000	1.231	0.1804	-	-				87.64	92.35	84.11
PBAA/EPON	85.6% PBAA + 14.4% EPON 828	1.000	1.535	0.03873	-	-	0.947	300-345	315	90.04	93.70	86.96
PBAN/MAPO	94.93% PBAN + 5.07% MAPO	1.000	1.507	0.02111	0.01950	P 0.001580	0.948	300-345	340	90.04	93.90	86.95
PBCT/EPOXY	94.8% PBCT + 5.2% ERL-0500	1.000	1.488	0.02127	0.002603	-	0.925	300-345	315	90.02	94.01	87.16
PBHT/TDI	94% PBD-45 + 6% TDI	1.000	1.475	0.02074	0.009612	-	0.923	300-345	110	90.14	93.97	87.08
PF	100% PRESSED PF	1.000	2.000	1.000	-	-			100	75.74	84.21	69.76
PIB/MAPO	83.1% PIB + 6.88% MAPO + 10.02% DOA	1.000	1.971	0.04904	0.01451	P 0.004837	0.949	165-195	315	90.15	93.97	87.09
POLYOL/TDI	88.40% PPG + 10.52% TDI + 1.05% TMP + 0.026% Ft. Oct.	1.000	1.878	0.3316	0.02358	Rh 0.0007356	1.048	<165	270	86.20	91.41	80.43
PVC/DBS	50% PVC + 50% DBS + (FERRO 121 OR 221)#	1.000	1.749	0.1425	-	Cl 0.1793				84.71	90.63	80.19

NOTES: *All atoms in empirical formula for binder have been normalized with respect to C atom.

+Stoichiometry defined as mixture ratio for which reactants burn to CO_2, H_2O, HCl, KCl, SO_2 and N_2.

#Small quantities of catalyst, etc. ignored for empirical formula and stoichiometry calculations.

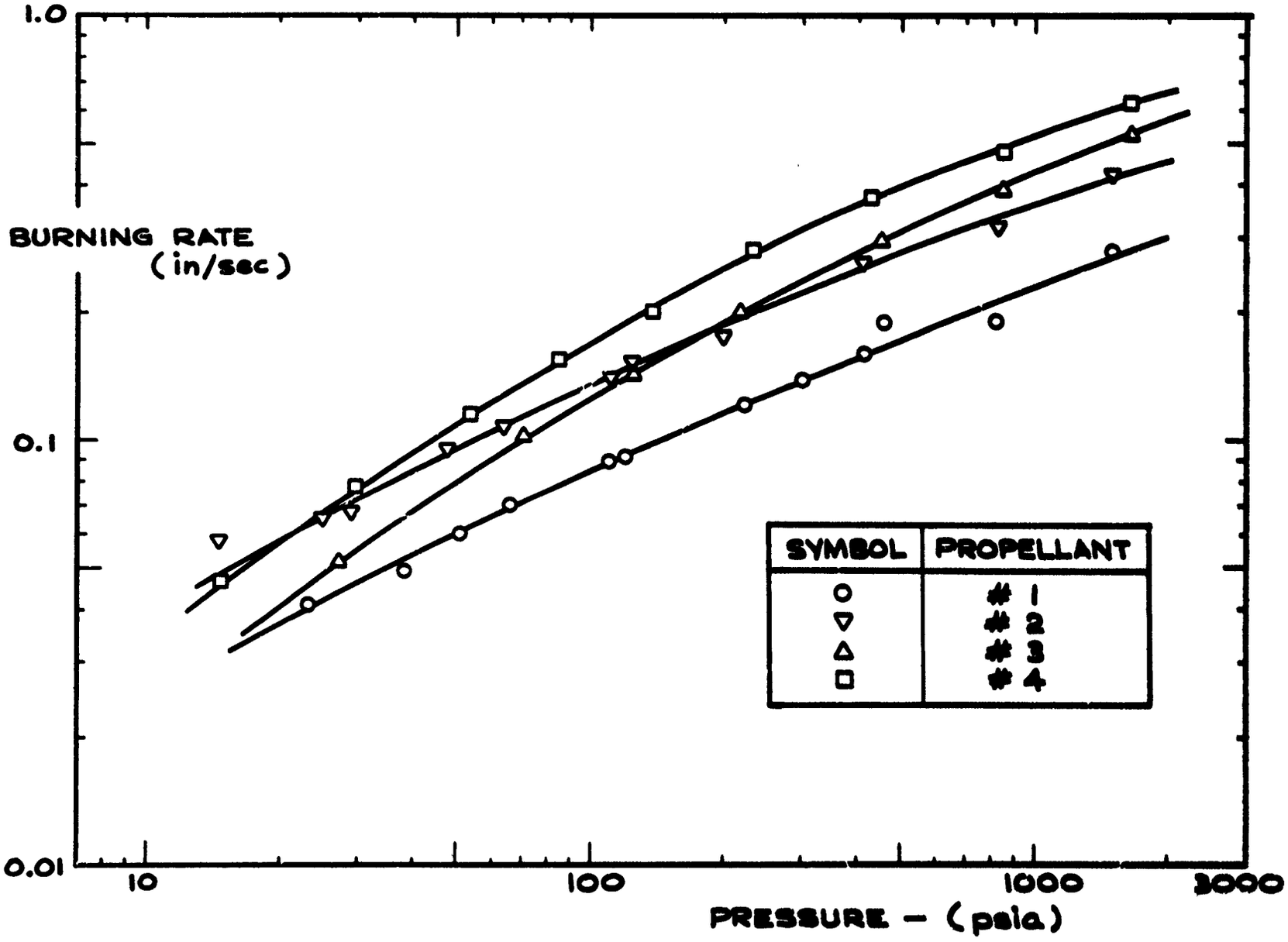

FIGURE B-1 DATA OF PROPELLANT NO.'S 1-4 IN TABLE III PLOTTED AS (log r) VS. (log p)

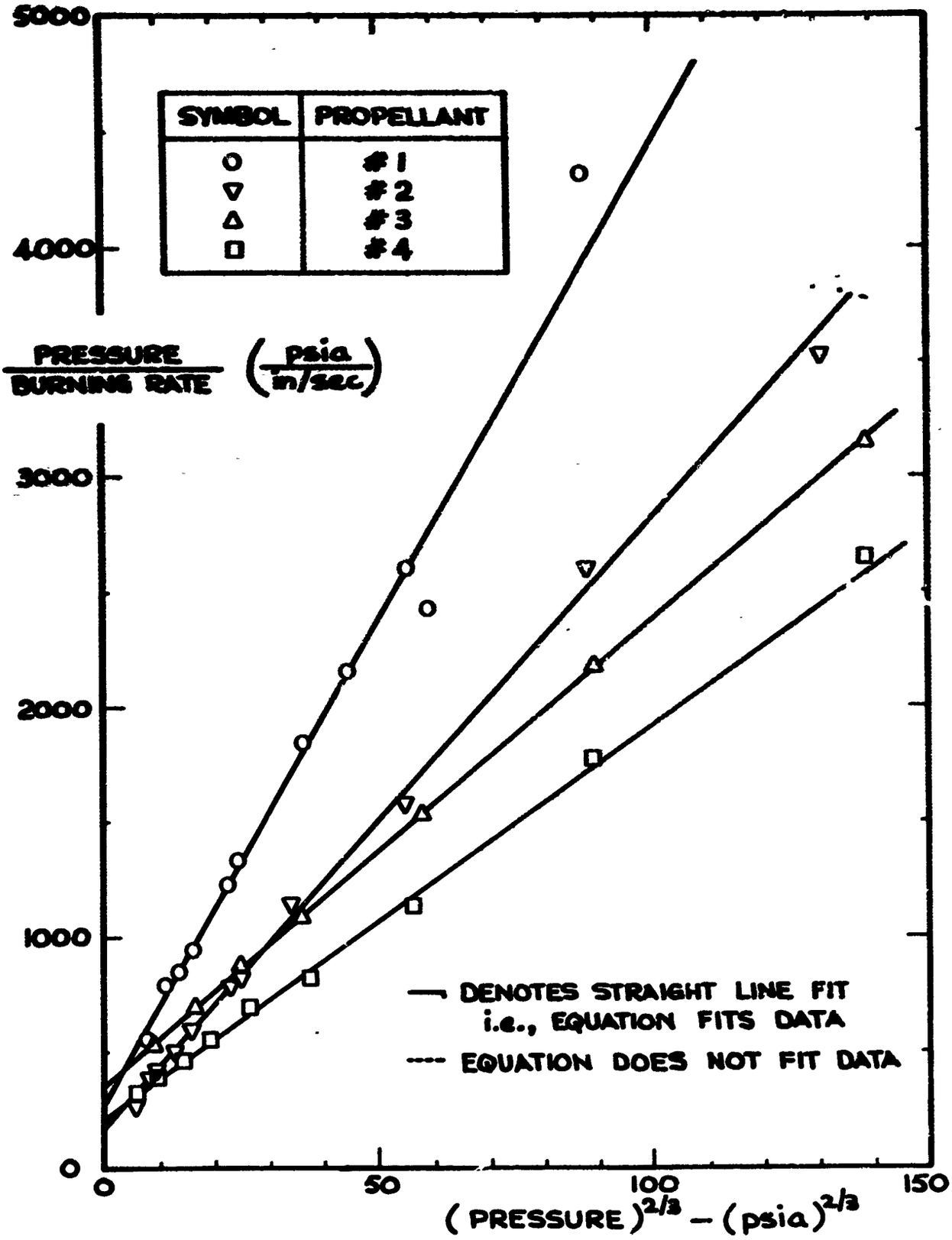

FIGURE B-2 DATA OF PROPELLANT NO.'S 1-4

CORRELATED WITH: $(1/r) = (a/p) + (b/p^{1/3})$

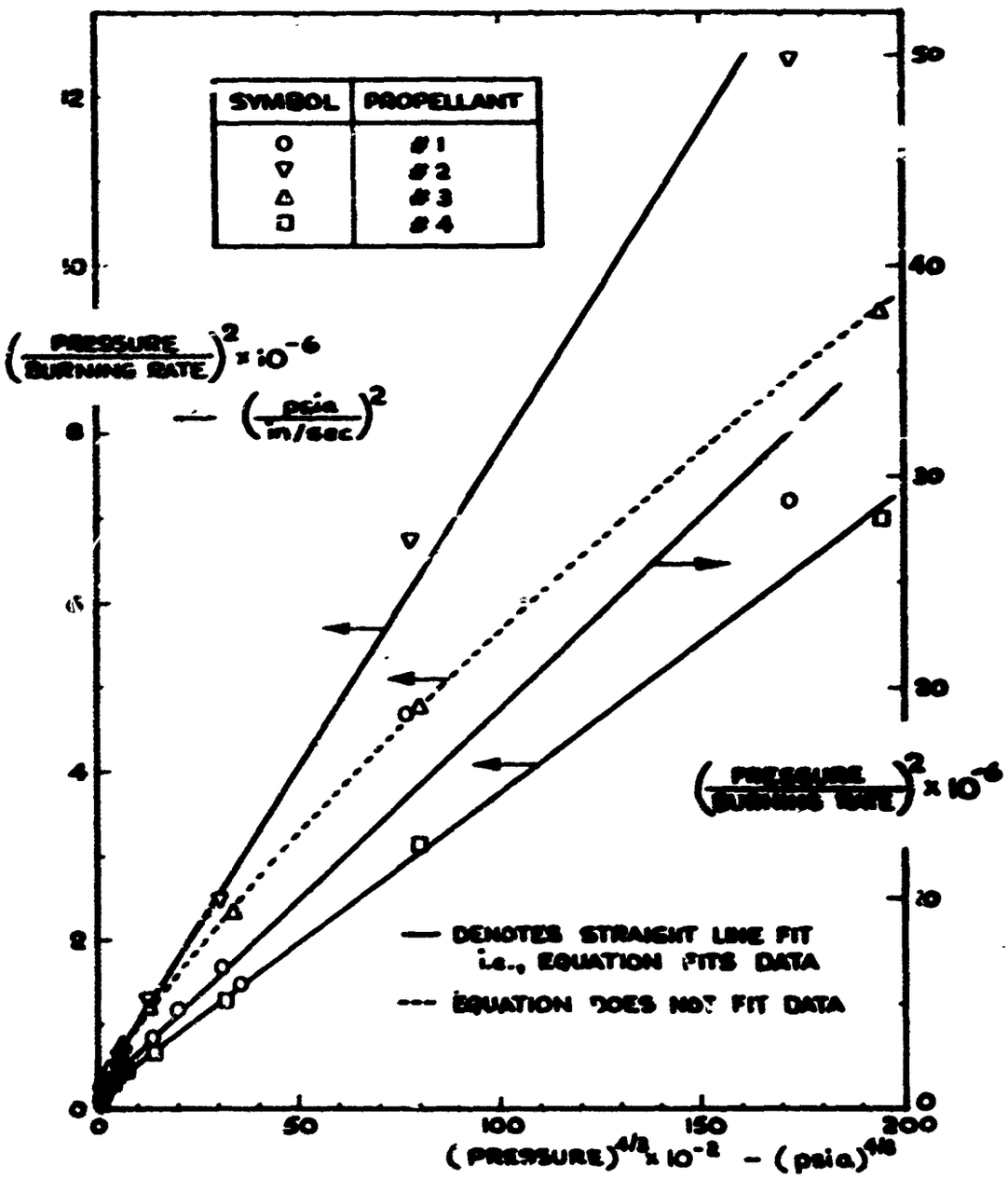

FIGURE B-3 DATA OF PROPELLANT NO.'S 1-4

CORRELATED WITH: $(1/r)^2 = (a/p)^2 + (b/p^{1/3})^2$

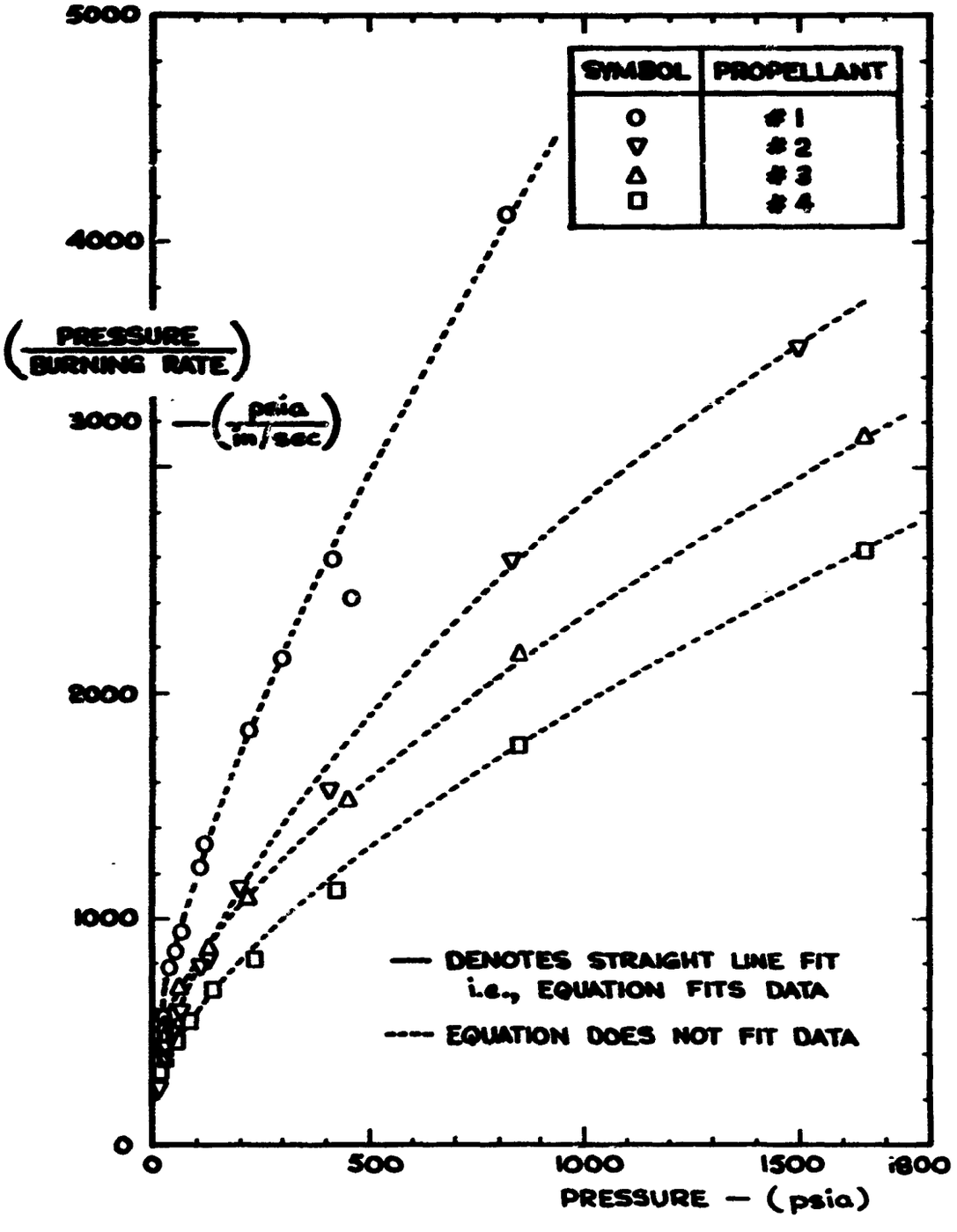

FIGURE B-4 DATA OF PROPELLANT NO.'S 1-4

CORRELATED WITH: $(1/r) = (a/p) + (c)$

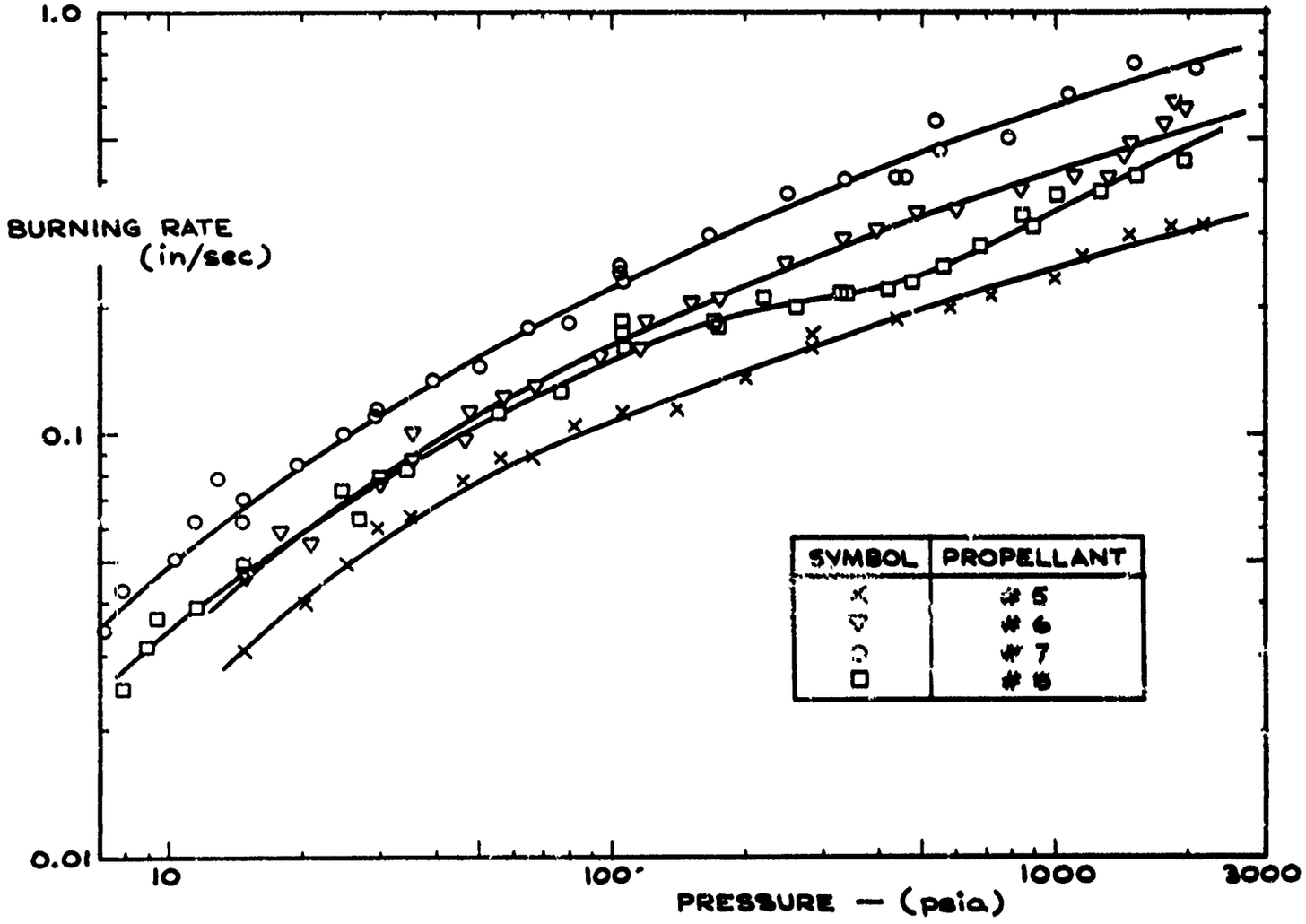

FIGURE B-5 DATA OF PROPELLANT NO.'S 5-8 IN TABLE III PLOTTED AS (log r) VS. (log p)

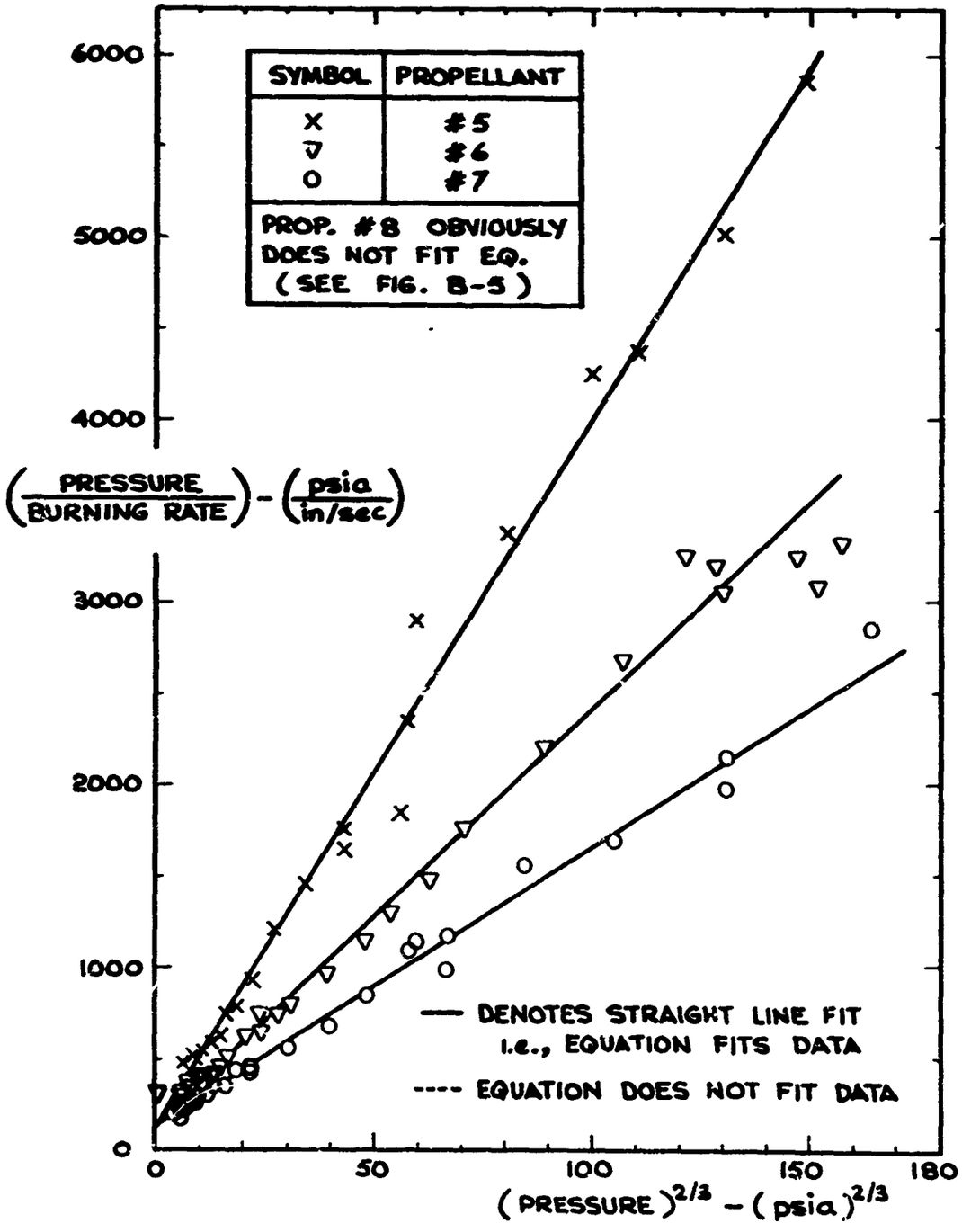

FIGURE B-6 DATA OF PROPELLANT NO.'S 5 - 8

CORRELATED WITH: $(1/r) = (a/p) + (b/p^{1/3})$

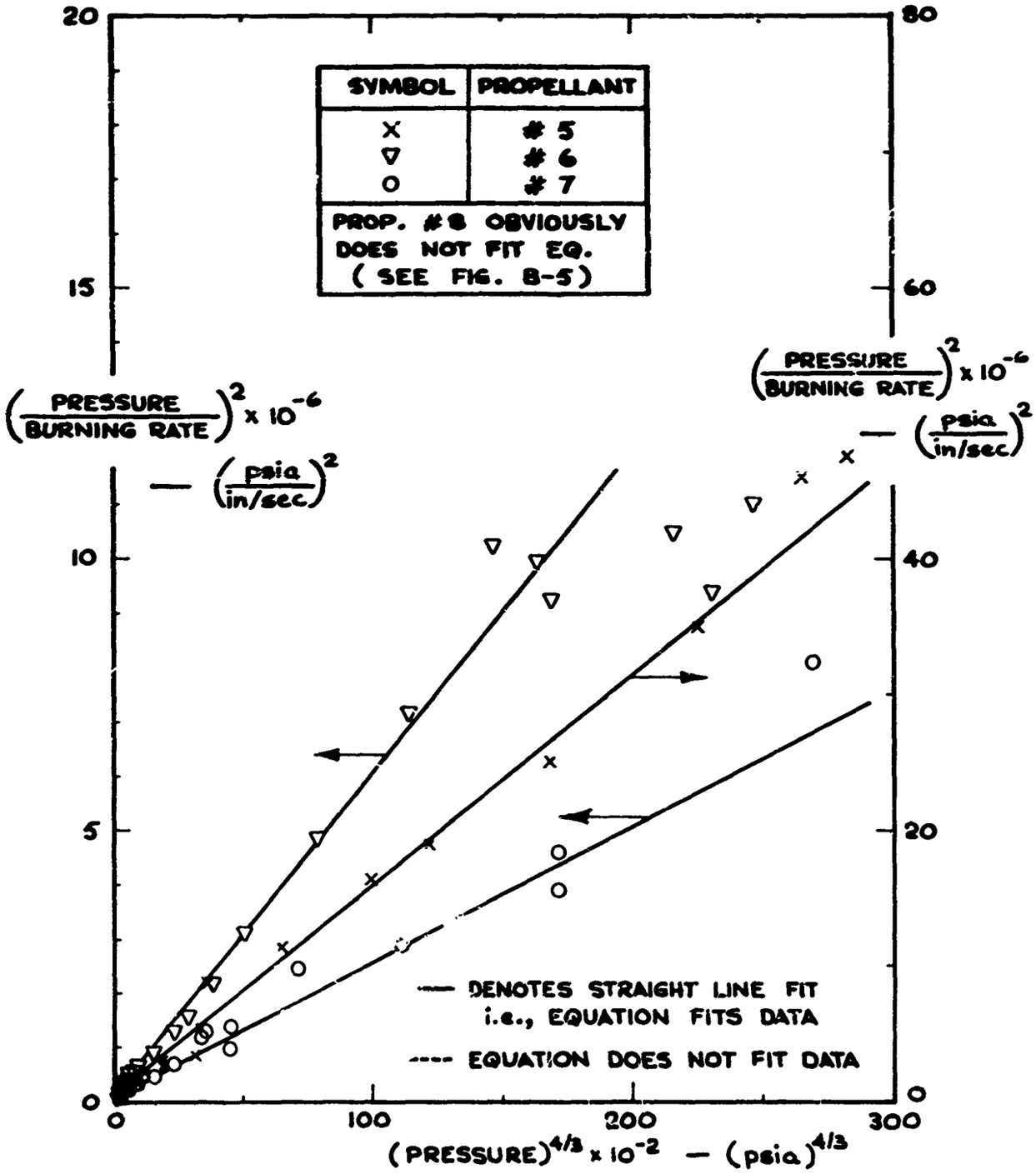

FIGURE B-7 DATA OF PROPELLANT NO'S 5-8 CORRELATED WITH: $(1/r)^2 = (a/p)^2 + (b/p^{1/3})^2$

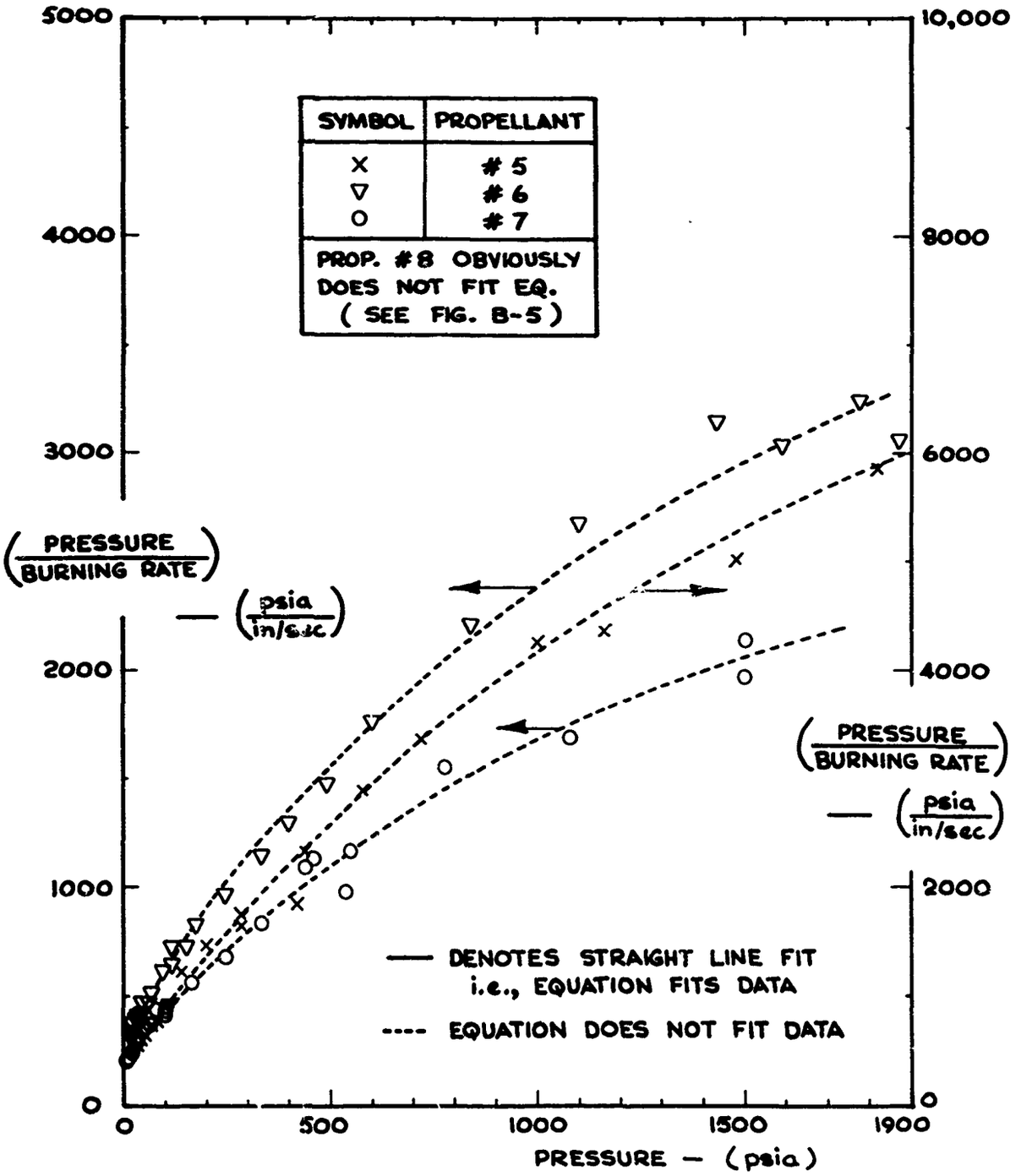

FIGURE B-8 DATA OF PROPELLANT NO.'S 5 - 8 CORRELATED WITH: $(1/r) = (a/p) + (c)$

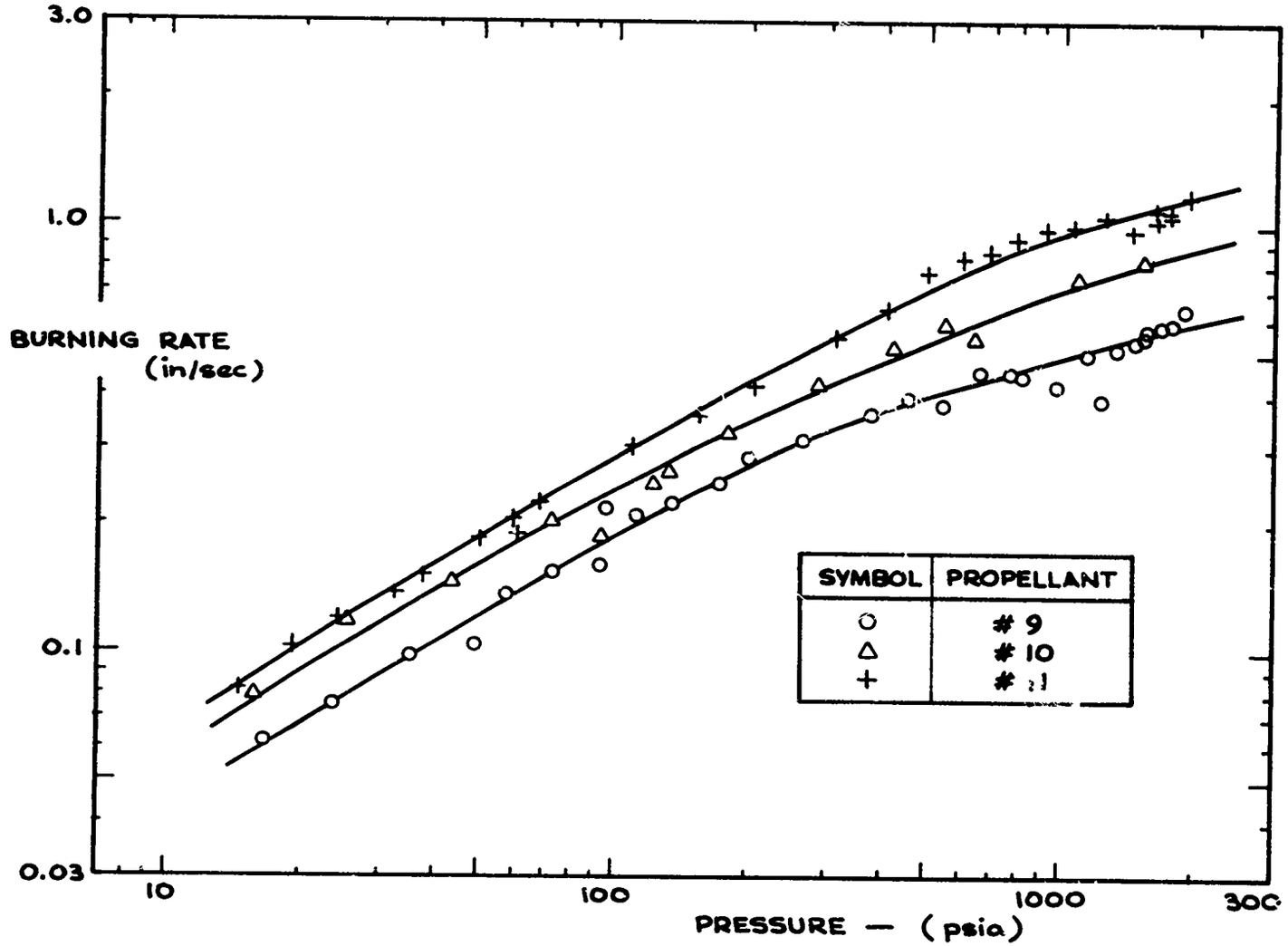

FIGURE B-9 DATA OF PROPELLANT NO.'S 9 - 11 IN TABLE III PLOTTED AS (log r) VS. (log p)

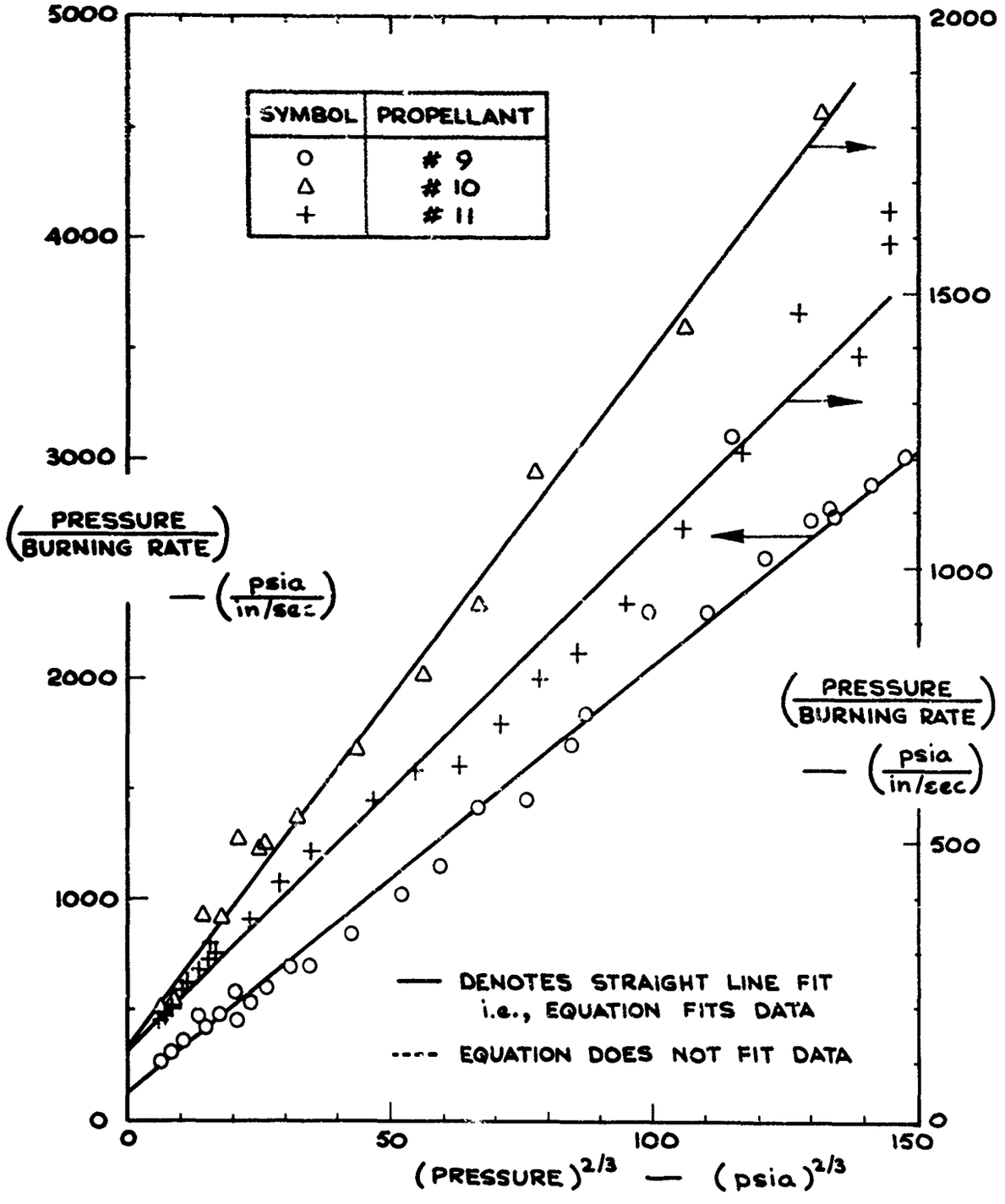

FIGURE B-10 DATA OF PROPELLANT NO'S 9 - 11

CORRELATED WITH: $(1/r) = (a/p) + (b/p^{1/3})$

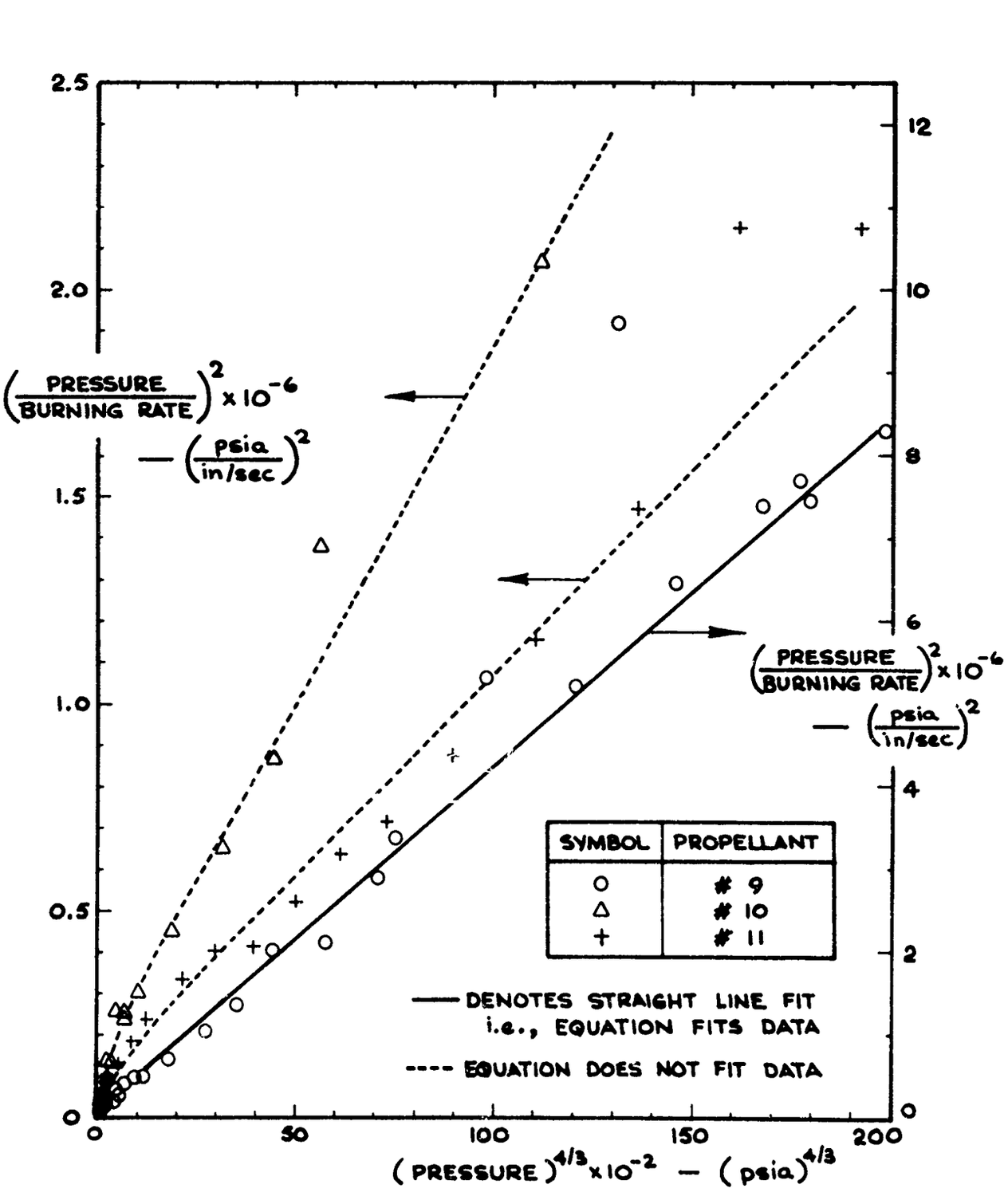

FIGURE B-11 DATA OF PROPELLANT NO.'S 9 - 11 CORRELATED WITH : $(1/r)^2 = (a/p)^2 + (b/p^{1/3})^2$

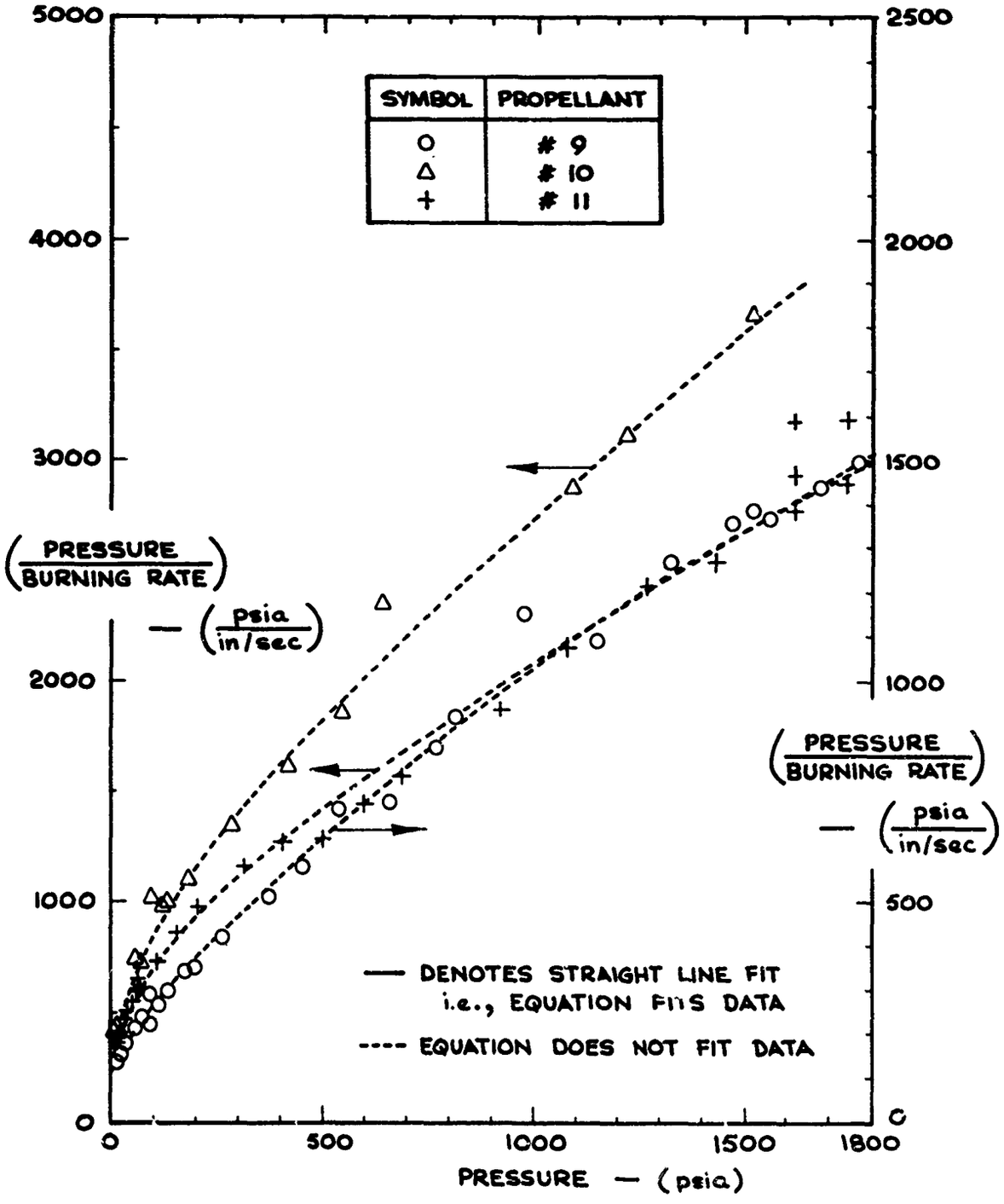

FIGURE B-12 DATA OF PROPELLANT NO'S 9 - 11

CORRELATED WITH : $(1/r) = (a/p) + (c)$

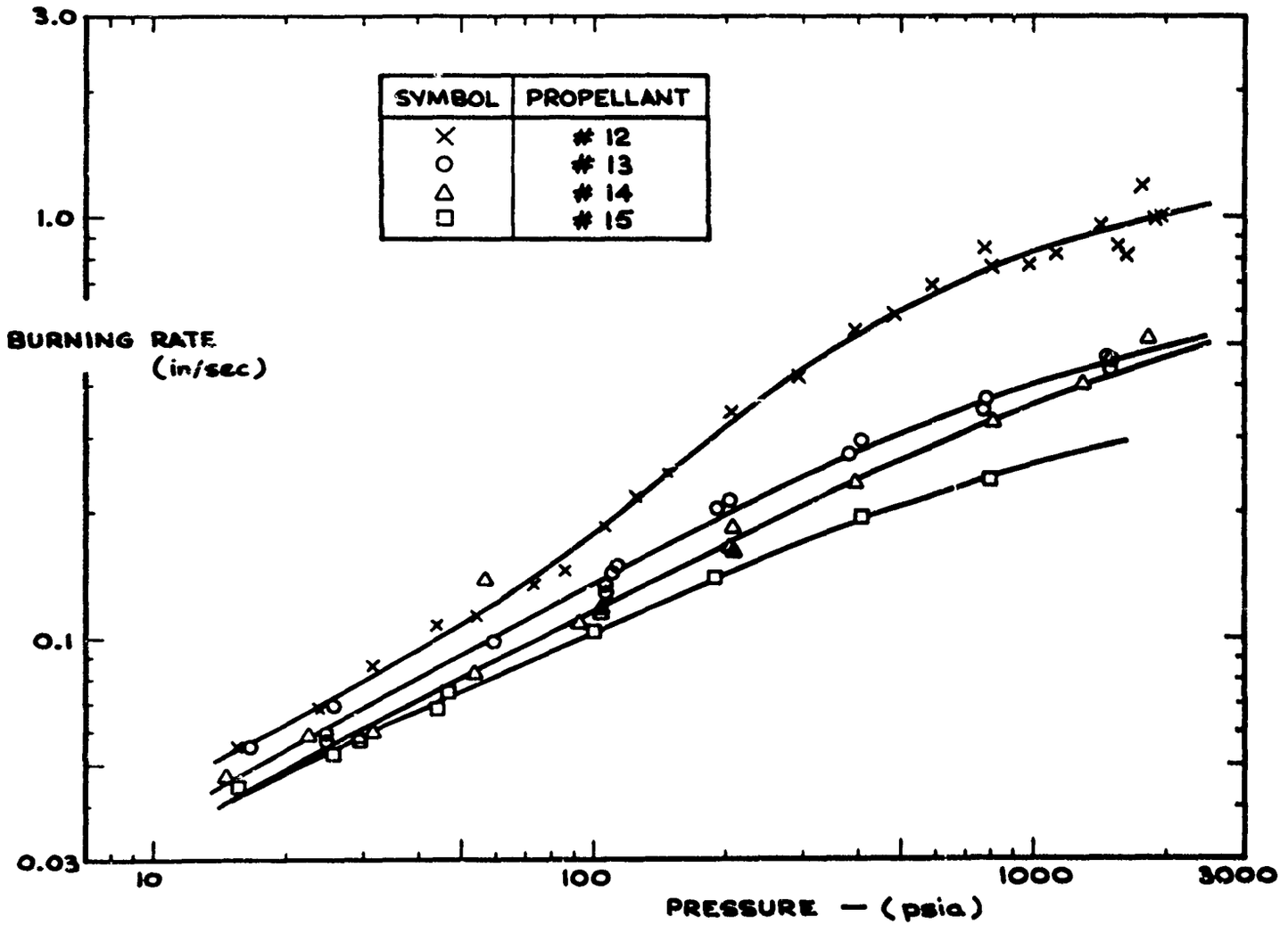

FIGURE B-13 DATA OF PROPELLANT NO'S 12-15 IN TABLE III PLOTTED AS (log r) VS. (log p)

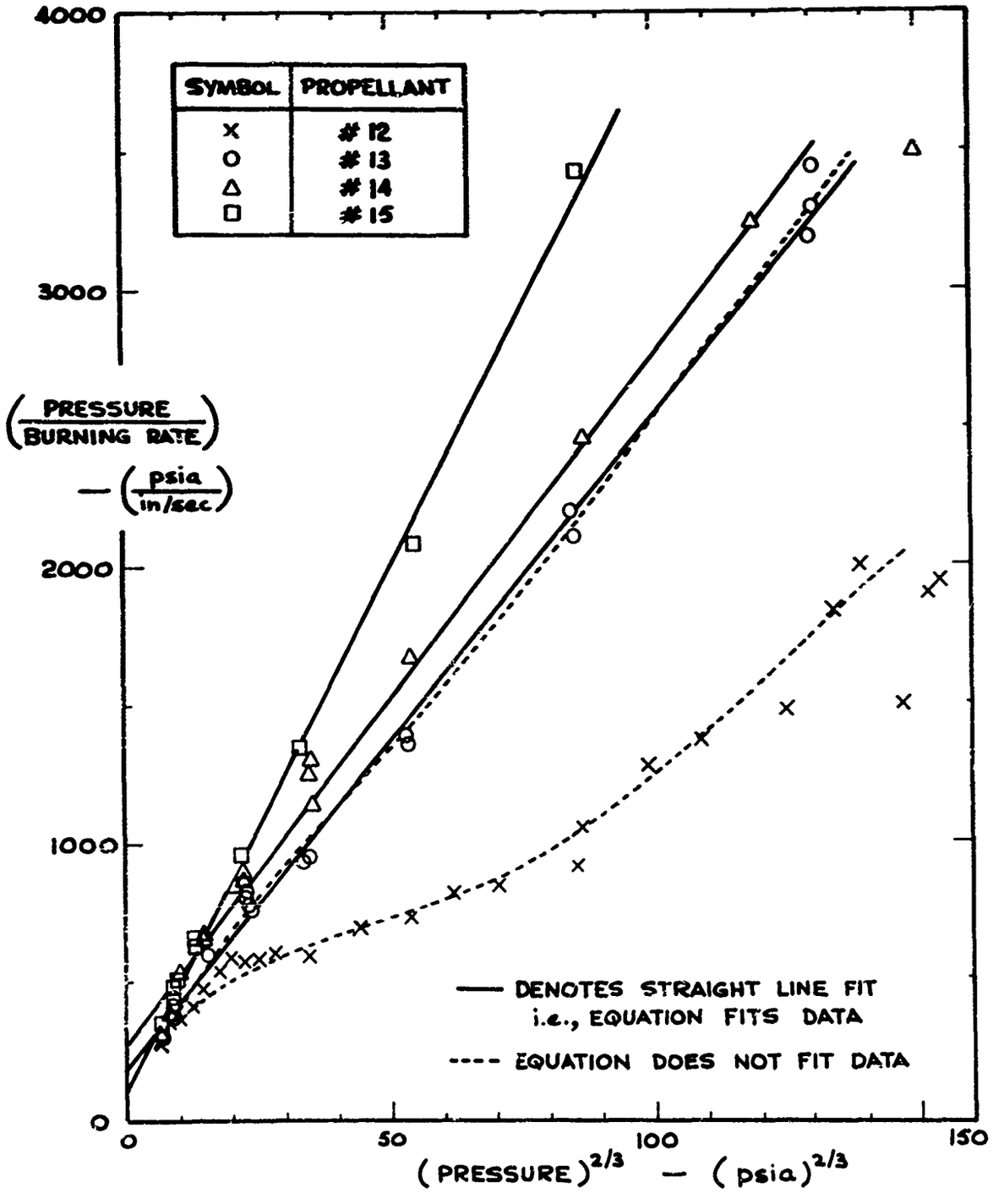

FIGURE B-14 DATA OF PROPELLANT NO.'S 12 - 15

CORRELATED WITH: $(1/r) = (a/p) + (b/p^{1/3})$

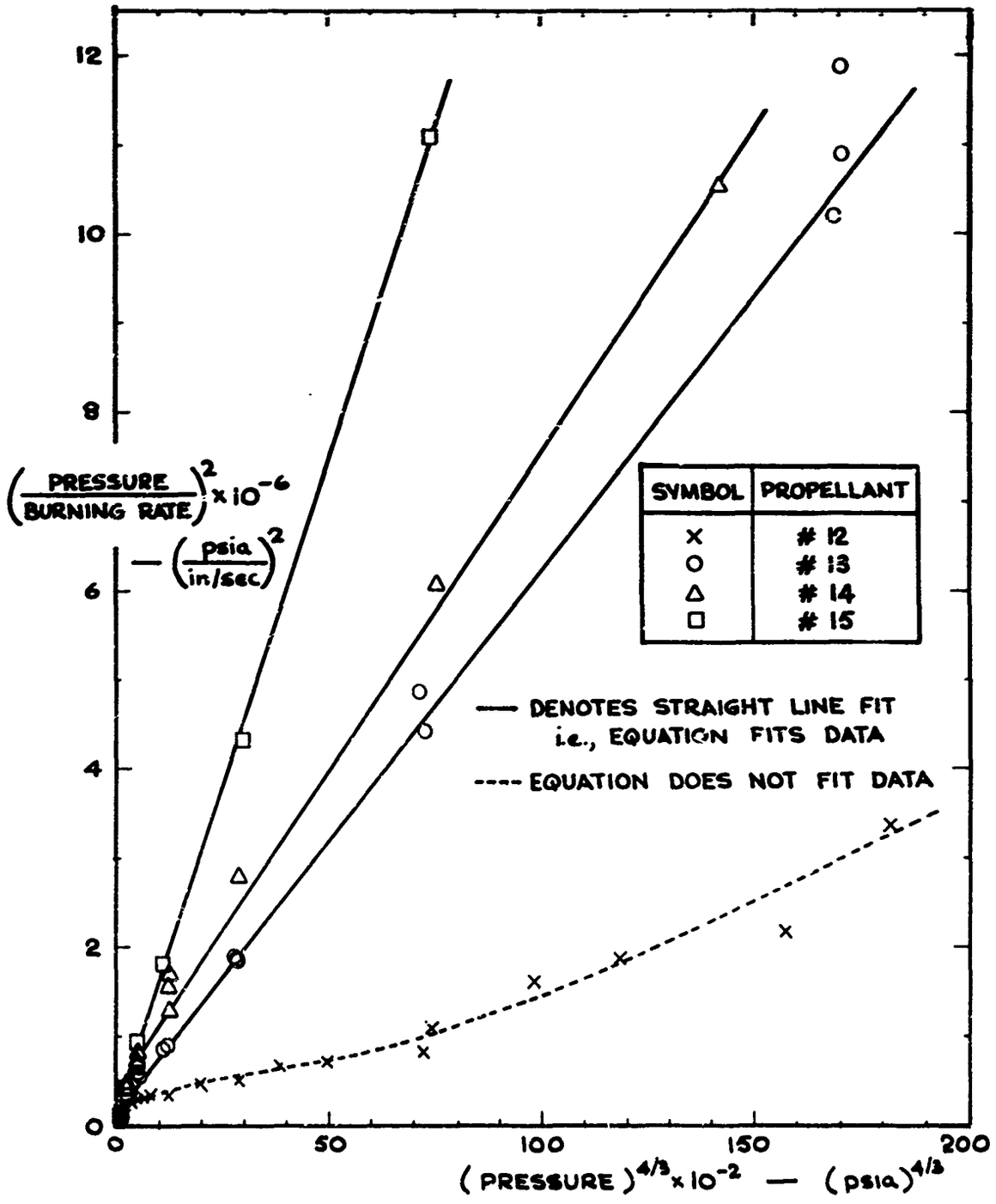

FIGURE B-15 DATA OF PROPELLANT NOS 12 - 15

CORRELATED WITH : $(1/r)^2 = (a/p)^2 + (b/p^{1/3})^2$

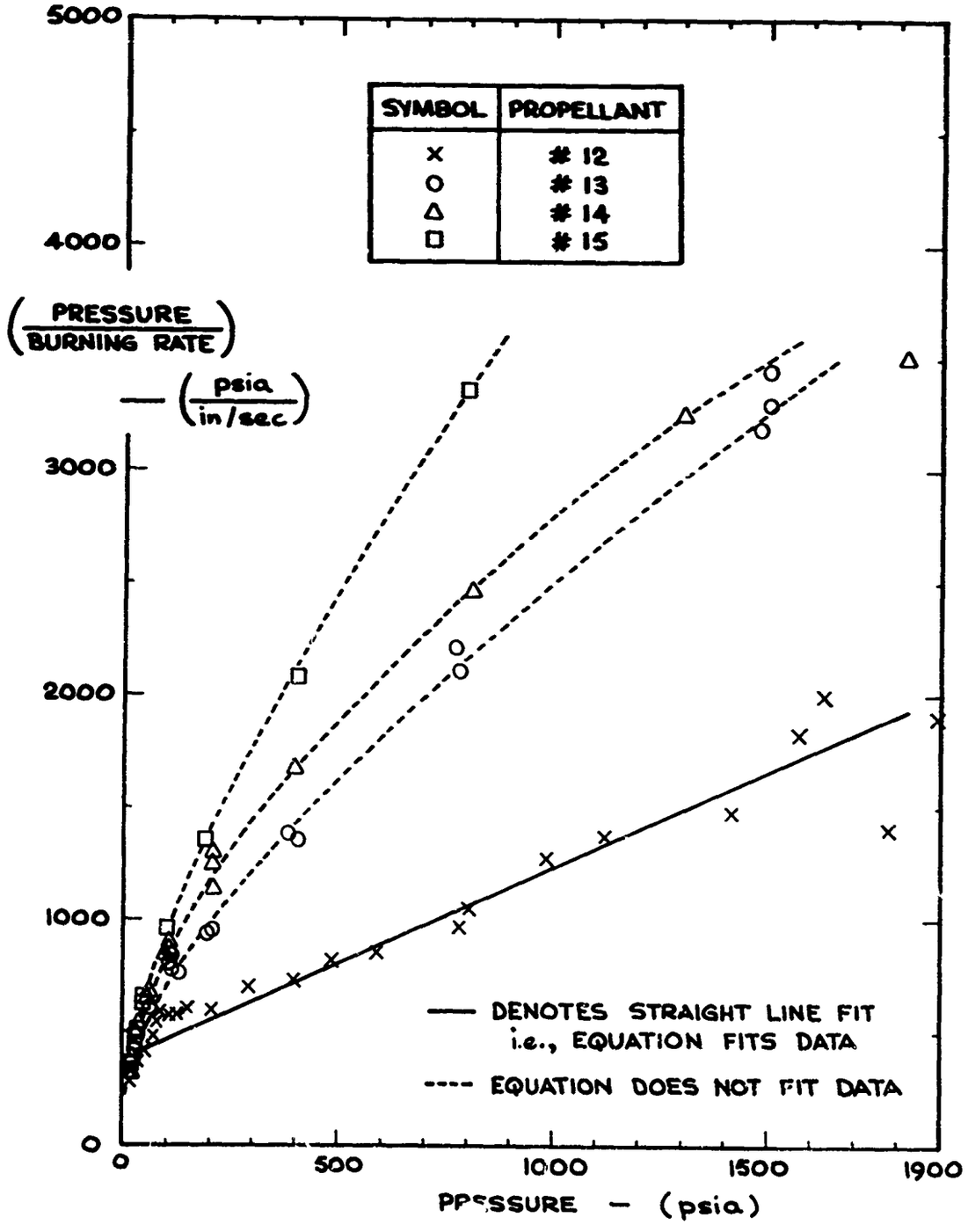

FIGURE B-16 DATA OF PROPELLANT NO.'S 12 - 15

CORRELATED WITH: $(1/r) = (a/p) + (c)$

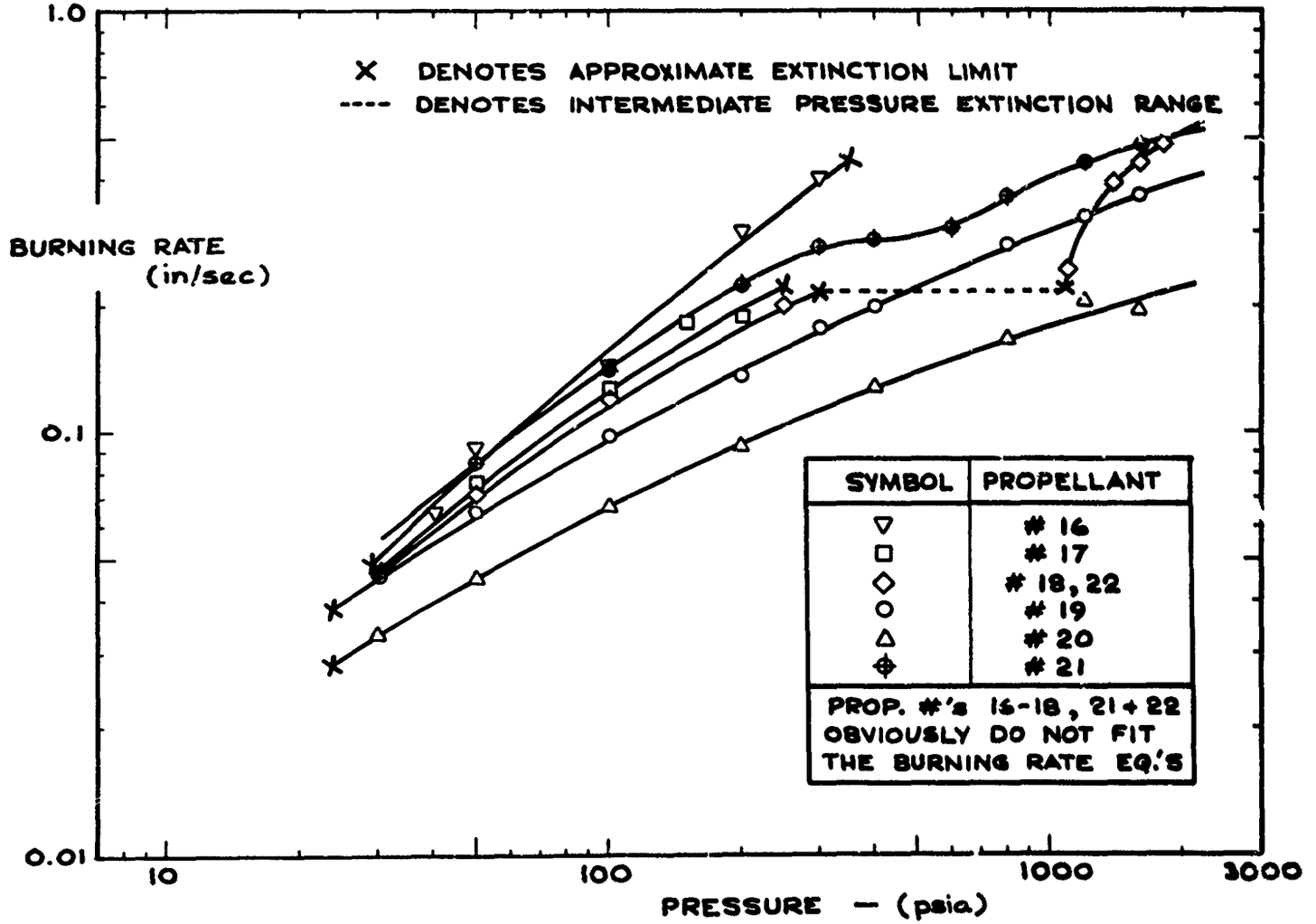

FIGURE B-17 DATA OF PROPELLANT NO.'S 16 - 22 IN TABLE III PLOTTED AS (log r) VS. (log p)

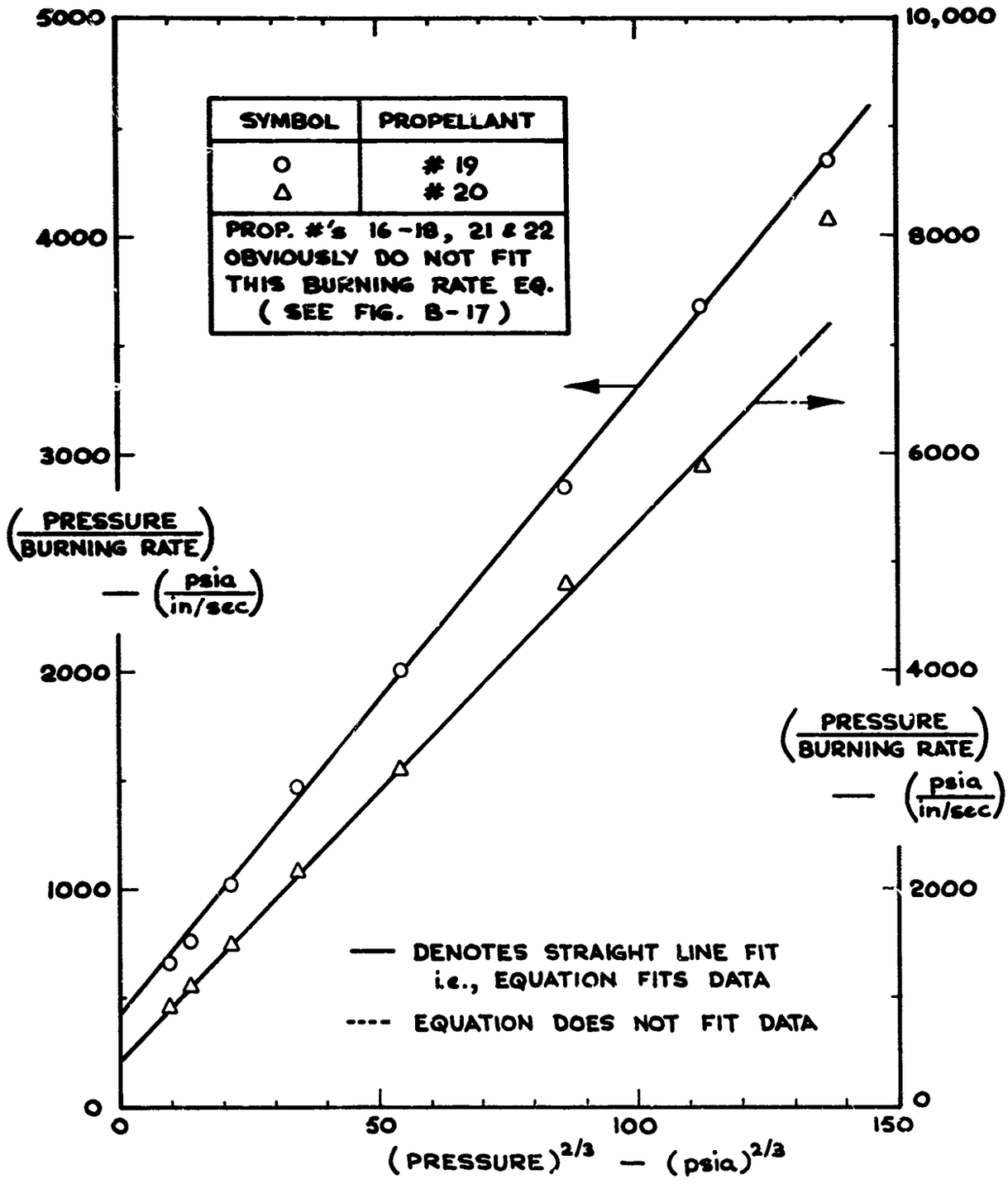

FIGURE B-18 DATA OF PROPELLANT NO.'S 16-22

CORRELATED WITH: $(1/r) = (a/p) + (b/p^{1/3})$

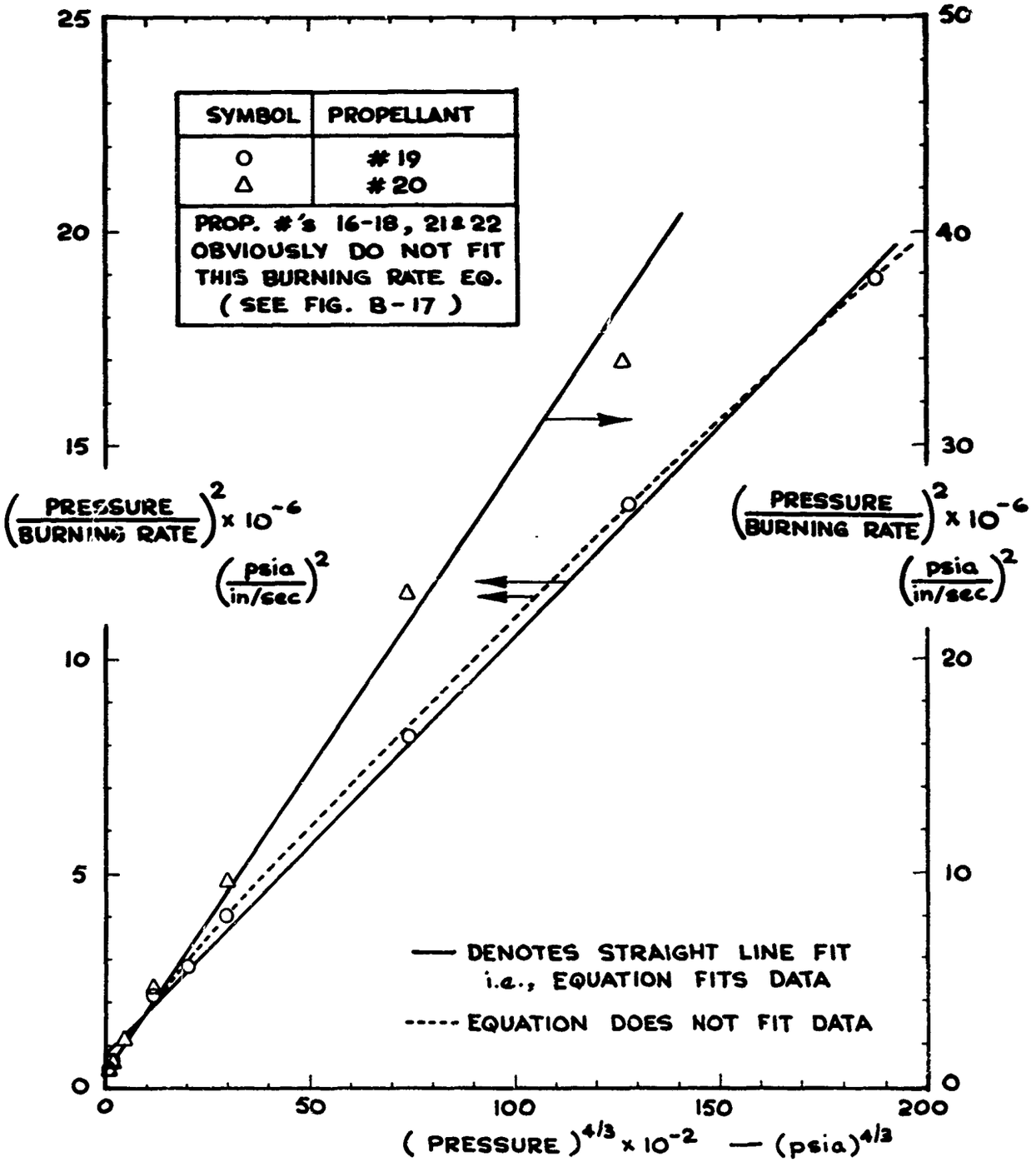

FIGURE B-19 DATA OF PROPELLANT NO.'S 16 - 22 CORRELATED WITH : $(1/r)^2 = (a/p)^2 + (b/p^{1/3})^2$

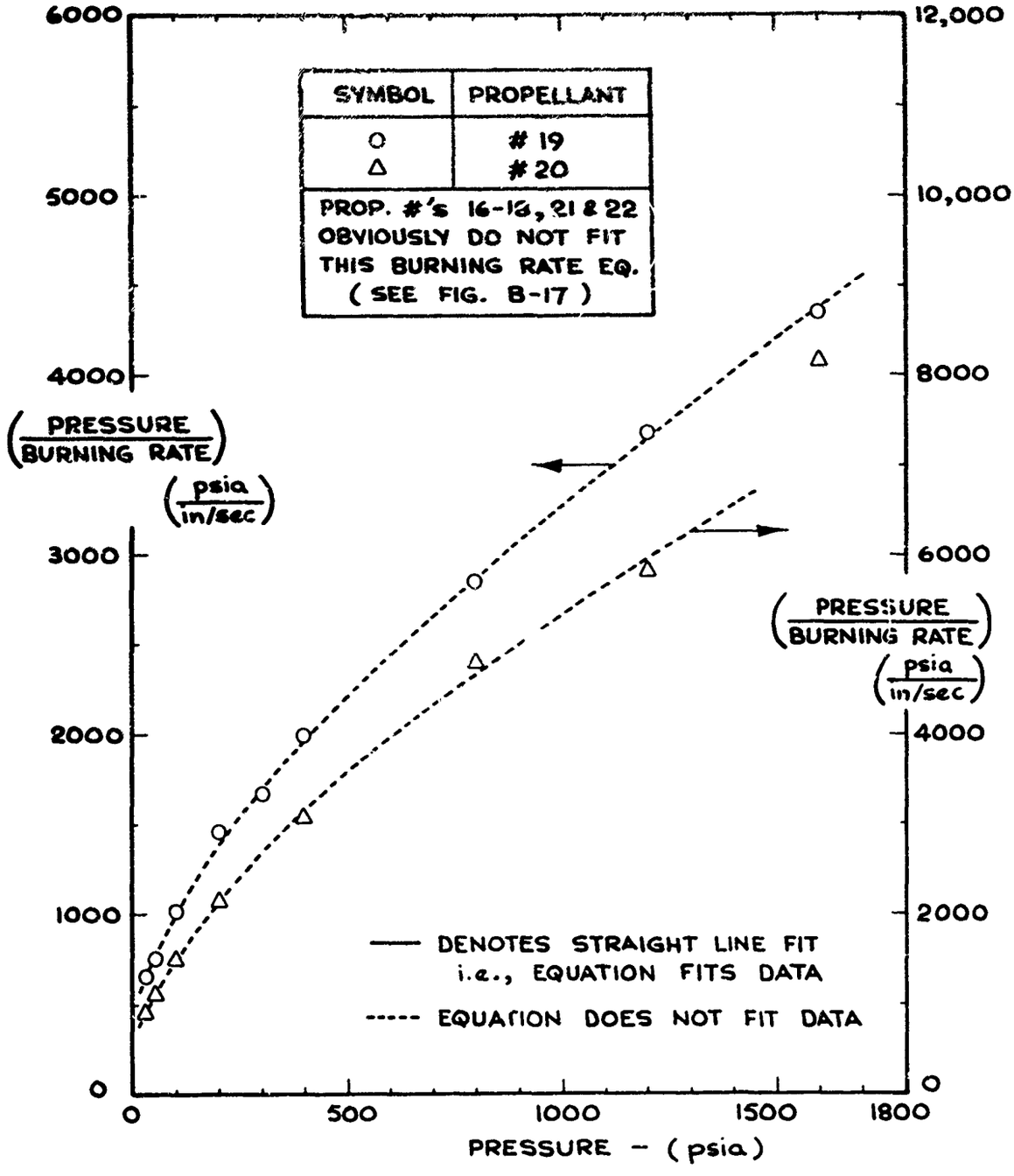

FIGURE B-20 DATA OF PROPELLANT NO.'S 16-22 CORRELATED WITH: $(1/r) = (a/p) + (c)$

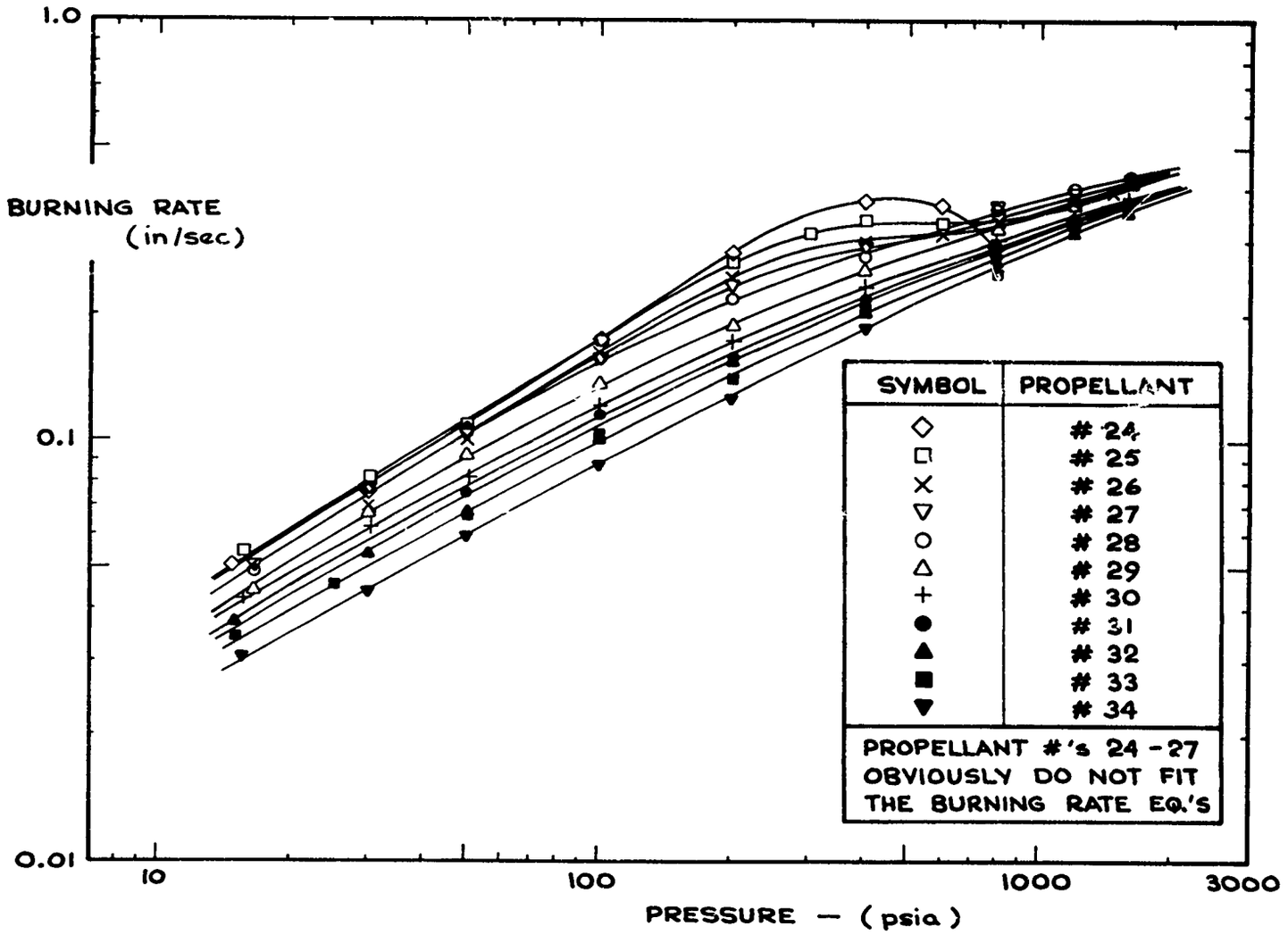

FIGURE B-21 DATA OF PROPELLANT NO.'S 24-34 IN TABLE III

PLOTTED AS (log r) VS. (log p)

(SEE FIG. B-42 FOR PROP. # 23)

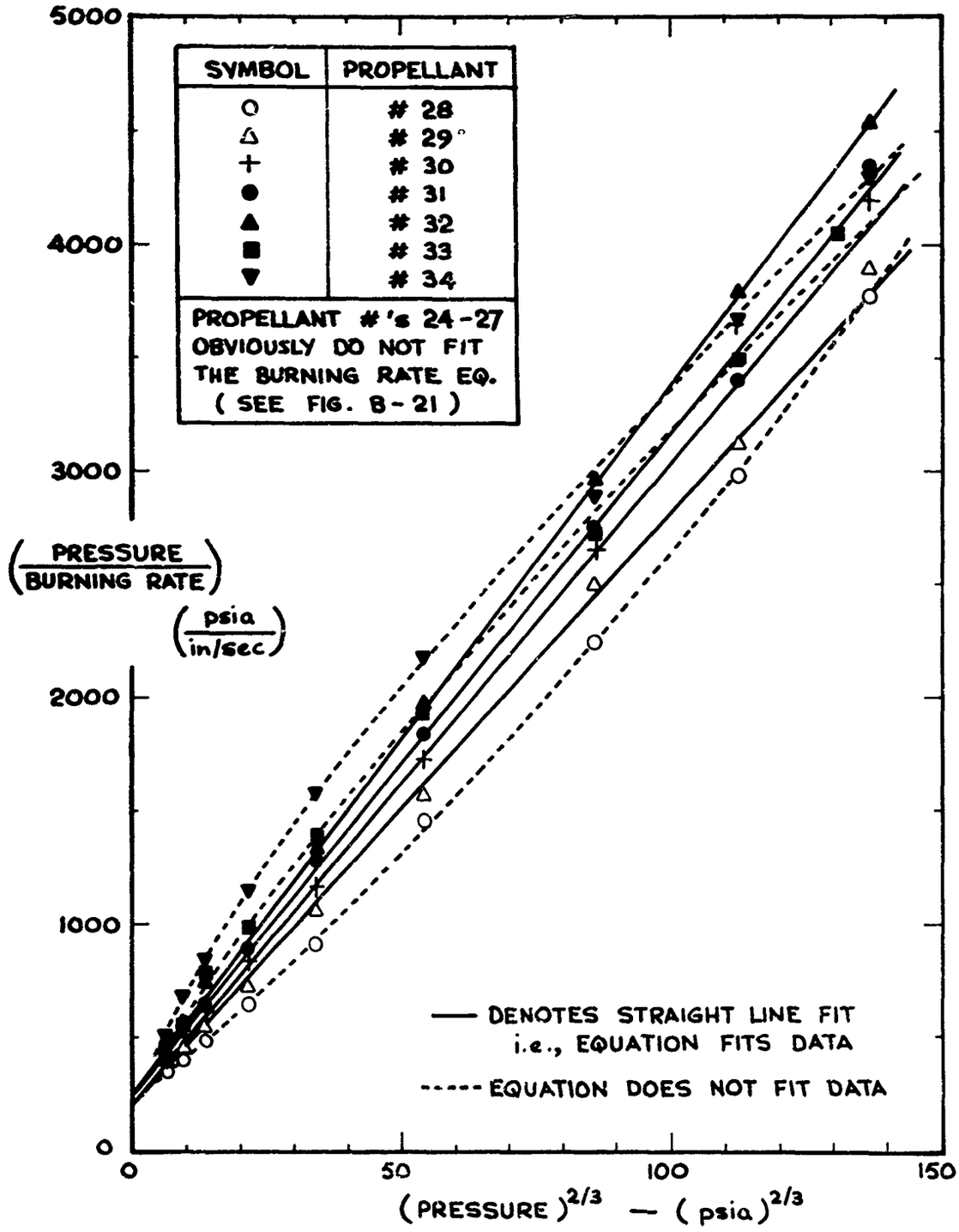

FIGURE B-22 DATA OF PROPELLANT NO.'S 24 - 34

CORRELATED WITH : $(1/r) = (a/p) + (b/p^{1/3})$

(SEE FIG. B-43 FOR PROP. # 23)

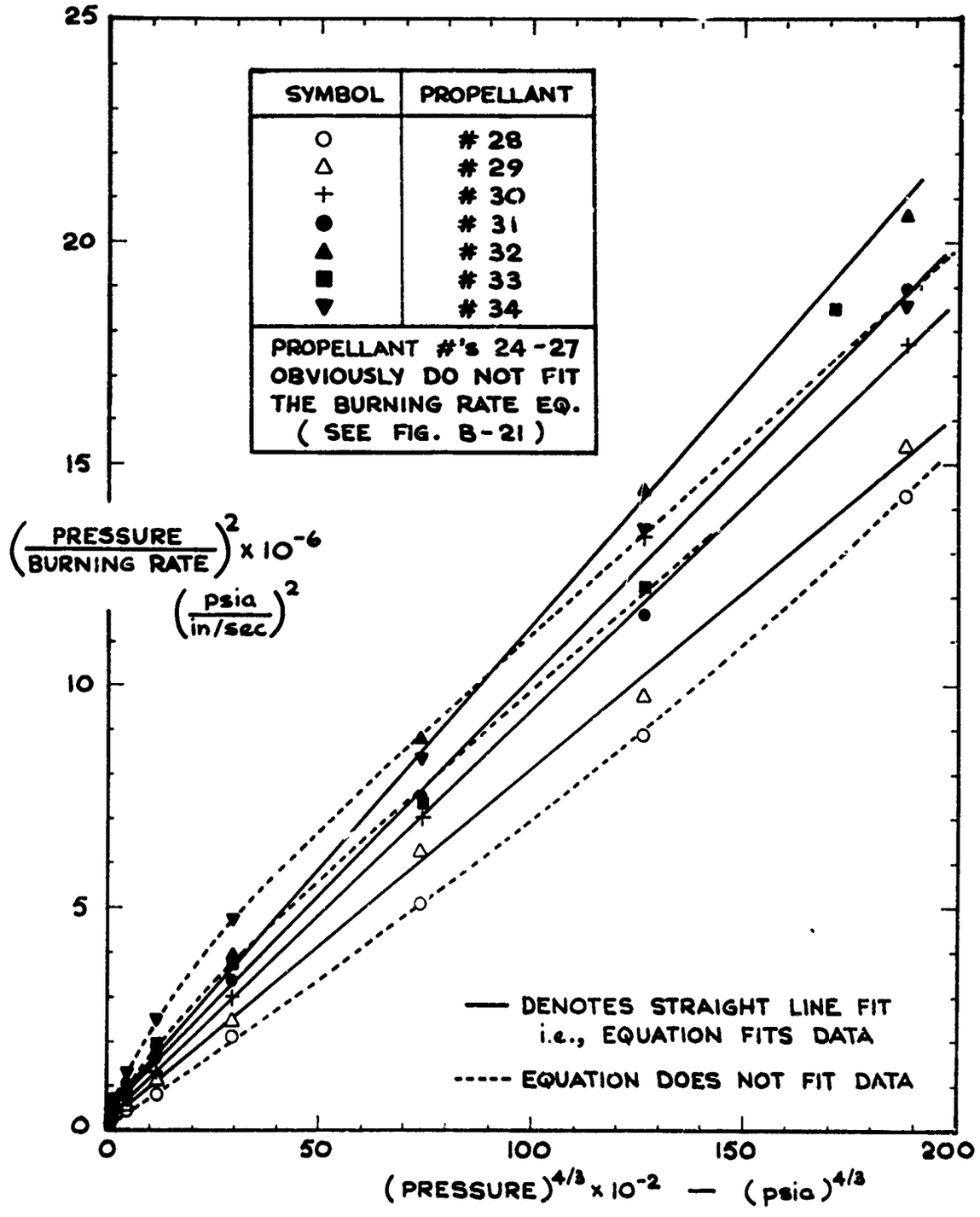

FIGURE B-23 DATA OF PROPELLANT NO.'S 24-34 CORRELATED WITH : $(1/r)^2 = (a/p)^2 + (b/p^{1/3})^2$

(SEE FIG. B-44 FOR PROP. # 23)

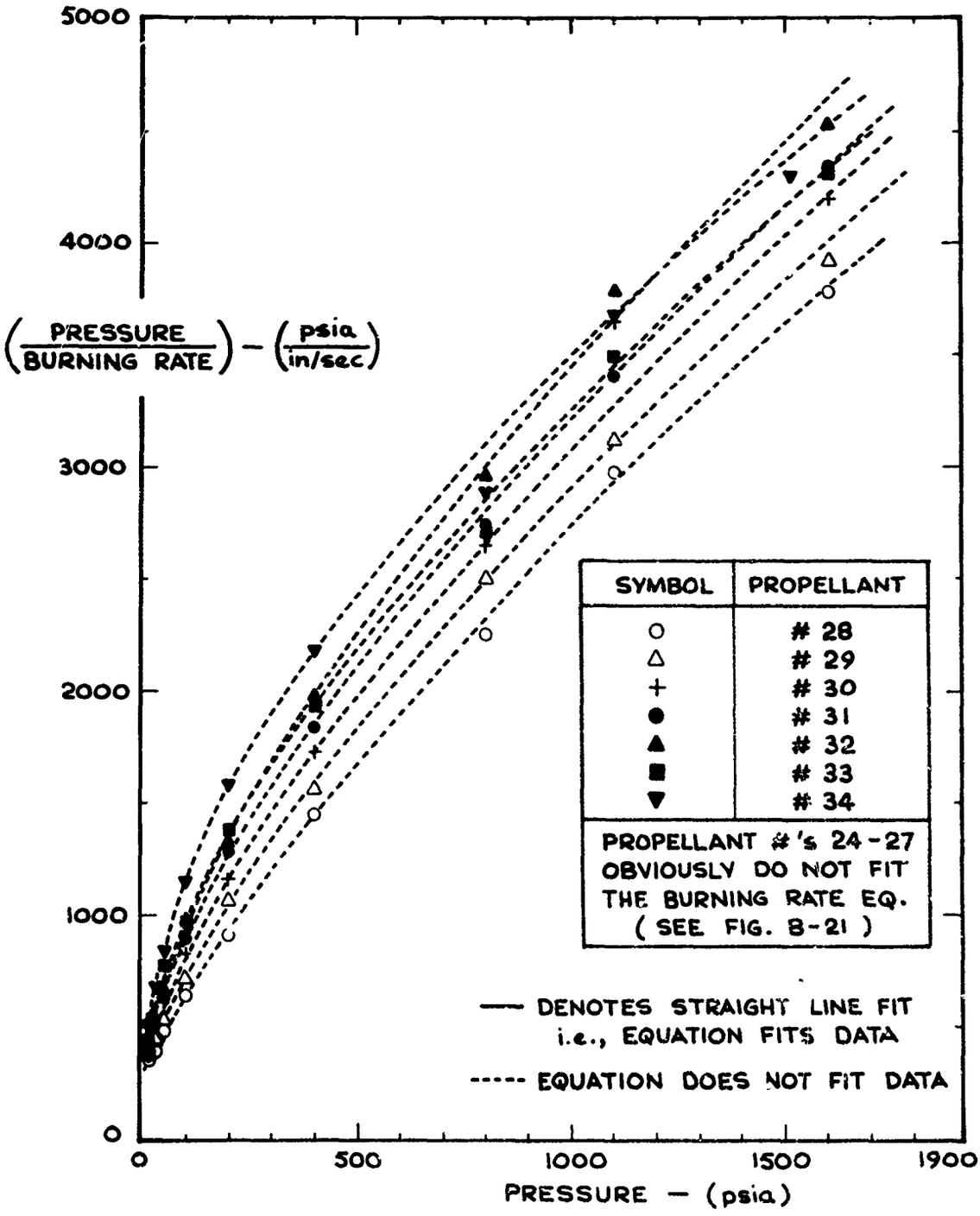

FIGURE B-24 DATA OF PROPELLANT NO.'S 24-34

CORRELATED WITH : $(1/r) = (a/p) + (c)$

(SEE FIG. B-45 FOR PROP. # 23)

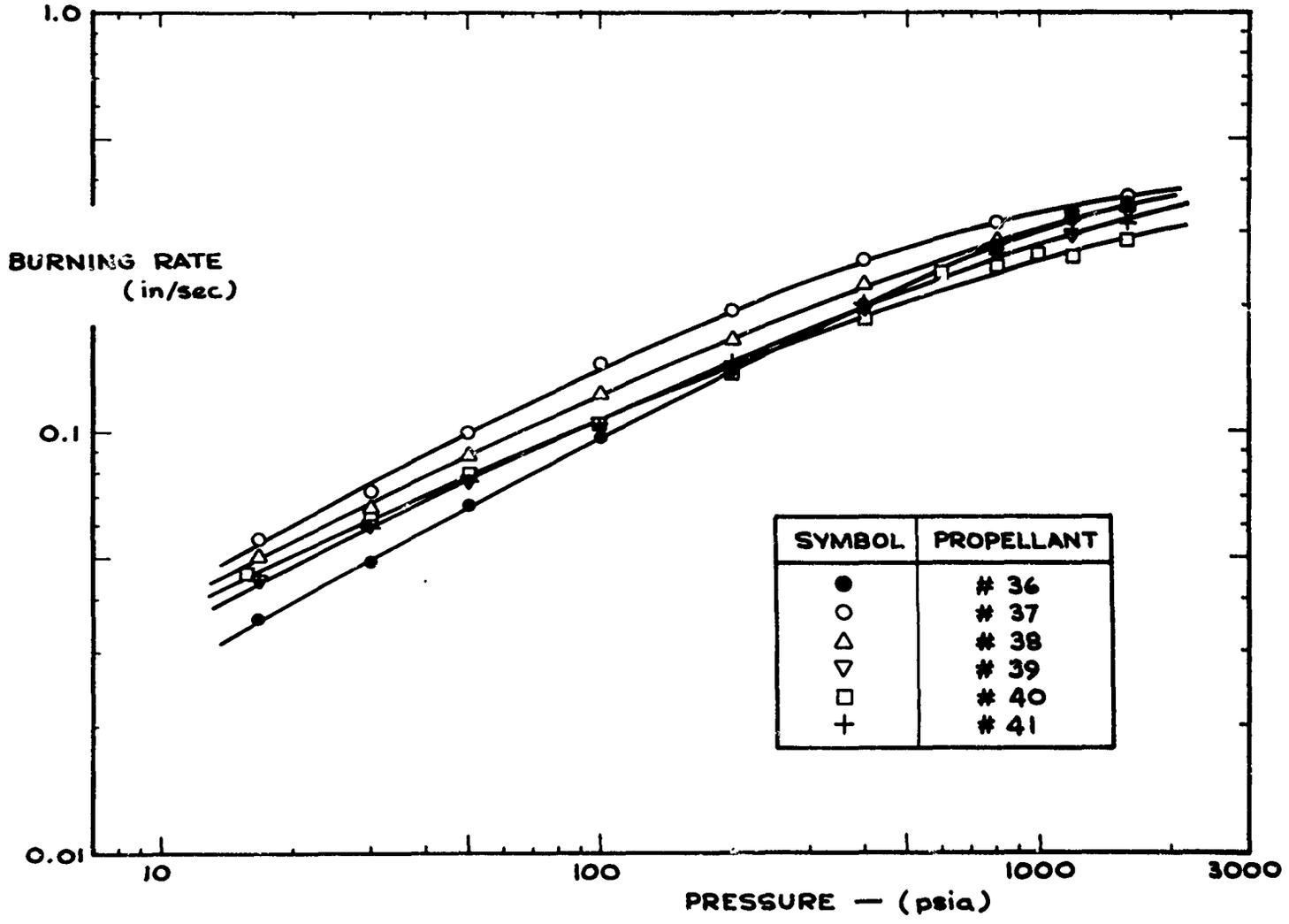

FIGURE B-25 DATA OF PROPELLANT NO.'S 36-41 IN TABLE III PLOTTED AS (log r) VS. (log p)

(SEE FIG. B-29 FOR PROPELLANT NO. 35)

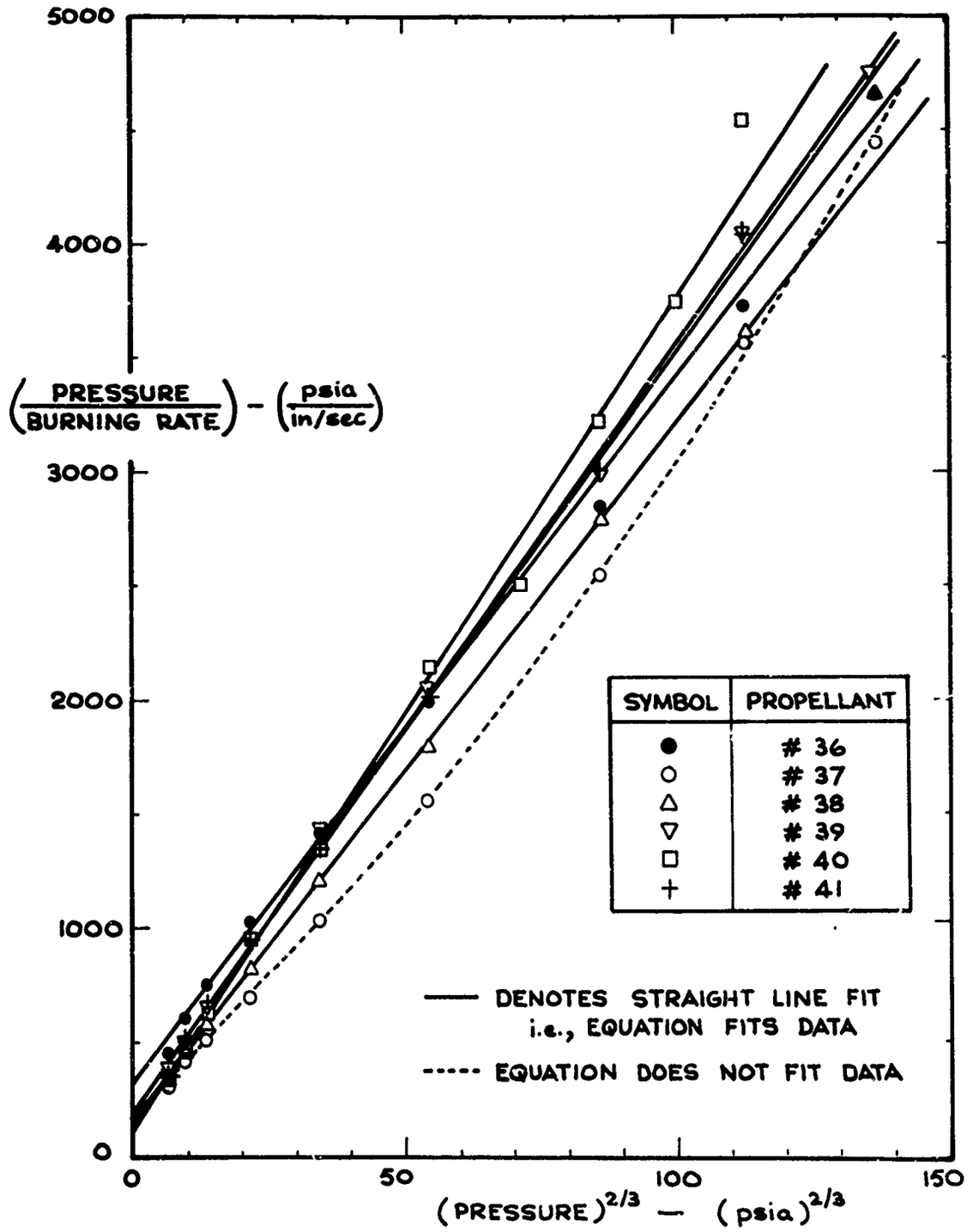

FIGURE B-26 DATA OF PROPELLANT NO.'S 36-41

CORRELATED WITH : $(1/r) = (a/p) + (b/p^{1/3})$

(SEE FIG. B-30 FOR PROPELLANT NO. 35)

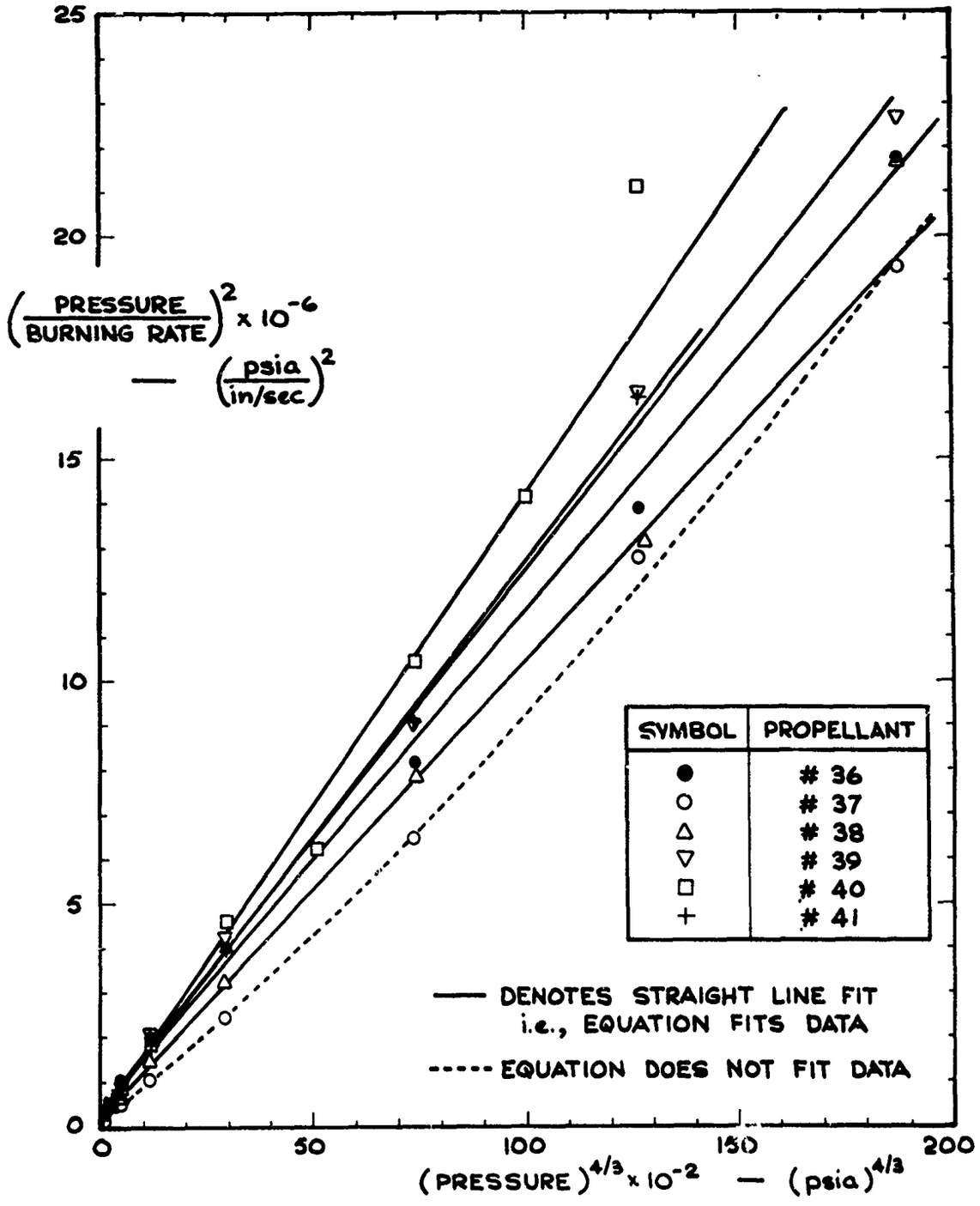

FIGURE B-27 DATA OF PROPELLANT NO.'S 36-41 CORRELATED WITH : $(1/r)^2 = (a/p)^2 + (b/p^{1/3})^2$

(SEE FIG. B-31 FOR PROPELLANT NO. 35)

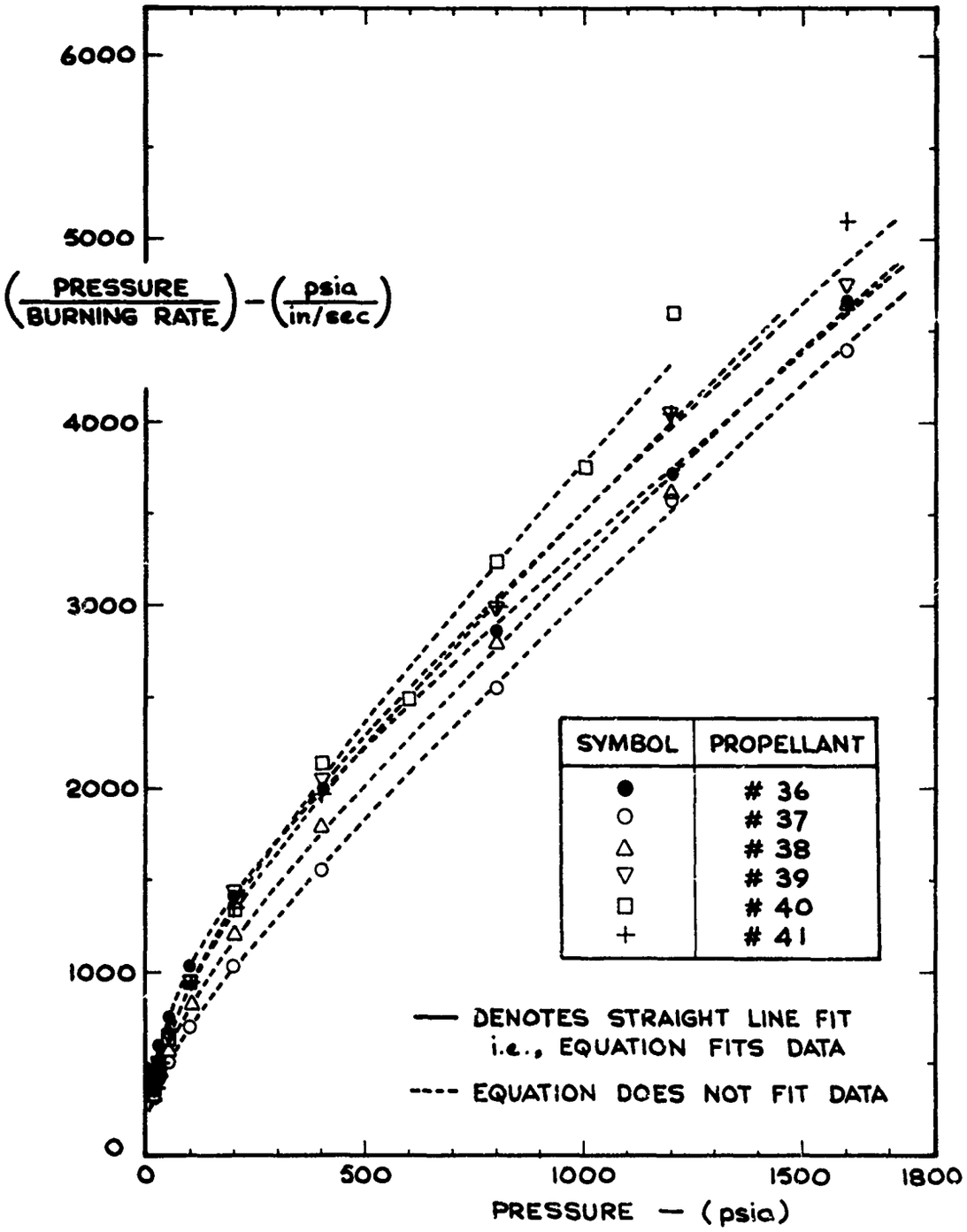

FIGURE B-28 DATA OF PROPELLANT NO.'S 36-41

CORRELATED WITH : $(1/r) = (a/p) + (c)$

(SEE FIG. B-32 FOR PROPELLANT NO. 35)

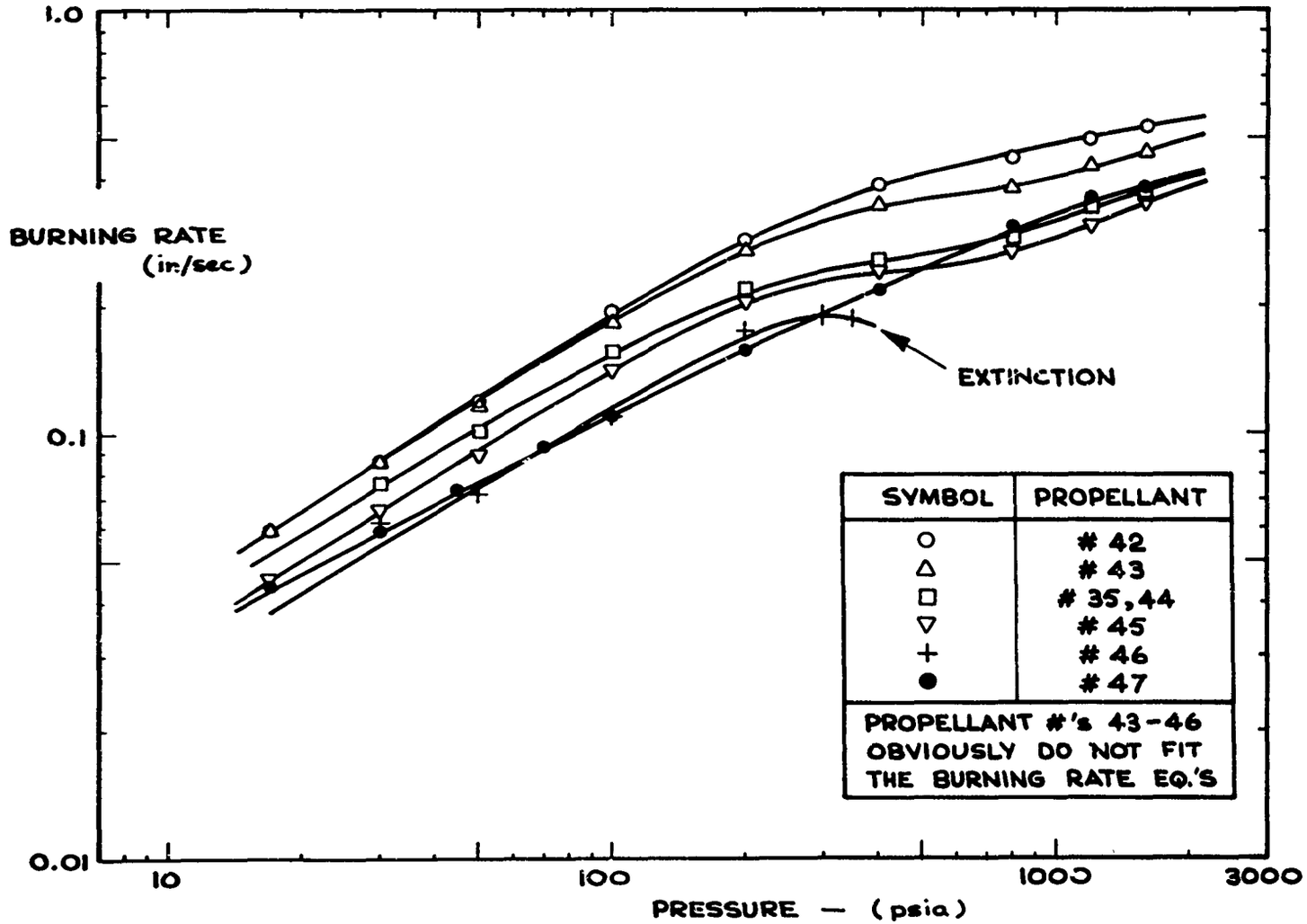

FIGURE B-29 DATA OF PROPELLANT NO.'S 35, 42-47 IN TABLE III PLOTTED AS (log r) VS. (log p)

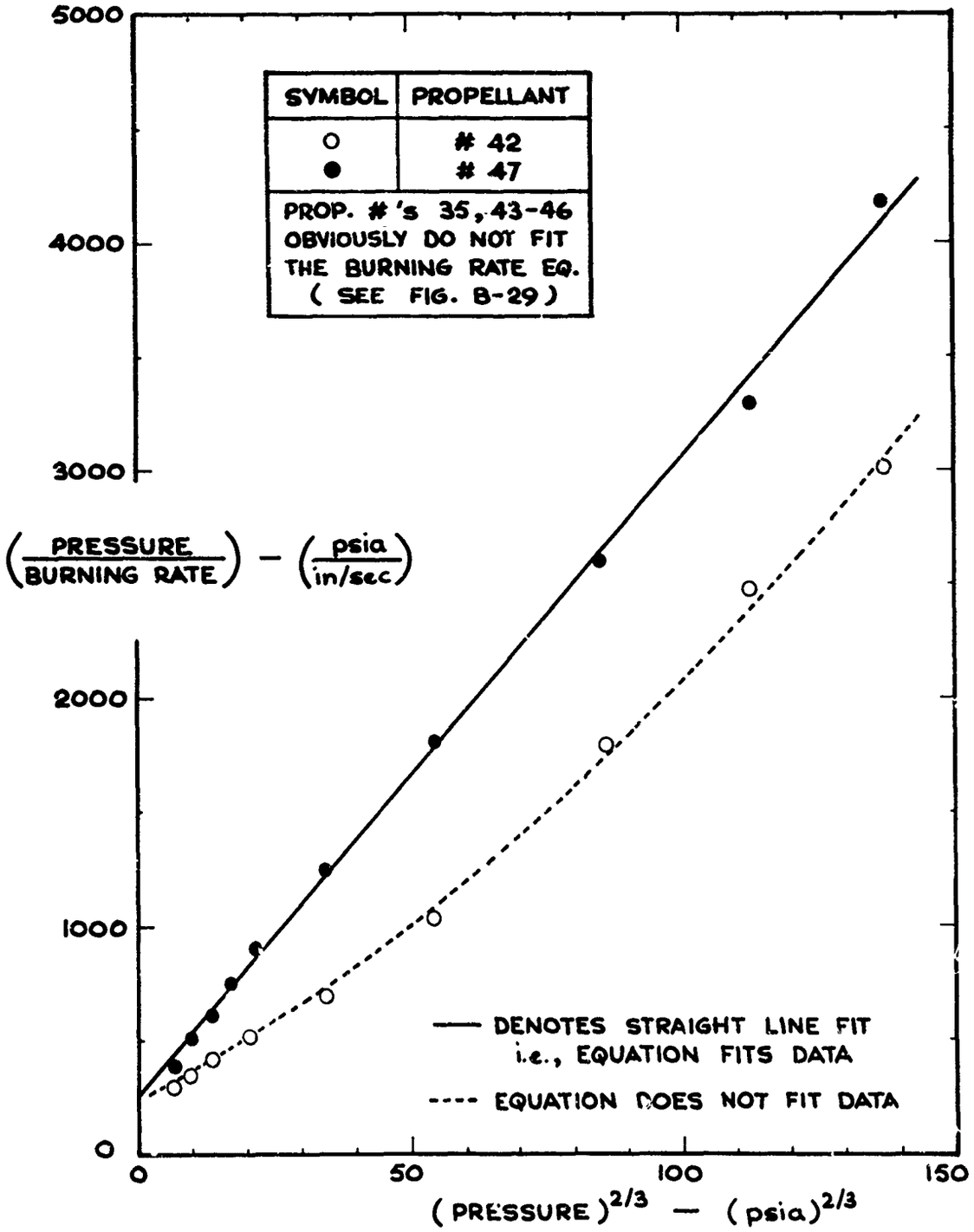

FIGURE B-30 DATA OF PROPELLANT NO.'S 35, 42-47

CORRELATED WITH : $(1/r) = (a/p) + (b/p^{1/3})$

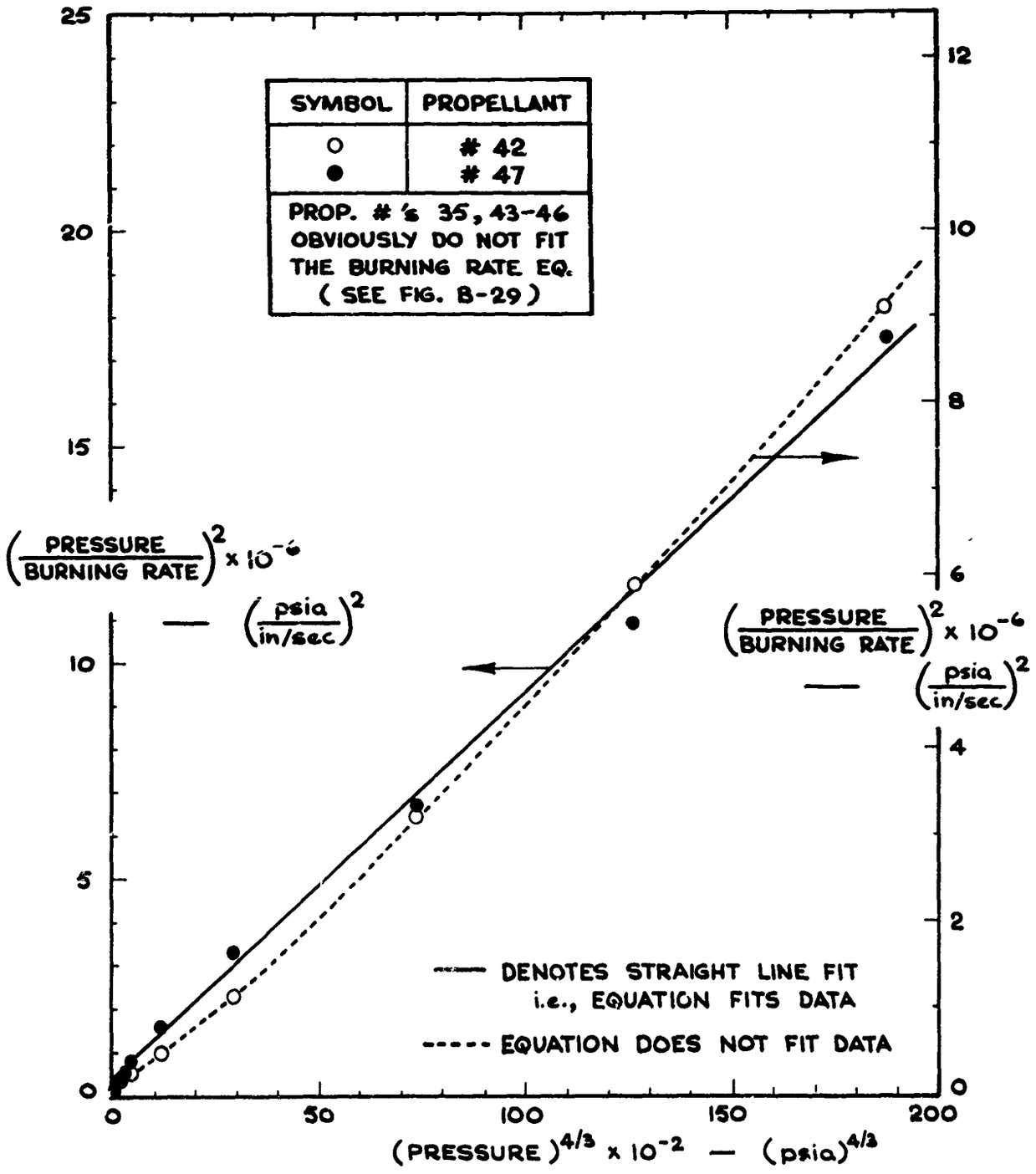

FIGURE B-31 DATA OF PROPELLANT NO.'S 35, 42-47 CORRELATED WITH : $(1/r)^2 = (a/p)^2 + (b/p^{1/3})^2$

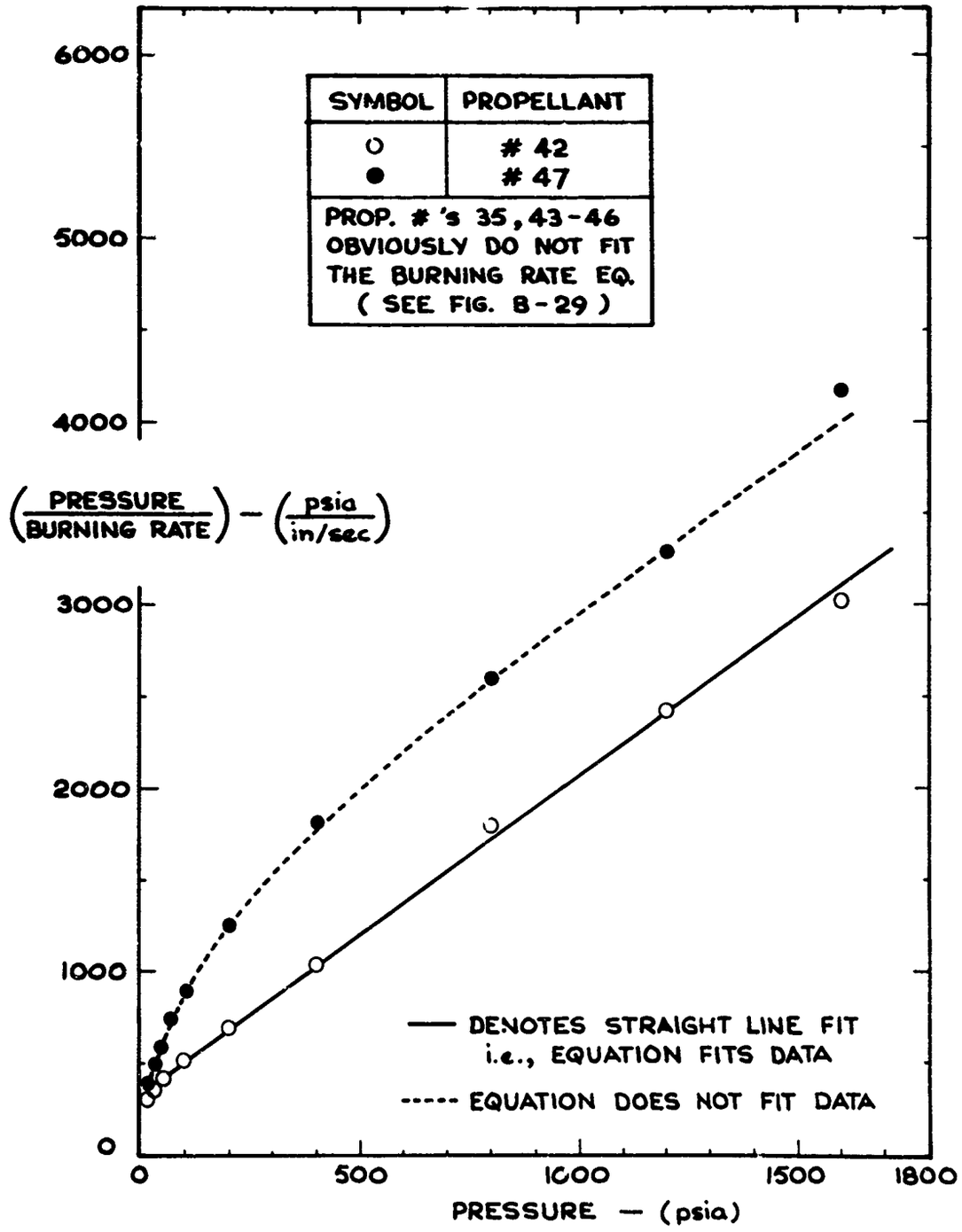

FIGURE B-32 DATA OF PROPELLANT NO.'S 35, 42-47

CORRELATED WITH : $(1/r) = (a/p) + (c)$

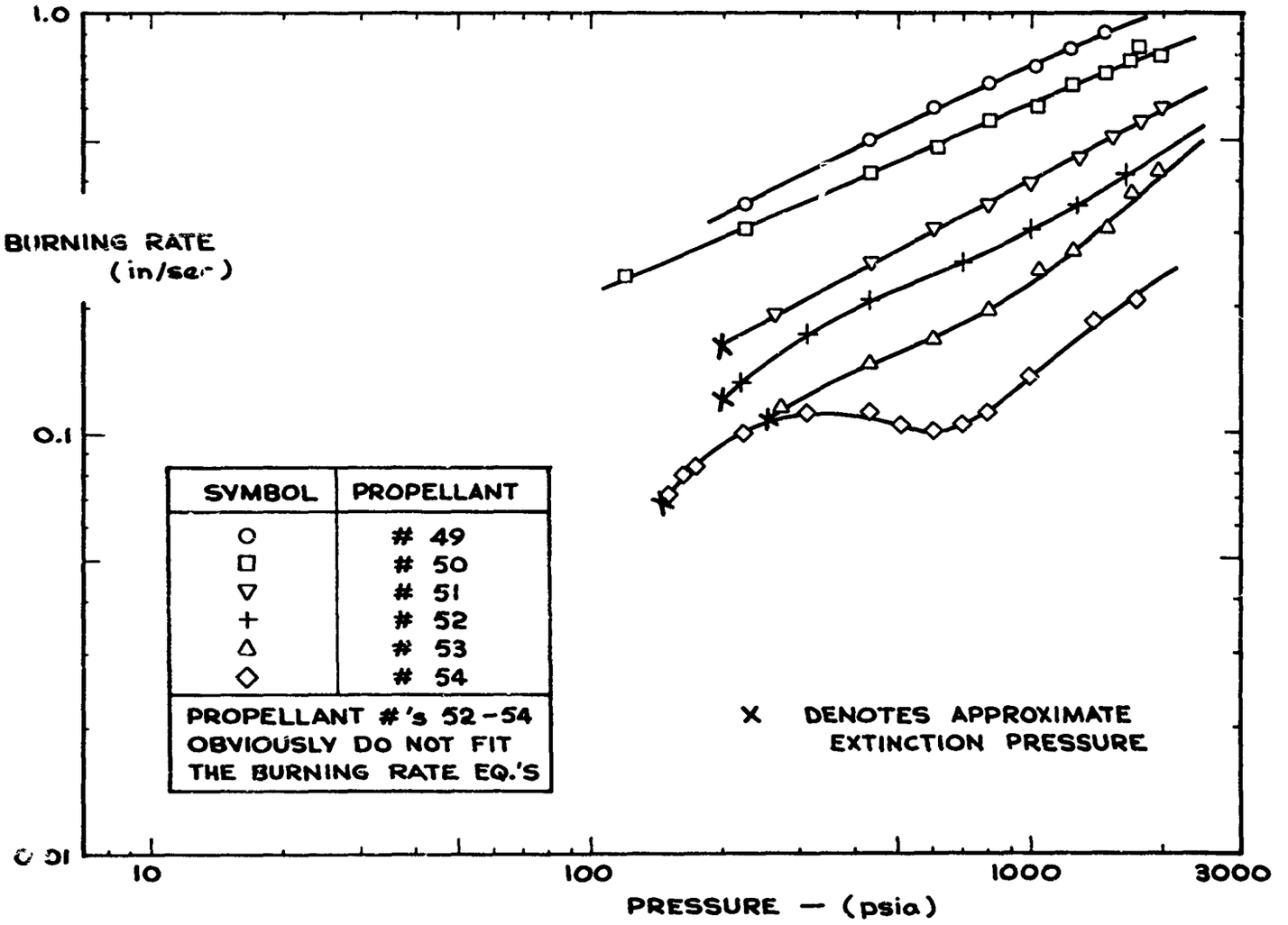

FIGURE B-33 DATA OF PROPELLANT NO.'S 49 - 54 IN TABLE III PLOTTED AS (log r) VS. (log p)

(SEE FIG. B-42 FOR PROPELLANT NO. 48)

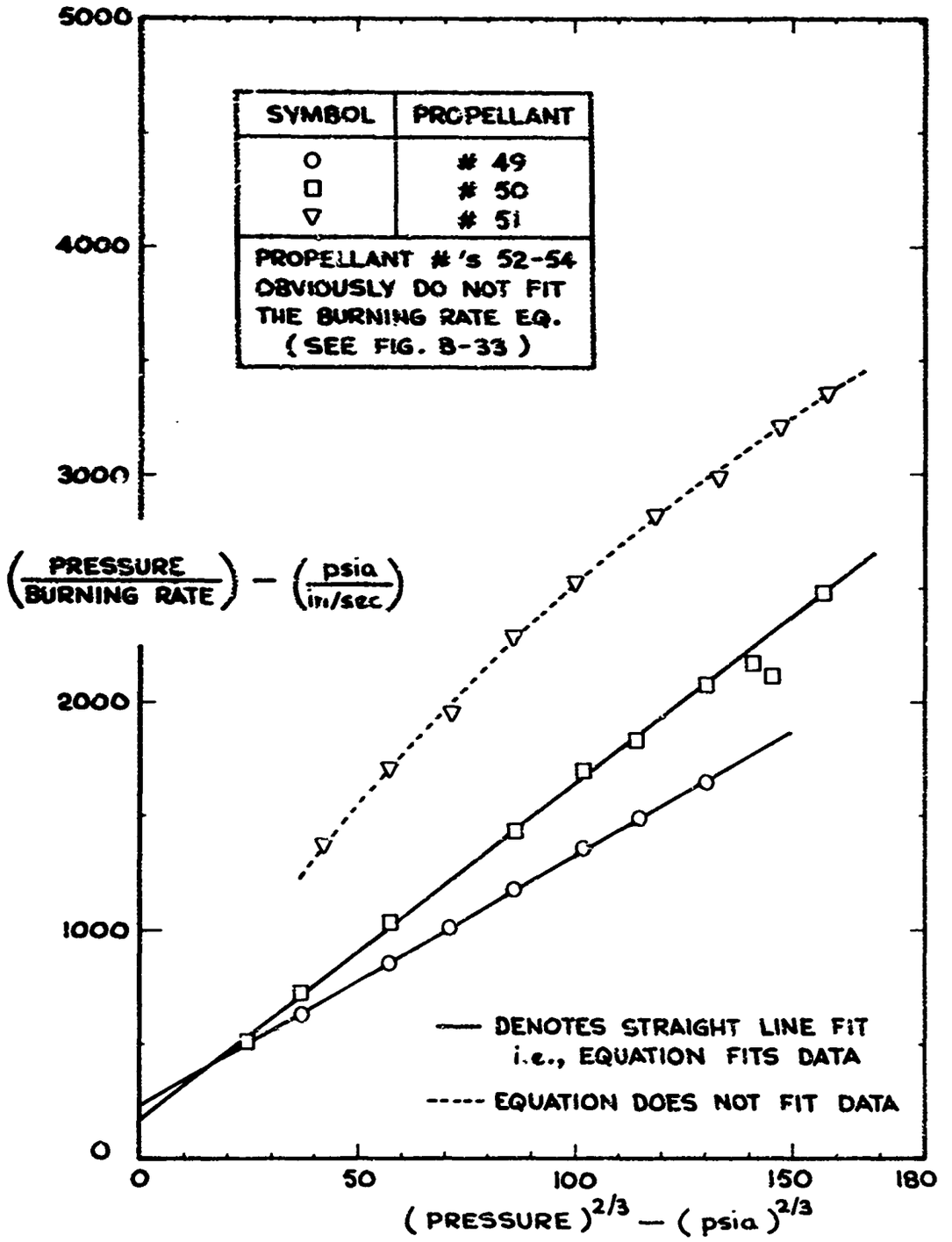

FIGURE B-34 DATA OF PROPELLANT NO.'S 49-54

CORRELATED WITH : $(1/r) = (a/p) + (b/p^{1/3})$

(SEE FIG. B-43 FOR PROP. #48)

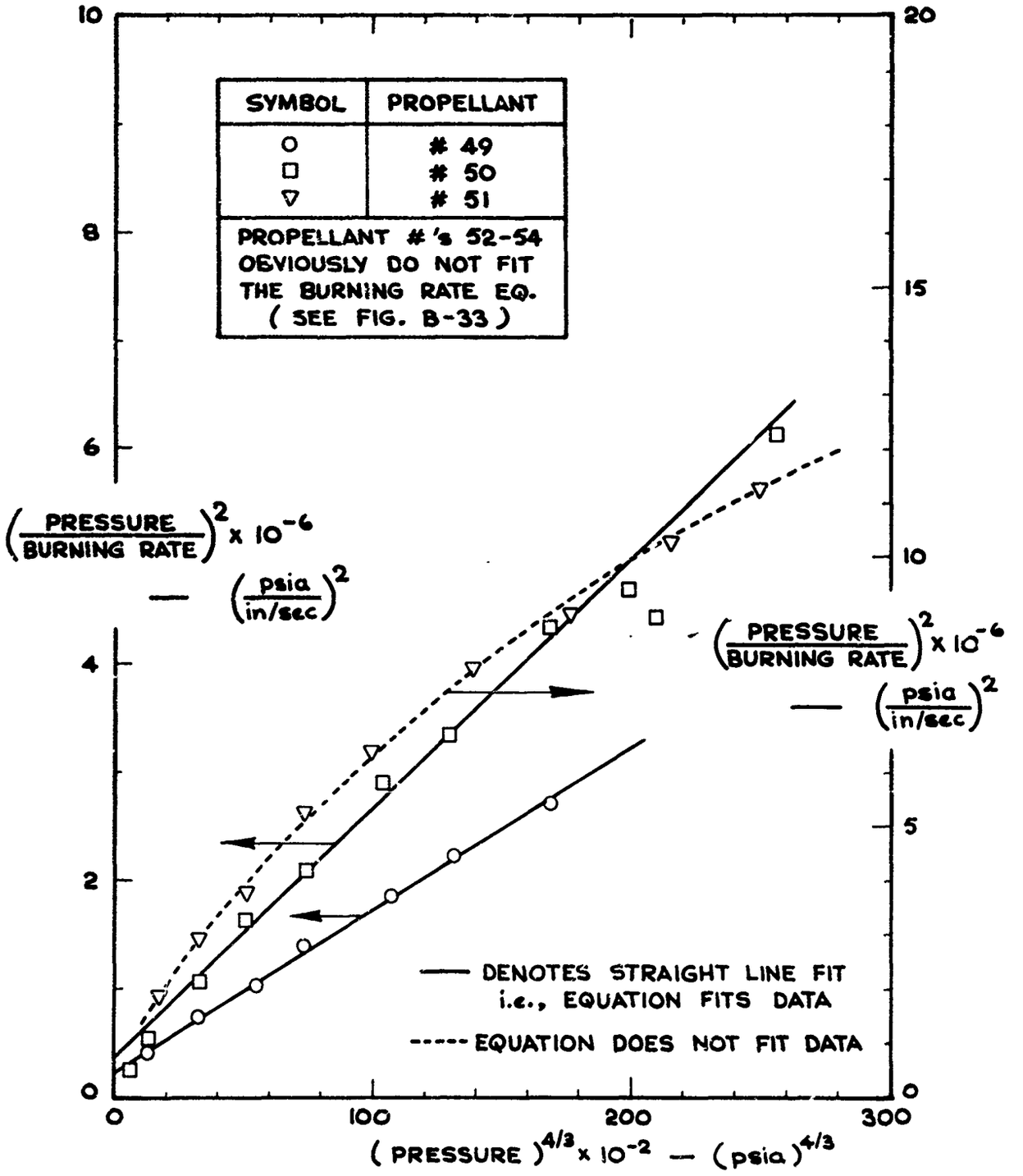

FIGURE B-35 DATA OF PROPELLANT NO.'S 49-54 CORRELATED WITH : $(1/r)^2 = (a/p)^2 + (b/p^{1/3})^2$

(SEE FIG. B-44 FOR PROP. # 48)

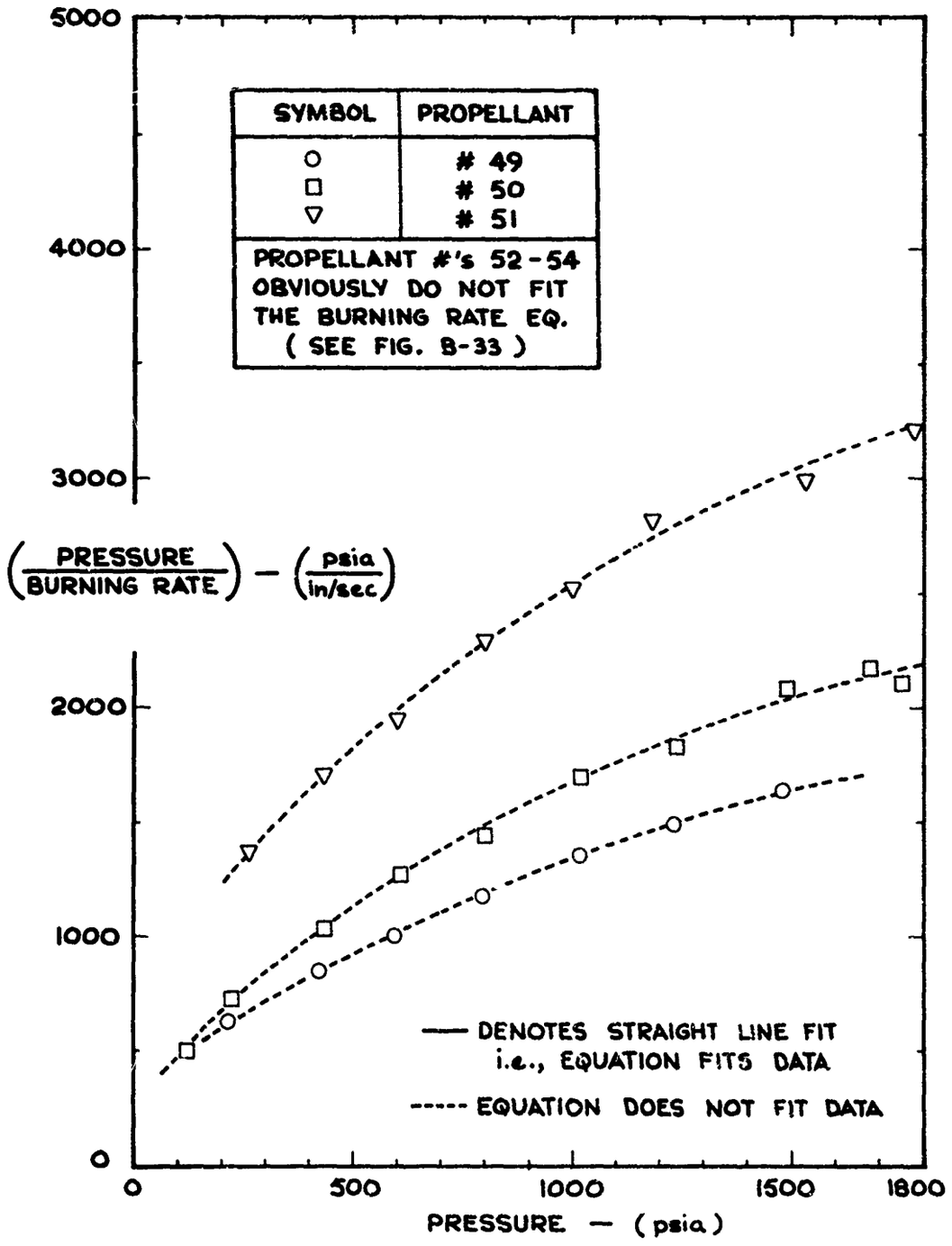

FIGURE B-36 DATA OF PROPELLANT NO.'S 49 - 54

CORRELATED WITH : $(1/r) = (a/p) + (c)$

(SEE FIG. B-45 FOR PROP. # 48)

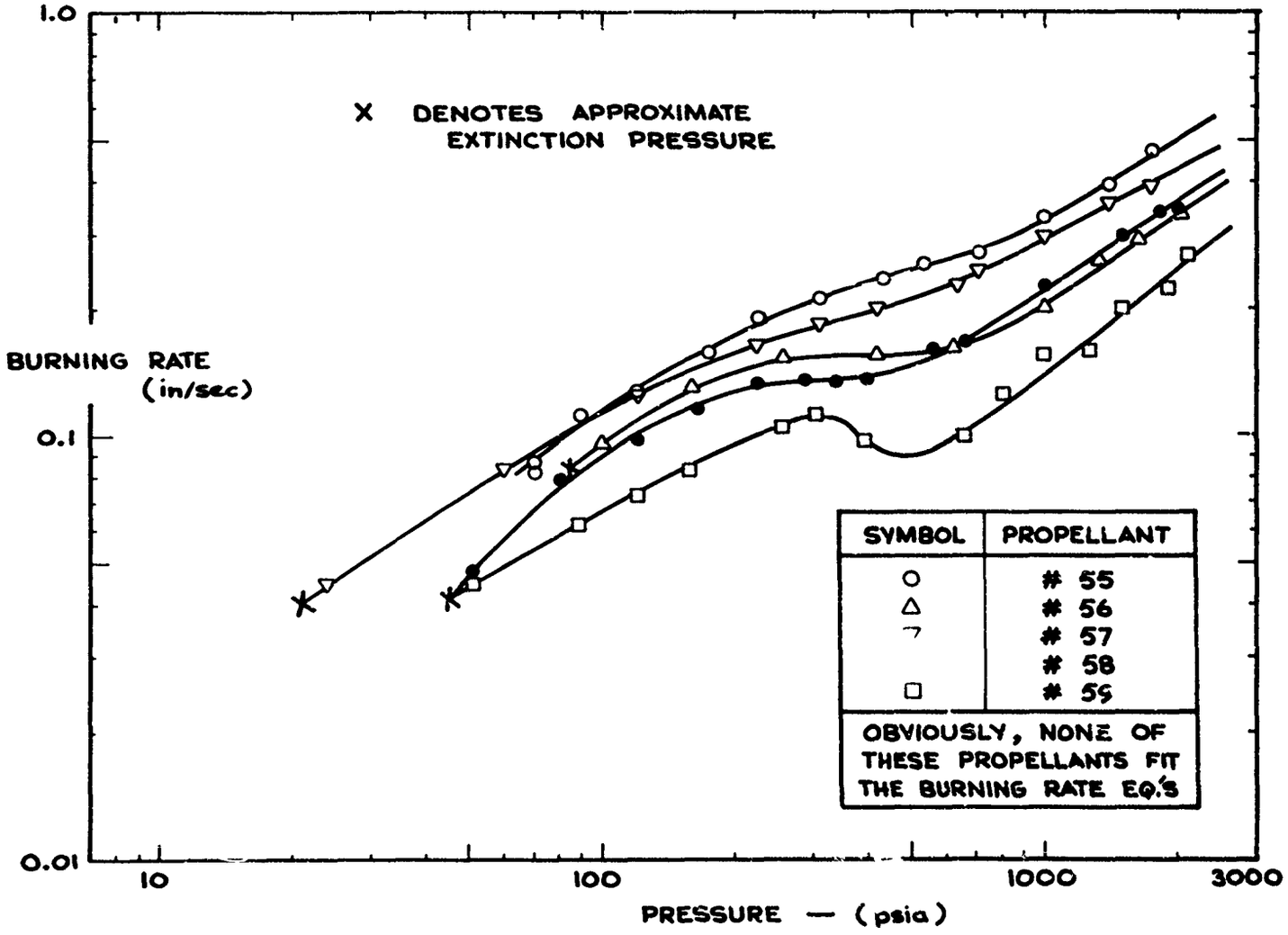

FIGURE B-37 DATA OF PROPELLANT NO.'S 55-59 IN TABLE III PLOTTED AS (log r) VS. (log p)

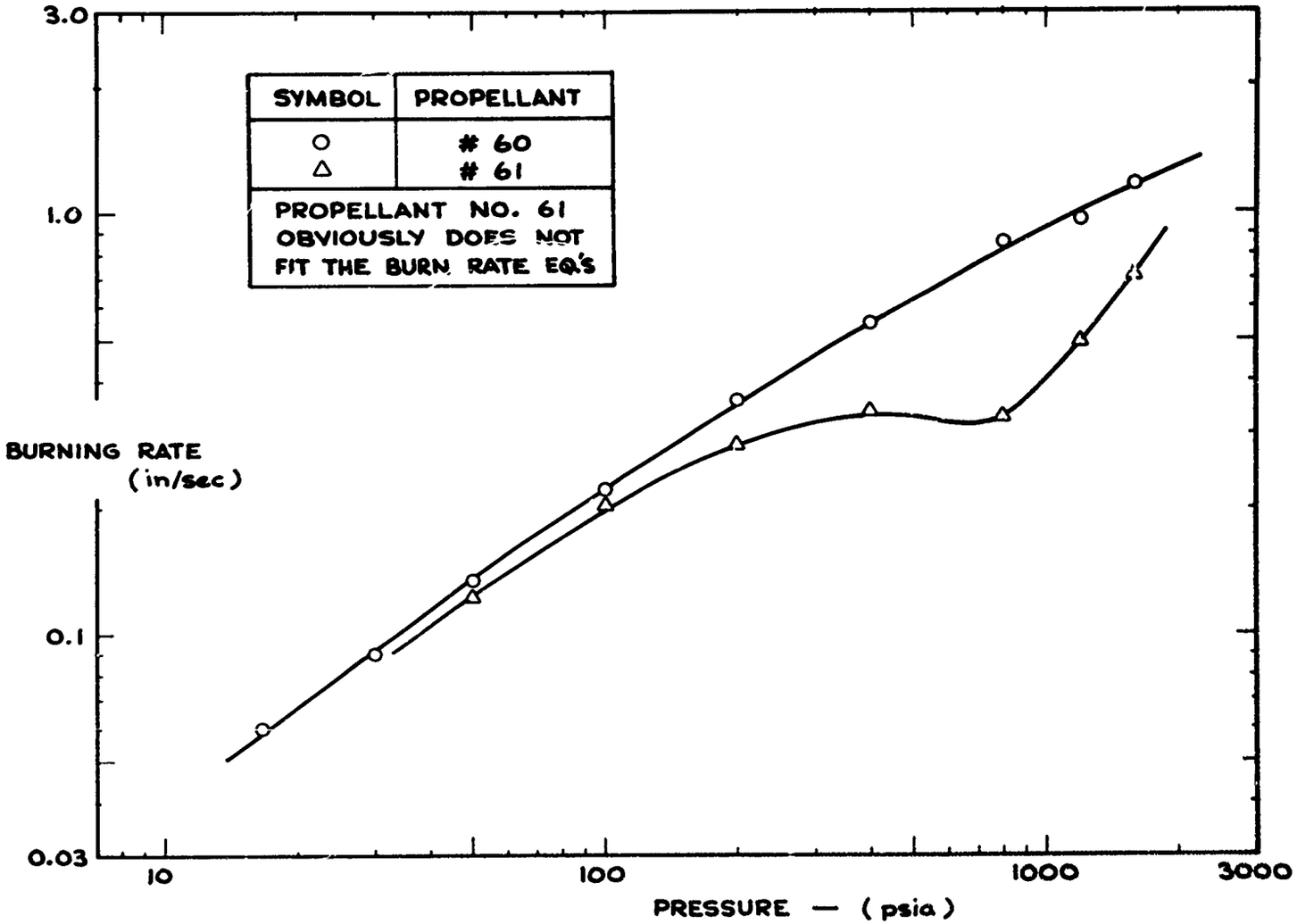

FIGURE B-38 DATA OF PROPELLANT NO.'S 60 & 61 IN TABLE III PLOTTED AS (log r) VS. (log p)

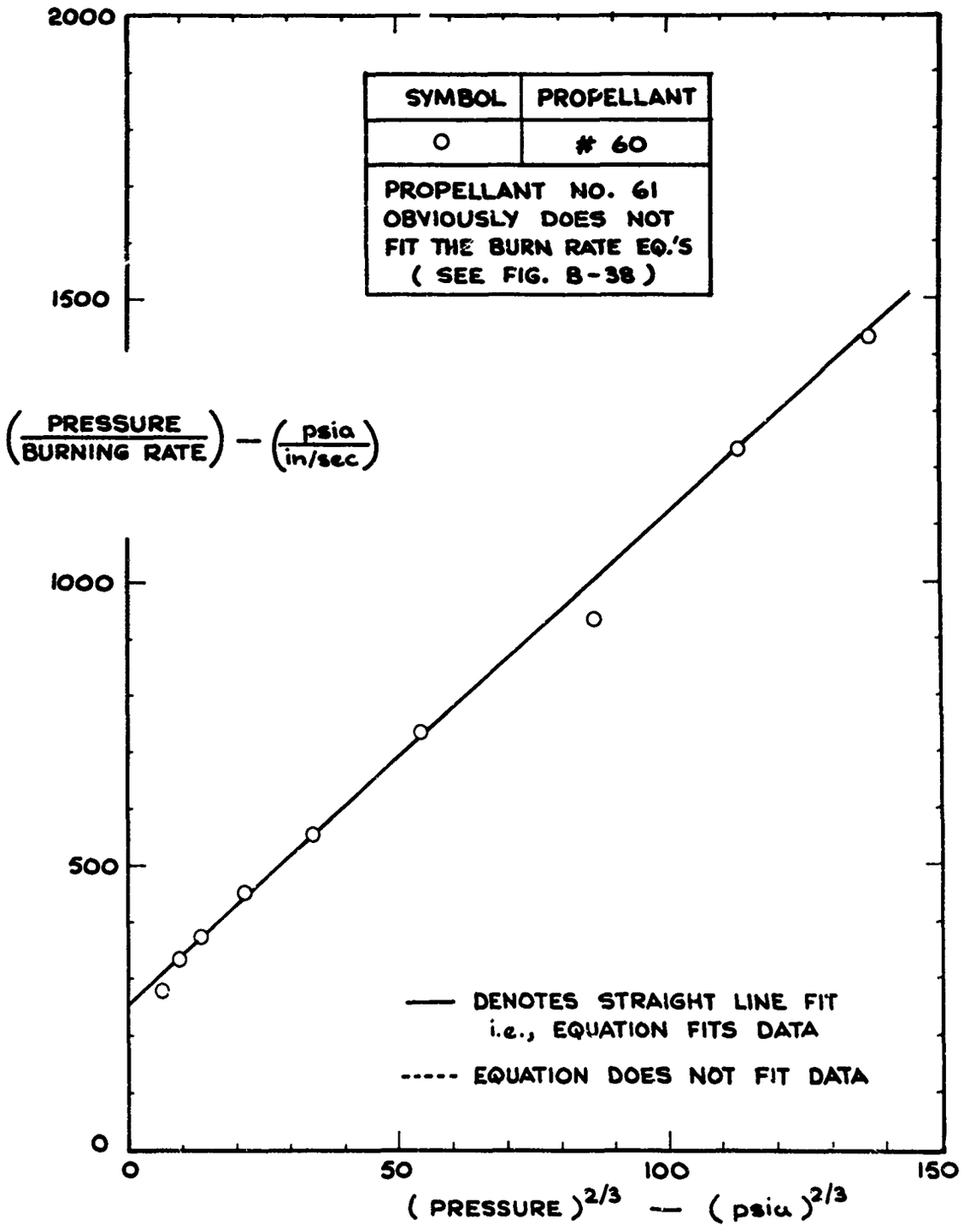

FIGURE B-39 DATA OF PROPELLANT NO.'S 60 + 61 CORRELATED WITH : $(1/r) = (a/p) + (b/p^{1/3})$

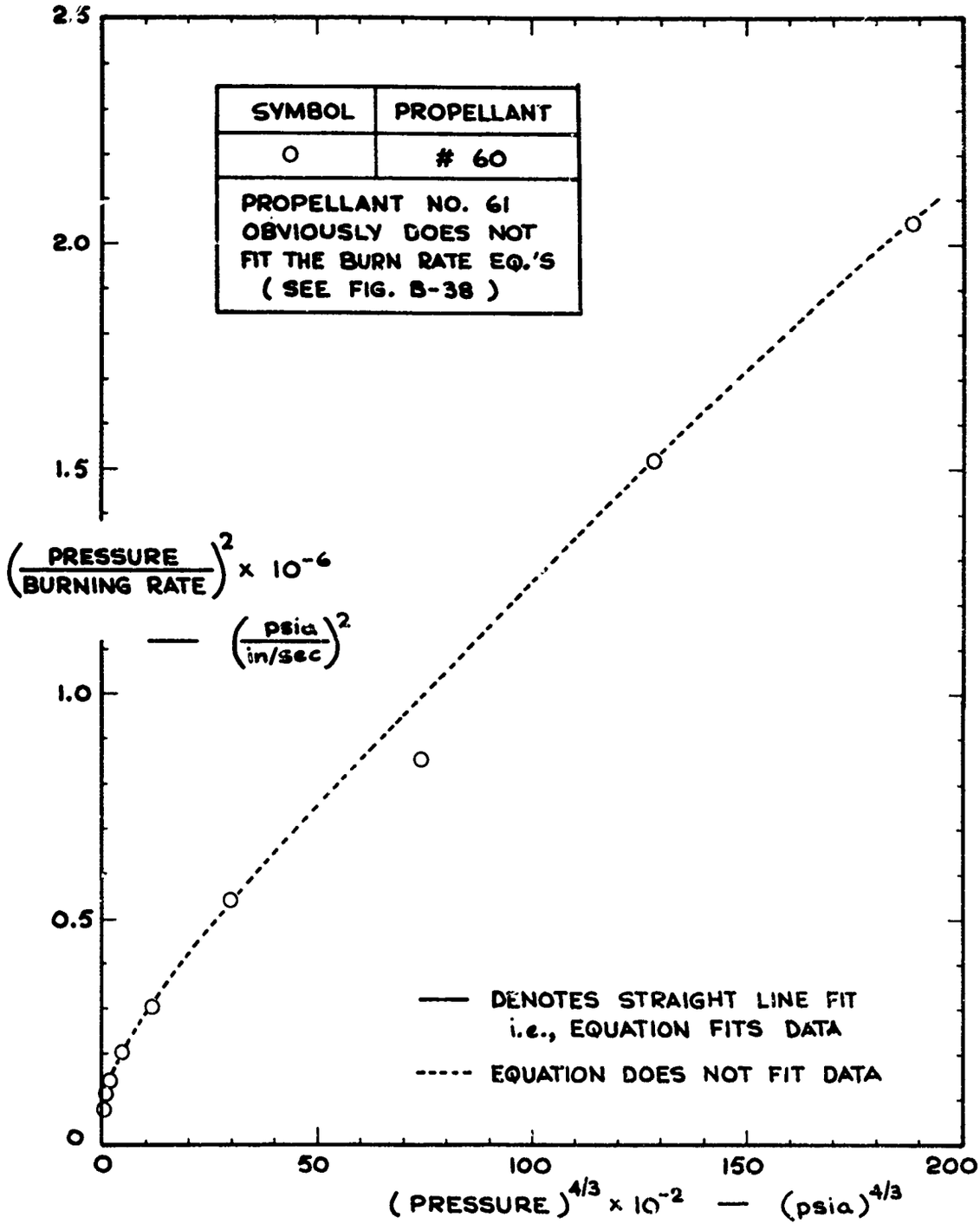

FIGURE B-40 DATA OF PROPELLANT NO.'S 60 + 61 CORRELATED WITH : $(1/r)^2 = (a/p)^2 + (b/p^{1/3})^2$

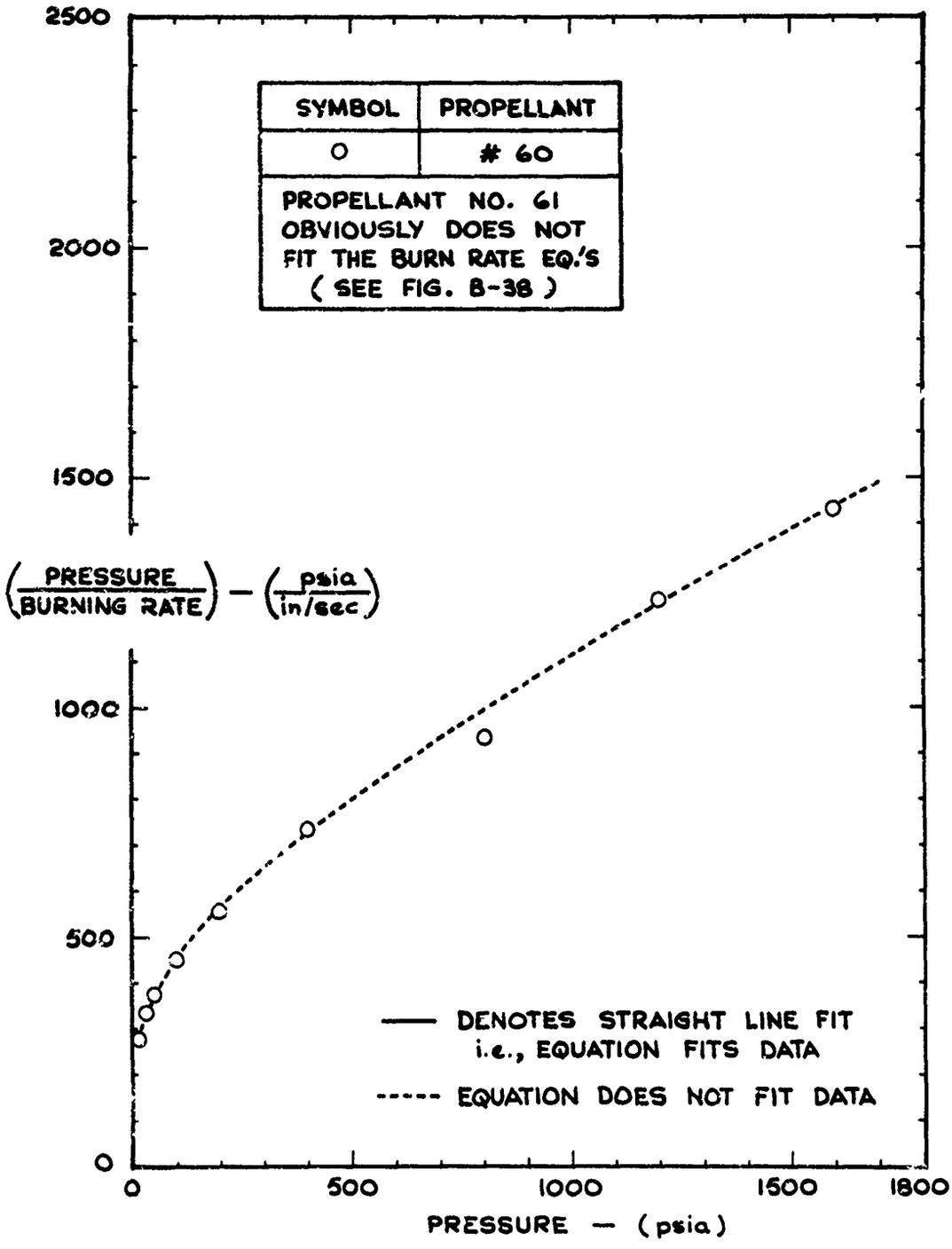

FIGURE B-41 DATA OF PROPELLANT NO.'S 60 + 61 CORRELATED WITH : $(1/r) = (a/p) + (c)$

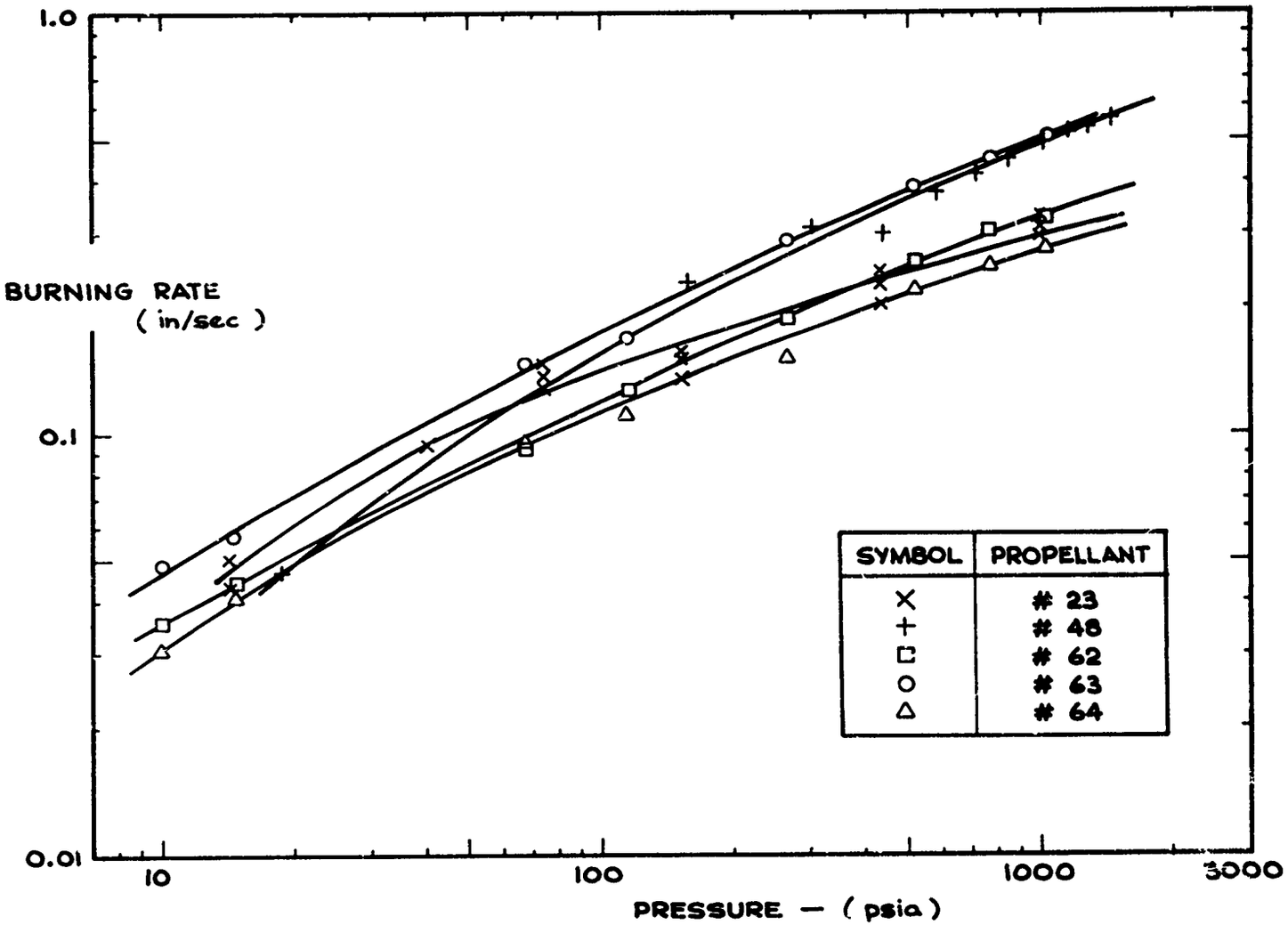

FIGURE B-42 DATA OF PROPELLANT NO.'S 23, 48, 62-64 IN TABLE III PLOTTED AS (log r) VS. (log p)

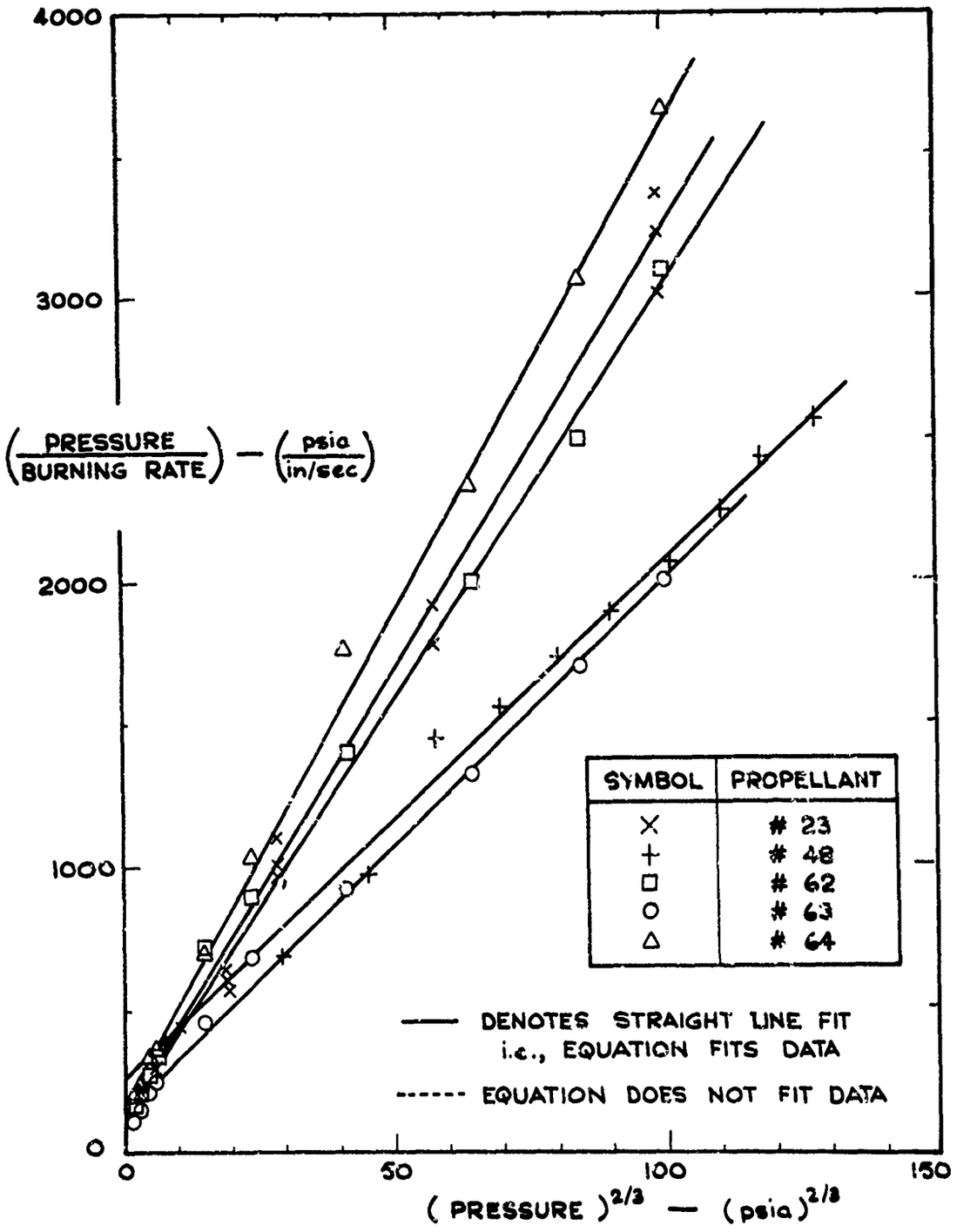

FIGURE B-43 DATA OF PROPELLANT NO.'S 23, 48, 62-64

CORRELATED WITH : $(1/r) = (a/p) + (b/p^{1/3})$

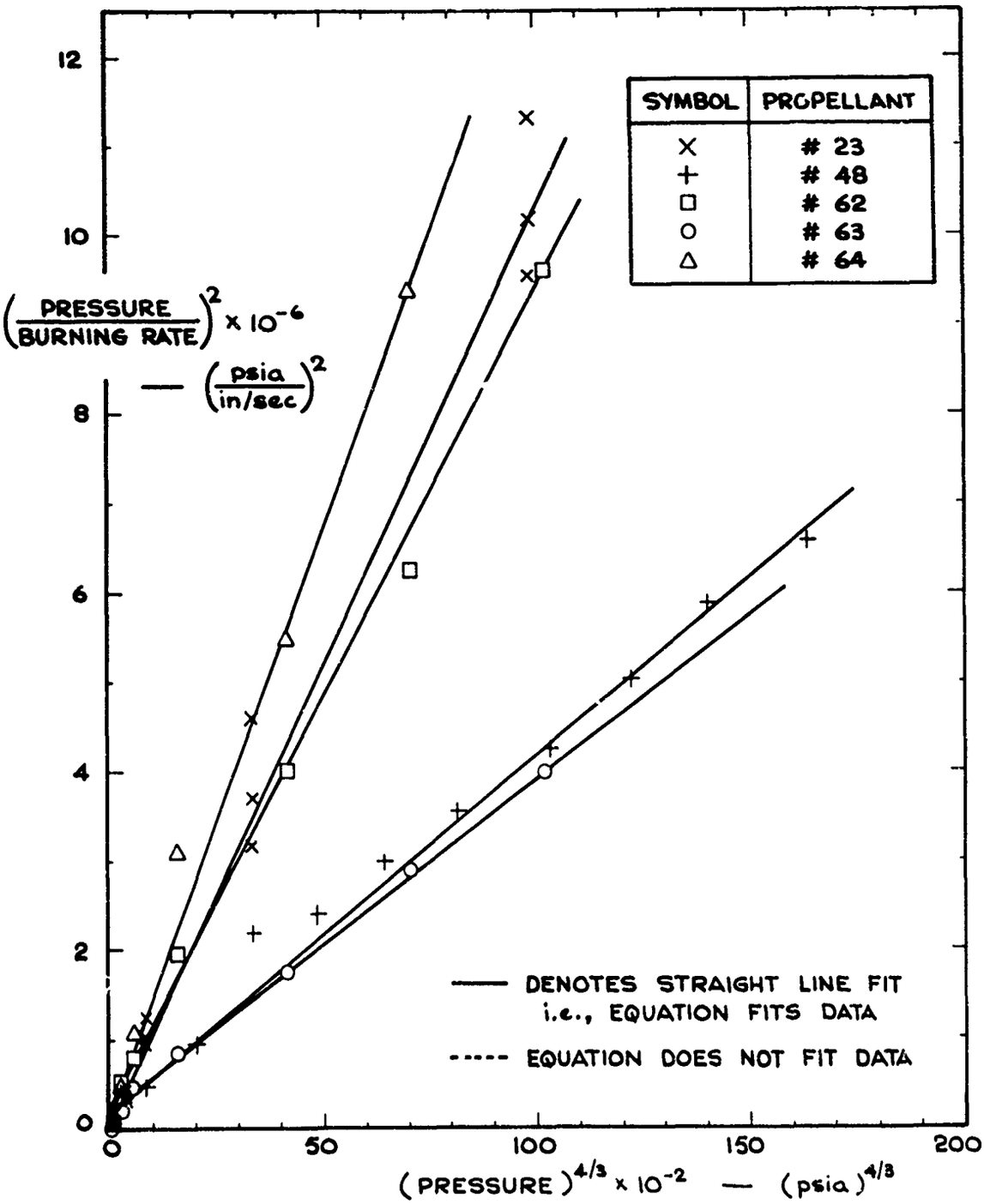

FIGURE B-44 DATA OF PROPELLANT NO.'S 23, 48, 62-64

CORRELATED WITH : $(1/r)^2 = (a/p)^2 + (b/p^{1/3})^2$

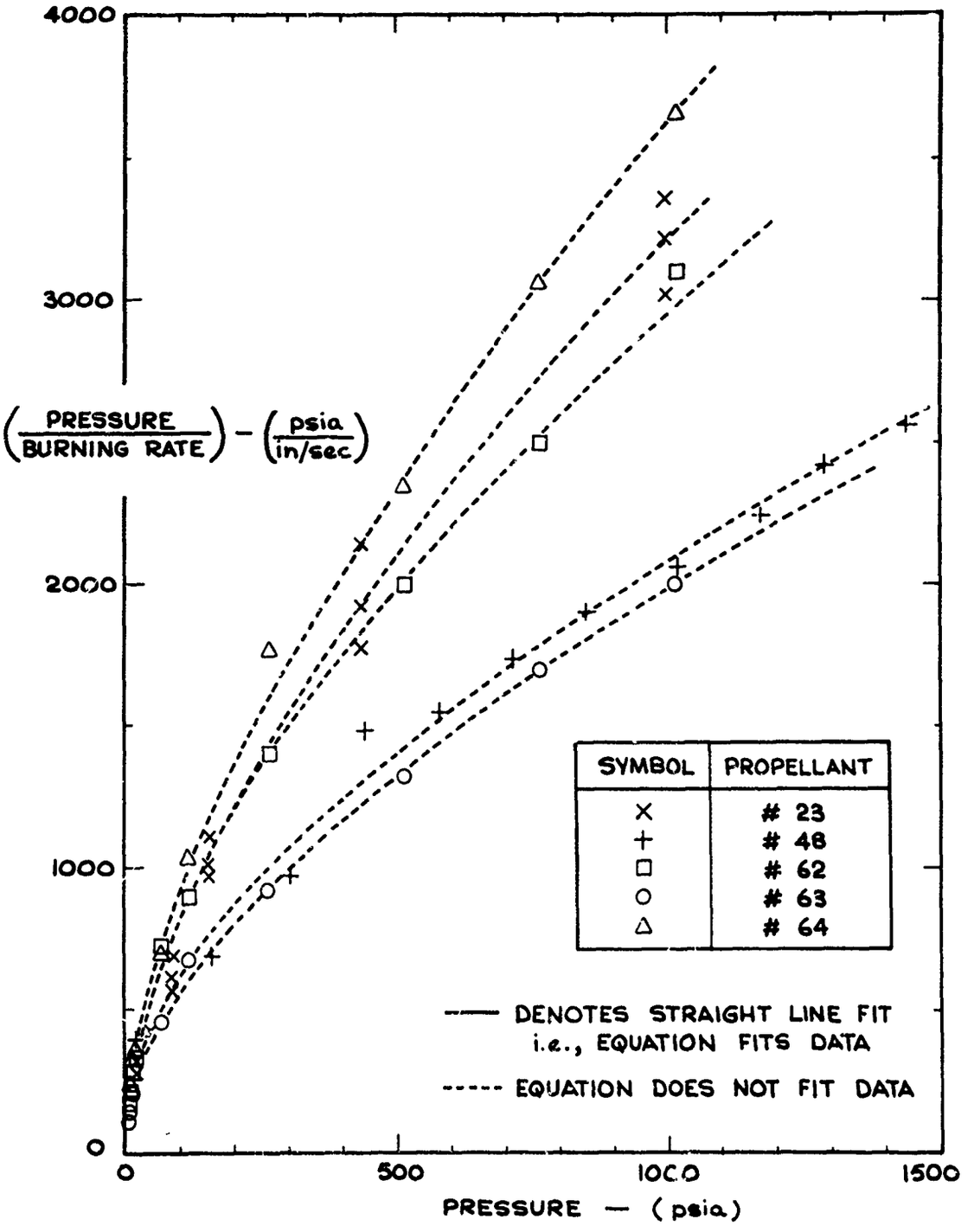

FIGURE B-45 DATA OF PROPELLANT NO.'S 23, 48, 62-64 CORRELATED WITH : $(1/r) = (a/p) + (c)$

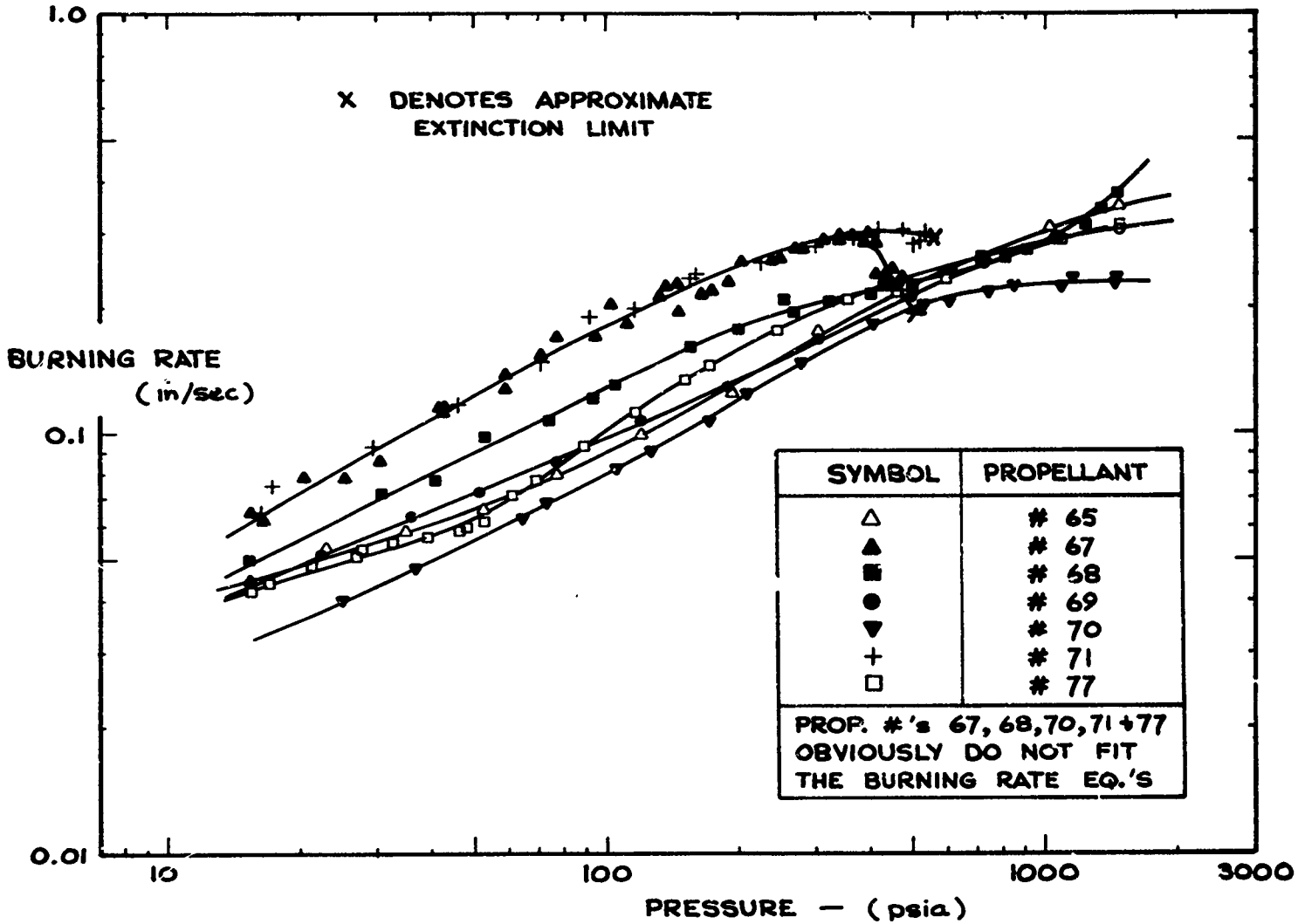

FIGURE B-46 DATA OF PROPELLANT NO.'S 65, 67-71, +77 IN TABLE III PLOTTED AS (log r) VS. (log p)

(SEE FIG. B-50 FOR PROP. # 66)

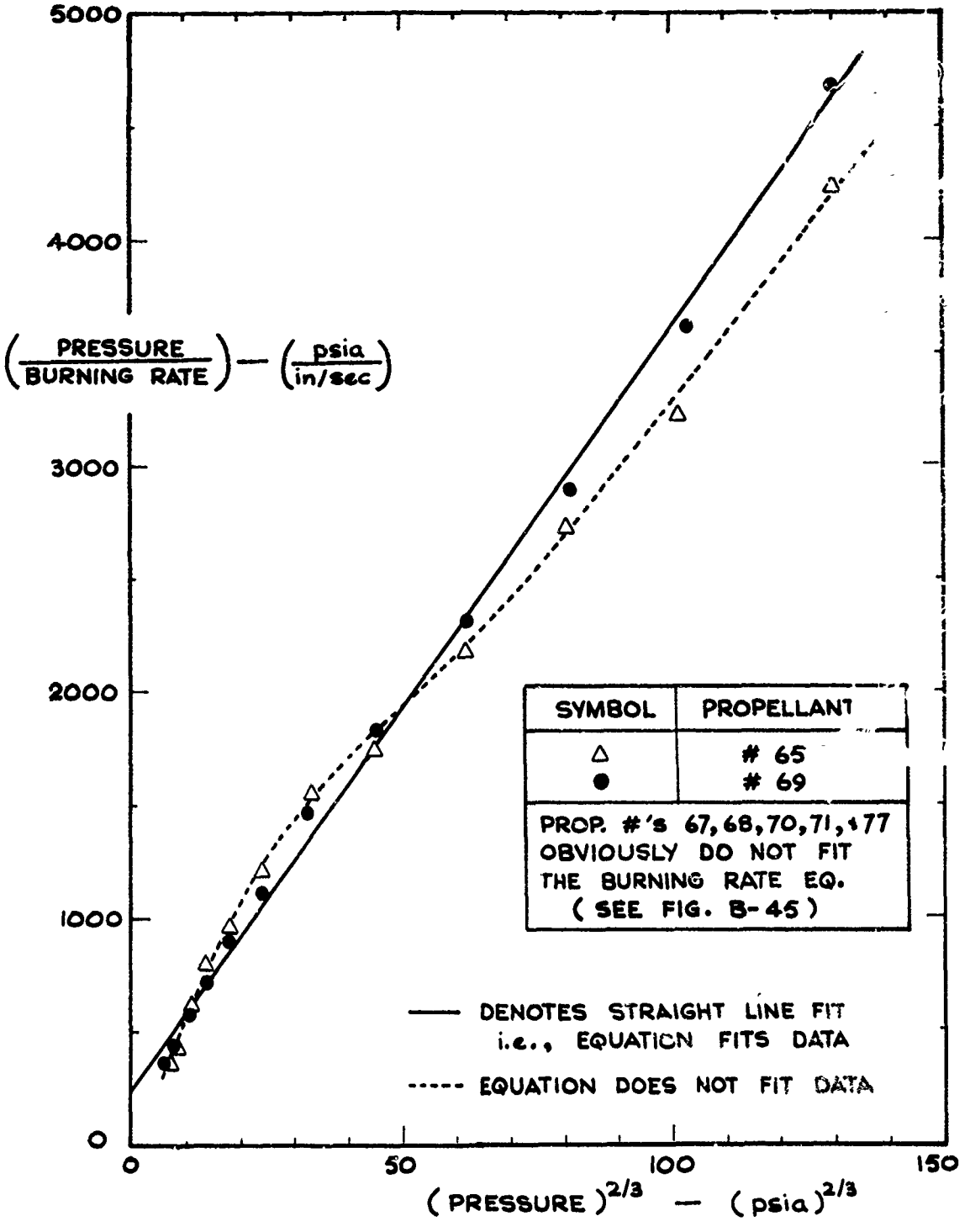

FIGURE B-47 DATA OF PROPELLANT NO.'S 65, 67-71, +77

CORRELATED WITH : $(1/r) = (a/p) + (b/p^{1/3})$

(SEE FIG. B-51 FOR PROP. # 66)

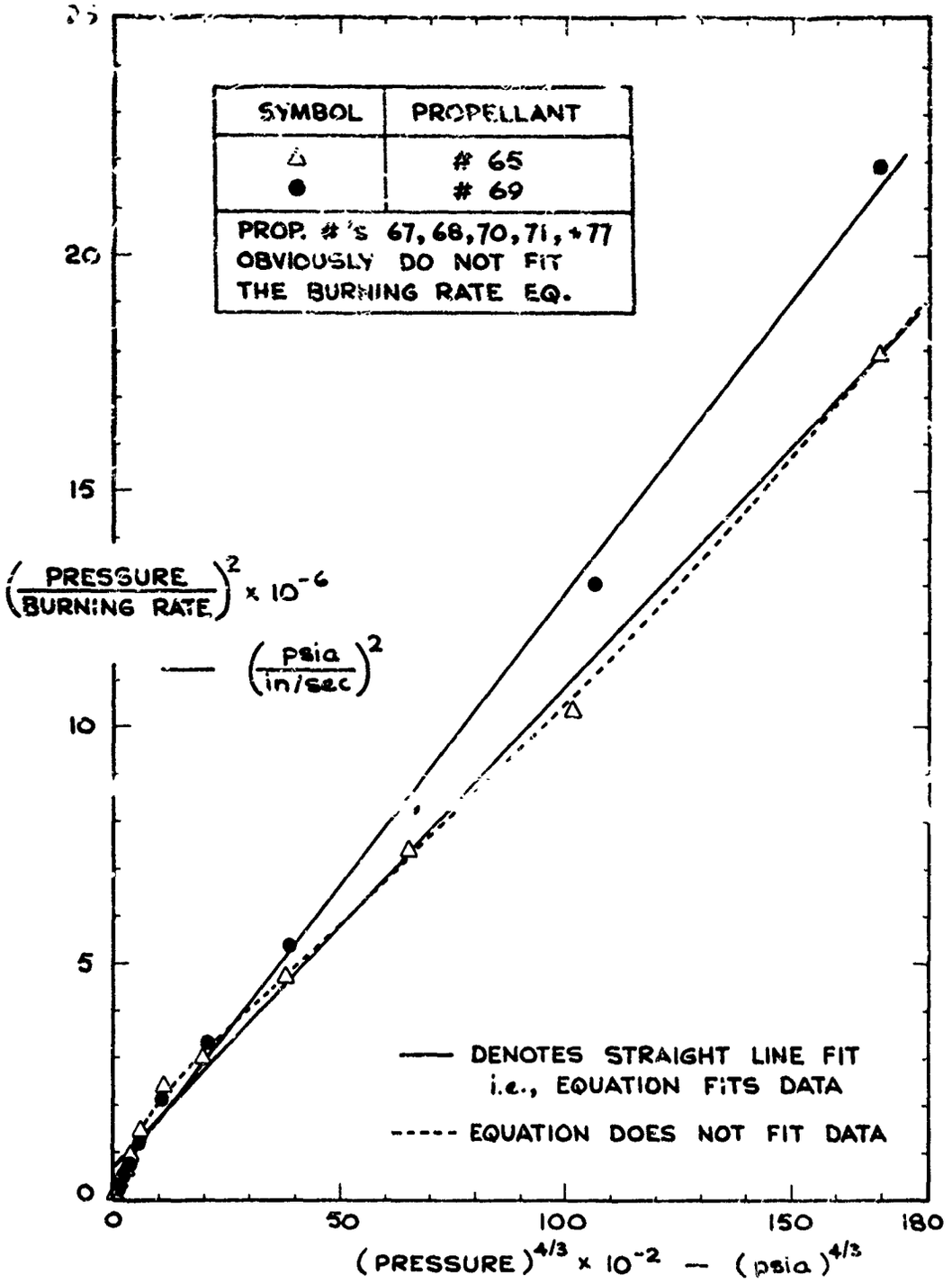

FIGURE B-48 DATA OF PROPELLANT NO.'S 65, 67-71, +77

CORRELATED WITH : $(1/r)^2 = (a/p)^2 + (b/p^{1/3})^2$

(SEE FIG. B-52 FOR PROP. # 66)

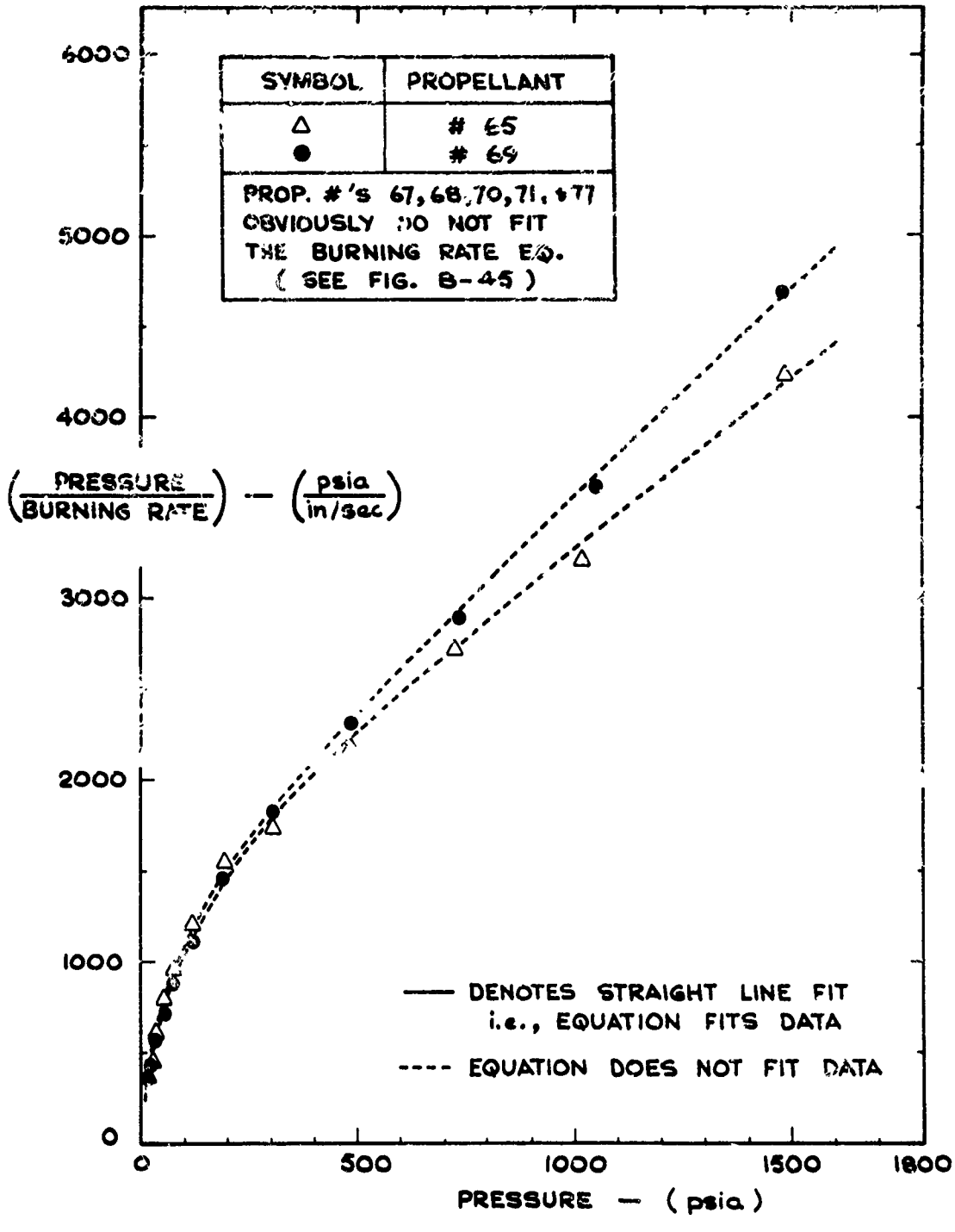

FIGURE B-49 DATA OF PROPELLANT NO.'S 65, 67-71, & 77

CORRELATED WITH : $(1/r) = (a/p) + (c)$

(SEE FIG. B-53 FOR PROP. # 66)

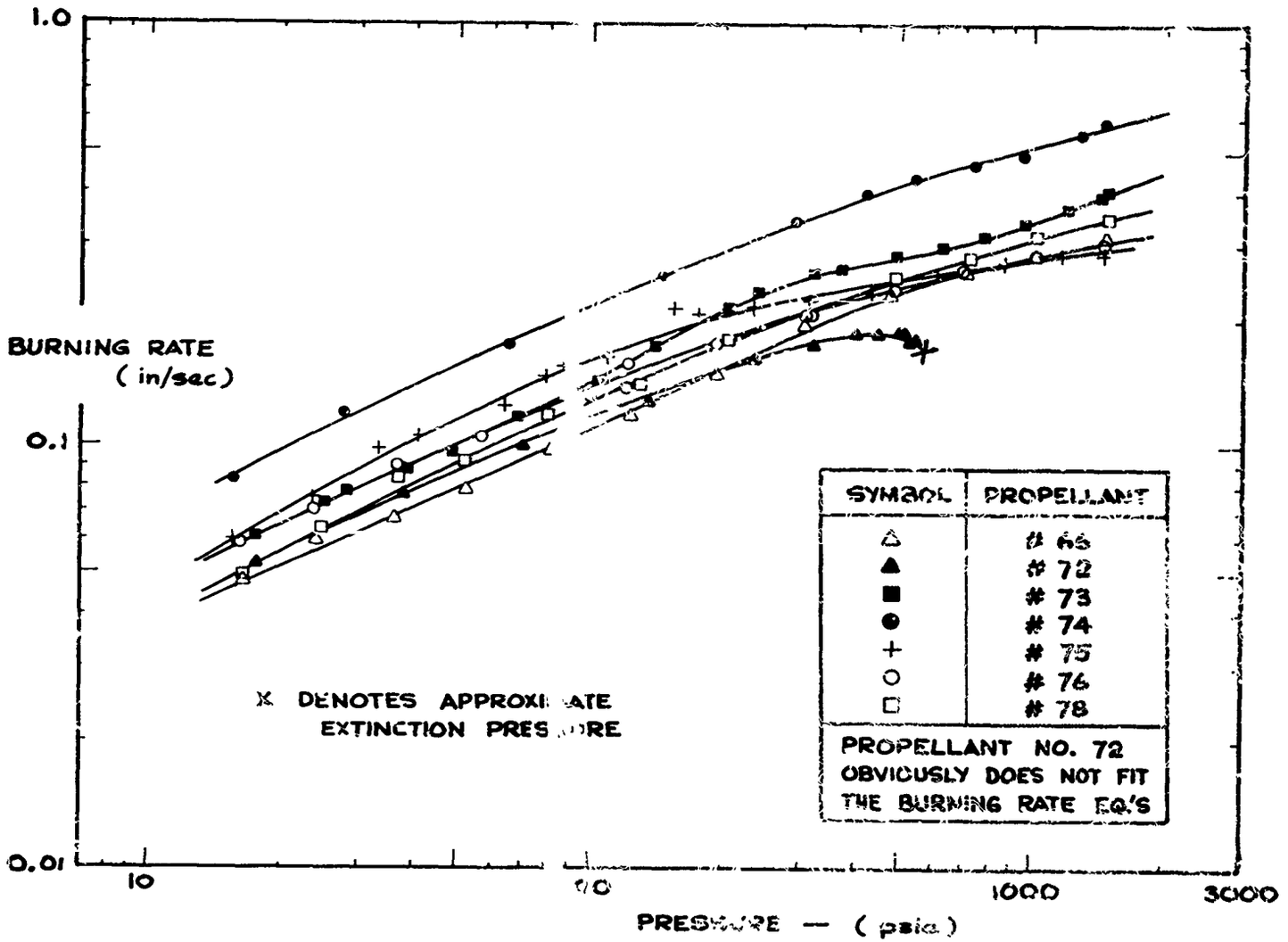

FIGURE B-50 DATA OF PROPELLANT NO.'S 66, 72-76, + 78 IN TABLE III

PLOTTED AS (log r) VS. (log p)

(SEE FIG B-46 FOR PROP. # 71)

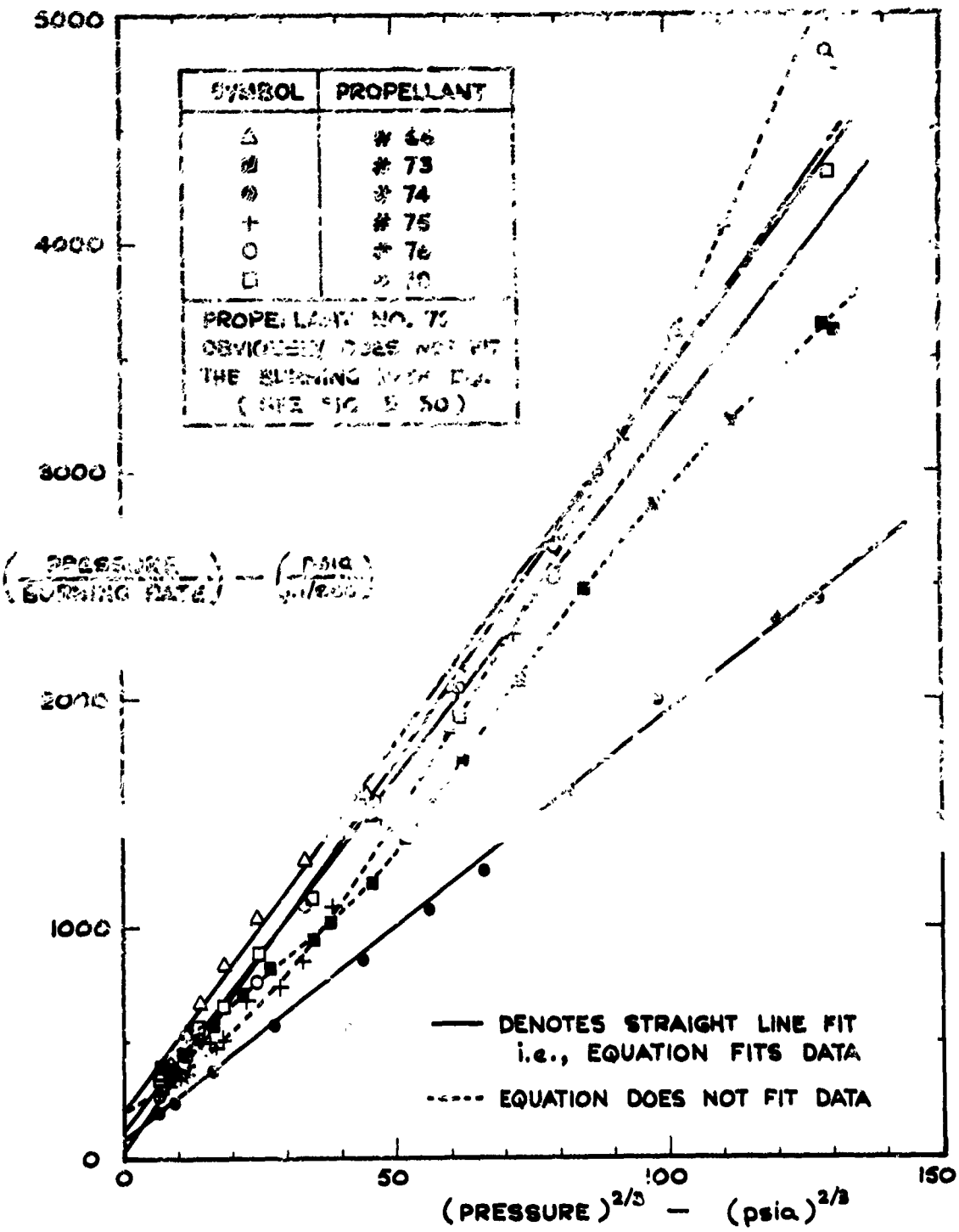

FIGURE B-51 DATA OF PROPELLANT NO.'S 66, 72-76, + 78

CORRELATED WITH : $(1/r) = (a/p) + (b/p^{1/3})$

(SEE FIG. B-47 FOR PROP. # 77)

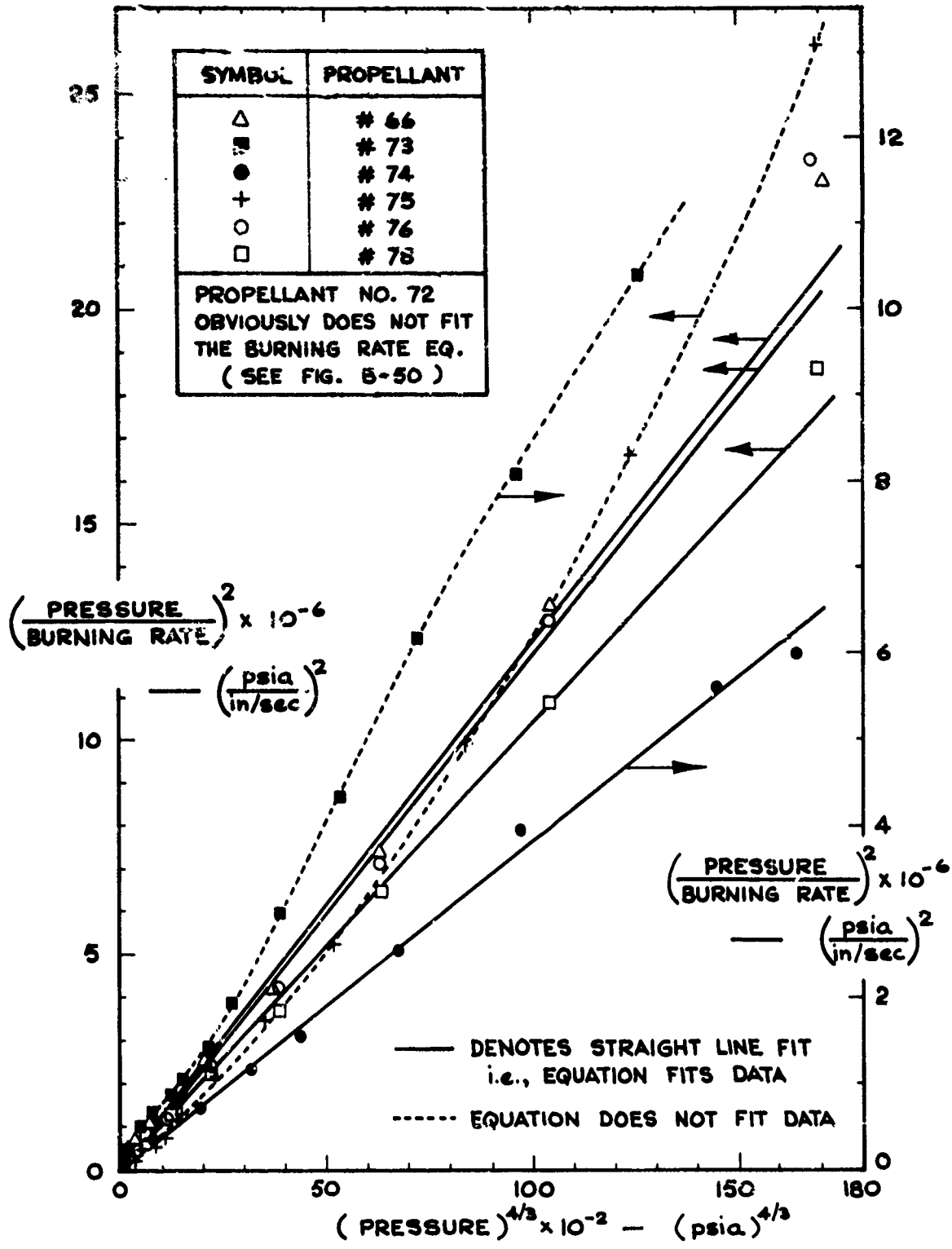

FIGURE B-52 DATA OF PROPELLANT NO.'S 66, 72-76, + 78

CORRELATED WITH : $(1/r)^2 = (a/p)^2 + (b/p^{1/3})^2$

(SEE FIG. B-48 FOR PROP. # 77)

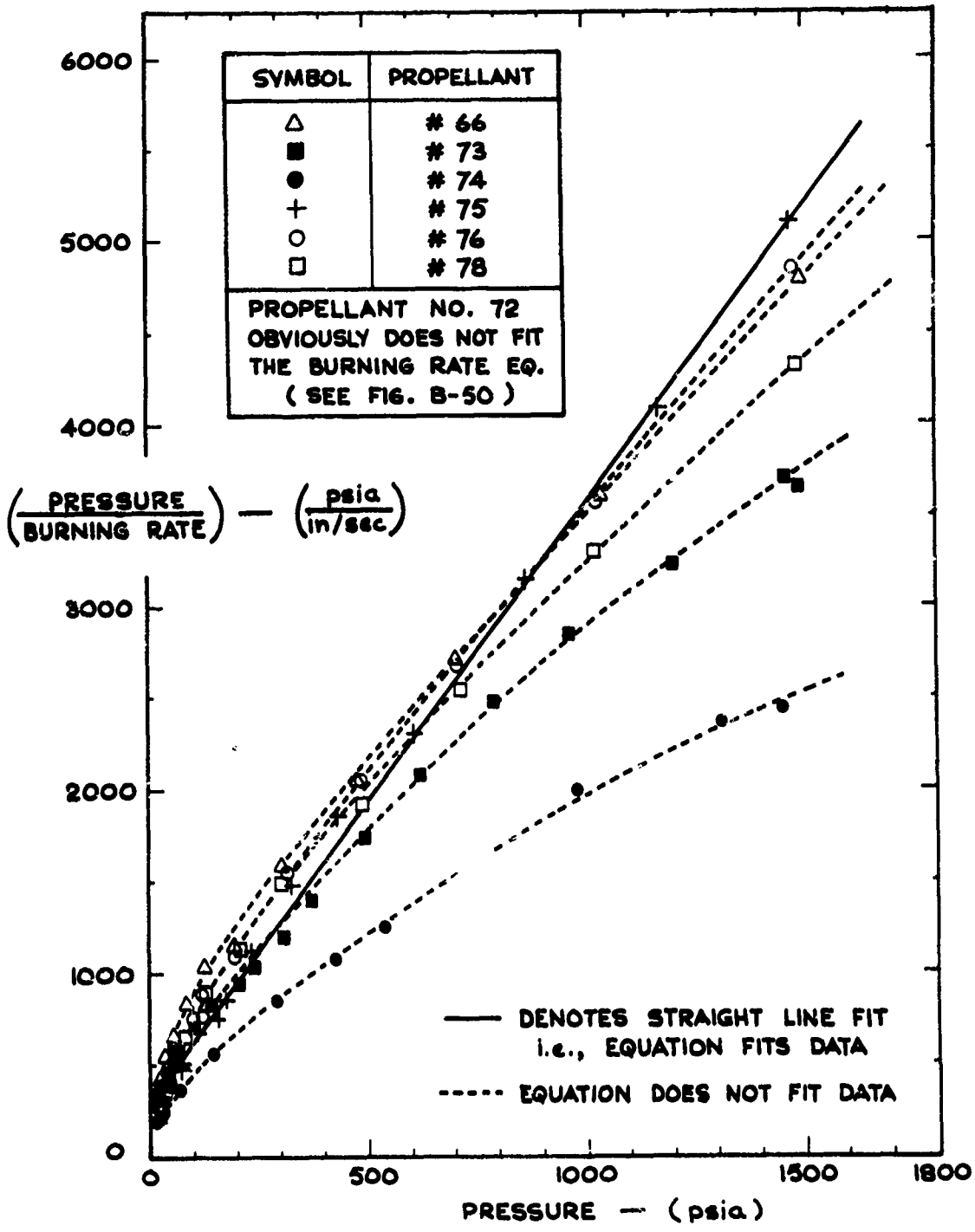

FIGURE B-53 DATA OF PROPELLANT NO.'S 66, 72-76, +78

CORRELATED WITH : $(1/r) = (a/p) + (c)$

(SEE FIG. B-49 FOR PROP. # 77)

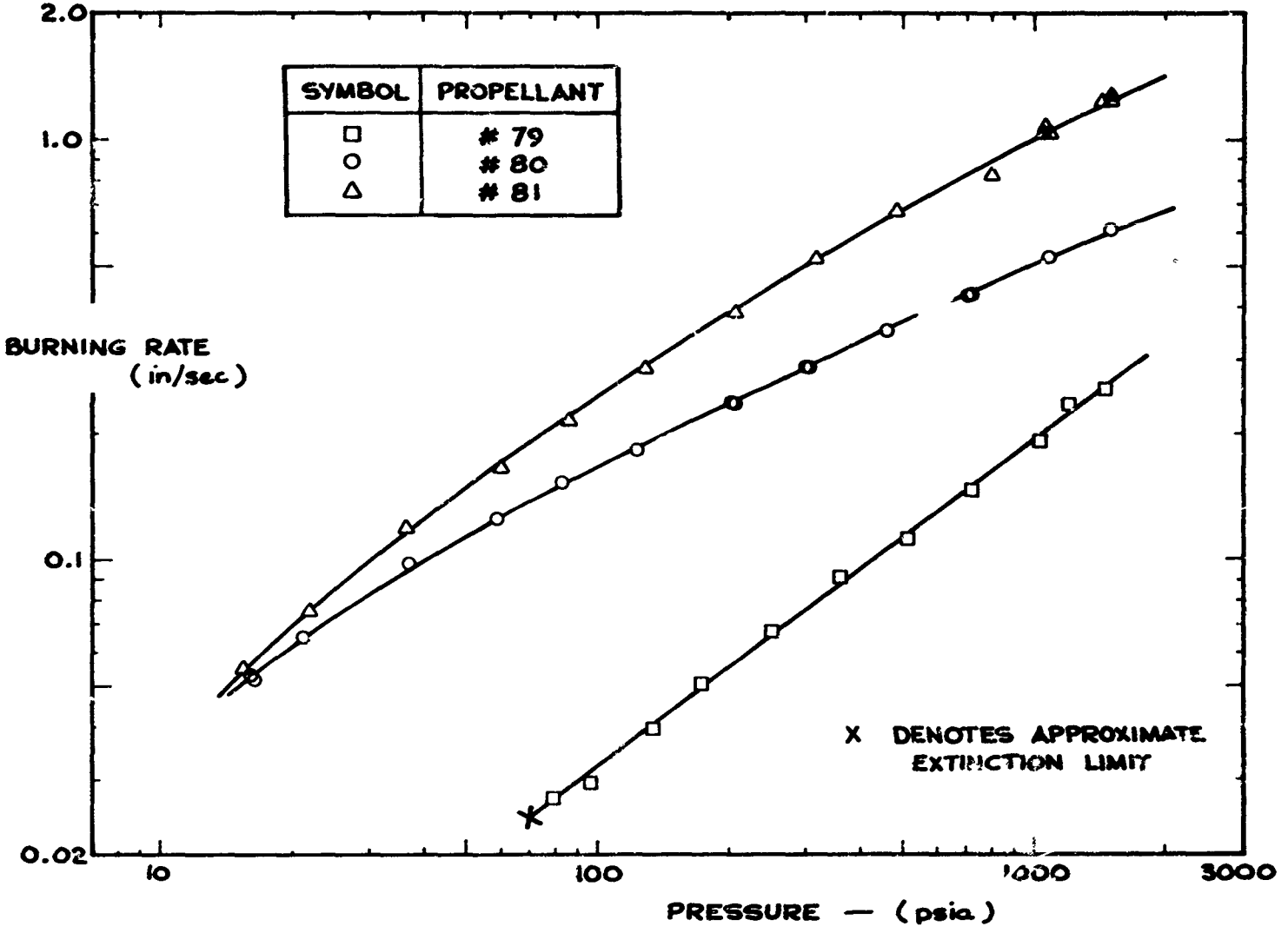

FIGURE B-54 DATA OF PROPELLANT NO.'S 79-81 IN TABLE III PLOTTED AS (log r) VS. (log p)

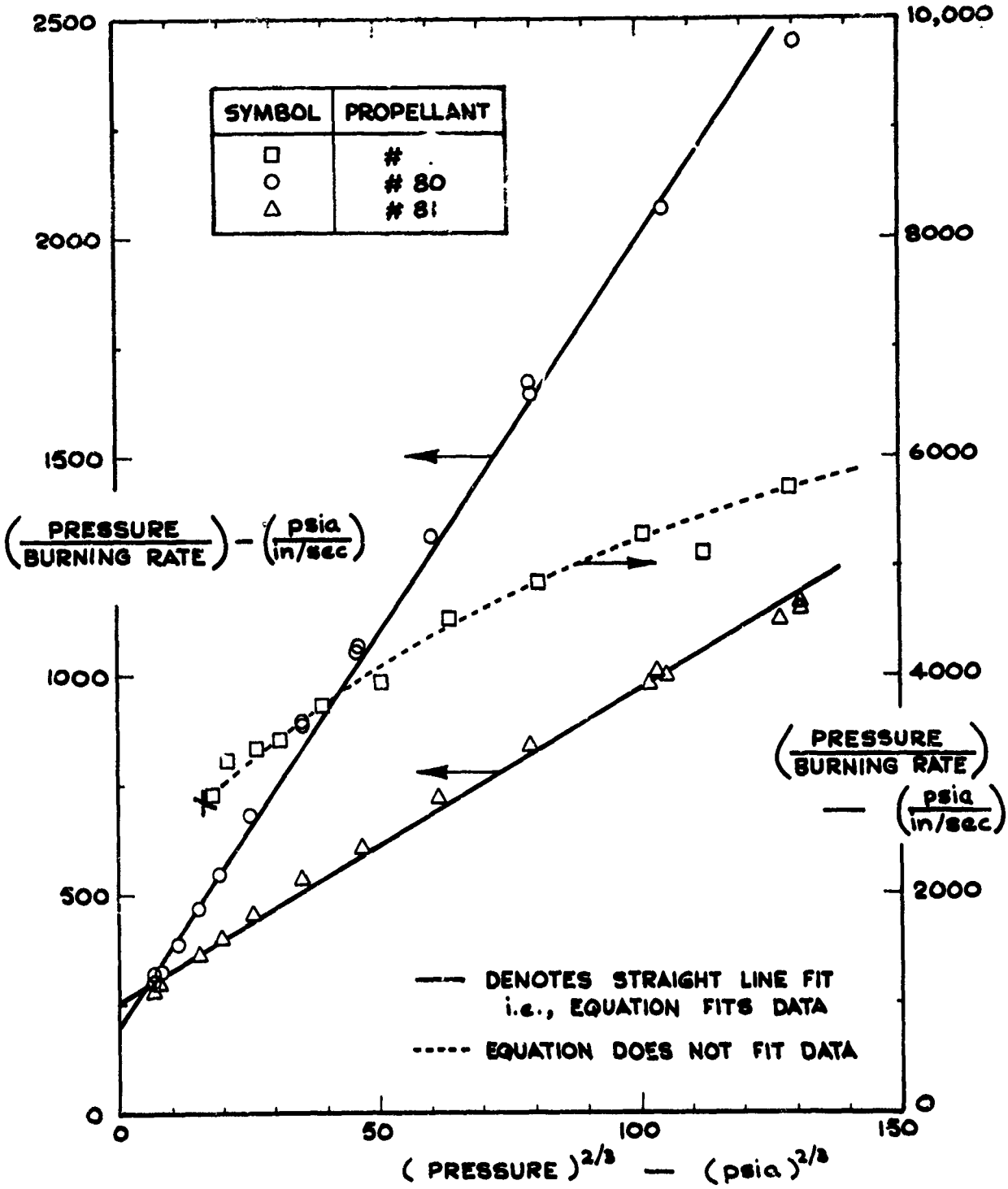

FIGURE B-55 DATA OF PROPELLANT NO.'S 79-81

CORRELATED WITH : $(1/r) = (a/p) + (b/p^{1/3})$

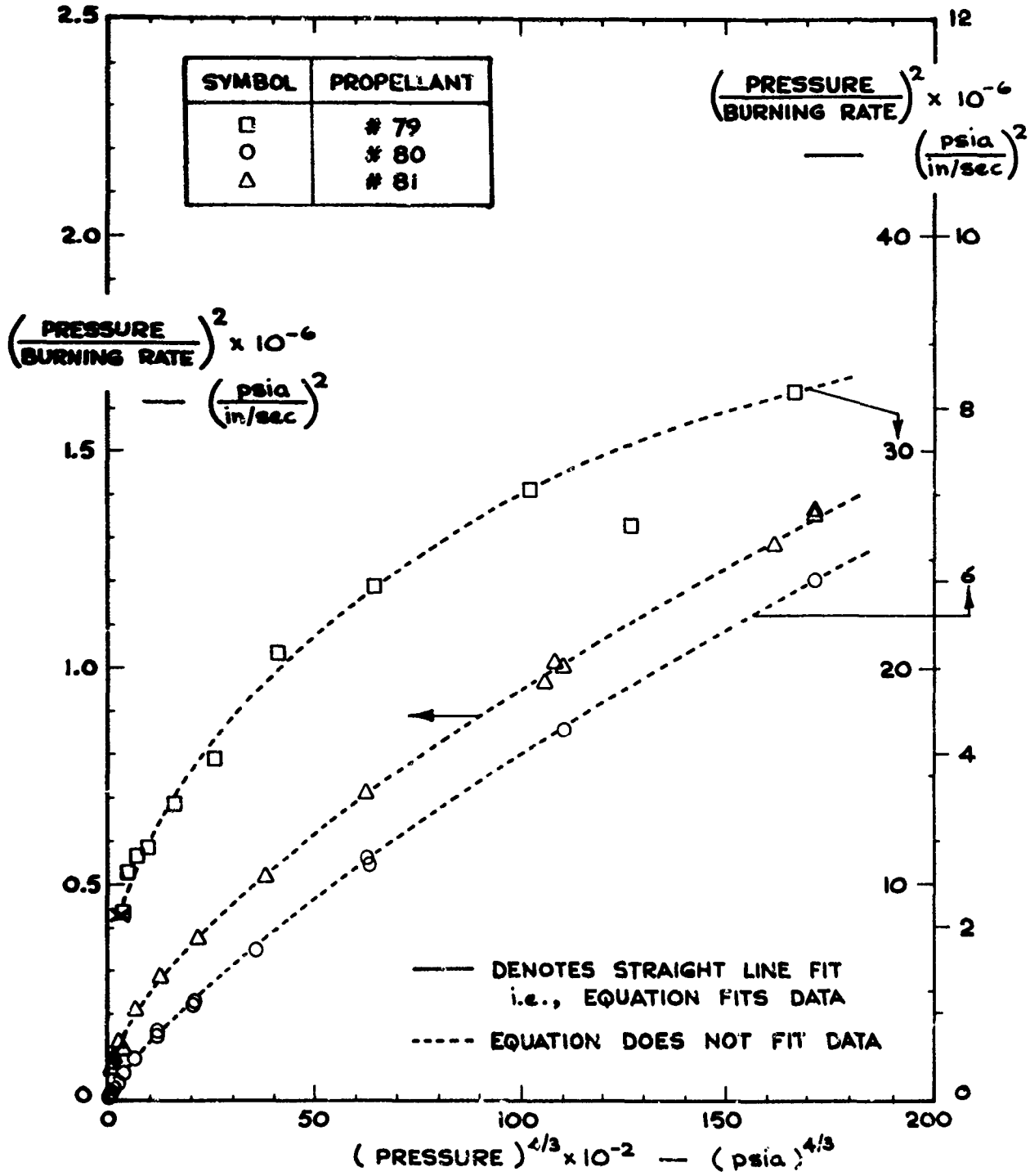

FIGURE B-56 DATA OF PROPELLANT NO.'S 79-81

CORRELATED WITH : $(1/r)^2 = (a/p)^2 + (b/p^{1/3})^2$

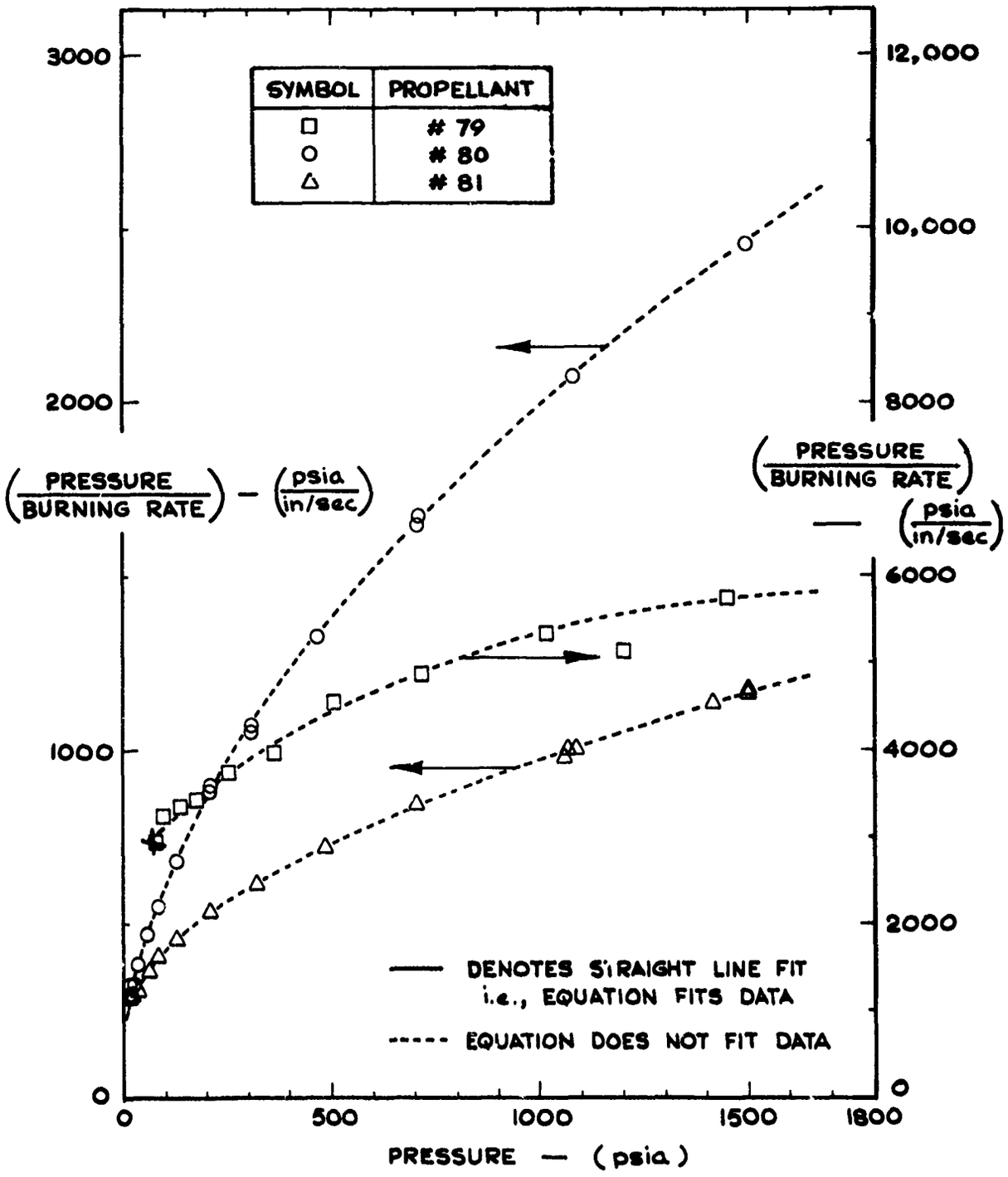

FIGURE B-57 DATA OF PROPELLANT NO.'S 79-81

CORRELATED WITH : $(1/r) = (a/p) + (c)$

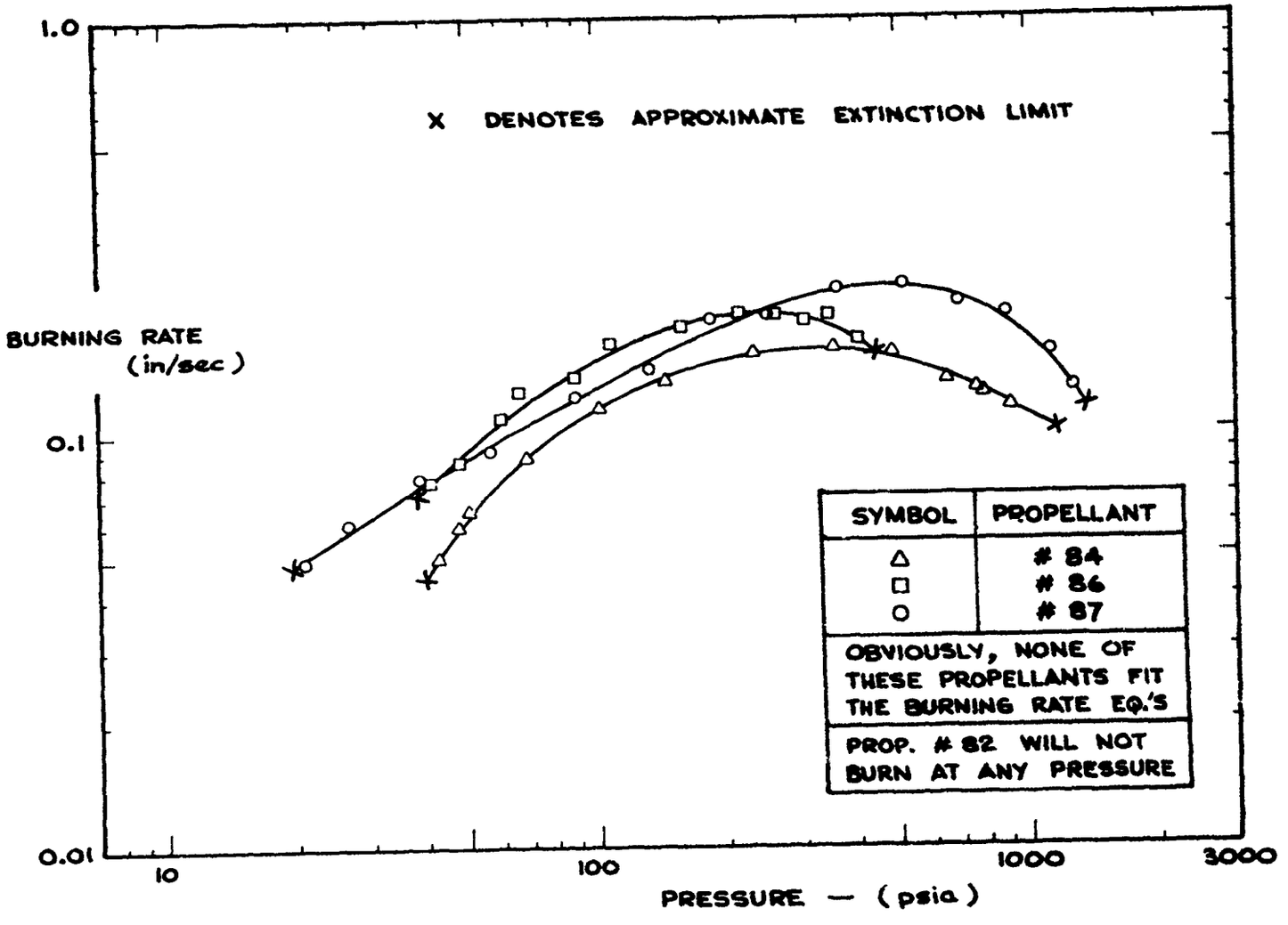

FIGURE B-58 DATA OF PROPELLANT NO.'S 82, 84, 86, + 87 IN TABLE III PLOTTED AS (log r) VS. (log p)

(SEE FIG. B-59 FOR PROP. #'s 83, 85, + 88)

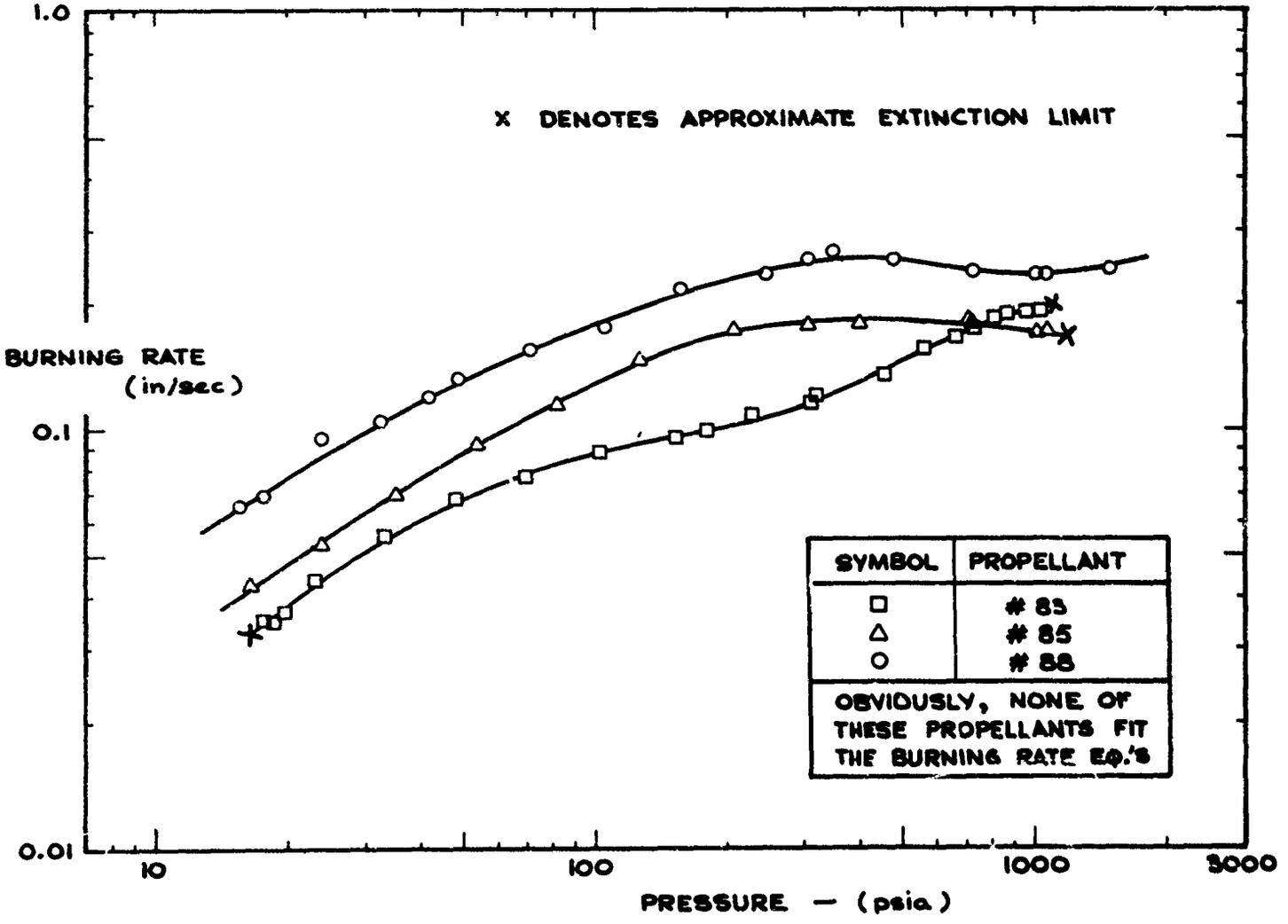

FIGURE B-59 DATA OF PROPELLANT NO.'S 83, 85, + 88 IN TABLE III PLOTTED AS (log r) VS. (log p)

(SEE FIG. B-58 FOR PROP. #'s 84, 86, + 87)

APPENDIX C

EXPERIMENTAL PROCEDURES AND ACCURACY OF MEASUREMENTS

The following sections describe the propellant manufacturing process, the propellant quality control methods used, and the techniques followed to measure the steady-state burning rate. Any improvement that has been made in a particular measurement or manufacturing technique during the course of this investigation is noted*. Wherever possible, the accuracy of a particular measurement technique is indicated.

(i) Propellant Manufacturing Process

Whenever possible, standard, as-received, "spherical" ammonium perchlorate obtained from American Potash Company was used. In cases where the required mean particle size was not available or where narrower size distributions were desired, standard non-spherical ammonium perchlorate (American Potash type AMS-C66F) was sieved and/or ground in a Bantam type SH Mikro-Pulverizer (hammer mill). All the oxidizer used in this program was dried before use for a period of at least 24 hours at 235°F.

In making a non-energetic fuel + AP composite propellant, the fuel pre-polymer and its curing agent are first thoroughly mixed into a thick paste and then placed into a 1500 gm capacity ARC (type 60 LP) propellant mixer‡, the walls of which were kept at a constant temperature of 135°F. The residue left

---

*If, in retrospect, it appeared that the improvement of a particular measurement did not make any difference, that is, the final interpretations as to the combustion mechanism do not change because the particular technique of measurement had been altered, the previous results were not repeated. Thus, not all propellants of this study have been made following the exact same techniques. In the interest of still preserving the information concerned with each batch of propellant, Appendix D is created: it summarizes the method of manufacture and the properties (oxidizer particle size distribution, finished propellant density, composition, etc.) of each propellant-type made.

‡During the early portion of this investigation, a 350 gm capacity ARC (type 35LP) Z-blade mixer was used. It has bearings that are submerged below the level of the uncured propellant in the mixer (as opposed to the 60 LP mixer now being used). This caused the finished propellant density to deviate from the theoretical by about 0.2% because, as noted in Section (ii) below, the liquid fuel seeps preferentially into these bearings. The implied 0.2% propellant composition error (excess AP) is acceptable for the purposes of this investigation. The propellants that have been made using this (submerged bearing) mixer, are indicated in Table VI of Appendix D.

in the beaker is weighed to the nearest 0.01 gm and noted. A previously weighed quantity of the desired AP is then slowly added while mixing under remote control. Once the AP has been thoroughly wetted (after 2 to 3 minutes mixing), vacuum is drawn (see Appendix D for exact pressure during mixing for each binder-type) and mixing is continued for another 30 minutes. Whenever possible, casting was done under vacuum as well (see Appendix D). In the cases of 5u and 15u mean particle size propellants which were very viscous, hand packing was sometimes necessary to prevent the inclusion of voids (also noted in Appendix D). After casting (or hand packing) the propellant was cured at 176°F for 48 hours. In the case of large particle size LP3 propellants for which the uncured mixture is very fluid, rotation of the mix while curing (at about 5 rpm), was found to minimize settling of the AP particles.

The DB and CMDB propellants of this study were made entirely under remote control. The main features of the mixing apparatus are that the mixer-rotor is driven pneumatically and that the propellant ingredients are entered into the mixing bowl by the opening of remote controlled, pneumatically-actuated valves. Also, casting is done under remote control by opening another pneumatically actuated valve at the bottom of the mixing bowl. This allows the propellant mix to be drawn, by vacuum, through a casting slit into the casting mould.

The manufacture of this class of propellants is largely a matter of skill. Such skill resides in the fact that the starting liquid must be thickened beforehand (by gelling at high temperature with a small amount of NC) to accomodate all the solids that are to be added to the propellant; if the mix is too viscous, the propellant will have many voids due to insufficient wetting of the solids (NC and AP)by the fluid (TEGDN); if the mix is too thin, the solids will settle to the bottom of the propellant block during the process of curing. The required amount of NC is determined by experience but generally it falls between 2% and 4% of the weight of TEGDN to be thickened.

The steps followed in making CMDB or DB propellant are:

(1) Weigh out the required quantities of NC, TEGDN, and AP.

(2) Place the TEGDN into the mixing bowl and place also the AP and NC into their respective storage hoppers.

(3) Enter the small quantity of NC needed for pregelling into the mixing bowl (with the TEGDN).

(4) Commence the mixing cycle and run hot water (150°F) through the jacket of the mixing bowl.

(5) After 10 min., run cool water at room temperature through the jacket and stop the mixer.

(6) Add the NC powder in three equal increments, mixing for 1 min. after each increment.

(7) Add the AP powder in three equal increments, mixing for 2 min. after each increment.

(8) Continue mixing for 30 minutes.

(9) Stop the mixer rotor and run the propellant mix into the casting bowl.

(10) Cure the propellant at 110°F for 24 hours.

(ii) Propellant Quality Control Tests

Propellant hardness and density tests were performed as a matter of routine. Uncured propellant viscosity tests were instituted but found to be a liability; so, these tests were later discontinued. The measurement of finished propellant density was found to be particularly valuable because it has the potential of detecting oxidizer particle settling during curing, the presence of voids as well as possible composition imperfections. These measurements are described in greater detail below.

(a) Propellant Hardness and Uncured Viscosity

The hardness of the cured propellant was measured with a Rex hardness gauge and the uncured viscosity with a Brookfield Synchro-Lectric Model RVT Viscosimeter. These hardness and viscosity measurements do not appear to be critically dependent on propellant imperfections. In fact, no propellant batches have been rejected on these grounds. Due to the fact that the propellant mix cools while taking the viscosity, making casting difficult, this measurement was discontinued. Hardness tests were, however, conducted for every batch of propellant made; testing of this property allowed for the easy recognition of gross propellant imperfections.

(b) Finished Propellant Density.

Owing to its potential of being able to detect void content, oxidizer particle settling and also possible composition errors, considerable effort has gone into perfecting the density measurement technique. As a result of these efforts more refined propellant manufacturing methods have been instituted.

The method of density measurement used, is based on Archimedes' principle where the volume of the propellant sample is determined by the loss of weight of the propellant when immersed in a fluid; the mass of the sample is measured directly.

Densities were measured at the top, middle, and bottom of each propellant block made. Thus, by comparison with the theoretical density, the presence of voids, and the occurence oxidizer particle settling and/or defective propellant composition can be inferred from such measurements of propellant density. The theoretical density is calculated on the basis of additive volumes of the fuel and oxidizer. For the purpose of these calculations, the density of the pure fuel, prepared under the same conditions as the propellant, was similarly determined. (Table IV of Appendix B gives the values of the fuel-binder densities so determined.) The published value of 1.952 gm/cc was used for the density of AP(204).

Isopropyl alcohol was chosen as the displacement fluid for all propellants other than those using LP3/GMF or NC/TEGDN fuels. It has a low density (for higher accuracy), low surface tension (no bubbles adhere to the surface of the sample) and repeated measurements varying the immersion time (see Fig. E-1) have shown that, as long as the immersion time is less than 30 sec, the error in density measurement caused by dissolving of the AP and swelling of the fuel, is only 0.02%. Owing to the fact that isopropyl alcohol dissolves polysulfide (LP3/GMF), heptane was chosen as the most suitable displacement fluid for propellants of this fuel-type. (As shown by Fig. E-1, heptane is inferior to isopropyl alcohol as a displacement fluid for PBAA propellant.) In the case of NC/TEGDN-AP, a silicone oil (type SF 96(100) made by General Electric) was used.

The possibility that the fluid might penetrate into the propellant, filling any voids which might be present and therefore render density determinations useless as a measure of void content, was checked. This was done by direct observation of cross-sections of pure fuel and propellant samples which had been immersed in isopropyl alcohol colored with nigrosin black, a biological stain. For immersion times less than 30 minutes, no penetration could be detected, and for 24 hours, the depth of penetration was 0.03" for both propellant and pure fuel samples. This shows that there are no hairline cracks in the propellant and that during an actual density determination, the fluid is only absorbed in the surface layers of the propellant sample.

It was necessary also, to determine the accuracy of the density measurements. A detailed error analysis (Appendix E) has shown that the random error is $\pm$ 0.2% and that the systematic error is -0.04%.

To determine whether densities very close to theoretical could indeed be obtained with the manufacturing methods in use at the time, several batches of 25% PBAA/EPON + 75% 80u AP propellant* were made. The propellant, then made with the 35 LP mixer (has submerged bearings), often had densities which, on the average, were 0.2% above the theoretical. It was observed

that after processing, the submerged bearings of this mixer were filled with a liquid that appeared to be the fuel constituent of the propellant mix; very little of the solid AP particles was mixed in with this liquid. Consequently, the mixer was replaced with the ARC 60LP model which has no submerged bearings. The first two batches of the above propellant after replacement of the mixer, then had densities, measured at seven different points in the propellant block, of 100.04 $\pm$ 0.15% and 100.02 $\pm$ 0.05% of the theoretical. The reproducibility with repeated measurements of the same sample was found to be within $\pm$ 0.05%.

Another source of loss of fuel during the manufacturing process, it was expected, is the drawing of some volatile components into the vacuum system. (AP is not volatile by comparison.) Careful measurements show that roughly 0.6% of the weight of fuel is lost during the mixing cycle. This results in a density measurement error of about 0.12%. This error is systematic from batch to batch and can therefore be accounted for, to an approximation.

It is extremely difficult to make propellants of all formulations that have no voids or errors in composition; the very nature of this project often demands propellants that are difficult to process and that would not be ordinarily used in practice. Thus, reasonable tolerance limits as dictated by considerations of obtaining the best possible propellant without having to sustain an inordinately high rate of failures, must be set. Generally, propellants with a uniform density throughout the block (within 0.4%) and with an average density that falls between 99.0% and 100.4% of the theoretical, were considered acceptable for the program. These limits imply a maximum void content of 1.0% and a maximum error in composition of $\pm$ 0.5%*. In some exceptional circumstances, it was necessary to widen these limits even further. Such cases are listed in Appendix D.

As a final remark, it is noted that any deviation from the theoretical can not be attributed exclusively to any one cause. Thus, the routine measurement of density does not guarantee propellant of the high quality desired (see footnote below concerning possible errors in composition). However, this method of quality control does eliminate the possibility of unknowingly accepting grossly inferior propellant.

(iii) Oxidizer Particle Size Measurements.

The mean particle size of all AP used in this study was measured using the sedimentation technique. As a check on the accuracy of this method, three particle size distributions

*This particular propellant was chosen because the manufacturing problems are few and so, the chances of obtaining a propellant with no void content and no AP particle settling are highest with this formulation.

were also determined by direct measurement through a microscope. The values for the particle size so determined, were then compared with those quoted by the manufacturer, also determined by the microscopic method. In general, the mean particle sizes agree. However, the shapes of the distribution curves do not correspond exactly.

(a) Sedimentation Technique

The method as initially developed by Bastress(14,205) using a M-S-A particle size analyser obtained from Mines Safety Appliances, is followed closely. Here, the time taken for a particle to fall a set height through a liquid of known viscosity is a measure of its equivalent diameter. To keep the total sedimentation time within practical limits, centrifugal force and a low viscosity fluid was used for distributions with mean particle sizes less than about 50μ.

For the larger size distributions (above about 50μ), a dispersion was made by adding about 1 gm AP to 100 ml. benzene containing four drops Twitchell base 8240 (Emery Industries) wetting agent. This was followed by vigorous agitation using a counter-rotating mixer for two to ten minutes, depending on the approximate mean particle size; 10 minutes was found sufficient for 50μ but mixing beyond two to three minutes for 200μ and above, was found to cause severe distortion of the distribution curve at the lower particle size end (presumably due to breaking of the crystals by the blades of the mixer). A sedimentation tube which narrows down to 1 mm bore at the bottom is filled with ethyl phthalate. About 1 ml of the dispersion, benzene + AP particles, is placed on the sedimentation fluid, ethyl phthalate. The height of the column of

---

A density of 100.4% of theoretical implies that the composition is in error by about 0.5%. A variation of 0.4% density through the propellant block also implies a composition error of 0.5%. A density of 99.0% of theoretical, however, implies a considerably larger compositional error, at least as long as there are no voids present in the propellant. As a general observation, it is to be noted that whenever the density falls below 99.5% of theoretical, pinhole-voids become evident. Thus, the general guide was followed that if the density is as low as 99.5% of theoretical and there are no voids, then the propellant should be discarded; also, if there are obviously voids and the density is close to, or above 100.0% of theoretical, the propellant should be discarded. In this way, the possibility of accepting propellant with composition error much in excess of ±0.5% is minimized.

In actual fact, unless particle settling occurs or some mistake has been made in weighing out the propellant ingredients, the error in composition is much smaller than the ±0.5% indicated above. The error is then mainly due to loss of fuel into the vacuum system during mixing and is then 0.12%. This error can be eliminated by making direct measurements of this loss of fuel.

particles accumulated in the capillary at the bottom of the tube is then recorded as a function of time until all the particles have settled. Sedimentation time is converted to equivalent diameter and the distribution is plotted as column height verses particle diameter (see Fig. C-1 for example).

The method used for particle sizes less than 50μ differs from that described above, in that dibutyl-n-sebacate with wetting agent (4 drops Twitchell per 100 ml) is used as the dispersion fluid, that mixing time is set at 10-15 minutes, and that chlorobenzene is used as the sedimentation fluid. Also, to decrease the total settling time, the tube is placed in a centrifuge supplied with the M-S-A analyser equipment.

Typical distributions obtained with this method are shown in Figure C-1. On probability vs. log scales the curves tend to be linear. As a check on the accuracy of the method, the same distributions were measured using the microscopic technique described below.

(b) Microscopic Technique.

Three particle size distributions quoted by the manufacturer as 4.7, 12.5, and 44.5μ mean size (based on equivalent volume) were measured using the microscopic technique. (Same distributions as measured by sedimentation technique above.) Agglomerates occurring in the two smaller particle size distributions were broken up by forming a dispersion of about 0.5 gm of the powder in benzene containing 1 drop of wetting agent (Twitchell) per 100 ml. After five minutes of vigorous agitation, a few drops of the dispersion were placed on a glass slide and the liquid allowed to evaporate. It was sufficient to merely spread the 45μ mean particle size powder on the slide. These particles were then individually measured against calibrated graticules in the eye pieces of a 75-250 power microscope. As recommended in Ref. 206, the dimension of each particle was taken in one direction only. Because the particles are randomly oriented on the glass slide, an accurate value for the average diameter is obtained only if a sufficiently large number of the particles are measured; in this study, the number of AP particles actually measured in each case, was that number for which the finally plotted distribution curve does not change if more AP particles are measured. The possibility that most particles may lie flat on the glass slide and thereby distort the measurement, is of course not accounted for when measuring particle size distributions this way. The number of particles of each diameter were counted and the equivalent diameter calculated. The distribution was then plotted as the fraction of AP particles (by weight) with a size less than the diameter indicated on the abscissa.

The results obtained for the three distributions measured are shown in Figure C-2. It is seen that with probability versus log scales the distribution follows a straight line in all cases. It was found that to obtain such a regular plot, at

least 1500 particles had to be measured in the cases of the 5 and 15.5μ mean particle size powders. However, 500 was sufficient for the 45μ mean particle size sample.

(c) Accuracy of the Sedimentation Technique.

A great many sets of measurements (see Figure D-1 and D-2) have shown the sedimentation method to be reproducible to within about ± 10% over the entire 5μ to 200μ AP particle size range investigated. Table V (at the end of this Appendix) shows the values of mean particle diameters found by both the microscopic and sedimentation methods in this study. The same table shows the values obtained by the manufacturer(207), also using the microscopic method. It is seen that for a mean particle size of 12μ and above, all measured values of mean particle size fall within 10% of each other. Below 10μ, the accuracy of the sedimentation technique drops drastically -- possibly agglomerates are not broken up sufficiently when making up a dispersion of such small particles. Further work is necessary to resolve this point. For our purposes, however, the sedimentation technique is sufficiently accurate.

(iv) Burning Rate Measurements

In this investigation, burning rates were measured in two pressure ranges, the subatmospheric pressure range and the 1-100 atm range. The apparatus used and experimental procedure followed for each of these pressure ranges, is described separately below. These sections are then followed by a section that deals with the accuracy of the burning rate determinations.

(a) Burning Rates at Subatmospheric Pressures

(1) Apparatus

An overall view of the apparatus used for subatmospheric pressure burning rate measurements is shown in Figure C-3. It consists of a bell jar serving as the test chamber which is connected to a vacuum pump through a large surge tank below the bench. The panel on the left houses a mercury manometer, pressure regulator, pressure gauges, nitrogen flow controls, and various electrical controls. Figure C-4 shows a closer view of the optical set-up used for burning rate measurements. The propellant strand is mounted vertically about 2 inches behind the window of the bell-jar. The system of beamsplitters and lenses is aligned in such a way that the 35 mm camera simultaneously records the propellant strand, steel rule, stopwatch and bourdon vacuum gauge situated on the control panel in Figure C-2. Figure C-5 shows two typical sequences of records obtained during actual tests. The first was taken through an oil film (silicone diffusion pump fluid) running past the window. This was necessary at pressures below 0.05 atm to avoid coating of the bell-jar window by large amounts of white fumes which are evolved whenever ash is formed with

LP3/GMF-AP propellant (see Section VB). The second sequence was obtained at higher pressure where no oil film was needed.

(2) Experimental Procedure and Data Reduction.

A finished propellant block was cut into strands 0.25 inch square and approximately 6 inches long. All strands were inhibited by leaching in water for 10-15 seconds and thin nichrome ignition wires threaded through the ends of each of these.

To measure the burning rate of a specific strand, the strand was mounted vertically in the bell-jar and the ends of the ignition wire wound around the appropriate terminals. The bell jar was then thoroughly purged with nitrogen for 3-5 minutes and evacuated to the desired pressure. After adjusting the camera speed such that at least 10 photographs will be taken during the course of a test, both firing and camera release buttons were depressed. The camera was turned off as soon as the flame passed out of the field of view of the camera. The pressure during the test was read from a mercury manometer (relative to atmospheric pressure which was measured by a barometer), a U-tube mercury manometer, or Mcloed gauge, depending upon the pressure in the bell jar: the U-tube manometer (graduated in millimeters) was used below 20 cm Hg abs and the Mcloed gauge (smallest pressure for which graduation exists, is 0.02 mm Hg abs) was used below 15 mm Hg abs.

The photographs obtained during the test were projected onto a screen so that the time and position of the regressing surface relative to the scale could be noted; in cases where a ripple in the oil film caused the image to be out of focus, the photograph was disregarded. Since the scale was calibrated, the actual position of the burning surface could be plotted as a function of time. The burning rate was then taken as the slope of the best straight line drawn through these points. A typical burning rate versus pressure plot is shown in Figure C-6. This figure is for the 35% LP3/GMF + 65% 5μ AP propellant that leaves an ash as a combustion product below about 0.05 atm (discussed in Section VB). It is seen that the scatter is somewhat larger in the range of pressure where ash is found. This is due to the fact that use of the oil film was necessary. To help in the judgment of drawing the pressure-dependence curves, burning rates were also calculated by taking the slope of a line determined by least mean squares. The bars in Figure C-6 indicate the 90% confidence limits on burning rates calculated in this way. It is seen that it is difficult to draw any other pressure dependence curve if the spread in error limits of all points are taken into account.

(b) Burning Rates in the Range 1-100 Atm.

(1) Apparatus

Burning rates were measured in a 0-2200 psig pressure vessel.

As shown in the exploded view of Figure C-7, the pressure vessel consists of a long 1-5/8 inch internal diameter stainless steel tube. Nitrogen and combustion products escape to the atmosphere via a choked orifice at the upper end of the tube and enters through a long coil immersed in water at room temperature. With the present set-up, the nitrogen temperature remained at $23.5 \pm 1.5^{o}C$ throughout the test series reported here. This temperature is measured by a calibrated chromel-alumel thermocouple placed below the strand in the bomb. The signal is amplified (by a Dana model 2200A DC amplifier) and measured by a digital voltmeter (Digitec model 201 manufactured by United Systems Corp.)

Figure C-8 shows the propellant strand in position between two electrical terminal posts. Ignition is accomplished by passing a current through a nichrome wire threaded through the top end of the strand. Burning rates are measured by determining the instant of melting of each of 7 low melting-point (98.5% Pb, 0.5 amp) fuse wires threaded through the strand at accurately known separation distances (0.50 inch). These 7 fuse wires, each in series with a resistor, form 7 parallel arms of an electrical circuit, the output voltage of which when driven by a battery, changes discontinuously as soon as a fuse wire melts.

Also shown in Figure C-8 are a Dynisco PT-76U-2M (0-2000 psi) strain-gauge pressure transducer and a thermocouple placed in the nitrogen flow close to the strand surface ($\sim 1/2$ mm) at the height of one of the fuse wires. The purpose of the former is to record any pressure oscillations that may exist in the combustion chamber. The purpose of the latter is to sense possible reverse flow of the hot combustion gases so that the possibility of preheating the strand, or of the flame flashing down the side of the strand, may be guarded against. The outputs of this thermocouple, the incoming nitrogen temperature thermocouple, the transient pressure transducer, and the fuse-wire circuit, are separately amplified (using respectively, Dana DC amplifier models 2200, 2200A, 3420, and 2200). These amplified signals are continuously recorded by a high response multi-channel galvanometer recorder (Honeywell Visicorder model 1508 with type M-3300 galvanometers).

The steady-state chamber pressure during a burning rate measurement test is measured by one of two bourdon gauges (manufactured by Heise and with guaranteed accuracy of 0.1% of full-scale), depending on the test pressure: below 200 psig, a 0-250 psig gauge with 0.5 psi graduations was used, and in the range

200-1500 psig, a 0-2000 psig gauge with 2.0 psig graduations was used. Both gauges were periodically calibrated with a dead-weight tester; the calibrations on the 0-250 psig gauge fell within 0.2 psig of each other and the calibrations of the 0-2000 psig gauge fell within 2.0 psig of each other.

Figure C-9 depicts an overall view of the instrumentation and control panels. A typical trace produced by the galvanometer recorder during the course of a test is shown by Figure C-10.

(2) Experimental Procedure

Before conducting an actual test, an exhaust orifice with throat area large enough to pass approximately 5 times as much gas as is generated by the propellant (at the desired test pressure), is fitted to the combustion chamber. The propellant is then placed in position, the bomb is closed and all electrical and pressure connections are made. The pressure vessel is brought to the desired pressure and purged for several seconds until all temperatures have reached equilibrium. As a check on the calibrations, while running the galvanometer recorder, the incoming nitrogen temperature and pressure are read on the digital voltmeter and bourdon pressure gauge, respectively. After ignition and during burning, these values are again read. They represent actual test conditions. After completion of the test, the bomb is purged of combustion product gases and pressure is released.

Burning rate for the particular test conditions is determined by calculating the slope of a straight line drawn through the seven points plotted as burning surface position versus time; if a straight line does not fit these seven points well, the test is discarded.

(c) Accuracy of Burning Rate Measurements.

The accuracy of a particular burning rate measurement cannot be determined directly because there are no absolute standards to compare with. However, there are many external factors (not concerned with the combustion mechanism) that could conceivably influence the burning rate and then burning rate is no longer an intrinsic property of the propellant - in that sense, the accuracy of the measurement is affected also. Thus, if the burning rate is to be meaningful from the standpoint of the burning mechanism, the possible effects of these external factors must be determined first. These are considered separately below.

(1) Effect of Strand Surface Treatment

As seen in Figure C-11, the condition of the surface of the strand makes very little difference on the burning rate. If the results on the untreated strands are excluded, they are reproducible to within $\pm$ 2.5%. Since untreated strands often burn

irregularly (presumably due to the flame flashing down the sides of the strand), the next easiest method of surface treatment, namely, leaching in water for 10 to 15 seconds, was followed throughout this program.

(2) Effect of Nitrogen Purge Rate

The effect of nitrogen purge rate on burning rate was investigated at four different pressure levels between 35 and 1200 psia. This was done by varying the throat diameter of the exhaust orifice of the pressure vessel. Figure C-12 shows the effect of nitrogen purge rate to be zero in the range of throat diameter from 0.04 to 0.3 inch. This range in orifice sizes corresponds approximately to a fifty fold change in nitrogen flow rate.

There are indications that reverse flow of the hot combustion gases can occur when the nitrogen mass flow rate becomes comparable to the mass flow rate of product gases generated by the propellant. Consequently, it was decided to always choose an orifice which will allow five times as much gas to escape to the atmosphere as is generated by the propellant.

The criterion above has been used to calculate orifice diameter as a function of pressure and burning rate for the particular propellant used here, i.e., PBAA with 75% 80μ AP, and is shown as the dotted line in Fig. C-12; the severe bend in the curve at low pressure is due to unchoking of the orifice below about 28 psia. This dotted curve shows that test corditions chosen such that the nitrogen purge rate is four times the mass of gas generated by the propellant, fall well within the range where burning rate is independent of nitrogen flow rate.

(3) Effect of Strand Size

The effect of strand size on the burning rate has been determined for a propellant for which this effect was expected to be the greatest, namely, an underoxidized, small AP particle size propellant which is prone to burning intermittently in the normal rocket pressure range. The results for 75% 5μ AP + 25% PBAA/EPON propellant with strand sizes varying from 1/8 inch square cross-section to 3/8 inch square cross-section are shown in Fig. C-13. It is seen that for all pressures investigated, strand size has no effect on the burning rate as long as the strand is of 1/4 inch square cross-section or larger. Thus, it was decided to use 1/4 inch square strands throughout the program.

It is to be noted that strand size has an effect on the extinction pressure: in the normal rocket pressure range, the large strands extinguish at higher pressures, as expected (Fig. C-13); at very low pressures, the larger strands extinguish at lower pressures, also as expected (see Section

VB & C). This dependence of the extinction pressure on strand size is not of profound importance from a combustion mechanistic standpoint.

(4) Effect of Fuse Wires.

The effect of the presence of fuse wires on the burning rate was determined in the subatmospheric pressure range where the effect is expected to be largest (the rate of generation of heat by the flame is low and so, the heat required to vaporize the fuse wire may cause a significant perturbation). No fuse wire effect could be discerned from comparison of photographically determined burning rates (as in Section (i) above), with burning rates determined by use of fuse wires (as in Section (ii) above), even very near the extinction pressure.

As expected, the low pressure extinction pressure is significantly raised by the presence of the fuse wire; at very low pressure ($\sim$0.1 atm), extinction occurs as soon as the flame front reaches the first fuse wire. So, burning rates can no longer be determined by use of fuse wires at these very low pressures.

(5) Condition of Regressing Surface: Flatness and Inclination to Direction of Travel.

It is essential that the burning surface be flat and perpendicular to its direction of travel if the burning rate determinations are to be accurate. A series of movies of various propellants burning at different pressures have shown that for the conditions of this investigation (i.e., N_2 flowing past strand that has been leached), all propellants that burn normally (as opposed to intermittent burning), burn with a flat surface that is perpendicular to its direction of travel. The same photographic movie survey showed that the underoxidized or readily meltable fuel propellants burn with an irregular surface; this is an essential manifestation of the intermittent burning phenomenon and so, the measured (mean) burning rates still have meaning for these cases.

(6) Accuracy and Reproducibility of Burning Rate Measurements.

Several error analyses(5,120) of burning rate measurements have already been done. These show that, as long as factors (1)-(4) above have no detectable effect on the burning rate and, as long as the burning surface is flat and perpendicular to its direction of travel, then the burning rate determinations should be accurate to within $\pm$ 2%. These conditions are all satisfied for "normal-burning" (highly oxidized-relatively non-meltable fuel) propellants but not for the propellants that burn intermittently. Propellants of the latter category are therefore expected to show more scatter in their burning rates.

Batch to batch reproducibility has been checked with a number of propellant formulations. Examples of two propellant formulations whose reproducibility has been checked, are shown in Fig. C-14. The 25% PBAA/EPON + 75% 80µ AP propellants are reproducible to within ± 1.0% over the entire pressure range investigated, regardless of the mixer used to make the propellant. The slight batch to batch variations in AP content (0.3%) do not have a noticeable effect on the absolute magnitude of burning rate. As expected, the same propellant with 5µ AP shows large scatter (Fig. 15). This is due to the phenomenon of intermittent burning, which by its very nature, is nonsteady and irregular (see Section IVC). Nevertheless, despite this obvious irregularity and unsteadiness, the burning rate behavior of this class of propellants is still surprisingly reproducible.

Fig. C-15 shows the results of this investigation for 35% LP3/GMF + 65% AP propellants, compared to those obtained by Bastress(14). We strove to reproduce the AP particle size distributions of Bastress as closely as possible (by methods indicated in the figure). In all other respects, however, these propellants were made with the more refined methods of this investigation. The results agree well, despite the different methods used to obtain the desired particle size distributions.

As is apparent from the density measurements listed in Fig. C-15, LP3/GMF-AP propellants are extremely difficult to make without imperfections. When the AP particle size is small (~5µ), voids can not be eliminated. Then the AP particles are larger (~100µ), these particles begin to settle during curing, even when the block is rotated constantly at 5 rpm during curing; the AP particles settle outwards when the block is rotated during curing. By the standards of this investigation, only the 12µ AP + LP3/GMF propellant can be classified as good propellant.

That the phenomenon of intermittent burning is not a result of propellant imperfections as revealed by the above-mentioned deviations from the theoretical density, is shown by the fact that the same intermittent burning behavior shows up in the many other more easily processable propellants of this study. In particular, PBAA/EPON-AP propellant which has excellant processing qualities, and which can be made with densities very close to the theoretical (see Table VI of Appendix D), also shows very pronounced intermittent burning behavior (see Fig. 15).

TABLE V

COMPARISON OF MEAN PARTICLE DIAMETERS OBTAINED BY MICROSCOPIC AND SEDIMENTATION TECHNIQUES FOR AS RECEIVED "SPHERICAL" AMMONIUM PERCHLORATE

Microscopic Method		Sedimentation Technique
Manufacturer(207)	This Study	This Study
4.7 μ	4.95 μ	8.5 μ
12.5 μ	12.5 μ	12 μ
44.5 μ	41 μ	41 μ
77.3 μ	--	82 μ
180 μ*	--	182 μ

*Determined by Sieve Analysis. (Information obtained from quality control sheet supplied by manufacturer.)

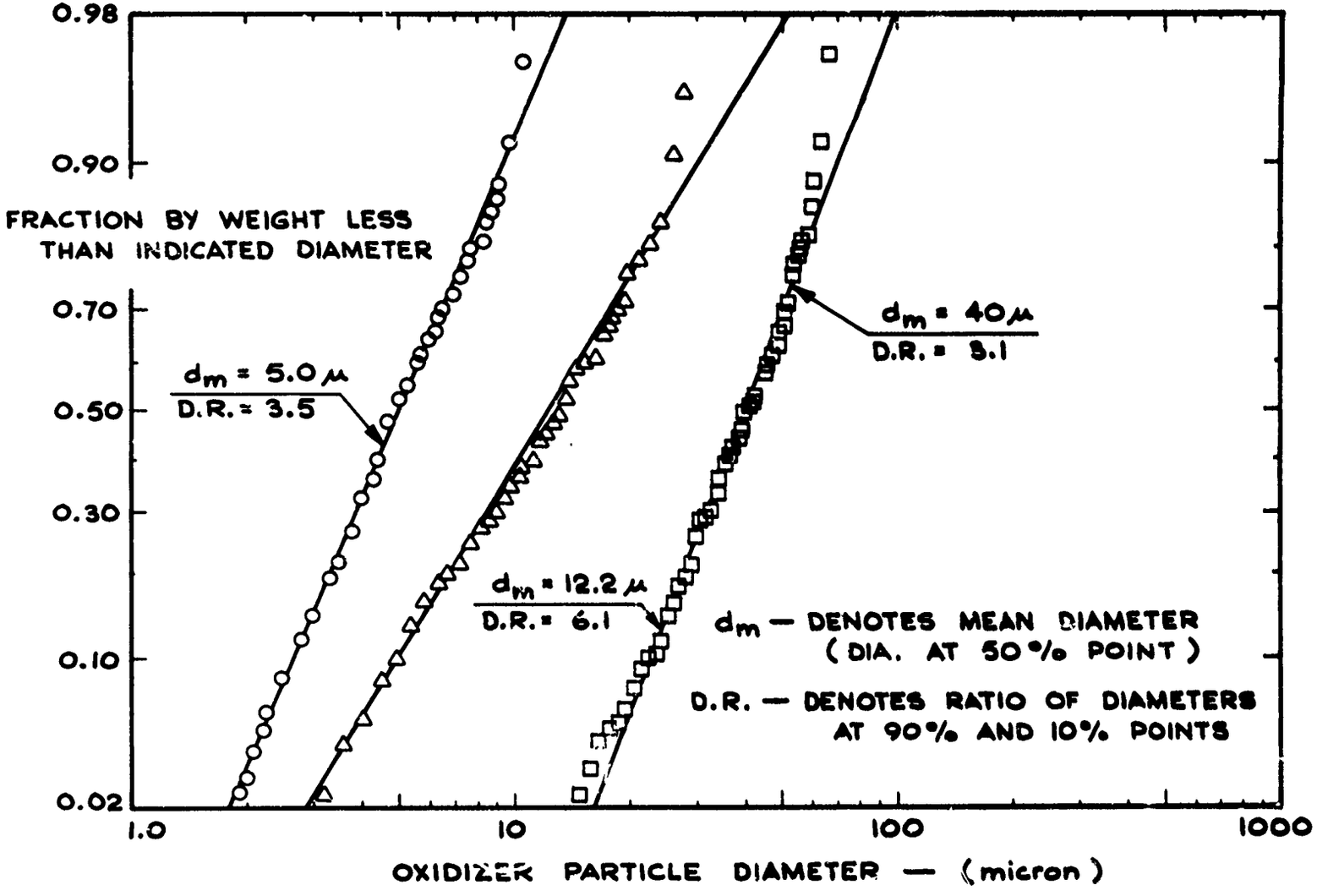

FIGURE C-1 AMMONIUM PERCHLORATE PARTICLE SIZE DISTRIBUTIONS DETERMINED BY MICROSCOPIC TECHNIQUE

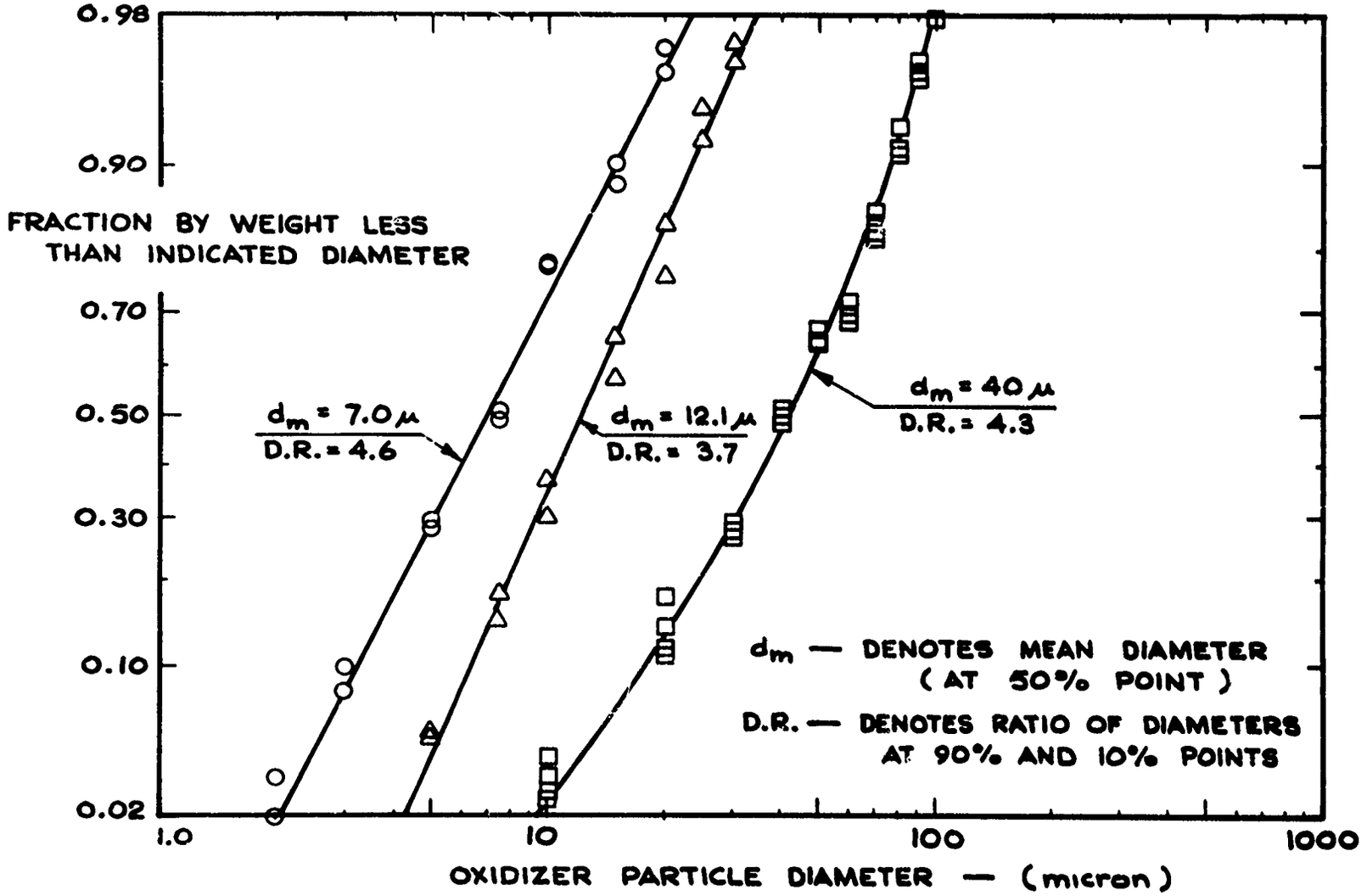

FIGURE C-2 AMMONIUM PERCHLORATE PARTICLE SIZE DISTRIBUTIONS DETERMINED BY SEDIMENTATION TECHNIQUE

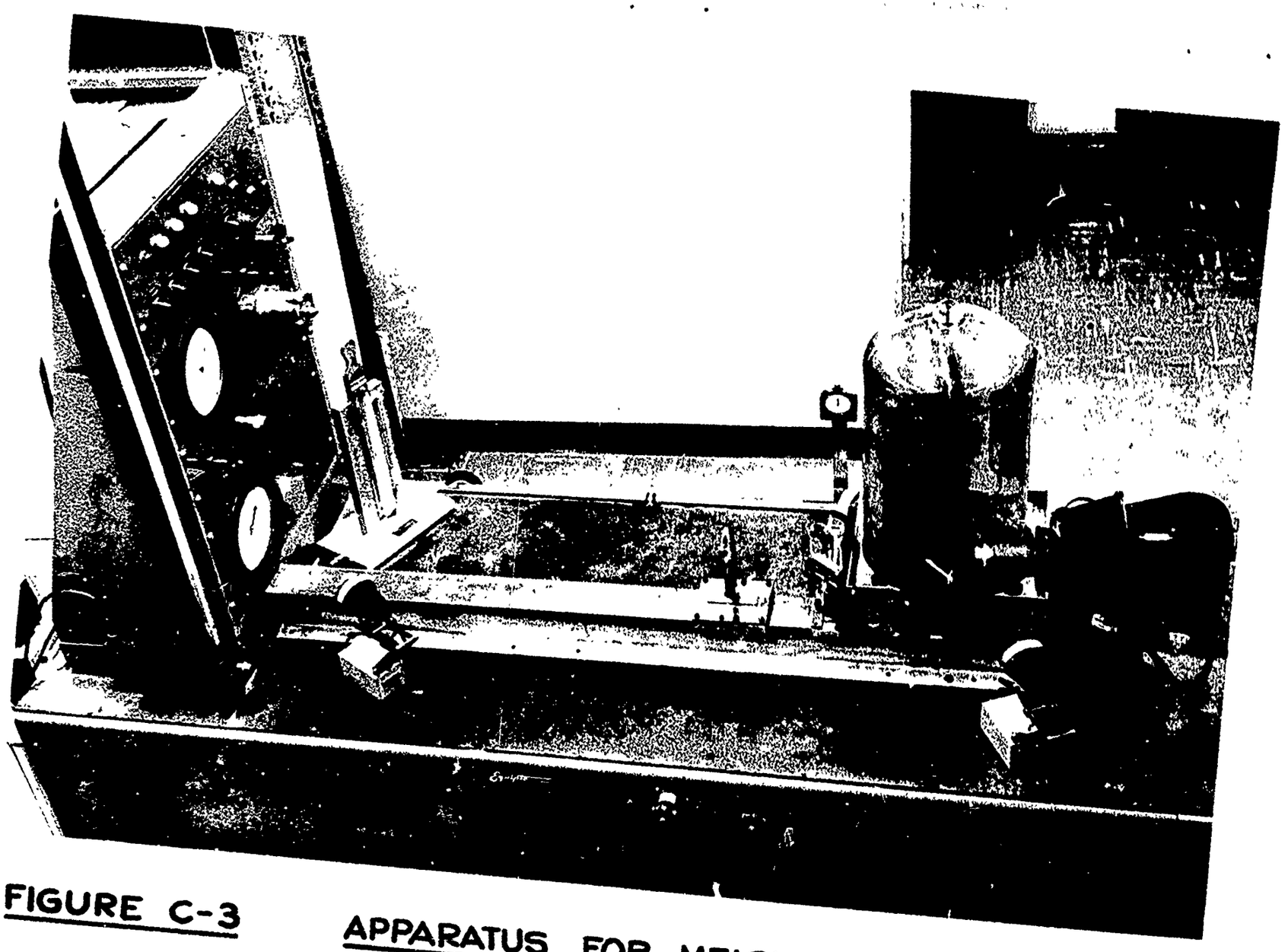

FIGURE C-3 APPARATUS FOR MEASURING BURNING RATES AT SUBATMOSPHERIC PRESSURES

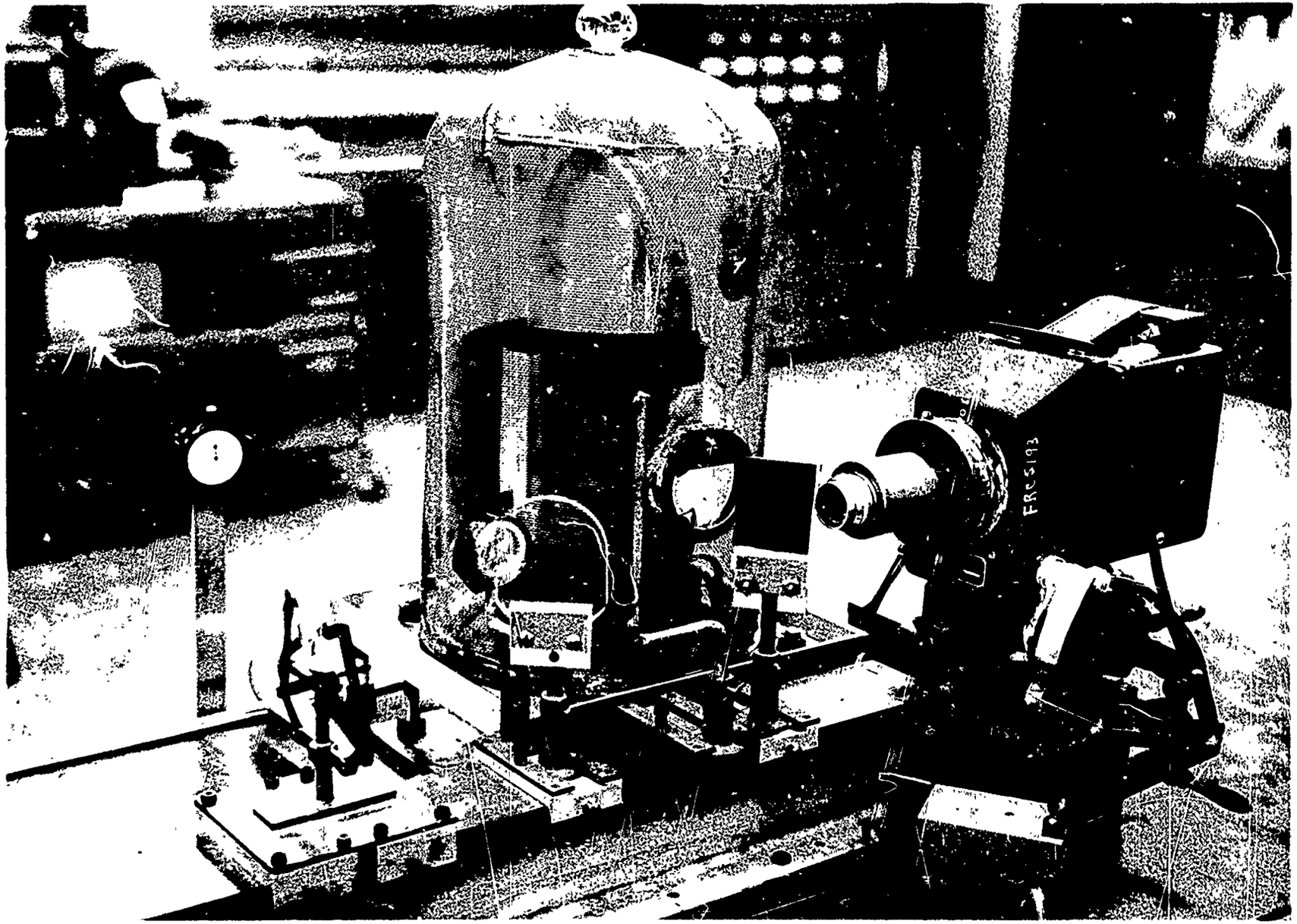

FIGURE C-4 CLOSE-UP OF OPTICAL SYSTEM USED TO MEASURE BURNING RATES AT SUBATMOSPHERIC PRESSURES

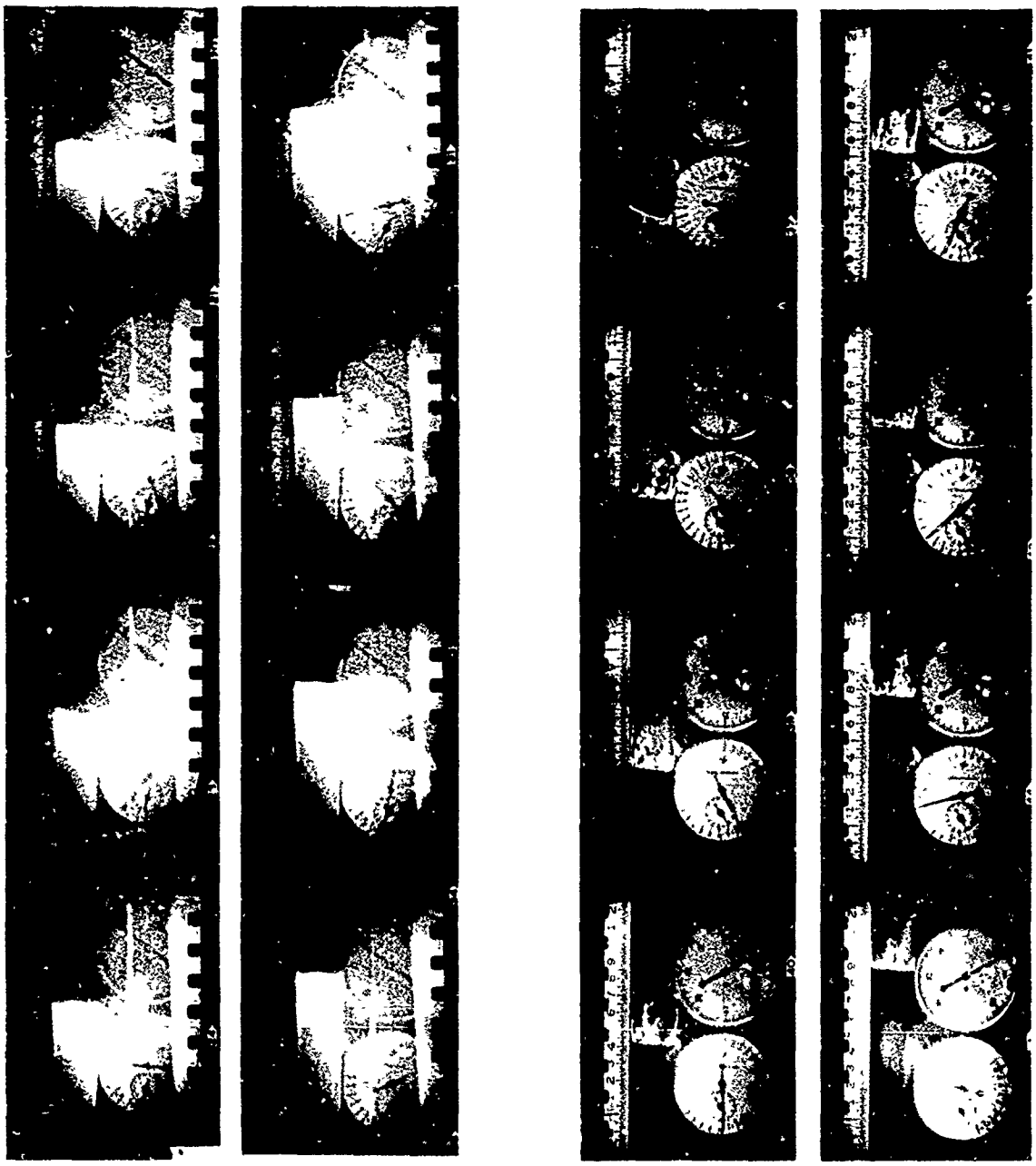

(a) IN "ASH FORMATION" REGION (WITH OIL SCREEN)

(b) IN "NORMAL COMBUSTION" REGIME (WITHOUT OIL SCREEN)

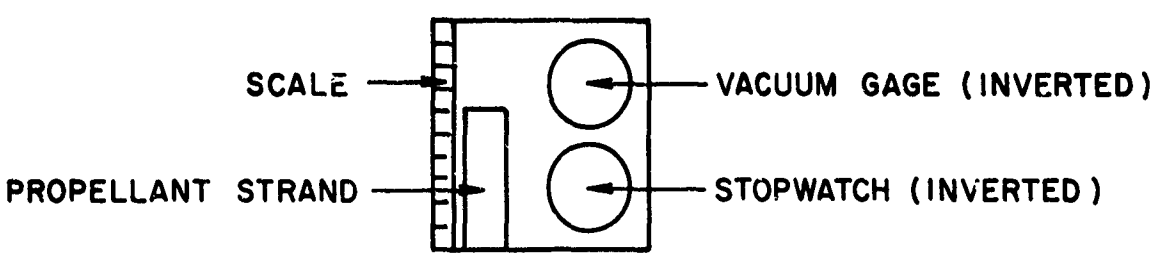

FIGURE C-5 PHOTOGRAPHIC RECORDS OF STRANDS BURNING AT SUBATMOSPHERIC PRESSURES

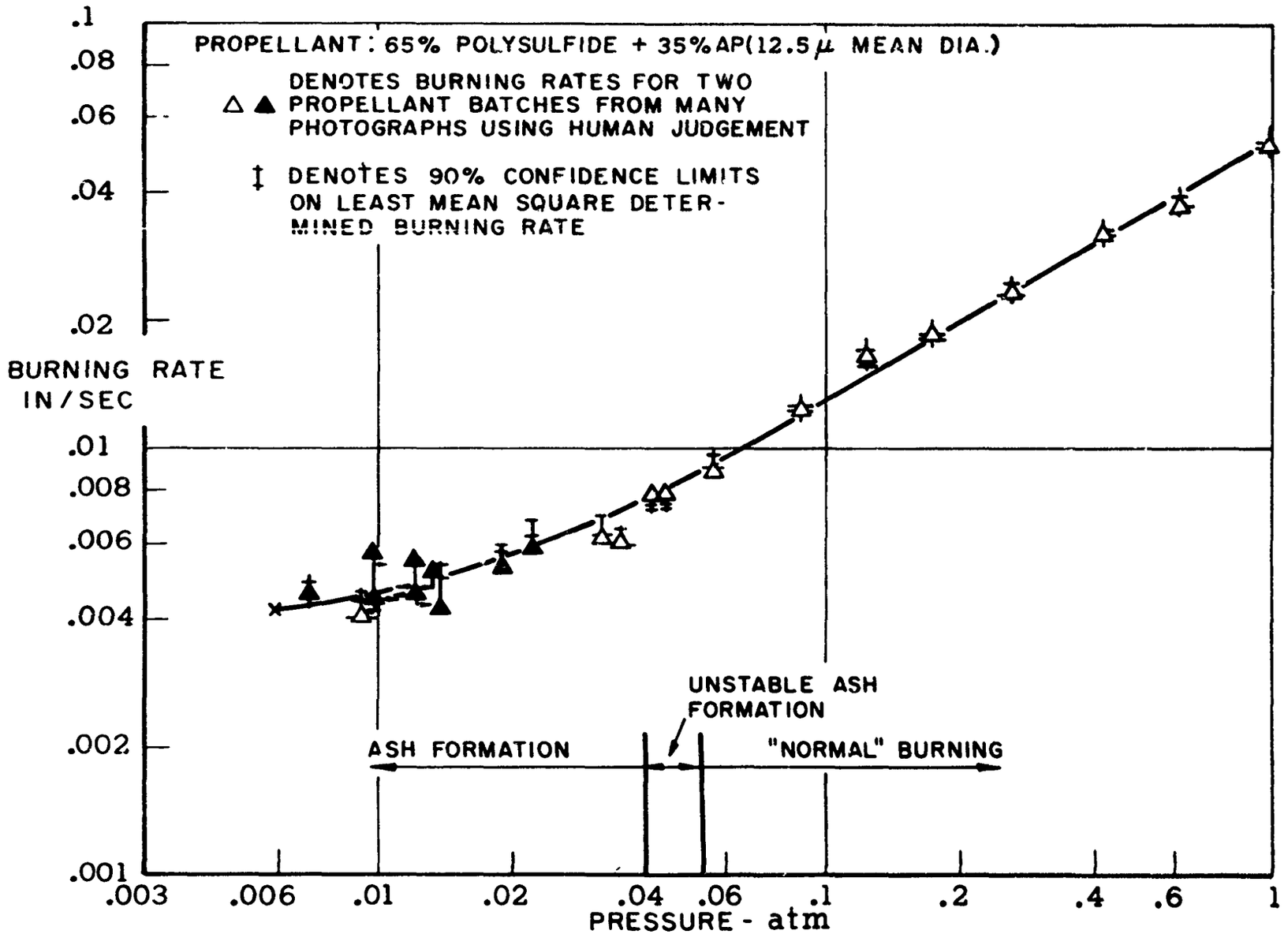

FIGURE C-6 PROPELLANT BURNING RATES DETERMINED BY TWO INDEPENDENT MEANS OF DATA REDUCTION

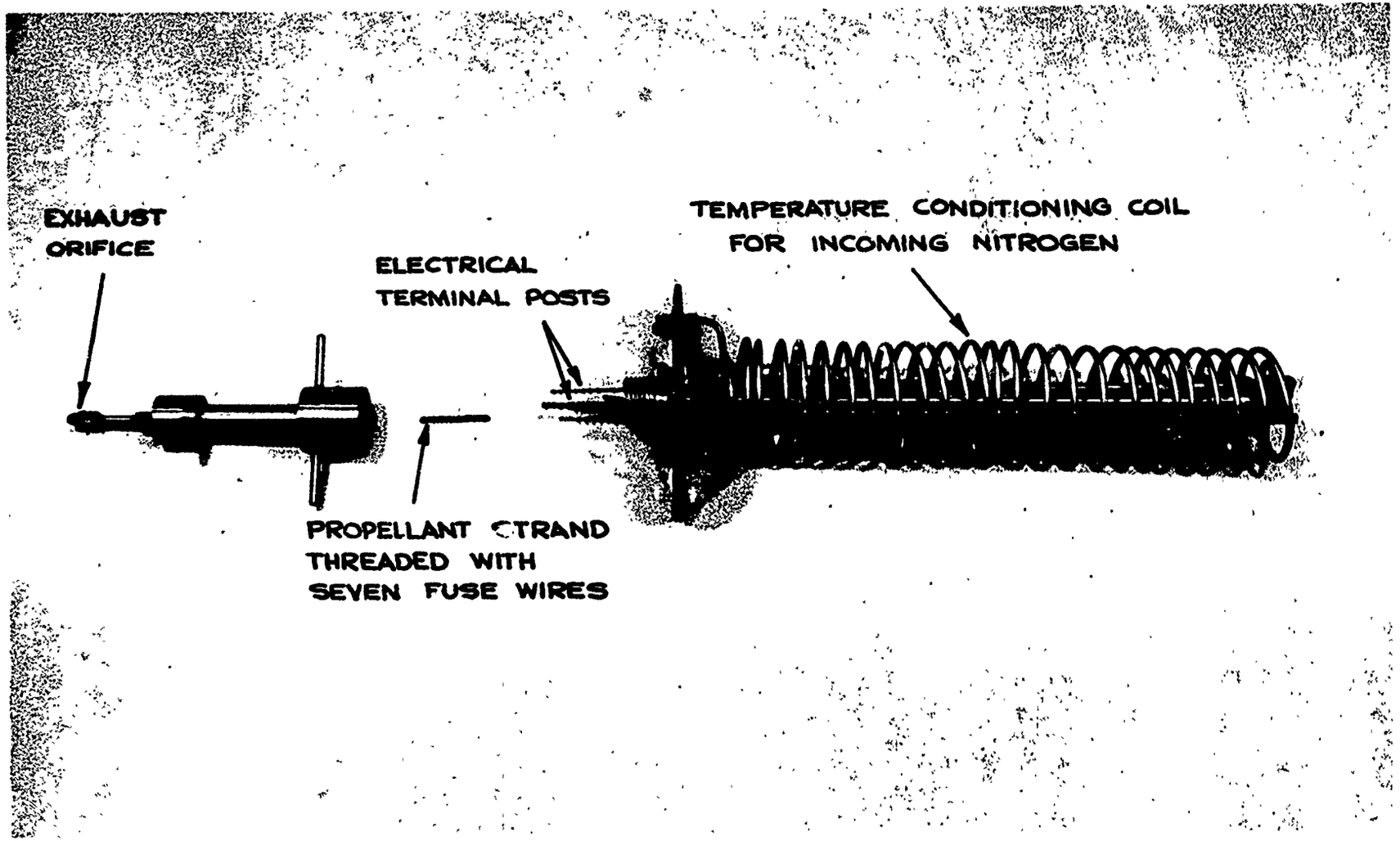

FIGURE C-7 EXPLODED VIEW OF STRAND BURNER FOR MEASURING BURNING RATES IN 1-100 atm RANGE

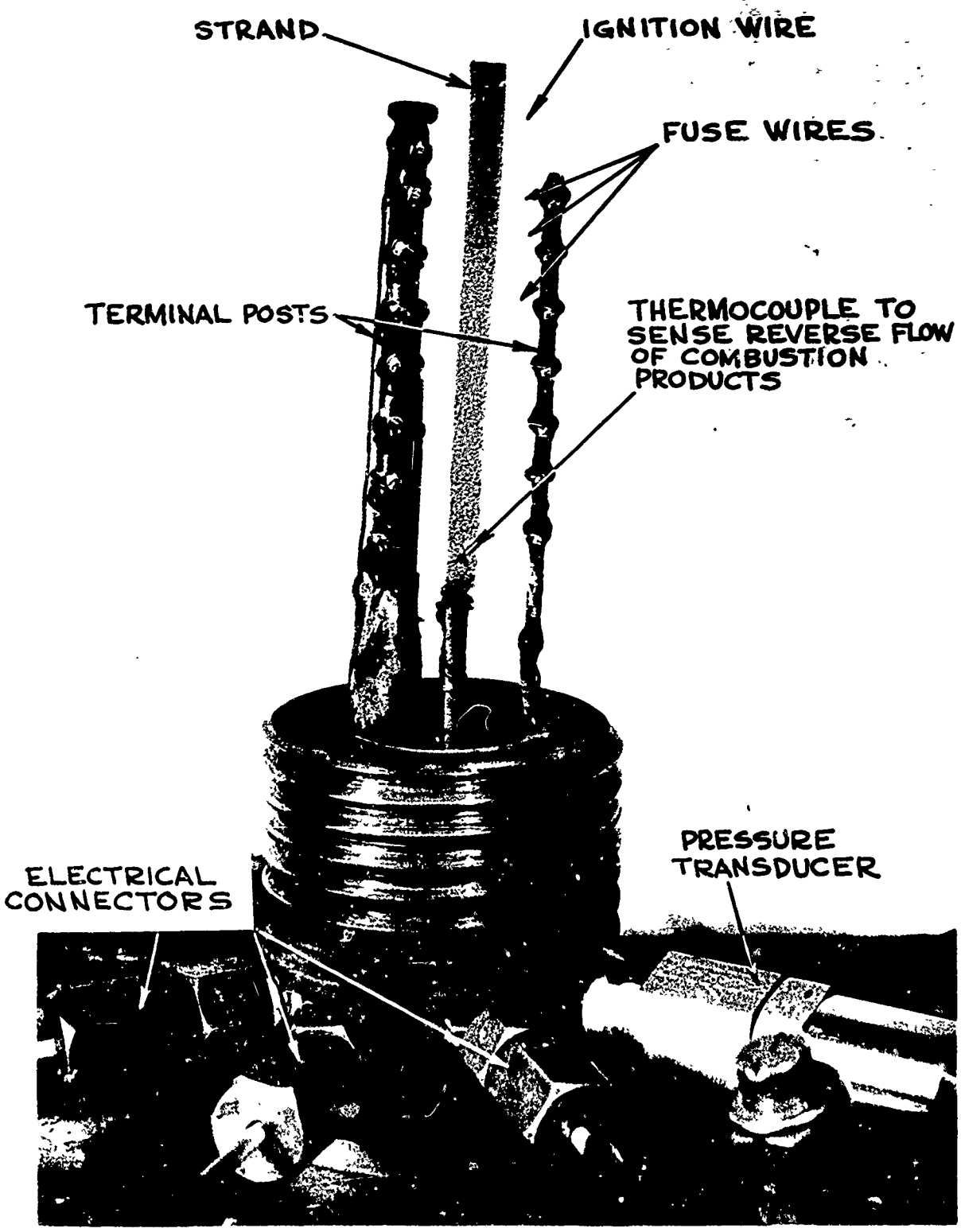

JP19-PB-66

FIGURE C-8 CLOSE-UP OF STRAND HOLDER PRIOR TO TEST (1-100 atm STRAND BURNER)

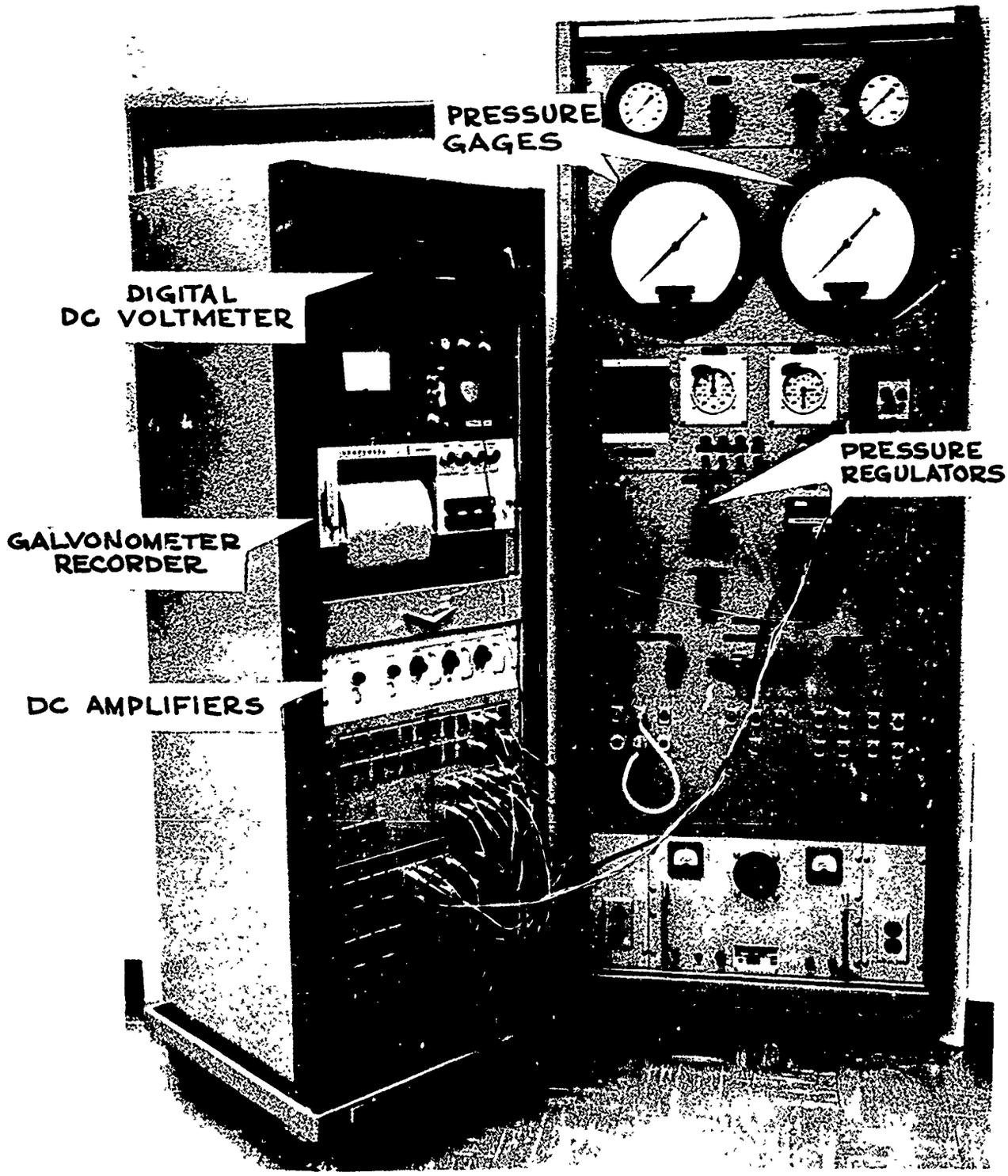

JPL 9-64

FIGURE C-9 INSTRUMENTATION FOR MEASURING BURNING RATES IN 1-100 atm RANGE

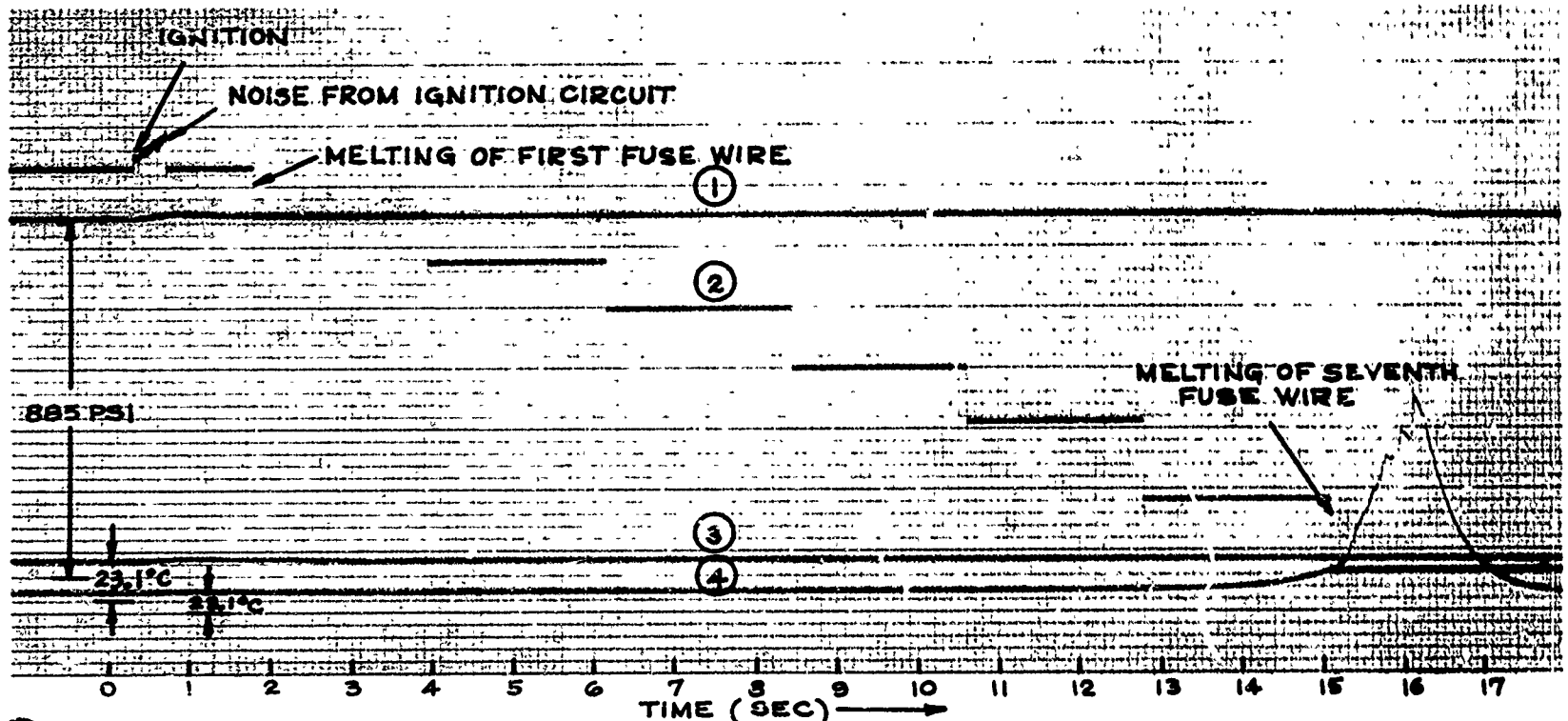

(1) PRESSURE TRACE

(2) TRACE INDICATING TIMES OF MELTING FUSE WIRES (AT 0.50 INCH SEPERATION DISTANCES)

(3) INCOMING NITROGEN FLOW TEMPERATURE TRACE

(4) TRACE DEPICTING TEMPERATURE OF NITROGEN NEXT TO STRAND SURFACE AT HEIGHT OF 7TH FUSE WIRE

FIGURE C-10 TYPICAL TEST RECORD FROM 1-100 atm STRAND BURNER

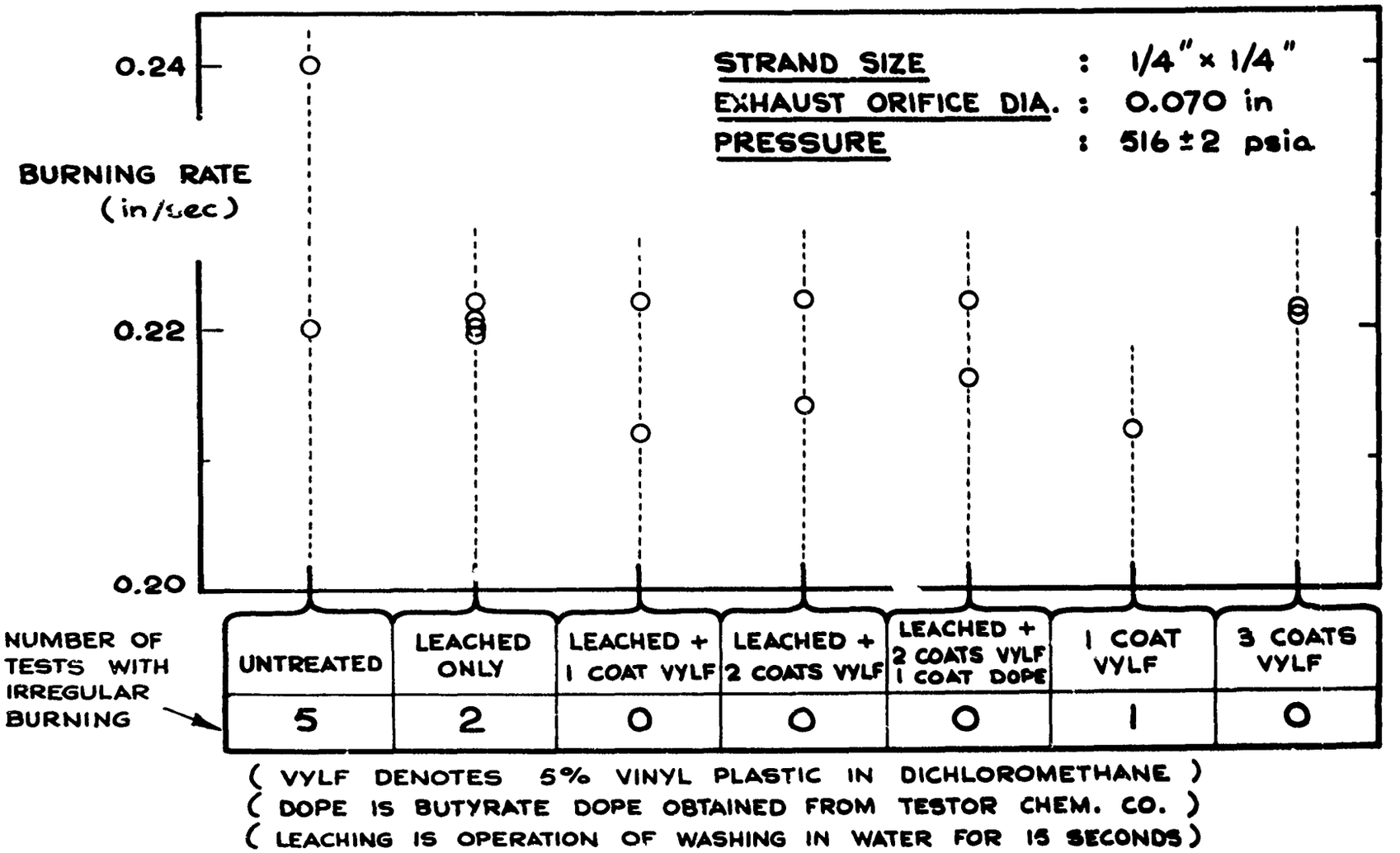

FIGURE C-11 EFFECT OF CONDITION OF SURFACE OF STRAND ON BURNING RATE OF 25% PBAA/EPON + 75% AP (80μ MEAN PARTICLE DIAMETER)

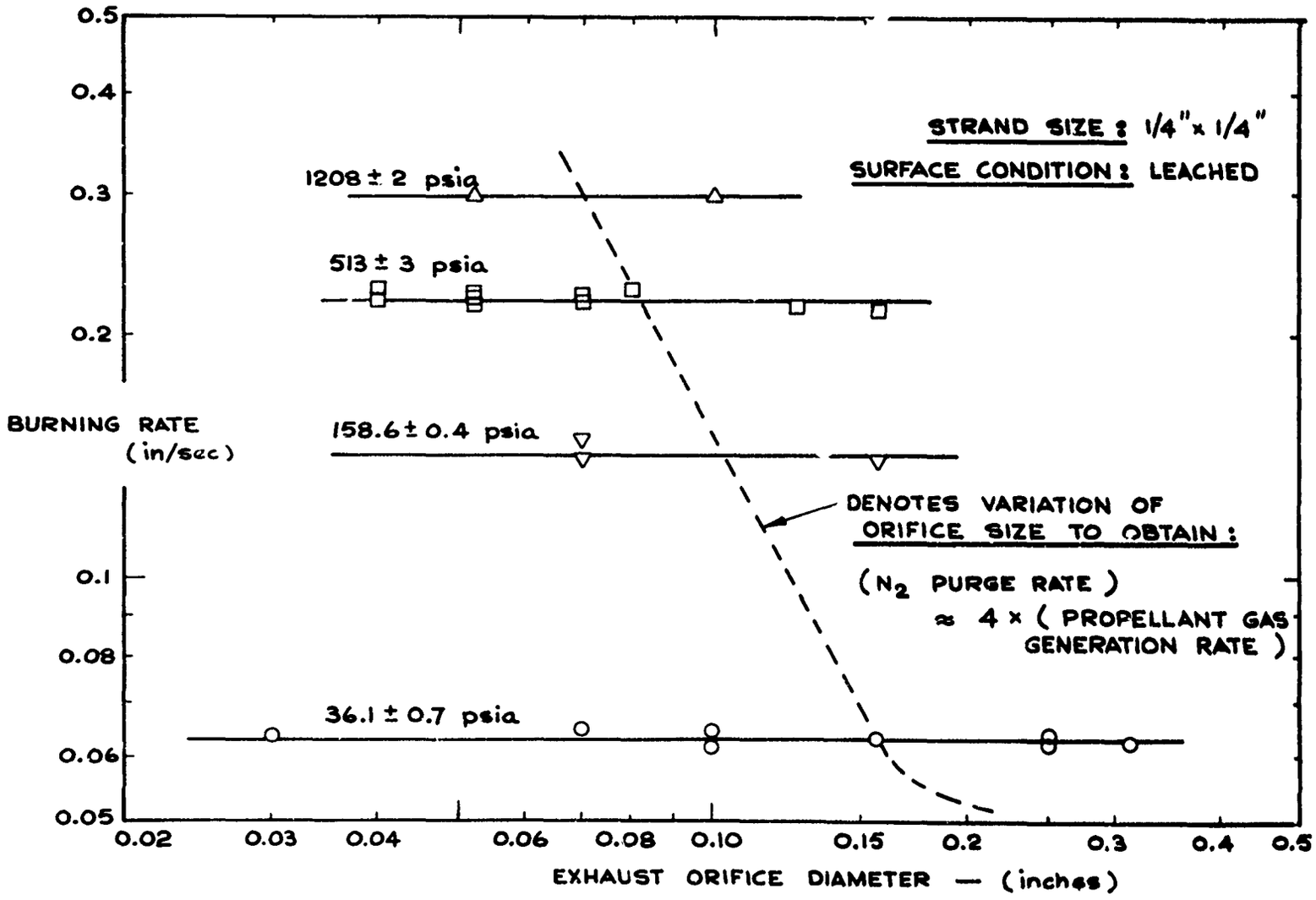

FIGURE C-12 EFFECT OF NITROGEN PURGE RATE ON BURNING RATE OF 25% PBAA + 75% AMMONIUM PERCHLORATE (MEAN SIZE = 80 μ)

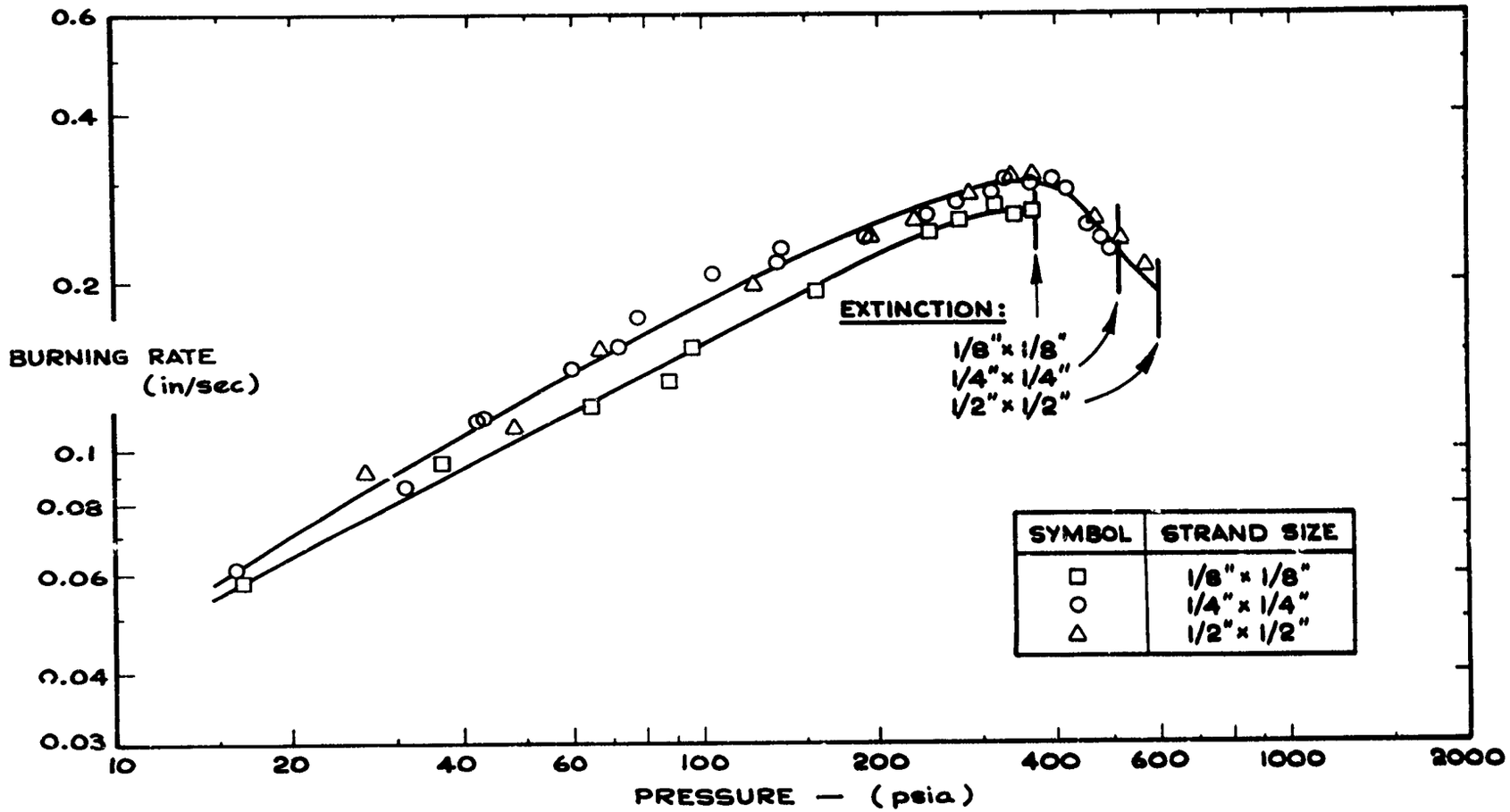

FIGURE C-13 EFFECT OF STRAND SIZE ON THE BURNING RATE BEHAVIOR OF 25% PBAA/EPON + 75% AMMONIUM PERCHLORATE (MEAN AP SIZE = 5 μ)

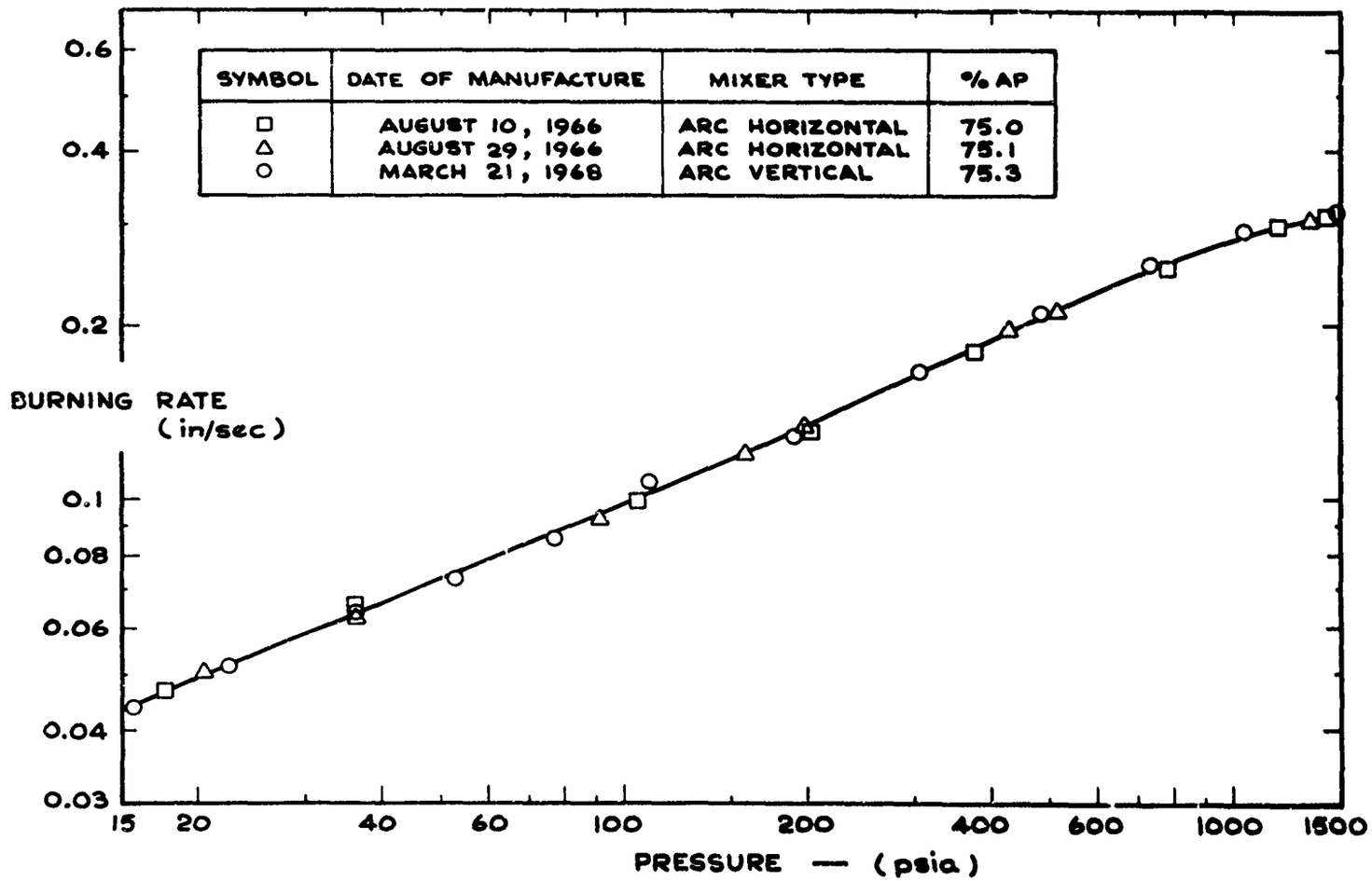

FIGURE C-14 BATCH TO BATCH REPRODUCIBILITY OF PBAA/EPON-AP PROPELLANT MEAN PARTICLE SIZE OF AP IS 80 MICRON

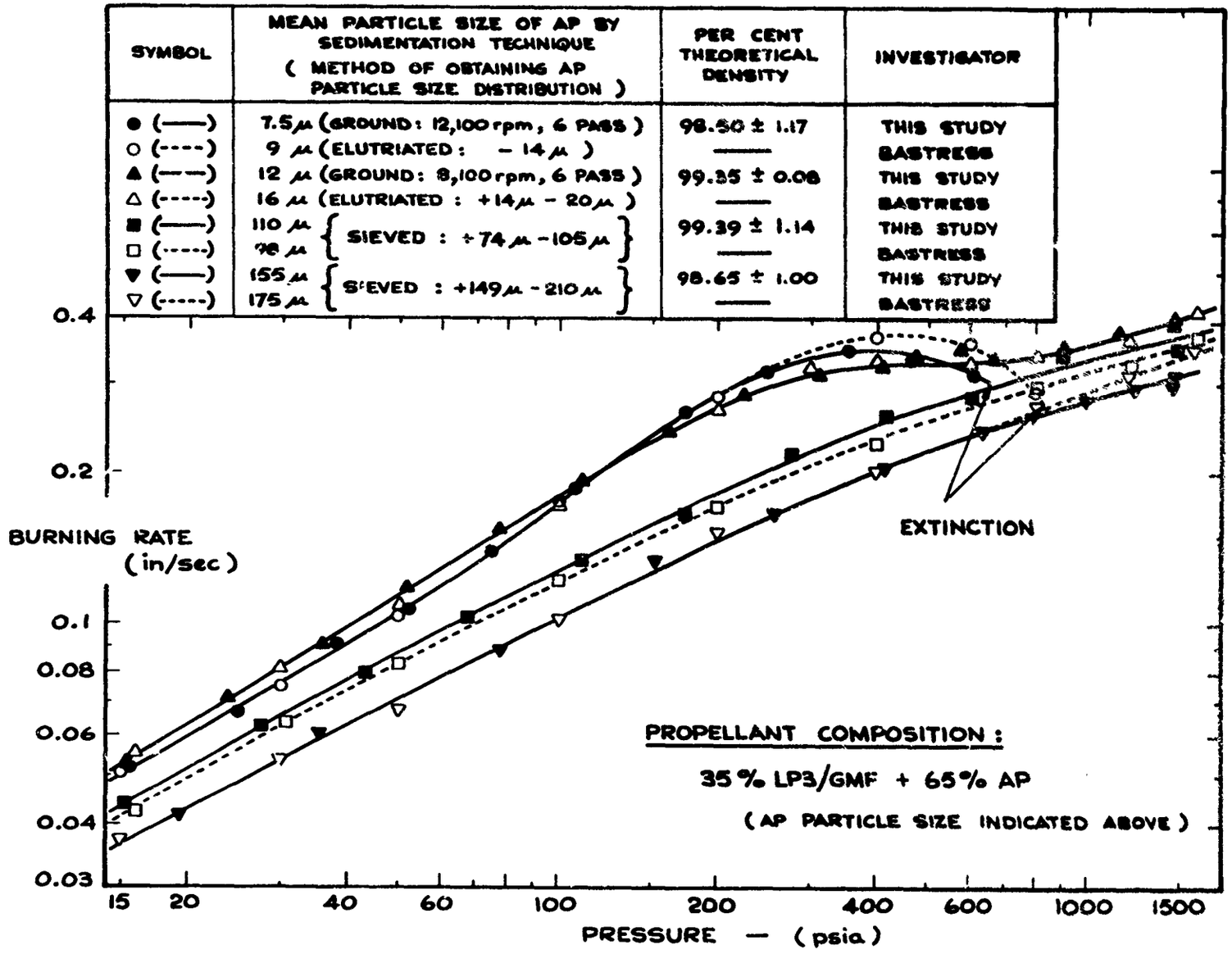

FIGURE C-15 DUPLICATION OF BASTRESS' DATA FOR POLYSULFIDE PROPELLANTS

APPENDIX D

SPECIFICATIONS OF ALL PROPELLANT FORMULATIONS USED IN THIS INVESTIGATION: Conditions of Manufacture, Propellant Composition, Propellant Density, and AP Particle Size

Tables VI (A) and VI (B) of this Appendix give the conditions of manufacture, the composition, the density, and the particle size of the AP of all propellants used in this study. The propellants are referred to by the number in the first column of Table VI. This code number corresponds to the number assigned to each propellant in Table III of Appendix B.

With the exception of the PBAA/EPON-AP propellants, all compositions listed in Table III (Appendix B) and Table VI (this Appendix) are based on the actual weights of ingredients that were entered into the mixer. In the case of the PBAA/EPON-AP propellants, the amount of fuel that was drawn into the vacuum system during the mixing operation, was measured directly and this loss of fuel was taken into account in the calculation of the mixture composition. Thus, in the case of the PBAA/EPON-AP propellants, the error in the quoted mixture composition is less than the 0.2% compositional error estimated for all the other propellant systems of this study (see Appendix E).

Tables III and VI give also the mean particle size of the AP used for each propellant. The corresponding size distribution curves of the AP of each propellant can be found in either Figures D-1, D-2, or D-3. Each distribution curve is identified by a different alphabetic symbol.

TABLE VI (A) SPECIFICATIONS OF ALL PROPELLANT FORMULATIONS USED FOR 1-100 atm BURNING RATE STUDIES

Propellant No. in Table III	Fuel	% AP	Mean Diameter of AP (Measured Size Distributions Given in Figs. D-1 and D-2 (Code in Parenthesis))	Percent Additive	Density (Percent of Theoretical)	Mixer Bearings Submerged?	Pressure During Mixing cm Hg abs	Pressure During Casting cm Hg abs	Remarks
#65	PBAN/MAPO	74.8	100% 80μ (C)	--	99.40 ± 0.46	No	6	6	
#66	PBAN/MAPO	82.5	30% 40μ(F) + 70% 180μ (D)	--	99.58 ± 0.17	No	6	6	
#67	PBAA/EPON	75.0	100% 5μ (A)	--	99.88 ± 0.03	No	6	6	
#68	PBAA/EPON	75.0	100% 45μ (B)	--	100.2 ± 0.1	Yes	6	6	
#69	PBAA/EPON	75.0	100% 80μ (C)	--	100.15 ± 0.05*	Yes	6	6	
#70	PBAA/EPON	75.0	100% 180μ (D)	--	100.5 ± 0.5**	Yes	6	6	
#71	PBAA/EPON	75.1	90% 5μ (A) + 10% 80μ (C)	--	100.09 ± 0.06	No	6	6	
#72	PBAA/EPON	70.0	30% 5μ (A) + 70% 45μ (G)	--	100.03 ± 0.04	No	6	6	
#73	PBAA/EPON	75.0	30% 5μ (A) + 70% 45μ (G)	--	99.97 ± 0.03	No	6	6	
#74	PBAA/EPON	80.0	30% 5μ (A) + 70% 45μ (G)	--	99.93 ± 0.07	No	6	6	
#75	PBAA/EPON	80.1	30% 8μ (E) + 70% 180μ (D)	--	100.25 ± 0.15*	Yes	6	6	
#76	PBAA/EPON	82.5	30% 40μ (F) + 70% 180μ (D)	--	100.03 ± 0.04	No	6	6	
#77	PBHT/TDI	75.0	100% 80μ (C)	--	100.10 ± 0.07	No	6	6	
#78	PBHT/TDI	82.7	30% 40μ (F) + 70% 180μ (D)	--	99.57 ± 0.16	No	6	6	
#79	NC/TEGDN	0	- - - -	--	- -	No	76	76	
#80	NC/TEGDN	40.0	100% 5μ (A)	--	99.29 ± 0.08	No	76	76	
#81	NC/TEGDN	40.0	100% 80μ (C)	--	99.66 ± 0.20	No	76	76	
#82	PIB/MAPO	74.8	100% 80μ (D)	--	99.69 ± 0.05	No	1.5	--	Too viscous; hand packed
#83	PIB/MAPO	80.1	30% 40μ (F) + 70% 180μ (D)	--	99.78 ± 0.29	No	1.5	3	
#84	ESTANE/POLYOL	72.5	100% 80μ (C)	--	99.54 ± 0.86	No	0.5	--	Too viscous; hand packed
#85	ESTANE/POLYOL	80.0	30% 40μ (F) + 70% 180μ (D)	--	99.85 ± 0.12	No	0.5	8	
#86	POLYOL/TDI	75.0	100% 45μ (B)	--	100.23 ± 0.37	No	0.5	8	
#87	POLYOL/TDI	75.0	100% 80μ (C)	--	99.82 ± 0.08	No	0.5	8	
#88	POLYOL/TDI	85.0	30% 40μ (F) + 70% 180μ (D)	--	99.45 ± 0.29	No	0.5	8	

Notes: *The density of these propellants is too high because of fuel leakage into the submerged bearings. Propellants #67 and 69 have since been remade in the new mixer. The densities were respectively, (99.98 ± 0.04)% and (99.40 ± 0.04)% of theoretical. No difference in burning rate behavior for the old and new propellant could be detected (see Figs. 15 and C-14). Thus densities of about 0.2% in excess of the theoretical do not appear to be important.

**This propellant is suspect. The density increased toward the bottom of the block, despite the fact that the block was rotated at 5 rpm during curing. The only possibility that remains, is that the AP particles settled during mixing or casting. To clarify this point it is necessary to re-process the propellant, using partially polymerized fuel.

TABLE VI (B) SPECIFICATIONS OF ALL PROPELLANT FORMULATIONS USED IN SUBATMOSPHERIC BURNING RATE STUDIES

Propellant Number	Fuel	%AP	Mean Diameter of AP (Measured Size Distributions Given in Fig. D-3 (Code in Parenthesis))	Percent Additive	Density (Percent of Theoretical)	Mixer Bearings Submerged?	Pressure During Mixing cm Hg abs	Pressure During Casting cm Hg abs	Remarks
#89	PBAA/EPON	75.0	100% 5μ (H)	--	100.03 ± 0.05	No	6	6	
#90	PBCT/ERL	75.0	100% 5μ (H)	--	100.18 ± 0.05	No	6	6	
#91	PBHT/TDI	75.0	100% 5μ (H)	--	100.20 ± 0.05	No	6	6	
#92	PBHT/TDI	74.75	100% 5μ (H)	0.75%CC	100.15 ± 0.02	No	6	6	
#93	LP3/GMF	65.0	100% 5μ (H)	--	94.69 ± 0.09	Yes	2	--	Too viscous; hand packed
#94	LP3/GMF	65.0	100% 12.2μ (I)	--	99.34 ± 0.11	Yes	2	2	
#95	LP3/GMF	65.0	100% 26μ (J)	--	99.14 ± 0.45	Yes	2	2	
#96	LP3/GMF	65.0	100% 51μ (K)	--	99.99 ± 0.09	Yes	2	2	

Note: *This propellant is very viscous. It cannot be made without voids.

SYMBOL	SYMBOL FOR DISTRIBUTION (LISTED IN TABLE VI)	SUPPLIER'S CLASSIFICATION (MEAN DIA. IN MICRON)	MEAN DIA. IN MICRON BY SEDIMENTATION TECHNIQUE	NUMBER OF RUNS WITH SEDIMENTATION TECHNIQUE	MEAN DIA. BY MICROSCOPE (BY MANUF.) (SEE TABLE V AND FIG. C-1)	MEAN DIA. BY MICROSCOPE (THIS STUDY)
▽	A	5 μ	8.5 μ	5	4.75 μ	5.0 μ
□	B	45 μ	46 μ	7	44.5 μ	41 μ
△	C	90 μ	82 μ	9	77.3 μ	—
○	D	180 μ	178 μ	7	—	—

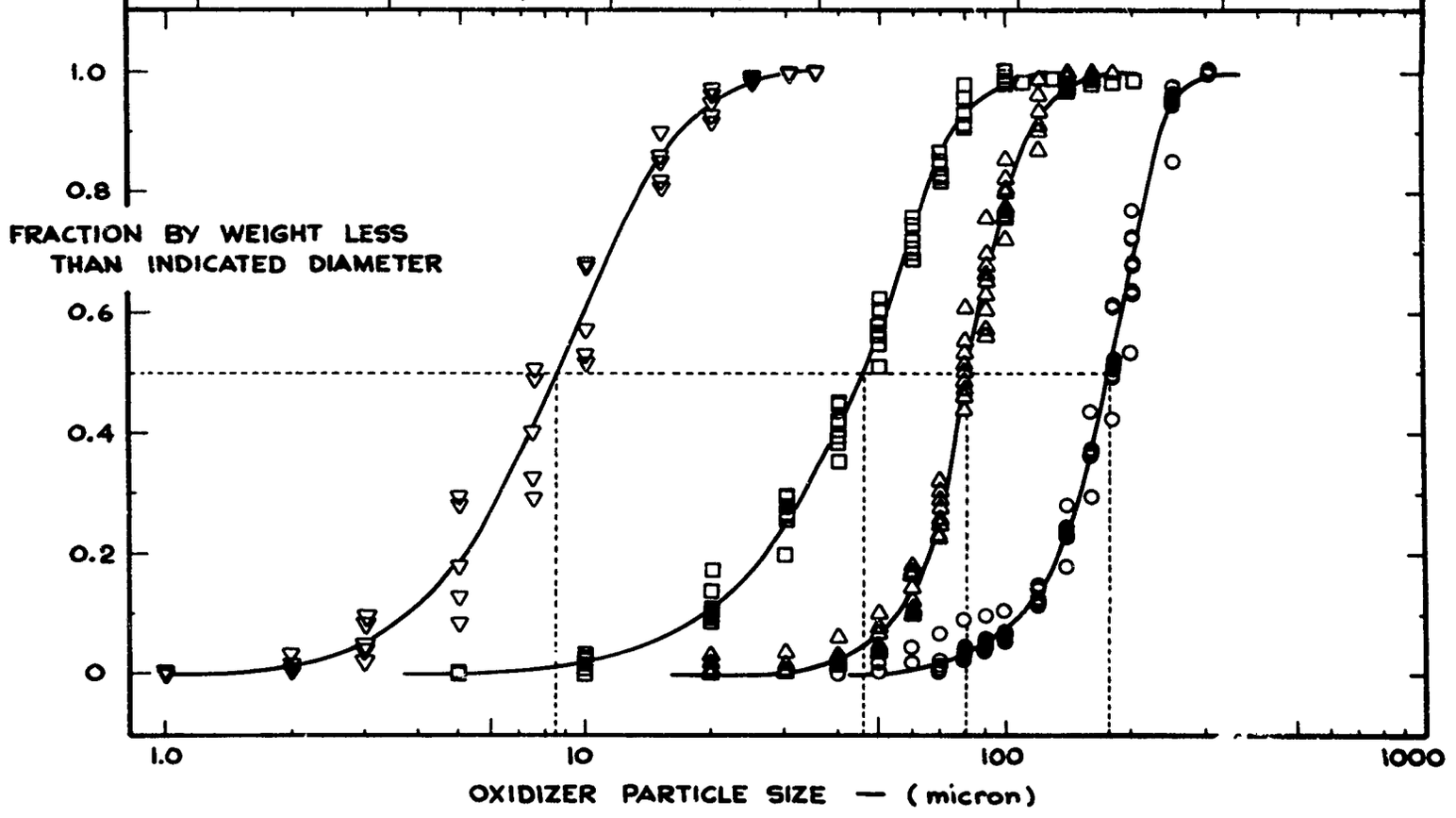

FIGURE D-1 AP PARTICLE SIZE DISTRIBUTIONS A to D (OF TABLE VI) DETERMINED BY SEDIMENTATION TECHNIQUE

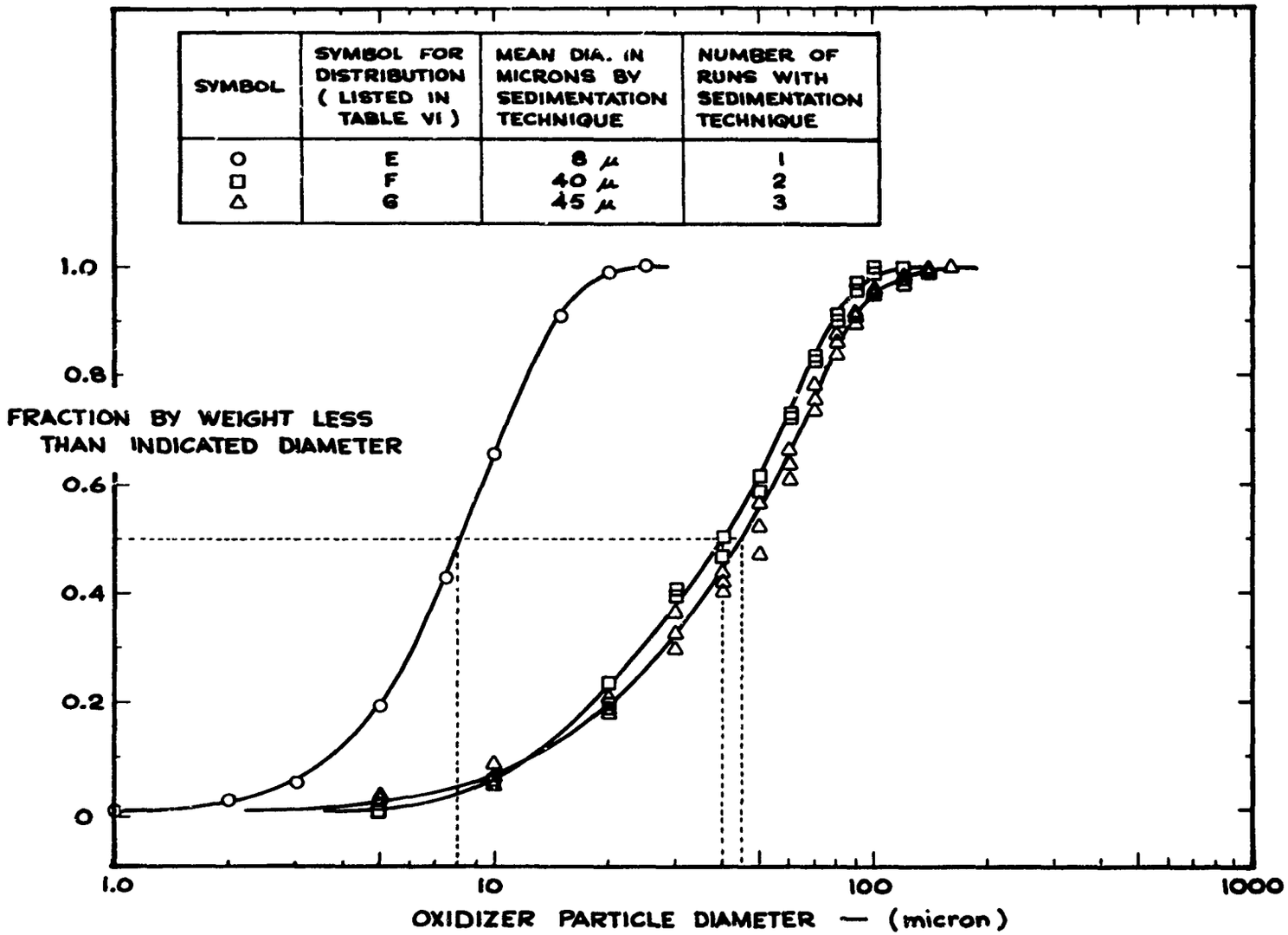

FIGURE D-2 AP PARTICLE SIZE DISTRIBUTIONS E to G (OF TABLE VI) DETERMINED BY SEDIMENTATION TECHNIQUE

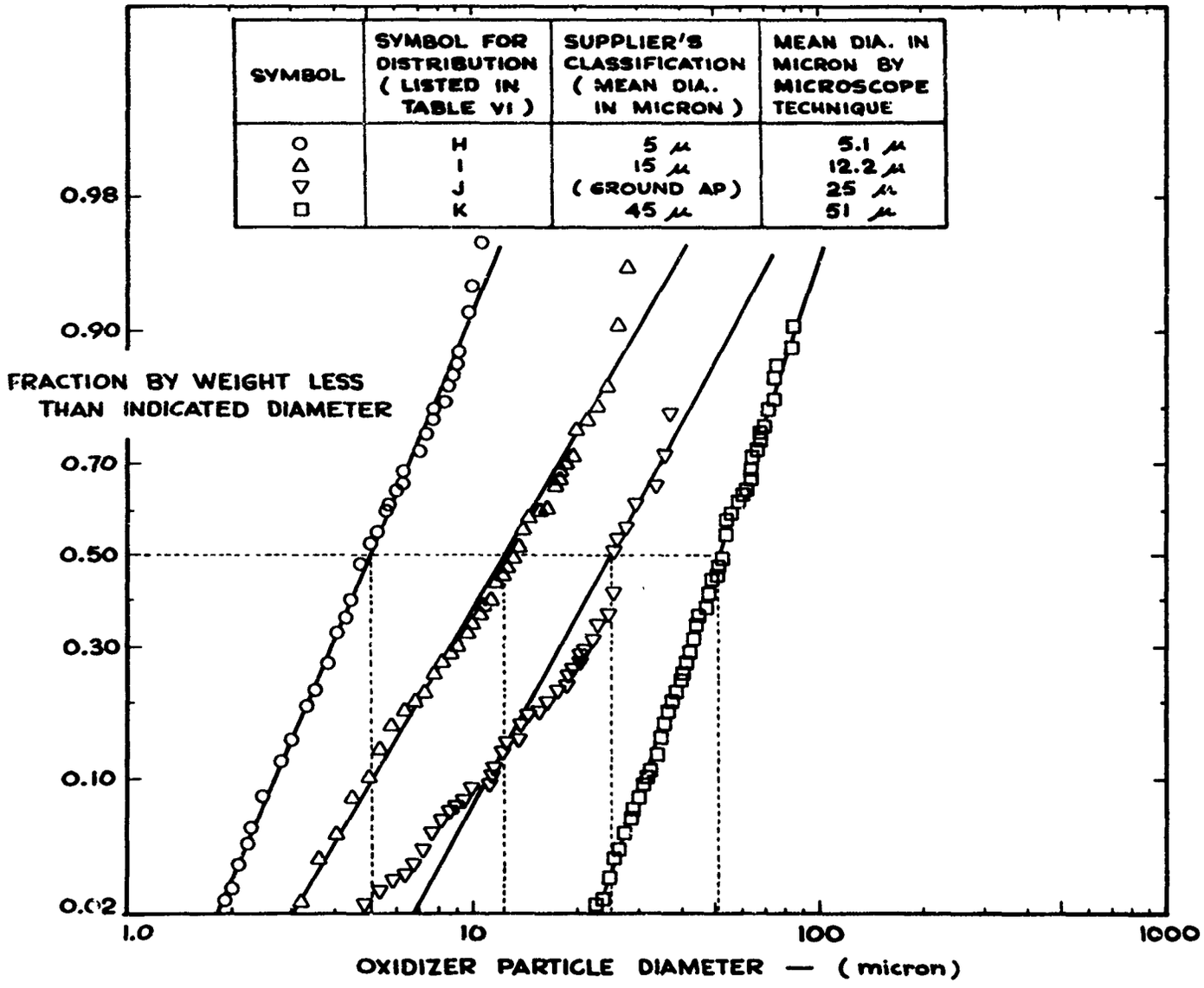

FIGURE D-3 AP PARTICLE SIZE DISTRIBUTIONS H to K (TABLE VI) DETERMINED BY MICROSCOPE METHOD

APPENDIX E

ERRORS ASSOCIATED WITH DENSITY MEASUREMENTS

In the search for accurate density measurements, the need for an error analysis was felt. Consequently all sources of density measurement error were identified and error bounds assigned to each of these. These sources of error are listed below and will be used in the error analysis that follows

(i) Loss of Fuel During Manufacturing.

As noted in Appendix C (Section (ii)(b)) fuel is drawn into the vacuum system during mixing. Weight loss measurements show this to amount to $(0.6 \pm 0.1)\%$ of the weight of the fuel in the mixer for 25% PBAA/EPON + 75% AP propellant, a typical propellant.

When the 35LP mixer is used, an additional amount of fuel is lost by preferential leakage into the bearings of the mixer. Crude estimates (based on weighing the amount of fuel wiped out of the bearing housing) show this loss to be of the order of $(1.0 \pm 0.3)\%$ of the weight of the fuel in the mixer.

(ii) Displacement fluid.

Preliminary testing showed heptane and isopropyl alcohol to be the most suitable displacement fluids. While AP is less soluble in heptane ($< 0.1\%$) than in isopropyl alcohol ($< 1.0\%$), PBAA fuel absorbs more heptane ($\sim 3.5\%$ by weight) than isopropyl alcohol ($\sim 0.3\%$ by weight). (All figures have been quoted for 30 min. soaking at room temperature). The density decrease due to dissolving of AP and absorbing by PBAA will be less with isopropyl alcohol because only a small percentage of AP particles in the propellant, namely those at the surface of the sample, are not covered by fuel. This density decrease is hard to calculate but can be estimated by soaking the propellant in the displacement fluid for varying times and measuring its density. The results for both heptane and isopropyl alcohol are shown in Figure E-1. It is seen the isopropyl alcohol is superior in this case; the actual to theoretical density ratio falls initially at a rate of 0.0073%/min. Considering that the strand does not remain in the alcohol for more than two minutes, the error due to the solubility of AP and the absorption of fluid by the fuel, is 0.02%. With heptane, this error is about 5 times larger in magnitude.

The specific gravity of the isopropyl alcohol is determined by a precision hydrometer with a guaranteed accuracy of 0.0005. As a check, the S.G. measured from 15-30°C was compared to that quoted by Ref. 208. The discrepancy was less than 0.001. This larger error is probably due to the differing grades of alcohol used.

(iii) Error incurred by neglecting volume displaced by the wire suspending the sample in the displacement fluid.

The weight of the wire is accounted for, but the volume displaced by it is assigned to the volume of the propellant sample in the method of density measurement used here. The wire is 0.0061 inch diameter and normally no more than 4 cm is below the surface of the liquid. This causes the measured density to be too low by 0.02%.

(iv) Error in weight measurements.

The weights used have been checked against a recently calibrated Mettler balance. If the worst combination or weights used in these measurements is taken, the error could be as high as 0.0006 gm.

(v) Error in fuel density.

Repeated density measurements of PBAA fuel, cured in the same way as the propellant, have shown it to be 0.947 ± 0.001 gm/cc.

(vi) Error in AP density.

Attempts at measuring the density of AP failed because a low viscosity, non-volatile fluid which does not dissolve the AP (for use as a displacement fluid in a specific gravity bottle), could not be found. The most accurate figure that could be found is that quoted by Ref. 204 as 1.952 gm/cc. An error of ± 0.001 gm/cc is estimated.

(vii) Error Analysis of Propellant Density Measurements.

For the case where there is only fuel lost to the vacuum system (no submerged bearings):

The mass of fuel used per 1000 gm propellant batch = 250.0 gm

From (i), the amount of fuel lost = (1.45 ± 0.20) gm

Therefore, mass of fuel left $m_f = 248.55 \pm 0.20$ gm

The mass of AP used per batch $m_o = 750.0$ gm

Therefore, the fuel oxidant ratio $x = \dfrac{m_f}{m_f + m_o} = 0.2489 \pm 0.0002$

(Residues left in the beakers used for weighing the propellant constituents, are accounted for in the calculation of the amount of ingredient that goes into the mixer.)

Further, from the previous:

PBAA density	$\rho_f = 0.947 \pm 0.001$ gm/cc
AP density	$\rho_o = 1.952 \pm 0.001$ gm/cc
S.G. of isopropyl alcohol	$\rho_l = 0.7833 \pm 0.0005$

and using typical figures for wt. measurements:

mass of propellant sample	$m_s = 6.7576 \pm 0.0006$ gm
mass of sample + wire	$M_w = 6.7804 \pm 0.0006$ gm
mass of sample + wire when immersed in alcohol	$M_l = 3.3597 \pm 0.0006$ gm

The theoretical density is expressed by:

$$(1/\rho_{th}) = (x/\rho_f) + (1-x)/\rho_o$$

Thus, the error in the theoretical density is:

$$\frac{\Delta\rho_{th}}{\rho_{th}} = \pm \frac{1}{\left(\frac{x}{\rho_f} + \frac{1-x}{\rho_o}\right)} \left\{ \left(\frac{1}{\rho_f} - \frac{1}{\rho_o}\right)\Delta x + \frac{x}{\rho_f^2}\Delta\rho_f + \frac{(1-x)}{\rho_o^2}\Delta\rho_o \right\}$$

$$= \underline{\pm\ 0.09\ \%}$$

Similarly, the actual density determined by the displacement method, is:

$$\rho_{act} = (m_s/v) = (m_s \rho_l)/(M_w - M_l)$$

Thus, the error in this measured density is:

$$\frac{\Delta\rho_{act}}{\rho_{act}} = \frac{\Delta m_s}{m_s} + \frac{\Delta\rho_l}{\rho_l} + \frac{\Delta M_w}{M_w - M_l} + \frac{\Delta M_l}{M_w - M_l}$$

$$= \underline{\pm\ 0.11\ \%}$$

Therefore, the error in the density ratio is:

$$\frac{\Delta(\rho_{act}/\rho_{th})}{(\rho_{act}/\rho_{th})} = \frac{\Delta\rho_{th}}{\rho_{th}} + \frac{\Delta\rho_{act}}{\rho_{act}} = \underline{\pm\ 0.20\ \%}$$

From (ii) and (iii) we have a systematic error of -0.04%. Therefore, if the fuel lost into the vacuum system is accounted for (i.e., loss measurements have been made), then the estimated error is $\underline{(-0.04 \pm 0.20)\%}$.

If no measurements of the loss of fuel into the vacuum system have been made, the systematic error in density measurements increases. Under these circumstances, the error is $\underline{(+0.05 \pm 0.20)\%}$. Similarly, if the 35LP mixer with submerged bearings is used, the error is of the order: $\underline{(+0.25 \pm 0.25)\%}$.

It is seen that replacement of the mixer with one that does not have submerged bearings, reduces mainly the systematic error. Since the loss into the bearings could only be roughly estimated (and the error could therefore not be accurately assessed), it was decided to always use the new mixer in the future.

With the new mixer in operation, the random error is now $\pm$0.2%. Further, the systematic error is now -0.05% or +0.05% depending on whether the fuel loss into the vacuum system has, or has not been accounted for, respectively.

(viii) Reproducibility of density measurements.

Repeated density measurements on the same strand have fallen within 0.05% of each other. This is considerably less than the predicted error of $\pm$0.2% determined in the previous section.

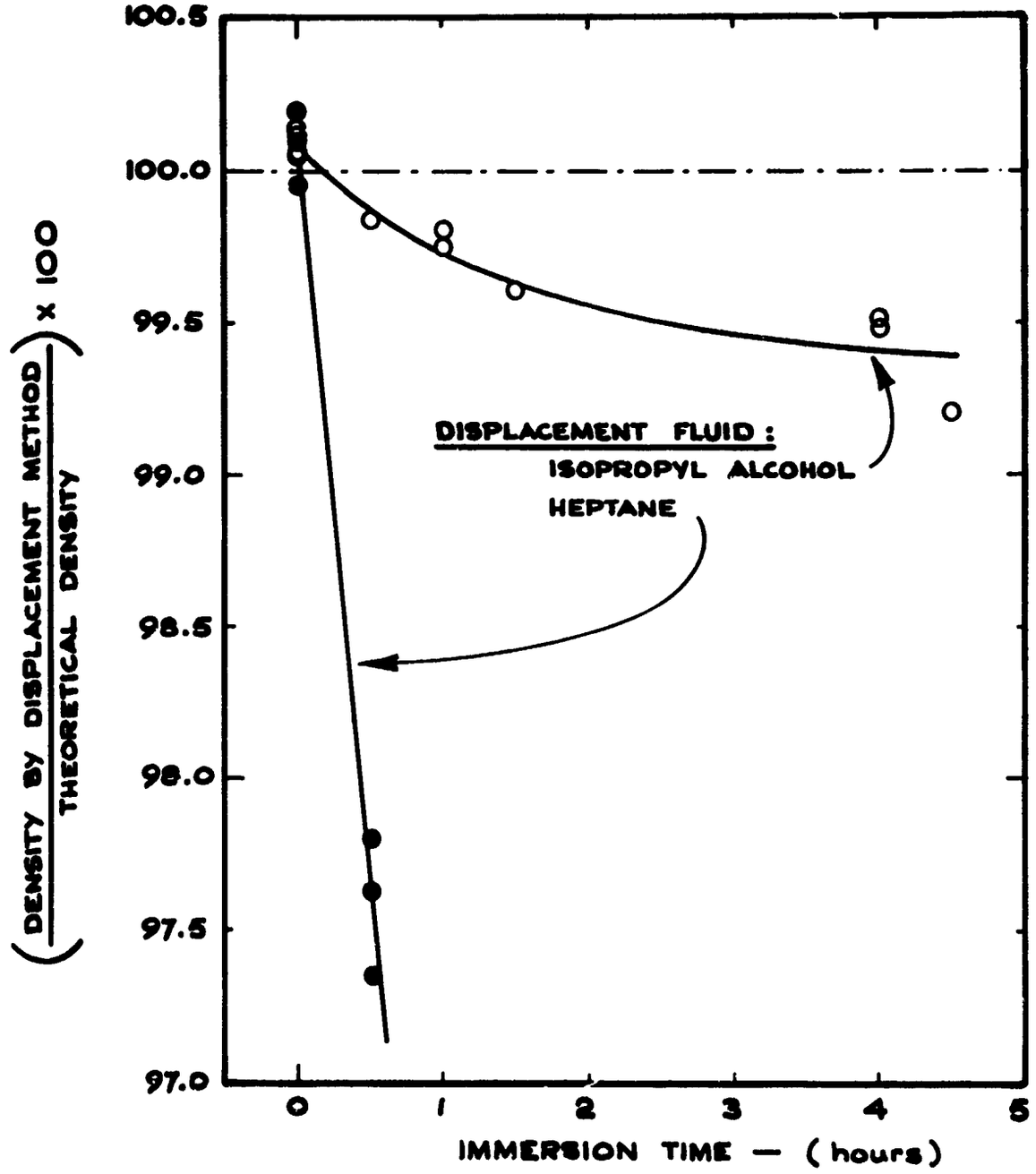

FIGURE E-1 EFFECT OF IMMERSION INTO DISPLACEMENT FLUID ON THE MEASURED DENSITY OF 25% PBAA/EPON + 75% AP (80μ UNIMODAL)

Unclassified
Security Classification

APPENDIX G

DOCUMENT CONTROL DATA - R & D

(Security classification of title, body of abstract and indexing annotation must be entered when the overall report is classified)

1 ORIGINATING ACTIVITY (Corporate author)
Princeton University
Department of Aerospace & Mechanical Science
Princeton, New Jersey 08540

2a. REPORT SECURITY CLASSIFICATION
Unclassified

2b. GROUP

3 REPORT TITLE
THE BURNING MECHANISM OF AMMONIUM PERCHLORATE-BASED COMPOSITE SOLID PROPELLANTS

4 DESCRIPTIVE NOTES (Type of report and inclusive dates)
Scientific Interim

5 AUTHOR(S) (First name, middle initial, last name)
J. A. Steinz, P. L. Stang, and M. Summerfield

6 REPORT DATE	7a. TOTAL NO OF PAGES	7b. NO OF REFS
February, 1969	242	208

8a CONTRACT OR GRANT NO	9a. ORIGINATOR'S REPORT NUMBER(S)
Nonr 1858(32)	AMS Report No. 830
b PROJECT NO	9b. OTHER REPORT NO(S) (Any other numbers that may be assigned this report)
c	
d	

10 DISTRIBUTION STATEMENT
1. Distribution of this document is unlimited

11 SUPPLEMENTARY NOTES	12 SPONSORING MILITARY ACTIVITY
Tech., Other	Power Program, Code 473 Office of Naval Research Dept. of the Navy, Washington, D.C.

13 ABSTRACT

The applicability of the granular diffusion flame model (GDF) and of the resulting theoretical burning rate equation has been tested on a wide variety of AP propellants, most of them of standard formulation but some of non-standard formulation. A remarkable degree of agreement has been demonstrated for the standard formulations in the usual range of pressure (1-100 atm). Burning rate measurements were carried out at sub-atmospheric pressures also, all the way down to 0.01 atm, and here, too, the data are in line with the GDF theory, but with an extended version. In this extension, the overall gas phase flame is recognized as consisting of two stages, first the exothermic AP decomposition flame and then the fuel-oxidant diffusion flame. With various non-standard propellants, particularly those with small AP particle size, low AP loading and/or readily meltable fuel binders, plateau burning rate curves and, in extreme cases, intermediate pressure extinctions (20-70 atm) have been found. This behavior is caused by temporary localized extinctions of the flame and seems to be due to intermittent but widespread covering of the AP particles on the surface by a molten fuel layer. The melting fuel is important also in determining extinction at low pressure($\lesssim$1 atm). Combustion inefficiency and convective cooling by the ambient gases are the main causes of low pressure extinction (0.1-0.01 atm) for strands of propellants with a dry (charred) burning surface. These findings on flame structure are important for understanding steady state burning rates, non-steady burning (instability), extinguishment, and ignition.

DD FORM 1 NOV 65 1473

Unclassified
Security Classification

14 KEY WORDS	LINK A		LINK B		LINK C	
	ROLE	WT	ROLE	WT	ROLE	WT
Combustion mechanism						
Composite solid propellant						
Ammonium perchlorate						
Flame structure						
Burning rate behavior						
Plateau burning						
Mesa burning						
Rocket pressure extinction						
Low pressure extinction						
Fuel-binder melt layer						
Combustion inefficiency						